UNIVERSITY OF CALIFORNIA,
IRVINE

Averaging and Singular Perturbation on Multiple Time Scales: From Sperm Chemotaxis to 3D Source Seeking

DISSERTATION

submitted in partial satisfaction of the requirements
for the degree of

DOCTOR OF PHILOSOPHY

in Mechanical and Aerospace Engineering

by

Mahmoud Abdelgalil

Dissertation Committee:
Associate Professor Haithem Taha, Co-Chair
Distinguished Professor Tryphon Georgiou, Co-Chair
Associate Professor Solmaz Kia
Distinguished Professor Mirlosav Kristć
Professor Anton Gorodetski

2023

DEDICATION

To my mentors, family, and friends.

TABLE OF CONTENTS

LIST OF FIGURES

ACKNOWLEDGMENTS

I would like to thank my mentors, Professor Mostafa Abdalla, Professor Ashraf Badawi, and Professor Tryphon Georgiou who is also my committee co-chair, each of whom inspired and mentored me during a part of my journey up to this point.

I would also like to thank my mother Amal Mahrous, my father Abdelazim Abdelgalil, my uncle Mahmoud Abdelgalil, and my wife and soulmate Asmaa Eldesoukey. None of this could have been possible without their unwavering support.

Moreover, I would like to thank my committee co-chair and advisor Professor Haithem Taha, and my committee members Professor Miroslav Krstić, Professor Solmaz Kia, and Professor Anton Gorodetski for their guidance and help. In addition, I would like to thank Professor Yasser Aboelkassem for his supervision of parts of the work done in this thesis.

Furthermore, I would like to thank all my friends and family.

Finally, I would like to acknowledge the funding support from the MAE department through TAships, Holmes Endowed Fellowship, and Henry Samueli Endowed Fellowship, and the partial funding support from NSF through grant number CMMI-1846308.

VITA

Mahmoud Abdelgalil

EDUCATION

PhD in Mechanical and Aerospace Engineering — **March 2020 - March 2023**
University of California, Irvine — *Irvine, California*

MSc in Mechanical and Aerospace Engineering — **September 2018 - March 2020**
University of California, Irvine — *Irvine, California*

BSc in Aerospace and Aeronautical Engineering — **September 2013 - June 2018**
University of Science and Technology at Zewail City — *Giza, Egypt*

REFEREED JOURNAL PUBLICATIONS

Sea urchin sperm exploit extremum seeking control to find the egg — **December 2022**
Physical Review E

Recursive Averaging with Application to Bio-Inspired 3D Source Seeking — **May 2022**
IEEE Control Systems Letters

Lie bracket approximation-based extremum seeking with vanishing input oscillations — **November 2021**
Automatica

REFEREED CONFERENCE PUBLICATIONS

Singularly Perturbed Averaging with Application to Bio-Inspired 3D Source Seeking — **June 2023**
American Control Conference 2023

Feedback Oscillatory Control of Roll Instability During Stall Using the LIBRA Mechanism — **January 2023**
AIAA SCITECH 2023

On the motion planning and feedback stabilization of control affine systems with drift — **January 2021**
AIAA SCITECH 2021

MANUSCRIPTS IN PREPARATION

Averaging and Singular Perturbation on Multiple Scales: From Sperm Chemotaxis to 3D Source Seeking

Second-order Averaging of Time-Delayed Systems

HONORS & AWARDS

Henry Samueli Endowed Fellowship **March 2019 – June 2019**
University of California, Irvine *Irvine, California*

Holmes Endowed Fellowship **January 2022 – June 2022**
University of California, Irvine *Irvine, California*

Finalist in ACC Best Student Paper Competition **June 2023**
University of California, Irvine *Irvine, California*

EMPLOYMENT

Teaching Assistant **September 2019 – January 2022**
University of California, Irvine *Irvine, California*

Teaching Assistant **July 2022 – March 2023**
University of California, Irvine *Irvine, California*

ABSTRACT OF THE DISSERTATION

Averaging and Singular Perturbation on Multiple Time Scales: From Sperm Chemotaxis to 3D Source Seeking

By

Mahmoud Abdelgalil

Doctor of Philosophy in Mechanical and Aerospace Engineering

University of California, Irvine, 2023

Associate Professor Haithem Taha, Co-Chair
Distinguished Professor Tryphon Georgiou, Co-Chair

This work revisits higher order averaging with a focus on the analysis of high-amplitude, high-frequency oscillatory systems; a class of systems that arises in the motion planning and stabilization of control-affine systems via oscillatory inputs, and in extremum seeking control. Traditional extremum seeking control suffers from persistent oscillations in the steady state. As a first contribution of this thesis, we extend recent results in the literature to allow for vanishing oscillations in steady state even when the optimal value of the function is unknown apriori.

Next, we investigate the effect of multiple periodic time scales on the average behavior of highly oscillatory systems through a recursive application of averaging methods. By exploiting the multiple-scale nature of our analysis, it is possible to separate the dither signals used for gradient estimation in extremum seeking on a slower time-scale, thereby relaxing the non-resonance conditions that are otherwise necessary in multi-dimensional extremum seeking.

Then, we consider a singularly perturbed version of highly oscillatory systems. In contrast to the results in the literature, we provide explicit formulas for the reduced order averaged

system that accounts for the interaction between the fast periodic time scale and the singularly perturbed part of the system. Moreover, we combine recursive averaging results with singular perturbation on multiple time-scales and provide explicit formulas for the reduced order averaged system.

In addition, we provide two applications of the methods studied in this thesis. The first application is concerned with klinotaxis in microorganisms. Specifically, we show that the chemotactic strategy of sea urchin sperm cells is a natural implementation of an extremum seeking control law under a nonholonomic integrator.

In the light of this novel connection, we propose bio-inspired 3D source seeking algorithms for rigid bodies with collocated and non-collocated sensors. Unlike all the results in the literature, our proposed algorithms do not assume any global attitude information.

Finally, we investigate, through formal calculations and numerical simulations, the effects of time delays on highly oscillatory systems. We provide explicit formulas for second order averaging of retarded differential equations with a constant time delay when the delay is infinitesmal or is finite. We show that the dynamics of the second-order averaged system depends on a twice-delayed state of the original system when the delay is finite. Moreover, we show that even an infinitesmal delay may bifurcate a single periodic orbit of the original system into multiple orbits and affect their stability. Our analysis highlights a fundamental trade-off between robustness to infinitesmal time-delays and the domain and speed of attraction for highly oscillatory systems when the frequency of oscillation is large compared to the natural time-scale of the dynamics.

Chapter 1

Introduction

Perturbation theory is concerned with the study of dynamical systems with small parameters. The trivial approach in perturbation theory is to substitute with zero for the small parameters, thereby obtaining as a *zeroth-order* approximation of the system under consideration in the limit where the small parameters vanish. This simple approach, however, fails in various ways and for various reasons. The problems where the simple approach fails are called singular perturbation problems, and, depending on the nature of the problem, more advanced tools are needed to approximate the behavior of the system.

This thesis considers a class of singular perturbation problems that arises in extremum seeking control [2, 3, 4] and the motion planning and stabilization of control-affine systems [5]. In particular, we employ higher-order averaging [6] and various extensions of the classic theorem of Tikhonov [7, Theorem 11.1] in our analysis. This introductory chapter provides a brief tour of the tools we use in this thesis, starting with the classical averaging method in the next section.

1.1 The classical averaging method

The method of averaging has a rich history going back as far as the early works of Laplace and Lagrange on the study of secular planet motions in celestial mechanics during the 1700s. Over the course of three centuries, the method continued to evolve thanks to the contributions of many great mathematicians [6, Appendix A].

Averaging received strong interest from Soviet Union mathematicians during the 1900s, which led to the formulation of the Krylov-Bogoliubov-Mitropolskii (KBM) averaging method with application to nonlinear oscillations in physics and engineering [8]. The emphasis has been on constructing asymptotically accurate solutions to nonlinear time varying differential equations in the presence of weak oscillations.

Not long after, the *chronological calculus* was developed to provide a representation for the flow of time varying vector fields as an exponential-like series [9]. The framework of chronological calculus naturally lends itself to the method of averaging. For example, Bullo utilized the chronological calculus framework in the averaging analysis and vibrational stabilization of mechanical systems [10, 11]. Concurrently, the framework was employed by Sarychev [12] and later Vela [13] as a geometric formulation of the standard averaging theorem, and, in combination with nonlinear Floquet theory, as a tool for the stability analysis of nonlinear time periodic systems. For more details on the connection between the chronological calculus approach to averaging and the KBM method, we refer the reader to the recent article [14].

Although the method of averaging applies to a general class of vector fields (the class of so-called KBM vector fields [6, Chapter 4]), the averaging method is well developed for the class of periodic vector fields and has been generalized to arbitrarily high orders under close-to-minimal regularity assumptions [15]. In this introductory section, we focus on periodic systems. The presentation in this chapter is largely based on the excellent book by Sanders and Verhulst [6].

Consider the following perturbation problem:

$$\dot{\mathbf{x}} = \sum_{i=1}^{k} \varepsilon^i \, \mathbf{f}_i(\mathbf{x}, t) + \varepsilon^{k+1} \mathbf{f}_{[k+1]}(\mathbf{x}, t, \varepsilon), \qquad \mathbf{x}(0) = \mathbf{x}_0 \tag{1.1}$$

where the vector fields $\mathbf{f}_i$, $\mathbf{f}_{[k+1]}$ are T-periodic in t, $k \in \mathbb{N}$ is some constant integer, and $\varepsilon \in [0, \varepsilon_0]$ is the perturbation parameter. We are interested in obtaining an approximation of the behavior of the trajectories of the system (1.1). To achieve this task, the so-called *near-identity* transform:

$$\mathbf{x} = \mathbf{U}(\boldsymbol{\xi}, t, \varepsilon) = \boldsymbol{\xi} + \sum_{i=1}^{k} \varepsilon^i \mathbf{u}_i(\boldsymbol{\xi}, t) \tag{1.2}$$

can be utilized as a coordinate transform, where in the new coordinate $\boldsymbol{\xi}$ we have that:

$$\dot{\boldsymbol{\xi}} = \sum_{i=1}^{k} \varepsilon^i \, \bar{\mathbf{f}}_i(\boldsymbol{\xi}) + \varepsilon^{k+1} \bar{\mathbf{f}}_{[k+1]}(\boldsymbol{\xi}, t, \varepsilon), \qquad \boldsymbol{\xi}(0) = \mathbf{x}_0 \tag{1.3}$$

Now, we see that according to (1.2), we have that:

$$\dot{\mathbf{x}} = \partial_t \mathbf{U}(\boldsymbol{\xi}, t, \varepsilon) + \partial_{\boldsymbol{\xi}} \mathbf{U}(\boldsymbol{\xi}, t, \varepsilon) \, \dot{\boldsymbol{\xi}} = \sum_{i=1}^{k} \varepsilon^i \Big(\partial_t \mathbf{u}_i(\boldsymbol{\xi}, t) - \mathbf{K}_{1,i}(\boldsymbol{\xi}, t) \Big) + O(\varepsilon^{k+1}) \tag{1.4}$$

where $\mathbf{K}_{1,i}$ for $i \in \{1, \ldots, k\}$ is the coefficient of the $O(\varepsilon^i)$ term in the product $\partial_{\boldsymbol{\xi}} \mathbf{U}(\boldsymbol{\xi}, t, \varepsilon) \, \dot{\boldsymbol{\xi}}$. At the same time, we have from (1.1) that:

$$\begin{aligned} \dot{\mathbf{x}} &= \sum_{i=1}^{k} \varepsilon^i \, \mathbf{f}_i(\mathbf{U}(\boldsymbol{\xi}, t, \varepsilon), t) + \varepsilon^{k+1} \mathbf{f}_{[k+1]}(\mathbf{U}(\boldsymbol{\xi}, t, \varepsilon), t, \varepsilon) \\ &= \sum_{i=1}^{k} \varepsilon^i \, \mathbf{K}_{2,i}(\boldsymbol{\xi}, t) + O(\varepsilon^{k+1}) \end{aligned} \tag{1.5}$$

where the right-hand-side is to expand as a Taylor series in ε up to order ε^k, and $\mathbf{K}_{2,i}$ is the

coefficient of ε^i in that expansion. By matching the coefficients of like-powers for the two series in (1.4) and (1.5) up to order ε^k, we arrive at the so called *homological equations*:

$$\partial_t \mathbf{u}_i(\boldsymbol{\xi}, t) = \mathbf{K}_{1,i}(\boldsymbol{\xi}, t) + \mathbf{K}_{2,i}(\boldsymbol{\xi}, t), \qquad i \in \{1, \dots, k\} \tag{1.6}$$

The remaining terms of order $O(\varepsilon^{k+1})$ and higher are grouped into the vector field $\bar{\mathbf{f}}_{k+1}$. Because (1.2) is a near identity transform, the homological equations take the form:

$$\partial_t \mathbf{u}_i(\boldsymbol{\xi}, t) = \mathbf{K}_i(\boldsymbol{\xi}, t) - \bar{\mathbf{f}}_i(\boldsymbol{\xi}), \qquad i \in \{1, \dots, k\} \tag{1.7}$$

where $\mathbf{K}_i$ depends on $\mathbf{f}_j$, $\bar{\mathbf{f}}_j, \mathbf{u}_j$ for $j \in \{1, \dots, i-1\}$ and $\mathbf{f}_i$, but not on $\bar{\mathbf{f}}_i$. Utilizing this structure, the homological equations can be solved sequentially by defining $\bar{\mathbf{f}}_i$ as the time average of $\mathbf{K}_i$ over one period:

$$\bar{\mathbf{f}}_i = \frac{1}{T} \int_0^T \mathbf{K}_i(\boldsymbol{\xi}, t) dt, \qquad i \in \{1, \dots, k\} \tag{1.8}$$

In this case, the homological equations (1.5) are solvable via direct integration:

$$\mathbf{u}_i(\boldsymbol{\xi}, t) = \int_0^T \Big(\mathbf{K}_i(\boldsymbol{\xi}, t) - \bar{\mathbf{f}}_i(\boldsymbol{\xi}) \Big) dt, \qquad i \in \{1, \dots, k\} \tag{1.9}$$

since the right-hand-side is a periodic function with zero average. The actual definition of the near-identity transform and the averaged system can now be constructed by reversing the arguments above. We provide here the first and second order terms in the expansion because they will play important roles in subsequent sections:

$$\mathbf{K}_1(\boldsymbol{\xi}, t) = \mathbf{f}_1(\boldsymbol{\xi}, t) \tag{1.10}$$

$$\mathbf{K}_2(\boldsymbol{\xi}, t) = \mathbf{f}_2(\boldsymbol{\xi}, t) + \partial_{\boldsymbol{\xi}} \mathbf{f}_1(\boldsymbol{\xi}, t)\, \mathbf{u}_1(\boldsymbol{\xi}, t) - \partial_{\boldsymbol{\xi}} \mathbf{u}_1(\boldsymbol{\xi}, t)\, \bar{\mathbf{f}}_1(\boldsymbol{\xi}) \tag{1.11}$$

We refer the reader to [14] for exact expressions of the third and fourth order terms, and to

[6, Chapter 3] for a systematic procedure of obtaining higher order expansions using the so called *Lie transforms*.

Now that we have defined the near-identity transform and the averaged system (1.2), we would like to obtain estimates on the error between the trajectories of the original system (1.1), and the trajectories of the averaged system (1.2). To state this relation, we introduce a shorter version of the near identity transform:

$$\mathbf{U}_j(\boldsymbol{\xi}, t, \varepsilon) = \boldsymbol{\xi} + \sum_{i=1}^{j} \varepsilon^i \mathbf{u}_i(\boldsymbol{\xi}, t) \tag{1.12}$$

and the truncated averaged system:

$$\dot{\overline{\boldsymbol{\xi}}} = \sum_{i=1}^{k} \varepsilon^i \, \overline{\mathbf{f}}_i(\overline{\boldsymbol{\xi}}), \qquad\qquad \overline{\boldsymbol{\xi}}(0) = \mathbf{x}_0 \tag{1.13}$$

The following theorem, adapted from [6], summarizes the relation between the trajectories of (1.1) and (1.13):

Theorem 1.1.1. The exact solution to (1.1), denoted as $\mathbf{x}(t)$, and its approximation $\overline{\mathbf{x}}(t) = \mathbf{U}_{k-1}(\overline{\boldsymbol{\xi}}(t), t, \varepsilon)$, where $\overline{\boldsymbol{\xi}}(t)$ is the solution to the system (1.13), satisfy the error estimate:

$$\|\mathbf{x}(t) - \overline{\mathbf{x}}(t)\| = O(\varepsilon^k) \tag{1.14}$$

for $t \sim O(1/\varepsilon)$ and small ε.

The theorem above provides a direct relationship between the trajectories of the time-varying system (1.1) and the time-invariant system (1.13). Therefore, by studying the simpler system (1.13), we may be able to conclude qualitative properties of the original time-varying system (1.1). As an example, when the averaged system possesses an exponentially stable equilibrium point, one can show that the original system possesses an exponentially stable periodic orbit.

Despite the fact that the class of problems studied in this section are singular perturbation problems in the general sense of the term, a truly singular behavior arises when a reduction of the order of the differential equation under consideration happens in the limit $\varepsilon \to 0$, which is not the case for the system (1.1). The next section provides a brief introduction to the main method in tackling such behavior.

1.2 Tikhonov's Theorem

In later chapters, we will be primarily concerned with singular perturbation problems in which a part of the system state (the fast states) converges sufficiently fast to an equilibrium manifold. The typical setting for this type of problems (e.g. [7]) is the following. Let $\mathbf{x}_1 \in \mathbb{R}^{n_1}$ and $\mathbf{x}_2 \in \mathbb{R}^{n_2}$, and consider the following system of differential equations:

$$\dot{\mathbf{x}}_1 = \mathbf{f}_1(\mathbf{x}_1, \mathbf{x}_2), \qquad \mathbf{x}_1(0) = \mathbf{x}_{1,0} \tag{1.15a}$$

$$\varepsilon\, \dot{\mathbf{x}}_2 = \mathbf{f}_2(\mathbf{x}_1, \mathbf{x}_2), \qquad \mathbf{x}_2(0) = \mathbf{x}_{2,0} \tag{1.15b}$$

In the limit $\varepsilon \to 0$, the order of the differential equations drops to n_1 due to the fact that ε multiplies a part of the highest order derivative in the equations. Consequently, the equations of the system reduce to:

$$\dot{\tilde{\mathbf{x}}}_1 = \mathbf{f}_1(\tilde{\mathbf{x}}_1, \mathbf{x}_2), \qquad \tilde{\mathbf{x}}_1(0) = \mathbf{x}_{1,0} \tag{1.16a}$$

$$0 = \mathbf{f}_2(\tilde{\mathbf{x}}_1, \mathbf{x}_2) \tag{1.16b}$$

If there exists a sufficiently smooth unique function $\varphi(\mathbf{x}_1)$ such that:

$$\mathbf{f}_2(\tilde{\mathbf{x}}_1, \varphi(\tilde{\mathbf{x}}_1)) = 0 \tag{1.17}$$

and the *boundary layer model* given by:

$$\frac{d\mathbf{y}_2}{d\tau} = \mathbf{f}_2(\mathbf{x}_1, \mathbf{y}_2 + \varphi(\mathbf{x}_1)) \tag{1.18}$$

where $\mathbf{x}_1$ is treated as a constant parameter, possesses the origin as a globally exponentially stable equilibrium point, then under sufficiently regularity conditions a classical result known as Tikhonov's theorem provides a relation between the trajectories of the system (1.15) and the system (1.16) and (1.18).

Theorem 1.2.1. *[7] There exists a sufficiently small* $\varepsilon^* \in (0, \infty)$ *such that* $\forall \varepsilon \in (0, \varepsilon^*)$ *we have:*

$$\mathbf{x}_1(t) - \tilde{\mathbf{x}}_1(t) = O(\varepsilon) \tag{1.19}$$

$$\mathbf{x}_2(t) - \boldsymbol{\varphi}(\tilde{\mathbf{x}}_1(t)) - \mathbf{y}_2(t/\varepsilon) = O(\varepsilon) \tag{1.20}$$

$\forall t \in [t_0, t_1]$ *where the interval* $[t_0, t_1]$ *is the interval of existence and uniqueness of the solution* $\tilde{\mathbf{x}}_1(t)$.

The key idea behind Tikhonov's theorem is to exploit the exponential stability of the boundary layer model (1.18) to replace the singularly perturbed part of the system (i.e. $\mathbf{x}_2$) with its quasi-steady state $\boldsymbol{\varphi}(\mathbf{x}_1)$. However, Tikhonov's theorem is concerned only with first order behavior as is evident from the nature of the approximate relation between the trajectories (i.e. the error is $O(\varepsilon)$). In later chapters, we shall encounter situations in which the first-order behavior of the system vanishes and it becomes necessary to proceed to at least second-order so as to capture the leading order behavior of the system under consideration. Consequently, we shall have to obtain an asymptotic approximation of the motion around the quasi-steady state $\boldsymbol{\varphi}(\mathbf{x}_1)$ using a perturbative expansion in the small parameter ε.

The archetype application of the combination of singular perturbation and averaging, and

to which a major part of this thesis is a contribution, is the well-known adaptive control technique called extremum seeking [2]. In the next section, we give a brief introduction to extremum seeking control.

1.3 Extremum Seeking Control

Extremum Seeking (ES) control is an adaptive control technique designed to steer a dynamical system towards the extremum of an objective function that depends on the state of the system, without access to information about the gradient of the function (only the value of the objective function is available for measurement at each instant in time). The first ES control law can be traced back to the century old paper due to Leblanc [16], but the recent interest in ES control was sparked by Krstić's seminal paper [2]. In the simplest setting, an ES controller is designed to find the optimal value of a single-variable static objective function by dynamically estimating the gradient. Let $c(x)$ be the objective function, and consider the following dynamical system [17]:

$$x = \bar{x} + a\,\sin(\omega t) \tag{1.21a}$$

$$\dot{\bar{x}} = 2\,k\,(\zeta_2 - \zeta_1)\,\sin(\omega t), \tag{1.21b}$$

$$\dot{\zeta}_1 = \omega\,(\zeta_2 - \zeta_1), \tag{1.21c}$$

$$\dot{\zeta}_2 = \omega\,(c(x) - \zeta_2), \tag{1.21d}$$

which is depicted in the block diagram shown in figure 1.1, where $\bar{x}$ is the estimate of the optimal value of the independent variable x, ζ_1 and ζ_2 are the states of a band-pass filter centered around the constant frequency ω, and k, a are tuning parameters. The flow of the block diagram in figure 1.1 can be traced as follows. First, a sinusoidal perturbation is injected to sample the objective function near the estimate $\bar{x}$. Using Taylor expansion, the

instantaneous cost can be written as:

$$c(x) = c(\bar{x}) + \frac{dc(\bar{x})}{d\bar{x}}\, a\, \sin(\omega t) + O(a^2). \tag{1.22}$$

We observe how the gradient appears as the amplitude of the sinusoidal perturbation. In engineering terms, injecting the perturbation around the current estimate $\bar{x}$ 'modulates' the local gradient information on the amplitude of the sinusoidal 'carrier' signal $\sin(\omega t)$. Therefore, to extract the gradient information, the measured objective function $c(x)$ goes through a band-pass filter centered around the frequency ω as defined by equations (1.21c)-(1.21d). The output of the filter ζ can be approximated in a quasi-steady sense by:

$$\zeta_2 - \zeta_1 \approx \frac{1}{2}\frac{dc(\bar{x})}{d\bar{x}}\, a\, \sin(\omega t), \tag{1.23}$$

Next, the gradient information is 'demodulated' (i.e., extracted from the carrier signal) through multiplication with another sinusoid having the same frequency and phase as the carrier signal:

$$2\,(\zeta_2 - \zeta_1)\, k \sin(\omega t) \approx \frac{a\, k}{2}\frac{dc(\bar{x})}{d\bar{x}}\,(1 - \cos(2\omega t)), \tag{1.24}$$

where the time-average of the right hand side of equation (1.24) is proportional to the gradient. Finally, the demodulated gradient information is used in adjusting the current estimate $\bar{x}$. Through a simple averaging argument, we obtain that the estimate $\bar{x}$ evolves on average according to:

$$\dot{\bar{x}} \approx \overline{2\,(\zeta_2 - \zeta_1)\, k\, \sin(\omega\, t)} = \frac{a\, k}{2}\frac{dc(\bar{x})}{d\bar{x}}, \tag{1.25}$$

where the overline $\bar{}$ indicates the time average of the overlined quantity. That is, the estimate $\bar{x}$ evolves, in a quasi-steady average sense, along the gradient of the objective function under

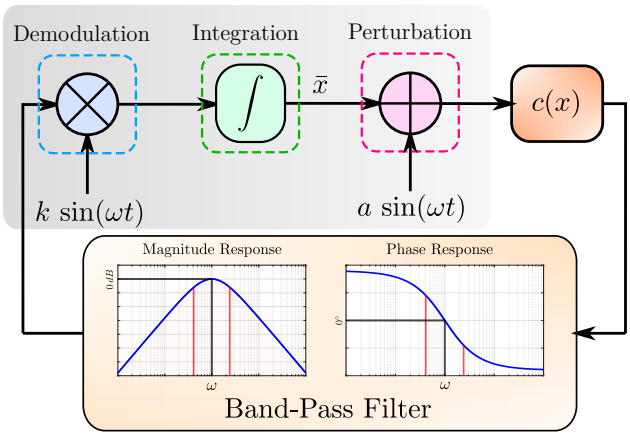

Figure 1.1: A block diagram description of the simplest extremum seeking control scheme as represented by equations (1.21).

the extremum seeking control law (1.21). The interested reader is referred to [2, 17, 18] for more details.

A key feature of extremum seeking control is that it employs zeroth-order information (i.e. objective function evaluation) to extract first-order information (i.e. objective function gradient). As such, extremum seeking control arises as a second-order effect in a dynamical system. In particular, it is clear that the oscillations around the current estimate $\bar{x}$ in equation (1.21a) have zero mean. Therefore, from an averaging perspective, the first-order behavior of extremum seeking vanishes and the leading order behavior is second-order. This aspect of extremum seeking is analogous to a situation that arises in nonholonomic control affine systems typically studied in geometric control theory. The following section provides a brief introduction to this connection with extremum seeking control.

1.4 Highly Oscillatory Systems

The development of geometric control theory in the second half of the 20th century rejuvenated the interest in the use of oscillatory inputs for the stabilization and motion planning of nonlinear control affine systems. This approach culminated in the results obtained by

Sussmann and Liu [19, 20, 5] who extended the earlier work of Kurzweil and Jarnik [21] on the limits of solutions of sequences of systems of ordinary differential equations. Notably, Sussmann and Liu's techniques on trajectory approximation and tracking may be combined with the notion of *practical stability* [22, 23] to analyze the long time behavior of time varying control-affine nonlinear systems. This approach is based on establishing the so-called 'convergence-of-trajectories' property between the system in consideration and the 'extended system' in which the high-frequency, high amplitude-oscillation is replaced by accounting for its average effect on the trajectories. In recent years, this approach was utilized in analyzing extremum seeking systems with the introduction of the Lie Bracket Approximation framework [3, 24, 1].

1.4.1 Lie Bracket Approximation Framework

The basic setting of the Lie Bracket Approximation framework, which is quite similar to the second order case in Sussman and Liu's results, is as follows. Consider the time varying control affine system defined by:

$$\dot{\mathbf{x}} = \mathbf{b}_0(\mathbf{x}, t) + \sum_{i=1}^{r} \sqrt{\omega}\, u_i(t, \omega t)\mathbf{b}_i(\mathbf{x}, t) \tag{1.26}$$

where the functions u_i are periodic in their second argument and have zero average over the period. Through a combination of Grönwall's inequality and integration by parts, the authors in [3] establish the convergence of the trajectories of the system (1.26) on compact time intervals and compact sets in the limit as $\omega \to \infty$ to the trajectories of the so called Lie Bracket system:

$$\dot{\mathbf{x}} = \mathbf{b}_0(\mathbf{x}, t) + \sum_{i<j}^{r} v_{ji}(t)[\mathbf{b}_i, \mathbf{b}_j](\mathbf{x}, t) \tag{1.27}$$

where:

$$v_{ji}(t) = \frac{1}{T}\int_0^T u_j(t,\tau)\int_0^\tau u_i(t,\nu)d\nu\, d\tau \tag{1.28}$$

$$[\mathbf{b}_i, \mathbf{b}_j] = \frac{\partial \mathbf{b}_j}{\partial \mathbf{x}}\,\mathbf{b}_i - \frac{\partial \mathbf{b}_i}{\partial \mathbf{x}}\mathbf{b}_j \tag{1.29}$$

The convergence-of-trajectories property is then employed to establish the practical stability as defined in [23] of the original system (1.26), provided that the Lie Bracket system (1.27) posses a globally uniformly asymptotically stable compact subset.

1.4.2 Lie Bracket Approximation of Extremum Seeking

The Lie Bracket Approximation framework has been applied to study and establish the practical stability of extremum seeking control. To illustrate, consider the following scalar system:

$$\dot{x} = \sqrt{\omega}\,\cos(\omega t) + J(x)\sqrt{\omega}\,\sin(\omega t) \tag{1.30}$$

which as the same form as the system (1.26). If we compute the Lie bracket system corresponding to (1.30), we obtain the system:

$$\dot{x} = \frac{1}{2}\frac{dJ}{dx} \tag{1.31}$$

which is a gradient ascent algorithm. Hence, in the limit as $\omega \to \infty$, the trajectories of (1.30) approximate the trajectories of (1.31), which drives the trajectories of the system in the direction of the gradient. Various extensions of the Lie bracket approximations has appear in the literature. Nevertheless, it seems that no attempts have been made to relate this approach to the standard method of averaging except for the discussion in [3, Section

5]. Moreover, [3, Section 5] claims that the averaging method is not directly application to the class of highly oscillatory systems, which is not true. We illustrate below how higher order averaging can be used to analyze the behavior of this class of systems.

1.4.3 Classical Averaging Treatment of Highly Oscillatory Systems

Consider the system (1.26), and apply the time scaling $\tau = \omega(t-t_0)+t_0$. Then, let $\varepsilon = 1/\sqrt{\omega}$ in order to obtain the system:

$$\frac{d\mathbf{x}}{d\tau} = \varepsilon \sum_{i=1}^{r} u_i(\varepsilon^2\tau, \tau)\mathbf{b}_i(\mathbf{x}, \varepsilon^2\tau) + \varepsilon^2\mathbf{b}_0(\mathbf{x}, \varepsilon^2\tau) \tag{1.32}$$

Observe that this system is on the averaging canonical form. If we attempt first-order averaging we obtain the trivial system:

$$\frac{d\bar{\mathbf{x}}}{d\tau} = 0 \tag{1.33}$$

due to the nature of the time-periodic signals u_i. Nevertheless, by applying the stroboscopic averaging theorem for systems with slow time dependence to second-order in ε, we obtain the system:

$$\frac{d\bar{\mathbf{x}}}{d\tau} = \varepsilon^2 \sum_{i<j}^{r} v_{ji}(\varepsilon^2\tau)\,[\mathbf{b}_i, \mathbf{b}_j](\mathbf{x}, \varepsilon^2\tau) + \varepsilon^2\mathbf{b}_0(\mathbf{x}, \varepsilon^2\tau) \tag{1.34}$$

By reversing the time scaling $t = \varepsilon^2(\tau - t_0) + t_0$, we obtain the averaged system:

$$\dot{\bar{\mathbf{x}}} = \mathbf{b}_0(\bar{\mathbf{x}}, t) + \sum_{i<j}^{r} v_{ji}(t)\,[\mathbf{b}_i, \mathbf{b}_j](\bar{\mathbf{x}}, t) \tag{1.35}$$

which is identical to the Lie bracket system (1.27). Hence, the higher-order averaging theorem is applicable to the class of systems considered in the Lie bracket approximations approach, and more generally the class of systems considered in Sussmann and Liu's results [19, 20, 5].

The key advantage of introducing the Lie Bracket approximation framework for extremum seeking control is that versatility that the framework brings to the design of extremum seeking systems. In particular, the approach made it possible to design extremum seeking control laws with various important and interesting properties [24, 25, 1] Moreover, it facilitated the study of extremum seeking systems when the underlying dynamics of the system has a nonholonomic nature. We exploit this particular feature in our treatment of the source seeking problem, a variant of extremum seeking control that has direct applications in robotic navigation.

Chapter 2

Extremum Seeking with Vanishing Input Oscillations

One of the main issues with the traditional extremum seeking control [17, 3] is the inevitable oscillation of the steady state response around the optimum point, which is a consequence of continuously changing the control input. Only *practical stability* is guaranteed [3]; the system converges to a periodic orbit around the optimum point whose size diminishes as the frequency of the dither increases. However, because the amplitude of the dither signal is typically scaled with frequency [3, 5], shrinking the size of the periodic orbit around the optimum point will necessitate large-amplitude control signals, risking control saturation. This issue can be resolved by using nonsmooth control vector fields as was demonstrated by Scheinker and Krstic [24]. To show this interesting feature, they extended Liu and Sussmann's averaging techniques [5] to nonsmooth systems (not differentiable at the minimum point). This extension enabled analysis for a class of nonsmooth control vector fields that possesses interesting properties for extremum seeking control such as vanishing at minimum points and bounded update rates. Suttner and Dashkovskiy [25] proposed another type of nonsmooth control vector fields that allow sharper results than that of Scheinker and Krstic

[24]; the former proved exponential/asymptotic stability of the minimum point using extremum seeking control where as the latter only showed that the oscillations in the control input will vanish if the system ever reaches the minimum point. Then, Grushkovskaya et al. [1] presented a unifying class of generating vector fields for extremum seeking control with vanishing control oscillations that subsumes the types used by Suttner and Dashkovskiy [25] and Scheinker and Krstic [24]. They provided a detailed proof of exponential/asymptotic stability for this class of vector fields. Moreover, their proof is constructive; it illustrates how to pick the frequency of oscillation for the dither signals in terms of some constants that define bounds on the cost function and the vector fields.

Nevertheless, one of the main assumptions in these efforts [24, 25, 1] to guarantee exponential/asymptotic stability of the minimum (and consequently to eliminate persistent oscillations) is that the function takes a minimum value of zero at the minimum point, or equivalently that the function value at the minimum point is known apriori, which is a strong requirement. Suttner [26] made an attempt to relax this assumption by adapting the frequency. In their framework, the minimum point is not assumed to be an equilibrium point of the uncontrolled dynamics and convergence to the minimum point(s) is guaranteed. However, asymptotic stability in the sense of Lyapunov is forfeited. More relevant to our work, the frequency update rule leads to unbounded frequency as the system approaches the minimum point. This behavior leads to a control input signal that grows without bound and oscillates infinitely fast around the minimum point, even in the absence of a drift vector field.

In this chapter, we propose a solution that resolves the two issues discussed above simultaneously: (i) achieving asymptotic convergence to the minimum point without requiring knowledge of the minimum value of the cost function, and (ii) doing so without persistent excitation of the control signal (i.e., the amplitude of the dither signal vanishes as the system approaches the minimum point). Specifically, we prove asymptotic convergence to the mini-

mum point with bounded amplitude and frequency for all initial conditions in an arbitrarily large compact subset of the *strict epigraph* of the cost function containing the minimum point. Although the presented proof is for the static cost case, it can be extended to the case of a dynamic cost function under reasonable assumptions on the dynamics similar to Suttner's [26] with additional requirements on the drift vector field.

Let $D \subset \mathbb{R}^n$ be a bounded subset with a nonempty interior. Suppose that $J : D \to \mathbb{R}$ is a cost function that has the following properties:

Assumption 2.0.1. *Assume that $J \in C^3(D;\mathbb{R})$ and that there exists a unique point $\mathbf{x}^* \in D$, such that $\tilde{J}(\mathbf{x}) = J(\mathbf{x}) - J^* > 0, \forall \mathbf{x} \neq \mathbf{x}^*$, where $J^* = J(\mathbf{x}^*)$ and*

$$\kappa_1 \tilde{J}(\mathbf{x})^{2-\frac{1}{m}} \leq \|\nabla J(\mathbf{x})\|^2 \leq \kappa_2 \tilde{J}(\mathbf{x})^{2-\frac{1}{m}} \tag{2.1a}$$

$$\gamma_1 \tilde{J}(\mathbf{x})^{1-\frac{1}{m}} \leq \|\nabla^2 J(\mathbf{x})\| \leq \gamma_2 \tilde{J}(\mathbf{x})^{1-\frac{1}{m}} \tag{2.1b}$$

where $\kappa_i, \gamma_i > 0$ and $m \geq 1$.

Next, define the *epigraph* and *strict epigraph* of J

$$\text{epi}(J) = \big\{(\mathbf{x}, z) \in D \times \mathbb{R} \big| J(\mathbf{x}) - z \leq 0\big\} \tag{2.2}$$

$$\text{epi}_S(J) = \big\{(\mathbf{x}, z) \in D \times \mathbb{R} \big| J(\mathbf{x}) - z < 0\big\}, \tag{2.3}$$

Let $\boldsymbol{\theta} = (\mathbf{x}, z) \in \text{epi}_S(J)$, and define the functions $g_i : \text{epi}_S(J) \to \mathbb{R},\ i \in \{1, 2, 3\}$

$$g_1(\boldsymbol{\theta}) = \tilde{J}(\mathbf{x}) - J_0, \tag{2.4a}$$

$$g_2(\boldsymbol{\theta}) = z - J^* - z_0 \tag{2.4b}$$

$$g_3(\boldsymbol{\theta}) = \frac{\tanh(\tilde{J}(\mathbf{x})^{2-\frac{1}{m}})}{z - J(\mathbf{x})} - y_0 \tag{2.4c}$$

where J_0, y_0, z_0 are positive constants. Let $\epsilon > 0$ and define the domains

$$\Delta_0 = \left\{ \boldsymbol{\theta} \in \mathrm{epi}_S(J) \middle| g_i(\boldsymbol{\theta}) \leq 0, \ \forall i \in \{1,2,3\} \right\} \tag{2.5a}$$

$$\Delta_\epsilon = \left\{ \boldsymbol{\theta} \in \mathrm{epi}_S(J) \middle| g_i(\boldsymbol{\theta}) \leq \epsilon, \ \forall i \in \{1,2,3\} \right\} \tag{2.5b}$$

Let Λ denote the set of all ordered pairs (j,s), where $j \in \{1,...,n\}, s \in \{1,2\}$. Then, consider the dynamical system

$$\dot{\boldsymbol{\theta}} = \mathbf{f}_0(\boldsymbol{\theta}) + \sum_{\lambda \in \Lambda} \mathbf{f}_\lambda(\boldsymbol{\theta}) u_\lambda(t) \tag{2.6a}$$

$$\mathbf{f}_0(\boldsymbol{\theta}) = -(z - J(\mathbf{x}))\ \boldsymbol{e}_{n+1} \tag{2.6b}$$

$$\mathbf{f}_{j,s}(\boldsymbol{\theta}) = F_s(z - J(\mathbf{x}))\ \boldsymbol{e}_j \tag{2.6c}$$

and the functions $u_{j,1}, u_{j,2}$ (the dithers) are given by

$$u_{j,1}(t) = 2\sqrt{\pi\omega_j\omega}\sin(2\pi\omega_j\omega t) \tag{2.7a}$$

$$u_{j,2}(t) = 2\sqrt{\pi\omega_j\omega}\cos(2\pi\omega_j\omega t) \tag{2.7b}$$

where $\omega \in (0,\infty),\ \omega_j \in \mathbb{N},\ \forall j \in \{1,2,...,n\}$, and the functions $F_1(\cdot), F_2(\cdot)$ satisfy the condition:

$$F_2(y) = F_1(y) \int \frac{1}{F_1(y)^2} dy, \tag{2.8}$$

where the integral is understood as an anti-derivative. Note that many choices for $F_s(\cdot)$ are possible. An example of such functions is $F_1(z) = z, F_2(z) = 1$, which is the simplest extremum seeking system. Another example of such functions is $F_1(z) = |z|^r, F_2(z) = |z|^{2-r}$, which was introduced by Scheinker and Krstic in [24]. Suttner and Dashkovskiy [25] introduced another set: $1, F_1(z) = \sqrt{z}\sin\ln z,\ F_2(z) = \sqrt{z}\cos\ln z$, which has the desirable property that if $J(\mathbf{x}^*) = 0$, then there is a critical frequency beyond which the point $\mathbf{x}^*$

becomes an asymptotically stable equilibrium point in the sense of Lyapunov. In particular, the system converges to the point $\mathbf{x}^*$ with vanishing control input oscillations. We remark that if $J(\mathbf{x}^*) > 0$, the point $\mathbf{x}^*$ is no longer an equilibrium point, and only practical stability holds. Moreover, if $J(\cdot)$ can take negative values, then the vector field introduced by Suttner and Dashkovskiy [25] is not well defined. In such a case, a large enough positive constant must be added to the function. However, this requires knowledge of a lower bound on $J(\mathbf{x}^*)$. If $J(\mathbf{x}^*)$ is known exactly, a shift of the form $\tilde{J}(\mathbf{x}) = J(\mathbf{x}) - J(\mathbf{x}^*)$ makes the new function $\tilde{J}(\cdot)$ satisfy the requirements of asymptotic stability. For simplicity, we will fix one choice of the functions F_1 and F_2 to be:

$$F_1(z) = \sqrt{z}\sin\ln z, \qquad F_2(z) = \sqrt{z}\cos\ln z \tag{2.9}$$

In this setting, we have the following theorem:

Theorem 2.0.1. Suppose that the function J satisfies Assumption 2.0.1, and consider the system defined by (2.6), (2.7) and (2.9). Fix a choice for the collection of frequencies $\omega_j \in \mathbb{N},\ \forall j \in \{1, 2, ..., n\}$ such that $\forall i \neq j,\ \omega_i \neq \omega_j$. Then, $\exists \omega^* \in (0, \infty)$ such that $\forall \omega \in (\omega^*, \infty),\ \forall \boldsymbol{\theta}(0) \in \Delta_0$ we have:

1. $\boldsymbol{\theta}(t) \in \Delta_\epsilon, \forall t \in [0, \infty)$,
2. $\boldsymbol{\theta}(t) \to (\mathbf{x}^*, J^*)$ as $t \to \infty$.

Since $J(x(0))$ is available via measurement, it is always possible to place $z(0)$, which is an internal state of the controller, such that the initial condition strictly lies in Δ_0. We emphasize that this does not require additional information other than online measurement of the function value. The proof of Theorem 2.0.1 employs several lemmas which we now state.

Consider the Initial Value Problem (**IVP**)

$$\dot{\boldsymbol{\zeta}}(t) = \mathbf{f}_0(\boldsymbol{\zeta}(t)) + \sum_{\lambda\in\Lambda} \mathbf{f}_\lambda(\boldsymbol{\zeta}(t))\ u_\lambda(t), \quad \boldsymbol{\zeta}(0) \in \Xi_0 \tag{2.10}$$

where $\Xi_0 \subset \Xi \subset \mathbb{R}^n$, Λ is the set of all ordered pairs $(j,s), j \in \{1,2,...,n\}, s \in \{1,2\}$, $\mathbf{f}_0, \mathbf{f}_\lambda \in \Gamma^2(\Xi)$ and the dither signals $u_\lambda(\cdot)$ are defined by Eq. (2.7)

Lemma 2.0.1. *[3, 5, 26] Let $g \in C^3(\Xi;\mathbb{R})$. Then, for every solution $\boldsymbol{\zeta} : I \to \Xi$ of (2.10), the function $g \circ \boldsymbol{\zeta} : I \to \mathbb{R}$ satisfies*

$$g(\boldsymbol{\zeta}(t))\big|_{t_1}^{t_2} = R_1^g(\boldsymbol{\zeta}(t),t)\big|_{t_1}^{t_2} + \int_{t_1}^{t_2} \big(F^g(\boldsymbol{\zeta}(t)) + R_2^g(\boldsymbol{\zeta}(t),t)\big)dt \tag{2.11a}$$

where I is the interval of existence and uniqueness of $\boldsymbol{\zeta}(\cdot)$, $t_1, t_2 \in I, t_2 > t_1$, and

$$F^g(\boldsymbol{\zeta}) = L_{\boldsymbol{f}_0} g(\boldsymbol{\zeta}) - \sum_{j=1}^{m} L_{[\boldsymbol{f}_{j,1}, \boldsymbol{f}_{j,2}]} g(\boldsymbol{\zeta}) \tag{2.12a}$$

$$R_1^g(\boldsymbol{\zeta},t) = \sum_{\lambda\in\Lambda} L_{\boldsymbol{f}_\lambda} g(\boldsymbol{\zeta})\ U_\lambda(t) - \sum_{\lambda_1,\lambda_2\in\Lambda} L_{\boldsymbol{f}_{\lambda_2}} L_{\boldsymbol{f}_{\lambda_1}} g(\boldsymbol{\zeta})\ U_{\lambda_1,\lambda_2}(t) \tag{2.12b}$$

$$R_2^g(\boldsymbol{\zeta},t) = -\sum_{\lambda\in\Lambda} L_{\boldsymbol{f}_0} L_{\boldsymbol{f}_\lambda} g(\boldsymbol{\zeta})\ U_\lambda(t) + \sum_{\lambda_1,\lambda_2\in\Lambda} L_{\boldsymbol{f}_0} L_{\boldsymbol{f}_{\lambda_2}} L_{\boldsymbol{f}_{\lambda_1}} g(\boldsymbol{\zeta})\ U_{\lambda_1,\lambda_2}(t) \tag{2.12c}$$

$$+ \sum_{\lambda_1,\lambda_2,\lambda_3\in\Lambda} L_{\boldsymbol{f}_{\lambda_3}} L_{\boldsymbol{f}_{\lambda_2}} L_{\boldsymbol{f}_{\lambda_1}} g(\boldsymbol{\zeta})\ U_{\lambda_1,\lambda_2}(t) u_{\lambda_3}(t) \tag{2.12d}$$

$$U_\lambda(t) = \int u_\lambda(t)\ dt, \qquad U_{\lambda_1,\lambda_2}(t) = \int \Big(v_{\lambda_1,\lambda_2} + U_{\lambda_1}(t)\ u_{\lambda_2}(t)\Big)d\tau \tag{2.13a}$$

$$v_{\lambda_1,\lambda_2} = \begin{cases} +1 & \lambda_1 = (j,1) \quad \& \quad \lambda_2 = (j,2) \\ -1 & \lambda_1 = (j,2) \quad \& \quad \lambda_2 = (j,1) \\ 0 & \textit{otherwise} \end{cases} \tag{2.13b}$$

Lemma 2.0.2. *Let $\Xi \subseteq \mathbb{R}^n, g_i \in C^3(\Xi;\mathbb{R})\ \forall i \in \{1,2,...,r\}$. Let $\epsilon > 0$ and define*

$$\Delta_0 = \left\{\boldsymbol{\zeta} \in \Xi \middle| g_i(\boldsymbol{\zeta}) \leq 0,\ \forall i \in \{1,2,..,r\}\right\} \tag{2.14a}$$

$$\Delta_\epsilon = \left\{\boldsymbol{\zeta} \in \Xi \middle| g_i(\boldsymbol{\zeta}) \leq \epsilon,\ \forall i \in \{1,2,..,r\}\right\} \tag{2.14b}$$

and the subsets $\Delta_\epsilon^i = \left\{\boldsymbol{\zeta} \in \Delta_\epsilon \middle| 0 \leq g_i(\boldsymbol{\zeta}) \leq \epsilon\right\}$. Suppose that $\forall i \in \{1,2,...,r\}$, whenever $\boldsymbol{\zeta} \in \Delta_\epsilon^i$, the following bounds hold

$$\left\|R_1^{g_i}(\boldsymbol{\zeta},t)\right\| \leq \frac{c_1^{g_i}}{\sqrt{\omega}}, \quad \left\|R_2^{g_i}(\boldsymbol{\zeta},t)\right\| \leq \frac{c_2^{g_i}}{\sqrt{\omega}}, \quad F^{g_i}(\boldsymbol{\zeta}) \leq -b^{g_i}$$

$\forall t \in \mathbb{R}$, where $c_1^{g_i}, c_2^{g_i}, b^{g_i} > 0$ are constants. Then $\exists \omega^* \in (0,\infty)$ such that $\forall \omega \in (\omega^*,\infty), \forall \boldsymbol{\zeta}(0) \in \Delta_0$ and maximal solution $\boldsymbol{\zeta} : I \to \Delta_\epsilon$ for the IVP (2.10), where $0 \in I = (t_e^-, t_e^+)$,

$$\limsup_{\tau \to t_e^+} g_i(\boldsymbol{\zeta}(\tau)) < \epsilon,\ \forall i \in \{1,2,..,r\}$$

Note that ω^* in the proof of Lemma 2.0.2 gives an estimate of the required frequency of oscillation in terms of the constants $c_1^{g_i}, c_2^{g_i}, b^{g_i}$ and a choice of $\delta \in (0,\epsilon)$. Thus, to choose a sufficiently large frequency, one needs to know the constants $c_1^{g_i}, c_2^{g_i}, b^{g_i}$. In the next lemma, we outline a procedure to estimate these constants under Assumption 2.0.1 for the static cost case. In fact, for a general dynamical system, if one can establish these bounds on the remainders, then the conclusions of Theorem 2.0.1 hold, as demonstrated by the numerical results provided above.

Lemma 2.0.3. *Consider the system (2.6) and the functions (2.4). Then, there exists constants $c_1^{g_i}, c_2^{g_i} > 0$ such that, $\forall \boldsymbol{\theta} \in \Delta_\epsilon^i, i \in \{1,2,3\}$ and $\forall t \in \mathbb{R}$:*

$$\left\|R_1^{g_i}(\boldsymbol{\theta},t)\right\| \leq \frac{c_1^{g_i}}{\sqrt{\omega}}, \quad \left\|R_2^{g_i}(\boldsymbol{\theta},t)\right\| \leq \frac{c_2^{g_i}}{\sqrt{\omega}}$$

The proofs of Theorem 2.0.1, Lemma 2.0.2, and Lemma 2.0.3 can be found in the appendix. We now give a numerical demonstration of the results presented in this chapter.

Example 2.0.1. Let $\mathbf{x} \in \mathbb{R}^2$, and consider the dynamical system

$$\dot{\mathbf{x}} = \mathbf{A}(t)(\mathbf{x} - \mathbf{x}^*) + \mathbf{B}\boldsymbol{u} \tag{2.15a}$$

$$J(\mathbf{x}, t) = \frac{3}{2}\|\mathbf{x} - \mathbf{x}^*\|^2 + 5(1 + \exp(-t)) \tag{2.15b}$$

where $\boldsymbol{u} \in \mathbb{R}^2$ is the control input, $\mathbf{x}^* = (1, -1)$, and

$$\mathbf{A}(t) = \begin{bmatrix} \cos(t)^2 & \sin(t)^2 \\ -\sin(t)^2 & \cos(t)^2 \end{bmatrix}, \quad \mathbf{B} = \begin{bmatrix} 1 & 1 \\ -1 & 1 \end{bmatrix}$$

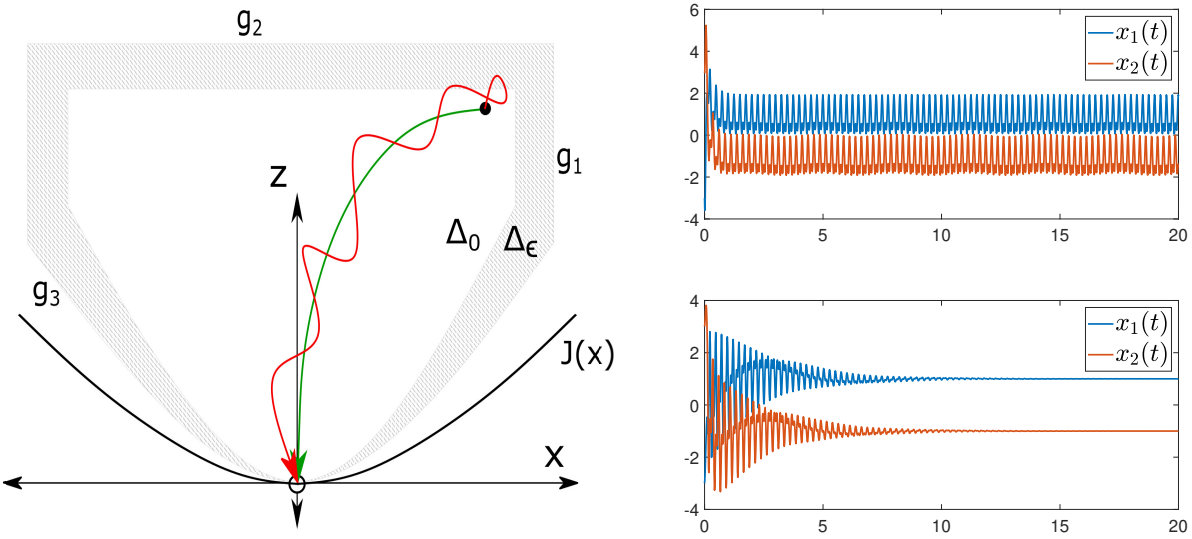

Figure 2.1: (left): Illustration of $\Delta_0, \Delta_\epsilon$ and sample trajectories, (right): Numerical results of Example 3.1 for the approach in [1] (top), and our approach (bottom)

The numerical results for the proposed control law are shown in figure 2.1 , where we used the initial conditions $\mathbf{x}(0) = (-3, 3)$, $z(0) = J(\mathbf{x}(0)) + 3 = 61$, and the frequency parameters

$\omega = 4,\ \omega_1 = 1, \omega_2 = 2.$

We remark that the proposed method can tolerate bounded monotonic decrease of the minimum value of the function as demonstrated in the provided example. However, we emphasize that it does not tolerate general time-dependent variations of the cost function in the current formulation. This is due to the nature of the dynamic upper bound on the cost function (i.e. $z(t)$).

Chapter 3

Averaging and Singular Perturbation on Multiple Time-Scales

In this chapter, we consider several situations in which the behavior of a dynamical system with a small parameter is governed by second-order effects. This situation arises when first-order effects vanish. A common feature among the systems we consider is the presence of multiple time-scales. We are interested in approximating the behavior of the system on the slowest time-scale. The main tools we employ in this chapter are: averaging, regular perturbation, and singular perturbation. In each situation, we provide explicit formulas for the vector fields that define a dynamical system whose trajectories approximate the trajectories of the original system, and a characterization of the nature of this approximation. Under a suitable trajectory approximation relation between the original system and the limit system, the stability of the limit system can be transferred to the practical stability of the original system. The approximations formulas and the theorems stated and proved in this chapter are used in subsequent chapters to study the behavior of novel source seeking algorithms and klinotaxis in microorganisms.

3.1 Convergence of Trajectories and Practical Stability

It is well known in the averaging literature that if the averaged system possesses an exponentially stable equilibrium, then the time-varying system possesses an exponentially stable periodic orbit [7, 6]. However, the requirement on exponential stability is usually strict in the sense that if only asymptotic as opposed to exponential stability is assumed then one can no longer assert the existence of a periodic orbit. This can be attributed to the method in which the existence of an orbit is established, which is typically done through the use of the implicit function theorem under the assumption that the jacobian of the averaged vector field does not drop rank near the equilibrium point [6, Theorem 6.3.2]. This requirement however is too strong when only asymptotic stability is assumed as the jacobian of the averaged vector field may indeed drop rank at the equilibrium point.

Nevertheless, if one is willing to sacrifice the assertion of the existence of a periodic orbit, the asymptotic stability of an equilibrium point for the averaged system may be transferred to a weaker notion of stability known as *practical stability*. This was first proven in [22] using advanced Lyapunov techniques. It was shown later in [23] that this transfer of stability is of a topological nature; it holds whenever the flows of two dynamical systems satisfy a certain property known as *the convergence of trajectories* property. We now give a precise definition of this property and of practical stability.

Let $\mathbf{x}, \mathbf{x}_0 \in \mathcal{D} \subset \mathbb{R}^{n_1}$ and $\varepsilon \in (0, \infty)$ and consider the system of differential equations:

$$\dot{\mathbf{x}} = \mathbf{f}(\mathbf{x}, t, \varepsilon), \qquad \mathbf{x}(t_0) = \mathbf{x}_0, \tag{3.1}$$

whose generating vector field depends on the parameter ε. Associated with the system (3.1) is the flow map $\mathbf{\Phi}^{\mathbf{f}}_t : \mathrm{Dom}(\mathbf{\Phi}^{\mathbf{f}}_t) \ni (\mathbf{x}, t, t_0) \mapsto \mathbf{\Phi}^{\mathbf{f}}_t(\mathbf{x}, t, t_0) \in \mathcal{D}$. Now consider another system

of differential equations:

$$\dot{\mathbf{x}} = \bar{\mathbf{f}}(\mathbf{x}, t), \qquad \mathbf{x}(t_0) = \mathbf{x}_0 \tag{3.2}$$

starting from the same initial condition, to which is associated the flow map $\mathbf{\Phi}_t^{\bar{\mathbf{f}}} : \mathrm{Dom}(\mathbf{\Phi}_t^{\bar{\mathbf{f}}}) \ni (\mathbf{x}, t, t_0) \mapsto \mathbf{\Phi}_t^{\bar{\mathbf{f}}}(\mathbf{x}, t, t_0) \in \mathcal{D}$.

Definition 3.1.1. *[23] The system (3.1) is said to satisfy the convergence-of-trajectories property w.r.t. the system (3.2) if: for every $T \in (0, \infty)$ and compact subset $\mathcal{K} \subset \mathcal{D}$ satisfying $\{(\mathbf{x}_0, t, t_0) \in \mathcal{D} \times \mathbb{R} \times \mathbb{R} : t \in [t_0, t_0 + T], \mathbf{x}_0 \in \mathcal{K}\} \subset \mathrm{Dom}(\mathbf{\Phi}_t^{\bar{\mathbf{f}}})$, and for every $\epsilon \in (0, \infty)$, there exists $\varepsilon^* \in (0, \infty)$ such that $\forall t_0 \in \mathbb{R}$, and $\forall \mathbf{x}_0 \in \mathcal{K}$, and $\forall \varepsilon \in (0, \varepsilon^*)$ we have that*

$$\begin{cases} \mathbf{\Phi}_t^{\mathbf{f}}(\mathbf{x}_0, t, t_0) \quad \text{exists} & \forall t \in [t_0, t_0 + T] \\ \|\mathbf{\Phi}_t^{\mathbf{f}}(\mathbf{x}_0, t, t_0) - \mathbf{\Phi}_t^{\bar{\mathbf{f}}}(\mathbf{x}_0, t, t_0)\| < \epsilon & \forall t \in [t_0, t_0 + T] \end{cases} \tag{3.3}$$

The meaning of the definition is as follows: whenever the trajectories of the system (3.2) exist for a compact set of initial conditions and compact time intervals, then the trajectories of the system (3.1) exist as well and converge to the trajectories of the system (3.2) on compact time intervals uniformly with respect to initial conditions and initial time in the limit $\varepsilon \to 0$. We now give the definition of practical stability. Let $\mathcal{S} \subset \mathcal{D} \subset \mathbb{R}^{n_1}$ be a compact subset and define the distance between a point $\mathbf{x} \in \mathcal{R}^n$ and the subset $\mathcal{S}$ to be:

$$d(\mathbf{x}, \mathcal{S}) = \inf\{\|\mathbf{x} - \mathbf{y}\|, \mathbf{y} \in \mathcal{S}\} \tag{3.4}$$

Definition 3.1.2. *The compact subset $\mathcal{S}$ is called semi-globally practically uniformly asymptotically stable (**SPUAS**) for the system (3.1) if the following conditions are satisfied:*

1. *For every $\epsilon \in (0, \infty)$, there exists $\delta \in (0, \infty)$ and $\varepsilon_0 \in (0, \infty)$ such that $\forall t_0 \in \mathbb{R}$, and*

$\forall \mathbf{x}_0 \in \mathbb{R}^{n_1}$ *with* $d(\mathbf{x}_0, \mathcal{S}) < \delta$, *and* $\forall \varepsilon \in (0, \varepsilon_0)$, *we have that:*

$$\begin{cases} \mathbf{\Phi}_t^{\mathbf{f}}(\mathbf{x}_0, t, t_0) \quad \text{exists} \qquad \forall t \in [t_0, \infty) \\ d(\mathbf{\Phi}_t^{\mathbf{f}}(\mathbf{x}_0, t, t_0), \mathcal{S}) < \epsilon \quad \forall t \in [t_0, \infty) \end{cases} \tag{3.5}$$

2. *For every* $\delta \in (0, \infty)$, *there exists* $\epsilon \in (0, \infty)$ *and* $\varepsilon_0 \in (0, \infty)$ *such that* $\forall t_0 \in \mathbb{R}$, *and* $\forall \mathbf{x}_0 \in \mathbb{R}^{n_1}$ *with* $d(\mathbf{x}_0, \mathcal{S}) < \delta$, *and* $\forall \varepsilon \in (0, \varepsilon_0)$, *we have that:*

$$\begin{cases} \mathbf{\Phi}_t^{\mathbf{f}}(\mathbf{x}_0, t, t_0) \quad \text{exists} \qquad \forall t \in [t_0, \infty) \\ d(\mathbf{\Phi}_t^{\mathbf{f}}(\mathbf{x}_0, t, t_0), \mathcal{S}) < \epsilon \quad \forall t \in [t_0, \infty) \end{cases} \tag{3.6}$$

3. *For every* $\delta \in (0, \infty)$, *and every* $\epsilon \in (0, \infty)$, *there exists* $T \in (0, \infty)$ *and* $\varepsilon_0 \in (0, \infty)$ *such that* $\forall t_0 \in \mathbb{R}$, *and* $\forall \mathbf{x}_0 \in \mathbb{R}^{n_1}$ *with* $d(\mathbf{x}_0, \mathcal{S}) < \delta$, *and* $\forall \varepsilon \in (0, \varepsilon_0)$, *we have that:*

$$\begin{cases} \mathbf{\Phi}_t^{\mathbf{f}}(\mathbf{x}_0, t, t_0) \quad \text{exists} \qquad \forall t \in [t_0, \infty) \\ d(\mathbf{\Phi}_t^{\mathbf{f}}(\mathbf{x}_0, t, t_0), \mathcal{S}) < \epsilon \quad \forall t \in [t_0 + T, \infty) \end{cases} \tag{3.7}$$

When the subset $\mathcal{S}$ satisfies Definition 3.1.2 independently from $\varepsilon \in (0, \infty)$, it is said that the subset $\mathcal{S}$ is *globally uniformly asymptotically stable (**GUAS**)* for the system (3.1) [3]. Having introduced Definition 3.1.1 and Definition 3.1.2, we are now ready to state the following theorem:

Theorem 3.1.1. *[3, 23] Suppose that the system (3.1) satisfies the convergence-of-trajectories property w.r.t. the system (3.2), and that* $\mathcal{S} \subset \mathbb{R}^{n_1}$ *is a compact GUAS set for the system (3.2). Then, the subset* $\mathcal{S}$ *is a SPUAS set for the system (3.1).*

The proof of this theorem can be found in [3]. In the following section, we will use higher order averaging to establish the convergence-of-trajectories property for a class of highly oscillatory systems with multiple scales. Then, by employing Theorem 3.1.1, we transfer the

stability properties of the averaged system to the practical stability of the original system under consideration.

3.2 Recursive Averaging

In this section, we consider the situation when a finite dimensional dynamical system contains two fast periodic time-scales in addition to the slowest time-scale. Specifically, we consider the class of systems that can be written on the form:

$$\dot{\mathbf{x}} = \sum_{k=1}^{2} \varepsilon^{k-2} \mathbf{f}_k(\mathbf{x}, t, \varepsilon^{-1}t, \varepsilon^{-2}t) + O(\varepsilon), \qquad \mathbf{x}(t_0) = \mathbf{x}_0 \tag{3.8}$$

We make the following assumption on the right hand side of equation (3.8):

Assumption 3.2.1. *The time-varying vector fields* $\mathbf{f}_k,\ k \in \{1, 2\}$ *are such that:*

A1 $\mathbf{f}_k(\cdot,\cdot,\cdot,\tau) \in \mathcal{C}^{3-k}(\mathbb{R}^{n+2};\mathbb{R}^{n_1})$, $\forall \tau \in \mathbb{R}$, $\mathbf{f}_k(\cdot,\cdot,\cdot,\cdot) \in \mathcal{C}^0(\mathbb{R}^{n+3};\mathbb{R}^{n_1})$

A3 $\mathbf{f}_k$ *is uniformly bounded in its second argument*

A4 $\exists T_1 > 0$ *s.t.* $\mathbf{f}_k(\cdot,\cdot,\sigma+T_1,\cdot) = \mathbf{f}_k(\cdot,\cdot,\sigma,\cdot)\ \forall \sigma \in \mathbb{R}$

A5 $\exists T_2 > 0$ *s.t.* $\mathbf{f}_k(\cdot,\cdot,\cdot,\tau+T_2) = \mathbf{f}_k(\cdot,\cdot,\cdot,\tau)\ \forall \tau \in \mathbb{R}$

A6 $\int_0^{T_1} \mathbf{f}_1(\cdot,\cdot,\cdot,\tau)d\tau = 0$

We note that assumptions of this nature are typical in the averaging literature [15]. Moreover, aside from some technical regularity conditions, the class of systems (3.8) includes as a special case the class of systems considered in the Lie Bracket Approximation framework and the second-order case in Sussmann and Liu's framework [5, 20, 19] when: i) the vector field $\mathbf{f}_1$ is independent from the time-scale $\varepsilon^{-1}t$ and can be decomposed as $\mathbf{f}_1(\mathbf{x}, t, \sigma, \tau) =$

$\sum_{\ell=1}^{r} \mathbf{b}_\ell(\mathbf{x},t)u_\ell(t,\tau)$ for some functions u_ℓ that are T-periodic in the second argument and some vector fields $\mathbf{b}_\ell$, and ii) the vector field $\mathbf{f}_2$ is independent from the fast periodic time scales $\varepsilon^{-1}t$ and $\varepsilon^{-2}t$. We show that the higher-order averaging method is directly applicable to this class of systems in contrast to the belief that it is not (see the discussion in [3, Section 5]).

Due to item A6 in Assumption 3.2.1, first order averaging does not yield any useful information about the average behavior of this system. It is, therefore, imperative to consider higher-order averages. For our purposes, second-order averaging suffices. Consider the system:

$$\dot{\bar{\bar{\mathbf{x}}}} = \bar{\bar{\mathbf{f}}}(\bar{\bar{\mathbf{x}}},t), \qquad \bar{\bar{\mathbf{x}}}(t_0) = \mathbf{x}_0 \tag{3.9}$$

where the time-varying vector field $\bar{\bar{\mathbf{f}}}$ is given by:

$$\bar{\bar{\mathbf{f}}}(\mathbf{x},t) = \frac{1}{T_1T_2}\int_0^{T_1}\int_0^{T_2}\left(\mathbf{f}_2(\mathbf{x},t,\sigma,\tau) + \frac{1}{2}\left[\int_0^{\tau}\mathbf{f}_1(\mathbf{x},t,\sigma,\nu)\,d\nu, \mathbf{f}_1(\mathbf{x},t,\sigma,\tau)\right]\right)d\tau\,d\sigma \tag{3.10}$$

Then, we have the following theorem concerning the relation between the trajectories of the systems (3.8) and (3.9):

Theorem 3.2.1. *Let a nonempty compact subset $\mathcal{K} \subset \mathbb{R}^{n_1}$ and a final time $t_f > 0$ be such that a unique trajectory $\bar{\bar{\mathbf{x}}} : [t_0, t_0+t_f] \ni t \mapsto \bar{\bar{\mathbf{x}}}(t) \in \mathbb{R}^{n_1}$ of the system (3.9) exists $\forall \mathbf{x}_0 \in \mathcal{K}$, $\forall t_0 \in \mathbb{R}$. Then $\exists \varepsilon^* \in (0,\infty)$ and a constant $C > 0$ independent of $\varepsilon \in (0,\varepsilon^*)$ such that $\forall \varepsilon \in (0,\varepsilon^*)$, $\forall \mathbf{x}_0 \in \mathcal{K}$, $\forall t_0 \in \mathbb{R}$, a unique trajectory of the system (3.8) exists and satisfies:*

$$\|\mathbf{x}(t) - \bar{\bar{\mathbf{x}}}(t)\| \leq C\,\varepsilon, \qquad \forall t \in [t_0, t_0+t_f] \tag{3.11}$$

Observe that we have not made any mention of the near-identity transforms. This is due to the fact the $O(\varepsilon)$ terms in the standard averaging procedure vanish, and so the contribution of the near-identity transform to the accuracy of the solution is of the same order as the neglected remainders in the averaging procedure, i.e. $O(\varepsilon)$. We refer the reader to [27] and the discussion in [6, Subsection 2.9.2] for more details.

Next, we have the following theorem which characterizes the relation between the stability of the averaged system (3.9) and the original system (3.8):

Theorem 3.2.2. *Suppose that a compact subset $\mathcal{S} \subset \mathbb{R}^{n_1}$ is GUAS for the system (3.9). Then the subset $\mathcal{S}$ is SPUAS for the system (3.8).*

Proof. The proof of this theorem follows from Theorem 3.1.1 [23, Theorem 1], provided that the vector fields defining the two systems (3.8) and (3.9) possess the local existence and uniqueness of trajectories property and the flow of (3.8) satisfies the convergence-of-trajectories property w.r.t. the flow of (3.9). Local existence and uniqueness of trajectories follows from Assumption 3.2.1, whereas Theorem 3.2.1 establishes the convergence-of-trajectories property. □

As a direct application of the theorem above, we consider the problem of steering a $6n$-dimensional driftless control-affine system towards the optimum of an objective function using extremum seeking. Traditional extremum seeking design [2] and Lie-Bracket based extremum seeking [3] require choosing $6n$ non-resonating frequencies on the time-scale ωt to estimate the gradient. Using a special feature of the extremum seeking vector fields introduced in [28], only $3n$ non-resonating frequencies are required. However, using the methods introduced in this section, only n frequencies can be used to steer the system.

Example 3.2.1. Let $n \geq 1$, $\mathbf{x} \in \mathbb{R}^{6n}$, $\mathbf{u} \in \mathbb{R}^{6n}$, and $J(\mathbf{x})$ be the objective function, then

consider the following driftless control-affine system:

$$\dot{\mathbf{x}} = \sum_{j=1}^{6} \sum_{k=1}^{n} \mathbf{f}_{j,k}(\mathbf{x}, t)\, u_{j,k} \tag{3.12}$$

It is required to design the control inputs $u_{j,k}$ to steer the system towards the extremum of the objective function $J(\mathbf{x})$. Consider the following time-varying output feedback control for $k \in \{1, \ldots, n\}$:

$$u_{1,k} = \varepsilon^{-1}\sqrt{2}\, \cos(\omega_k \varepsilon^{-2} t - J(\mathbf{x})), \tag{3.13a}$$

$$u_{2,k} = \varepsilon^{-1}\sqrt{2}\, \sin(\omega_k \varepsilon^{-2} t - J(\mathbf{x})), \tag{3.13b}$$

$$u_{3,k} = \varepsilon^{-1}\sqrt{4}\, \cos(\omega_k \varepsilon^{-2} t - J(\mathbf{x}))\cos(\varepsilon^{-1} t), \tag{3.13c}$$

$$u_{4,k} = \varepsilon^{-1}\sqrt{4}\, \sin(\omega_k \varepsilon^{-2} t - J(\mathbf{x}))\cos(\varepsilon^{-1} t), \tag{3.13d}$$

$$u_{5,k} = \varepsilon^{-1}\sqrt{4}\, \cos(\omega_k \varepsilon^{-2} t - J(\mathbf{x}))\sin(\varepsilon^{-1} t), \tag{3.13e}$$

$$u_{6,k} = \varepsilon^{-1}\sqrt{4}\, \sin(\omega_k \varepsilon^{-2} t - J(\mathbf{x}))\sin(\varepsilon^{-1} t), \tag{3.13f}$$

where $\omega_k \in \mathbb{Q}_+$ are positive rational numbers such that $\omega_{k_1} \neq \omega_{k_2}$ whenever $k_1 \neq k_2$. Then, a direct application of Theorem 3.2.1 in the limit $\varepsilon \to 0$ leads to the averaged system:

$$\dot{\bar{\bar{\mathbf{x}}}} = \mathbf{P}(\bar{\bar{\mathbf{x}}}, t) \nabla J(\bar{\bar{\mathbf{x}}}) \tag{3.14}$$

where the matrix $\mathbf{P}(\bar{\bar{\mathbf{x}}}, t)$ is a positive semi-definite matrix. If, in addition to sufficient regularity and boundedness assumptions, the driftless control system (3.12) is such that the span of the vector fields $\mathbf{f}_{j,k}$ is the entire tangent space $\mathbb{R}^{6n}$ everywhere in the manifold, and the objective function $J(\mathbf{x})$ is sufficiently smooth and possesses a compact maximizing set $\mathcal{S}$, then we may conclude that the subset $\mathcal{S}$ is GUAS for the system (3.14). Hence, we may also conclude using Theorem 3.2.1 and Theorem 3.1.1 that the subset $\mathcal{S}$ is SPUAS for the system (3.12). We observe that only n non-resonating frequencies $\{\omega_k\}_{k \in \{1,\ldots,n\}}$ are used on

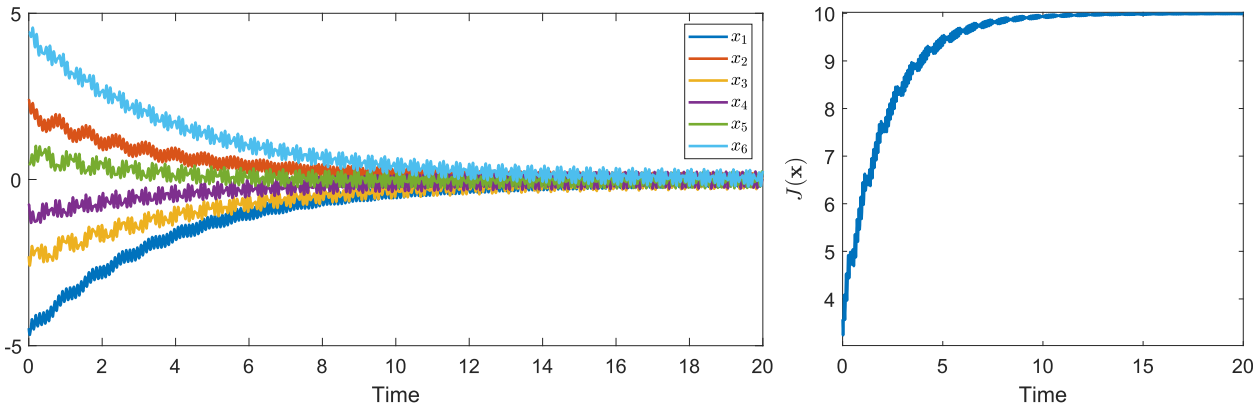

Figure 3.1: Numerical simulation results of Example 3.2.1.

the fast time-scale $\varepsilon^{-2}t$, whereas in any other method in the literature [3, 2, 28] at least *three* distinct frequencies must be used on the fast time-scale $\varepsilon^{-2}t$. Intuitively, the results of this section allow transferring the non-resonance requirement between the dithers used in extremum seeking to the intermediate time-scale $\varepsilon^{-1}t$.

We now give numerical simulation results for illustration. Suppose that $n = 1$, $J(\mathbf{x}) = 10 - 0.125\|\mathbf{x}\|^2$, and that the vector fields $\mathbf{f}_{j,1}$ are the canonical orthonormal basis on $\mathbb{R}^6$. Let $\omega_1 = 1$, $\varepsilon = 1/\sqrt{20\pi} \approx 0.126$, and apply the control inputs defined by (3.13). The trajectory of the system (3.12) with the control inputs (3.13) along with the time history of the objective function for a randomly generated initial condition are shown in Figure 3.1. We observe how the trajectories of the system converge to a small neighborhood around the origin which is the maximizer for the objective function $J(\mathbf{x})$.

Another application of the results in this section will be presented in the next chapter when we tackle the problem of 3D source seeking.

3.3 First-Order Singularly Perturbed Averaging

We now tackle the situation in which, in addition to the fast periodic time-scale, a part of the system state is singularly perturbed. That is, a part of the system state, henceforth referred to as the fast state, quickly converges to an equilibrium manifold parameterized by the slow state and (possibly) the fast time-scale. In such a situation, the averaged behavior of the slow state is affected by the fast periodic behavior (if any) of the equilibrium manifold. In this section, we consider the situation in which this interaction takes place to first-order. In the next section, we consider the situation in which such an interaction vanishes to first-order and it becomes necessary to consider second-order interactions.

Let $\mathbf{x}_1 \in \mathbb{R}^{n_1}, \mathbf{x}_2 \in \mathbb{R}^{n_2}$, and consider the following interconnected system:

$$\dot{\mathbf{x}}_1 = \mathbf{f}_{1,2}(\mathbf{x}_1, \mathbf{x}_2, t, \varepsilon^{-1}t) + O(\varepsilon), \qquad \mathbf{x}_1(t_0) = \mathbf{x}_{1,0} \tag{3.15a}$$

$$\dot{\mathbf{x}}_2 = \sum_{k=1}^{2} \varepsilon^{k-2} \mathbf{f}_{2,k}(\mathbf{x}_1, \mathbf{x}_2, t, \varepsilon^{-1}t) + O(\varepsilon), \qquad \mathbf{x}_2(t_0) = \mathbf{x}_{2,0} \tag{3.15b}$$

Suppose that the following assumption is satisfied:

Assumption 3.3.1. *Suppose that there exists a unique and sufficiently smooth map $\boldsymbol{\phi}_0(\mathbf{x}_1, t, \sigma)$ and a positive number $T_1 > 0$ such that the vector fields $\mathbf{f}_{j,k}$ are sufficiently smooth in all their arguments and T_1-periodic in the last argument, and that:*

$$\mathbf{f}_{2,1}(\mathbf{x}_1, \boldsymbol{\phi}_0(\mathbf{x}_1, t, \sigma), t, \sigma) = 0 \tag{3.16a}$$

$$\boldsymbol{\phi}_0(\mathbf{x}_1, t, \sigma + T_1) - \boldsymbol{\phi}_0(\mathbf{x}_1, t, \sigma) = 0 \tag{3.16b}$$

Moreover, let $\mathbf{y}_2 \in \mathbb{R}^{n_2}$, and

$$\tilde{\mathbf{f}}_{2,1}(\mathbf{x}_1, \mathbf{y}_2, t, \sigma) = \mathbf{f}_{2,1}(\mathbf{x}_1, \mathbf{y}_2 + \boldsymbol{\phi}_0(\mathbf{x}_1, t, \sigma), t, \sigma) - \partial_\sigma \boldsymbol{\phi}_0(\mathbf{x}_1, t, \sigma), \tag{3.17}$$

and suppose that there exists a Lyapunov function V and constants $\kappa_i > 0$ for $i \in \{1, \ldots, 4\}$ such that the inequalities:

$$\kappa_1 \|\mathbf{y}_2\|^2 \leq V(\mathbf{y}_2, \sigma) \leq \kappa_2 \|\mathbf{y}_2\|^2 \tag{3.18a}$$

$$\partial_2 V(\mathbf{y}_2, \sigma) + \partial_1 V(\mathbf{y}_2, \sigma) \tilde{\mathbf{f}}_{2,1}(\mathbf{x}_1, \mathbf{y}_2, t, \sigma) \leq -\kappa_3 \|\mathbf{y}_2\|^2 \tag{3.18b}$$

$$\|\partial_1 V(\mathbf{y}_2, \sigma)\| \leq \kappa_4 \|\mathbf{y}_2\| \tag{3.18c}$$

are satisfied globally in $\mathbf{y}_2$, uniformly in $t, \sigma, \mathbf{x}_1$.

In addition, consider the reduced-order averaged system:

$$\dot{\bar{\mathbf{x}}} = \bar{\mathbf{f}}(\bar{\mathbf{x}}, t), \qquad \bar{\mathbf{x}}(t_0) = \mathbf{x}_{1,0} \tag{3.19}$$

where the vector field $\bar{\mathbf{f}}$ is defined by:

$$\bar{\mathbf{f}}(\bar{\mathbf{x}}_1, t) = \frac{1}{T_1} \int_0^{T_1} \tilde{\mathbf{f}}_{1,2}(\bar{\mathbf{x}}_1, \boldsymbol{\phi}_0(\bar{\mathbf{x}}_1, t, \nu), t, \nu)\, d\nu \tag{3.20}$$

Then, we have the following lemma concerning the relation between the trajectories of the reduced order averaged system (3.19) to the trajectories of the original system (3.15).

Theorem 3.3.1. *Let Assumption* 3.3.1 *be satisfied, and let $\mathcal{B}_2 \subset \mathbb{R}^{n_2}$ be arbitrary but bounded and $D \in (0, \infty)$ be arbitrary. In addition, let a bounded subset $\mathcal{B}_1 \subset \mathbb{R}^{n_1}$, a compact subset $\mathcal{N} \subset \mathbb{R}^{n_1}$, and a positive constant $L \in (0, \infty)$ be such that unique trajectories $\bar{\mathbf{x}}_1(t; t_0, \mathbf{x}_{1,0})$ for the system (3.19) exist and $\bar{\mathbf{x}}_1(t; t_0, \mathbf{x}_{1,0}) \in \mathcal{N}$, $\forall t \in [t_0, t_0 + L]$, $\forall t_0 \in \mathbb{R}$, $\forall \mathbf{x}_{1,0} \in \mathcal{B}_1$. Then, $\exists \varepsilon^* \in (0, \varepsilon_0)$ and positive constants $\lambda_\sigma, \gamma_\sigma$ such that $\forall t_0 \in \mathbb{R}$, $\forall (\mathbf{x}_{1,0}, \mathbf{x}_{2,0} - \boldsymbol{\phi}_0(\mathbf{x}_{1,0}, t_0, t_0)) \in \mathcal{B}_1 \times \mathcal{B}_2$, $\forall t \in [t_0, t_0 + L]$, $\forall \varepsilon \in (0, \varepsilon^*)$, and $\sigma = \varepsilon^{-1}(t - t_0) + t_0$, unique trajectories $(\mathbf{x}_1(t; t_0, \mathbf{x}_{1,0}), \mathbf{x}_2((t; t_0, \mathbf{x}_{2,0}))$ for the system (3.15) exist and satisfy the estimates:*

$$\|\mathbf{x}_1(t;t_0,\mathbf{x}_{1,0}) - \bar{\mathbf{x}}_1(t;t_0,\mathbf{x}_{1,0})\| < D \tag{3.21a}$$

$$\|\mathbf{x}_2(t;t_0,\mathbf{x}_{1,0}) - \boldsymbol{\phi}_0(\bar{\mathbf{x}}_1(t;t_0,\mathbf{x}_{1,0}),t,\sigma)\| < \gamma_\sigma \|\mathbf{x}_{2,0} - \boldsymbol{\phi}_0(\mathbf{x}_{1,0},t_0,t_0)\| \mathrm{e}^{-\lambda_\sigma(\sigma-t_0)} + D \tag{3.21b}$$

This lemma provides a direct relation between the trajectories of the system (3.15) and the trajectories of the reduced order averaged system (3.19). In particular, it establishes a singularly perturbed version of the convergence-of-trajectories property given in Definition 3.1.1, which allows transferring the stability properties of the reduced order averaged system (3.19) to a singularly perturbed version of practical stability. We now give a precise definition of singular practical stability:

Definition 3.3.1. *The set $\mathcal{S}$ is said to be singularly semi-globally practically uniformly asymptotically stable (**sSPUAS**) for system (3.15) if the following is satisfied:*

1. $\forall \epsilon_1, \epsilon_2 \in (0,\infty)$ there exists $\delta_1, \delta_2 \in (0,\infty)$ and $\varepsilon^* \in (0,\infty)$ such that $\forall \varepsilon \in (0,\varepsilon^*)$, $\forall t_0 \in \mathbb{R}$, and $\forall t \in [t_0,\infty)$ we have:

$$\left.\begin{aligned} \mathbf{x}_{1,0} &\in \mathcal{U}^{\mathcal{S}}_{\delta_x} \\ \mathbf{x}_{2,0} - \boldsymbol{\phi}_0(\mathbf{x}_{1,0},t_0) &\in \mathcal{U}^0_{\delta_z} \end{aligned}\right\} \implies \left\{\begin{aligned} \mathbf{x}_1(t) &\in \mathcal{U}^{\mathcal{S}}_{\epsilon_x} \\ \mathbf{x}_2(t) - \boldsymbol{\phi}_0(\mathbf{x}_1(t),t) &\in \mathcal{U}^0_{\epsilon_z} \end{aligned}\right.$$

2. $\forall \epsilon_1, \epsilon_2 \in (0,\infty)$ and all $\delta_1, \delta_2 \in (0,\infty)$, there exists a time $t_f \in (0,\infty)$ and $\varepsilon^* \in (0,\infty)$ such that $\forall \varepsilon \in (0,\varepsilon^*)$, $\forall t_0 \in \mathbb{R}$, $\forall t_1 \in [t_0+t_f,\infty)$, and $\forall t_2 \in [t_0+t_f\eta(\varepsilon),\infty)$ we have:

$$\left.\begin{aligned} \mathbf{x}_{1,0} &\in \mathcal{U}^{\mathcal{S}}_{\delta_1} \\ \mathbf{x}_{2,0} - \boldsymbol{\phi}_0(\mathbf{x}_{1,0},t_0) &\in \mathcal{U}^0_{\delta_2} \end{aligned}\right\} \implies \left\{\begin{aligned} \mathbf{x}_1(t_1) &\in \mathcal{U}^{\mathcal{S}}_{\epsilon_1} \\ \mathbf{x}_2(t_2) - \boldsymbol{\phi}_0(\mathbf{x}(t_2),t_2) &\in \mathcal{U}^0_{\epsilon_2} \end{aligned}\right.$$

   where $\eta(\varepsilon)$ is such that $\lim_{\varepsilon\to 0}\eta(\varepsilon) = 0$.

3. $\forall \delta_1, \delta_2 \in (0, \infty)$ there exists $\epsilon_1, \epsilon_2 \in (0, \infty)$ and $\varepsilon^* \in (0, \infty)$ such that $\forall \varepsilon \in (0, \varepsilon^*)$, $\forall t_0 \in \mathbb{R}$, and $\forall t \in [t_0, \infty)$ we have:

$$\left.\begin{aligned} \mathbf{x}_{1,0} &\in \mathcal{U}^{\mathcal{S}}_{\delta_1} \\ \mathbf{x}_{2,0} - \boldsymbol{\phi}_0(\mathbf{x}_{1,0}, t_0) &\in \mathcal{U}^0_{\delta_2} \end{aligned}\right\} \implies \begin{cases} \mathbf{x}_1(t) \in \mathcal{U}^{\mathcal{S}}_{\epsilon_1} \\ \mathbf{x}_2(t) - \boldsymbol{\phi}_0(\mathbf{x}_1(t), t) \in \mathcal{U}^0_{\epsilon_2} \end{cases}$$

Having stated definition Definition 3.3.1, we are now ready to state the following theorem:

Theorem 3.3.2. *Let Assumption* 3.3.1 *be satisfied and suppose that the compact subset $\mathcal{S}$ is GUAS for the system (3.19). Then, the subset $\mathcal{S}$ is sSPUAS for the system (3.15).*

A version of Theorem 3.3.1 appears in [29] under different assumptions. In the next section, we extend the analysis above and the corresponding theorem to second-order behavior.

3.4 Second-Order Singularly Perturbed Averaging

We now analyze a class of singularly perturbed high-frequency, high-amplitude oscillatory systems in which the first-order effects vanish and it becomes necessary to account for second-order effects. To capture the behavior of this class of systems, we must account for the interaction between the fast periodic time scale and the singularly perturbed part of the system. We begin the discussion with a simple example to elucidate the motivation behind our results. Consider the interconnected system:

$$\frac{dx_1}{d\tau} = \mu\beta x_1 + \mu\sqrt{2\omega}\sin(x_1^2 + 4(x_4 - x_3) + \omega\mu\tau) \tag{3.22a}$$

$$\frac{dx_2}{d\tau} = \mu\beta x_2 + \mu\sqrt{2\omega}\cos(x_1^2 + 4(x_4 - x_3) + \omega\mu\tau) \tag{3.22b}$$

$$\frac{dx_3}{d\tau} = x_4 - x_3, \qquad \frac{dx_4}{d\tau} = x_2^2 - x_4 \tag{3.22c}$$

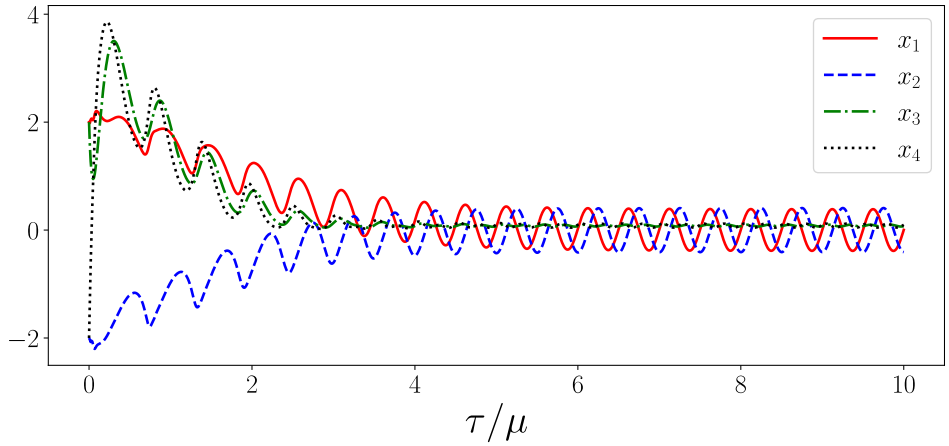

Figure 3.2: Numerical results for the motivational example. The initial condition is taken as $(-2, 2, 2, 2)$, and the parameters are $\beta = 1/2$, $\omega = 4\pi$ and $\mu = 1/(4\pi)$.

with an initial condition $(x_{1,0}, x_{2,0}, x_{3,0}, x_{4,0}) \in \mathbb{R}^4$, where β is fixed and positive, and μ and ω are positive parameters. Observe that the system (3.22) has the same form as the class of systems considered in [4]. If we attempt to apply the results in [4], we obtain the quasi-steady state $(x_3, x_4) = \boldsymbol{\varphi}_0(x_1, x_2) = (x_2^2, x_2^2)$ for the singularly perturbed part of the system. Hence, the reduced order system according to [4] becomes:

$$\frac{dx_1}{d\tau} = \beta x_1 + \sqrt{2\omega}\sin(x_1^2 + \omega\tau) \tag{3.23a}$$

$$\frac{dx_2}{d\tau} = \beta x_2 + \sqrt{2\omega}\cos(x_1^2 + \omega\tau) \tag{3.23b}$$

$$x_3 = x_2^2, \qquad x_4 = x_2^2 \tag{3.23c}$$

It is clear that the system (3.23) has no practically asymptotically stable subsets for any value of ω, and so the results in [4] are not useful here. However, numerical simulations shown in Figure 3.2 demonstrate that the original system (3.22) exhibits practical stability. The intuitive reason why this stable behavior is not captured by the singularly perturbed Lie Bracket Approximation framework [4] is that the latter neglects the interaction between the singularly perturbed part of the system and the fast periodic time-scale. We shall return to this motivational example after formulating a general result.

Consider the interconnected system:

$$\dot{\mathbf{x}}_1 = \sum_{k=1}^{2} \varepsilon^{k-2} \mathbf{f}_{1,k}(\mathbf{x}_1, \mathbf{x}_2, t, \varepsilon^{-2} t), \qquad \mathbf{x}_1(t_0) = \mathbf{x}_{1,0} \tag{3.24a}$$

$$\dot{\mathbf{x}}_2 = \sum_{k=0}^{2} \varepsilon^{k-2} \mathbf{f}_{2,k}(\mathbf{x}_1, \mathbf{x}_2, t, \varepsilon^{-2} t), \qquad \mathbf{x}_2(t_0) = \mathbf{x}_{2,0} \tag{3.24b}$$

where $\mathbf{x}_1, \mathbf{x}_{1,0} \in \mathbb{R}^{n_1}$, $\mathbf{x}_2, \mathbf{x}_{2,0} \in \mathbb{R}^{n_2}$, $t \geq 0$, and $\varepsilon \in (0, \infty)$. We adopt the following assumptions on the regularity of the right-hand side of the equations (3.24):

Assumption 3.4.1. *Suppose that there exists a unique and sufficiently smooth map $\boldsymbol{\varphi}_0(\mathbf{x}_1, t)$ and a positive number $T_2 > 0$ such that the vector fields $\mathbf{f}_{j,k}$ are sufficiently smooth in all their arguments and T_2-periodic in the last argument, and that:*

$$\mathbf{f}_{2,1}(\mathbf{x}_1, \boldsymbol{\varphi}_0(\mathbf{x}_1, t), t, \tau) = 0 \tag{3.25}$$

Moreover, let $\mathbf{y}_2 \in \mathbb{R}^{n_2}$, and

$$\tilde{\mathbf{f}}_{2,0}(\mathbf{x}_1, \mathbf{y}_2, t, \tau) = \mathbf{f}_{2,0}(\mathbf{x}_1, \mathbf{y}_2 + \boldsymbol{\varphi}_0(\mathbf{x}_1, t), t, \tau) \tag{3.26}$$

and suppose that there exists a Lyapunov function V and constants $\kappa_i > 0$ for $i \in \{1, \ldots, 4\}$ such that the inequalities:

$$\kappa_1 \|\mathbf{y}_2\|^2 \leq V(\mathbf{y}_2, \tau) \leq \kappa_2 \|\mathbf{y}_2\|^2 \tag{3.27a}$$

$$\partial_2 V(\mathbf{y}_2, \tau) + \partial_1 V(\mathbf{y}_2, \tau) \tilde{\mathbf{f}}_{2,0}(\mathbf{x}_1, \mathbf{y}_2, t, \tau) \leq -\kappa_3 \|\mathbf{y}_2\|^2 \tag{3.27b}$$

$$\|\partial_1 V(\mathbf{y}_2, \tau)\| \leq \kappa_4 \|\mathbf{y}_2\| \tag{3.27c}$$

are satisfied globally in $\mathbf{y}_2$, uniformly in $t, \tau, \mathbf{x}_1$.

In addition, consider the reduced order system:

$$\dot{\tilde{\mathbf{x}}}_1 = \sum_{k=1}^{2} \varepsilon^{k-2}\, \tilde{\mathbf{f}}_k(\tilde{\mathbf{x}}_1, t, \varepsilon^{-2}t), \qquad \tilde{\mathbf{x}}_1(t_0) = \mathbf{x}_{1,0}, \tag{3.28}$$

where the time-varying vector fields $\tilde{\mathbf{f}}_k$ are defined by:

$$\tilde{\mathbf{f}}_1(\mathbf{x}_1, t, \tau) = \mathbf{f}_{1,1}(\mathbf{x}_1, \boldsymbol{\varphi}_0(\mathbf{x}_1, t), t, \tau), \tag{3.29a}$$

$$\tilde{\mathbf{f}}_2(\mathbf{x}_1, t, \tau) = \mathbf{f}_{1,2}(\mathbf{x}_1, \boldsymbol{\varphi}_0(\mathbf{x}_1, t), t, \tau) + \partial_2 \mathbf{f}_{1,1}(\mathbf{x}_1, \boldsymbol{\varphi}_0(\mathbf{x}_1, t), t, \tau)\boldsymbol{\varphi}_1(\mathbf{x}_1, t, \tau), \tag{3.29b}$$

$$\boldsymbol{\varphi}_1(\mathbf{x}_1, t, \tau) = \big(\mathbf{I} - \boldsymbol{\Phi}_{\mathbf{A}_{\boldsymbol{\varphi}}}(\tau + T_2, \tau)\big)^{-1} \int_{\tau}^{\tau+T_2} \boldsymbol{\Phi}_{\mathbf{A}_{\boldsymbol{\varphi}}}(\tau + T_2, \nu)\mathbf{b}_{\boldsymbol{\varphi}}(\mathbf{x}_1, t, \nu)\, d\nu, \tag{3.29c}$$

$$\mathbf{b}_1(\mathbf{x}_1, t, \tau) = \mathbf{f}_{2,1}(\mathbf{x}_1, \boldsymbol{\varphi}_0(\mathbf{x}_1, t), t, \tau) - \partial_1 \boldsymbol{\varphi}_0(\mathbf{x}_1, t)\, \mathbf{f}_{1,1}(\mathbf{x}_1, \boldsymbol{\varphi}_0(\mathbf{x}_1, t), t, \tau), \tag{3.29d}$$

the matrix-valued map $\mathbf{A}_{\boldsymbol{\varphi}}$ is defined by:

$$\mathbf{A}_{\boldsymbol{\varphi}}(\mathbf{x}_1, t, \tau) = \partial_2 \mathbf{f}_{2,0}(\mathbf{x}_1, \boldsymbol{\varphi}_0(\mathbf{x}_1, t), t, \tau), \tag{3.30}$$

and the matrix-valued map $\boldsymbol{\Phi}_{\mathbf{A}_{\boldsymbol{\varphi}}}$ is the fundamental matrix associated with the linear time-periodic system:

$$\frac{d\mathbf{y}_2}{d\tau} = \mathbf{A}_{\boldsymbol{\varphi}}(\cdot, \tau)\mathbf{y}_2, \tag{3.31}$$

The second order averaging theorem may be applied [30, 6] to the reduced order system (3.28) to obtain the reduced order averaged system:

$$\dot{\bar{\mathbf{x}}}_1 = \bar{\mathbf{f}}(\bar{\mathbf{x}}_1, t), \qquad \bar{\mathbf{x}}_1(t_0) = \mathbf{x}_{1,0} \tag{3.32}$$

where the vector field $\bar{\mathbf{f}}$ is given by:

$$\bar{\mathbf{f}}(\mathbf{x}_1, t) = \frac{1}{T_2} \int_0^{T_2} \left(\tilde{\mathbf{f}}_2(\mathbf{x}_1, t, \tau) + \frac{1}{2} \left[\int_0^{\tau} \tilde{\mathbf{f}}_1(\mathbf{x}_1, t, \nu)\, d\nu, \tilde{\mathbf{f}}_1(\mathbf{x}_1, t, \tau) \right] \right) d\tau \tag{3.33}$$

Then, we have the following trajectory approximation result between the original system (3.24) and the reduced order averaged system (3.32):

Theorem 3.4.1. *Let Assumption* 3.4.1 *be satisfied, and let* $\mathcal{B}_2 \subset \mathbb{R}^{n_2}$ *be arbitrary but bounded and* $D \in (0, \infty)$ *be arbitrary. In addition, let a bounded subset* $\mathcal{B}_1 \subset \mathbb{R}^{n_1}$*, a compact subset* $\mathcal{N} \subset \mathbb{R}^{n_1}$*, and a positive constant* $L \in (0, \infty)$ *be such that unique trajectories* $\bar{\mathbf{x}}_1(t; t_0, \mathbf{x}_{1,0})$ *for the system (3.32) exist and* $\bar{\mathbf{x}}_1(t; t_0, \mathbf{x}_{1,0}) \in \mathcal{N}$*,* $\forall t \in [t_0, t_0 + L]$*,* $\forall t_0 \in \mathbb{R}$*,* $\forall \mathbf{x}_{1,0} \in \mathcal{B}_1$*. Then,* $\exists \varepsilon^* \in (0, \varepsilon_0)$ *and positive constants* $\lambda_\tau, \gamma_\tau$ *such that* $\forall t_0 \in \mathbb{R}$*,* $\forall (\mathbf{x}_{1,0}, \mathbf{x}_{2,0} - \boldsymbol{\varphi}_0(\mathbf{x}_{1,0}, t_0, t_0)) \in \mathcal{B}_1 \times \mathcal{B}_2$*,* $\forall t \in [t_0, t_0 + L]$*,* $\forall \varepsilon \in (0, \varepsilon^*)$*, and* $\tau = \varepsilon^{-2}(t - t_0) + t_0$*, unique trajectories* $(\mathbf{x}_1(t; t_0, \mathbf{x}_{1,0}), \mathbf{x}_2(t; t_0, \mathbf{x}_{2,0}))$ *for the system (3.24) exist and satisfy the estimates:*

$$\|\mathbf{x}_1(t) - \bar{\mathbf{x}}_1(t)\| < D \tag{3.34}$$

$$\|\mathbf{x}_2(t) - \boldsymbol{\varphi}_0(\mathbf{x}_1(t), t)\| < \gamma_\tau \|\mathbf{x}_{2,0} - \boldsymbol{\varphi}_0(\mathbf{x}_{1,0}, t_0)\| \, \mathrm{e}^{-\lambda_\tau (\tau - t_0)} + D \tag{3.35}$$

Having this trajectory approximation result, we are now able to state the following theorem:

Theorem 3.4.2. *Let Assumption* 3.4.1 *be satisfies and suppose that a compact subset* $\mathcal{S}$ *is GUAS for the system (3.32). Then, the subset* $\mathcal{S}$ *is sSPUAS for the system (3.24).*

Going back to the motivational example, we see that when $\mu = 1/\omega$, the system can be written in the timescale $t = \tau/\omega$ on the form:

$$\dot{x}_1 = \beta x_1 + \sqrt{2\omega} \sin(x_1^2 + 4(x_4 - x_3) + \omega t) \tag{3.36}$$

$$\dot{x}_2 = \beta x_2 + \sqrt{2\omega} \cos(x_1^2 + 4(x_4 - x_3) + \omega t) \tag{3.37}$$

$$\dot{x}_3 = \omega (x_4 - x_3), \qquad \dot{x}_4 = \omega (x_2^2 - x_4) \tag{3.38}$$

If we apply our results, we obtain the system:

$$\dot{\bar{x}}_1 = (\beta - 2)\bar{x}_1 \tag{3.39}$$

$$\dot{\bar{x}}_2 = (\beta - 2)\bar{x}_2 \tag{3.40}$$

It is clear that the reduced order averaged system has a GUAS equilibrium point at the origin when $\beta < 2$. Hence, we conclude from Theorem 3.4.2 that the origin $x_1 = x_2 = 0$ is a sSPUAS subset for the original system (3.22a)-(3.22c).

3.5 Recursive Singularly Perturbed Averaging

Finally, we consider the situation in which first-order and second-order singularly perturbed averaging take place in the same dynamical system but operate on different time-scales. The class of systems we consider in this section contains three distinct time-scales. We are interested in approximating the trajectories of the system on the slowest time-scale. Two parts of the system state are singularly perturbed but on two different time-scales. The motivation for considering this class of systems comes from the 3D source seeking algorithms that we propose and analyze in subsequent chapters.

Let $\mathbf{x}_1 \in \mathbb{R}^{n_1}$, $\mathbf{x}_2 \in \mathbb{R}^{n_2}$, $\mathbf{x}_3 \in \mathbb{R}^{n_3}$, and $\mathbf{x} = (\mathbf{x}_1, \mathbf{x}_2, \mathbf{x}_3) \in \mathbb{R}^{n_1+n_2+n_3}$. Next, consider the following dynamical system:

$$\dot{\mathbf{x}}_1 = \sum_{k=1}^{2} \varepsilon^{k-2} \mathbf{f}_{1,k}(\mathbf{x}_1, \mathbf{x}_2, \mathbf{x}_3, t, \varepsilon^{-1}t, \varepsilon^{-2}t) + O(\varepsilon), \qquad \mathbf{x}_1(t_0) = \mathbf{x}_{1,0} \tag{3.41a}$$

$$\dot{\mathbf{x}}_2 = \sum_{k=1}^{2} \varepsilon^{k-2} \mathbf{f}_{2,k}(\mathbf{x}_1, \mathbf{x}_2, \mathbf{x}_3, t, \varepsilon^{-1}t, \varepsilon^{-2}t) + O(\varepsilon), \qquad \mathbf{x}_2(t_0) = \mathbf{x}_{2,0} \tag{3.41b}$$

$$\dot{\mathbf{x}}_3 = \sum_{k=0}^{2} \varepsilon^{k-2} \mathbf{f}_{3,k}(\mathbf{x}_1, \mathbf{x}_2, \mathbf{x}_3, t, \varepsilon^{-1}t, \varepsilon^{-2}t) + O(\varepsilon), \qquad \mathbf{x}_3(t_0) = \mathbf{x}_{3,0} \tag{3.41c}$$

where $O(\varepsilon)$ refers to small terms that are neglected in the limit $\varepsilon \to 0$. We are interested in approximating the trajectories of the system (3.41) in the limit $\varepsilon \to 0$. It is clear that the system above contains three distinct time-scales: $t, \varepsilon^{-1}t, \varepsilon^{-2}t$. We are interested in

approximating the trajectories of the system on compact intervals in the slowest time-scale t. We assume that all the vector fields on the right hand side of the equations (3.41) are sufficiently smooth, T_2-periodic in the fastest time variable τ, and T_1-periodic in the intermediate time variable σ. In addition, we make the following assumption:

Assumption 3.5.1. *Suppose that there exists a unique and sufficiently smooth map $\boldsymbol{\varphi}_0$ such that:*

$$\mathbf{f}_{3,0}(\mathbf{x}_1, \mathbf{x}_2, \boldsymbol{\varphi}_0(\mathbf{x}_1, \mathbf{x}_2, t, \sigma), t, \sigma, \tau) = 0 \tag{3.42}$$

$$\int_0^{T_2} \mathbf{f}_{1,1}(\mathbf{x}_1, \mathbf{x}_2, \boldsymbol{\varphi}_0(\mathbf{x}_1, \mathbf{x}_2, t, \sigma), t, \sigma, \tau)\, d\tau = 0 \tag{3.43}$$

In addition, let $\mathbf{y}_3 \in \mathbb{R}^{n_3}$, and

$$\tilde{\mathbf{f}}_{3,0}(\mathbf{x}_1, \mathbf{x}_2, \mathbf{y}_3, t, \sigma, \tau) = \mathbf{f}_{3,0}(\mathbf{x}_1, \mathbf{x}_2, \mathbf{y}_3 + \boldsymbol{\varphi}_0(\mathbf{x}_1, \mathbf{x}_2, t, \sigma), t, \sigma, \tau) \tag{3.44}$$

and suppose that there exists a Lyapunov function V_3 and constants $\kappa_{3,i} > 0$ for $i \in \{1, \dots, 4\}$ such that the inequalities:

$$\kappa_{3,1}\|\mathbf{y}_3\|^2 \leq V_3(\mathbf{y}_3, \tau) \leq \kappa_{3,2}\|\mathbf{y}_3\|^2 \tag{3.45a}$$

$$\partial_2 V_3(\mathbf{y}_3, \tau) + \partial_1 V_3(\mathbf{y}_3, \tau)\tilde{\mathbf{f}}_{3,0}(\mathbf{x}_1, \mathbf{x}_2, \mathbf{y}_3, t, \sigma, \tau) \leq -\kappa_{3,3}\|\mathbf{y}_3\|^2 \tag{3.45b}$$

$$\|\partial_1 V_3(\mathbf{y}_3, \tau)\| \leq \kappa_{3,4}\|\mathbf{y}_3\| \tag{3.45c}$$

are satisfied globally in $\mathbf{y}_3$, uniformly in $t, \sigma, \tau, \mathbf{x}_1, \mathbf{x}_2$.

Moreover, suppose that there exists a unique T_1-periodic and sufficiently smooth map $\boldsymbol{\phi}_0$ such that:

$$\int_0^{T_2} \mathbf{f}_{2,1}(\mathbf{x}_1, \boldsymbol{\phi}_0(\mathbf{x}_1, t, \sigma), \boldsymbol{\varphi}_0(\mathbf{x}_1, \boldsymbol{\phi}_0(\mathbf{x}_1, t, \sigma), t, \sigma), t, \sigma, \tau)\, d\tau = 0 \tag{3.46}$$

Furthermore, let $\mathbf{y}_2 \in \mathbb{R}^{n_2}$*, and:*

$$\begin{aligned}\tilde{\tilde{\mathbf{f}}}_{2,1}(\mathbf{x}_1,&\mathbf{y}_2, t, \sigma) = \\ &\frac{1}{T_2}\int_0^{T_2} \mathbf{f}_{2,1}(\mathbf{x}_1, \mathbf{y}_2 + \boldsymbol{\phi}_0(\mathbf{x}_1, t, \sigma), \boldsymbol{\varphi}_0(\mathbf{x}_1, \boldsymbol{\phi}_0(\mathbf{x}_1, t, \sigma), t, \sigma), t, \sigma, \tau)\, d\tau\end{aligned} \tag{3.47}$$

and suppose that there exists a Lyapunov function V_2 *and constants* $\kappa_{2,i}$ *for* $i \in \{1, \ldots, 4\}$ *such that the inequalities:*

$$\kappa_1\|\mathbf{y}_2\|^2 \leq V(\mathbf{y}_2, \sigma) \leq \kappa_2\|\mathbf{y}_2\|^2 \tag{3.48a}$$

$$\partial_2 V(\mathbf{y}_2, \sigma) + \partial_1 V(\mathbf{y}_2, \sigma)\tilde{\tilde{\mathbf{f}}}_{2,1}(\mathbf{x}_1, \mathbf{y}_2, t, \sigma) \leq -\kappa_3\|\mathbf{y}_2\|^2 \tag{3.48b}$$

$$\|\partial_1 V(\mathbf{y}_2, \sigma)\| \leq \kappa_4\|\mathbf{y}_2\| \tag{3.48c}$$

are satisfied globally in $\mathbf{y}_2$*, uniformly in* $t, \sigma, \mathbf{x}_1$*.*

By changing to the fastest time variable $\tau = \varepsilon^{-2}(t - t_0) + t_0$, and with some notation abuse, we obtain the following system:

$$\frac{d\mathbf{x}_1}{d\tau} = \sum_{k=1}^{2} \varepsilon^k \mathbf{f}_{1,k}(\mathbf{x}_1, \mathbf{x}_2, \mathbf{x}_3, t, \sigma, \tau) + O(\varepsilon^3), \qquad \mathbf{x}_1(t_0) = \mathbf{x}_{1,0} \tag{3.49a}$$

$$\frac{d\mathbf{x}_2}{d\tau} = \sum_{k=1}^{2} \varepsilon^k \mathbf{f}_{2,k}(\mathbf{x}_1, \mathbf{x}_2, \mathbf{x}_3, t, \sigma, \tau) + O(\varepsilon^3), \qquad \mathbf{x}_2(t_0) = \mathbf{x}_{2,0} \tag{3.49b}$$

$$\frac{d\mathbf{x}_3}{d\tau} = \sum_{k=0}^{2} \varepsilon^k \mathbf{f}_{3,k}(\mathbf{x}_1, \mathbf{x}_2, \mathbf{x}_3, t, \sigma, \tau) + O(\varepsilon^3), \qquad \mathbf{x}_3(t_0) = \mathbf{x}_{3,0} \tag{3.49c}$$

where $t = \varepsilon^2(\tau - t_0) + t_0$, and $\sigma = \varepsilon(\tau - t_0) + t_0$. We apply a coordinate shift:

$$\mathbf{y}_3 = \mathbf{x}_3 - \boldsymbol{\varphi}_0(\mathbf{x}_1, \mathbf{x}_2, t, \sigma) - \sum_{i=1}^{2} \varepsilon^i \boldsymbol{\varphi}_i(\mathbf{x}_1, \mathbf{x}_2, t, \sigma, \tau) \tag{3.50}$$

where the maps $\boldsymbol{\varphi}_i(\mathbf{x}_1, \mathbf{x}_2, t, \sigma, \tau)$ are to be defined below. Under this coordinate shift, the

system takes the form:

$$\frac{d\mathbf{x}_1}{d\tau} = \sum_{k=1}^{2} \varepsilon^k \tilde{\mathbf{f}}_{1,k}(\mathbf{x}_1, \mathbf{x}_2, \mathbf{y}_3, t, \sigma, \tau) + O(\varepsilon^3), \qquad \mathbf{x}_1(t_0) = \mathbf{x}_{1,0} \tag{3.51a}$$

$$\frac{d\mathbf{x}_2}{d\tau} = \sum_{k=1}^{2} \varepsilon^k \tilde{\mathbf{f}}_{2,k}(\mathbf{x}_1, \mathbf{x}_2, \mathbf{y}_3, t, \sigma, \tau) + O(\varepsilon^3), \qquad \mathbf{x}_2(t_0) = \mathbf{x}_{2,0} \tag{3.51b}$$

$$\frac{d\mathbf{y}_3}{d\tau} = \sum_{k=0}^{2} \varepsilon^k \tilde{\mathbf{f}}_{3,k}(\mathbf{x}_1, \mathbf{x}_2, \mathbf{y}_3, t, \sigma, \tau) + O(\varepsilon^3), \qquad \mathbf{y}_3(t_0) = \mathbf{y}_{3,0} \tag{3.51c}$$

where $\tilde{\mathbf{x}} = (\mathbf{x}_1, \mathbf{x}_2, \mathbf{y}_3)$, and the new vector fields $\tilde{\mathbf{f}}_{j,k}$ are obtained from the older vector fields $\mathbf{f}$ through substitution with the coordinate shift (3.50), expanding using Taylor's theorem in the small parameter ε, and matching the coefficients of like-powers. The exact expressions can be found in Appendix E.

Since we are interested in a second-order approximation of the trajectories, we enforce a condition on the vector fields $\tilde{\mathbf{f}}_{3,1}$ and $\tilde{\mathbf{f}}_{3,2}$. Namely, we enforce the conditions that:

$$\tilde{\mathbf{f}}_{3,1}(\mathbf{x}_1, \mathbf{x}_2, 0, t, \sigma, \tau) = 0, \qquad \tilde{\mathbf{f}}_{3,2}(\mathbf{x}_1, \mathbf{x}_2, 0, t, \sigma, \tau) = 0 \tag{3.52}$$

which leads to the following simple partial differential equations for $i \in \{1, 2\}$:

$$\partial_\tau \boldsymbol{\varphi}_i(\mathbf{x}_1, \mathbf{x}_2, t, \sigma, \tau) = \mathbf{A}_{\boldsymbol{\varphi}}(\mathbf{x}_1, \mathbf{x}_2, t, \sigma, \tau)\boldsymbol{\varphi}_i(\mathbf{x}_1, \mathbf{x}_2, t, \sigma, \tau) + \mathbf{b}_{\boldsymbol{\varphi},i}(\mathbf{x}_1, \mathbf{x}_2, t, \sigma, \tau) \tag{3.53}$$

where the exact expressions for the vector-valued maps $\mathbf{b}_{\boldsymbol{\varphi},i}$ can be found in Appendix E. These partial differential equations are solvable when supplemented with a boundary condition. Since all vector fields are T_1-periodic, enforcing the periodicity of the maps $\boldsymbol{\varphi}_1$ and $\boldsymbol{\varphi}_2$ provides the missing boundary condition:

$$\boldsymbol{\varphi}_i(\mathbf{x}_1, \mathbf{x}_2, t, \sigma, \tau + T_1) = \boldsymbol{\varphi}_i(\mathbf{x}_1, \mathbf{x}_2, t, \sigma, \tau), \qquad \forall i \in \{1, 2\} \tag{3.54}$$

The maps $\boldsymbol{\varphi}_i$ are well-defined only when the solutions to the boundary value problems above are well-defined. A sufficient condition for solvability is that the matrix $\mathbf{A}_{\boldsymbol{\varphi}}$ is uniformly non-singular, which is guaranteed by Assumption 3.5.1 and converse Lyapunov theorems [7]. To summarize, we have the following two Boundary Value Problems (BVPs):

$$\partial_\tau \boldsymbol{\varphi}_i(\cdot,\tau) = \mathbf{A}_{\boldsymbol{\varphi}}(\cdot,\tau)\boldsymbol{\varphi}_i(\cdot,\tau) + \mathbf{b}_{\boldsymbol{\varphi},i}(\cdot,\tau) \tag{3.55}$$

$$\boldsymbol{\varphi}_i(\cdot,\tau+T) = \boldsymbol{\varphi}_i(\cdot,\tau), \tag{3.56}$$

where the variables $\mathbf{x}_1, \mathbf{x}_2, t, \sigma$ have been omitted since they appear only as constant parameters. The solutions are given by the formula:

$$\boldsymbol{\varphi}_i(\cdot,\tau) = \big(\mathbf{I} - \boldsymbol{\Phi}_{\mathbf{A}_{\boldsymbol{\varphi}}}(\tau+T_1,\tau)\big)^{-1} \int_\tau^{\tau+T_1} \boldsymbol{\Phi}_{\mathbf{A}_{\boldsymbol{\varphi}}}(\tau+T_1,\nu)\mathbf{b}_{\boldsymbol{\varphi},i}(\cdot,\nu)\,d\nu, \tag{3.57}$$

where $\boldsymbol{\Phi}_{\mathbf{A}_{\boldsymbol{\varphi}}}$ is the fundamental matrix associated with the linear system:

$$\frac{d\mathbf{y}_3}{d\tau} = \mathbf{A}_{\boldsymbol{\varphi}}(\cdot,\tau)\mathbf{y}_3, \tag{3.58}$$

which completely defines the coordinate shift (3.50).

Consequently, we have that:

$$\tilde{\mathbf{f}}_{3,k}(\mathbf{x}_1,\mathbf{x}_2,0,t,\sigma,\tau) = 0, \qquad \forall k \in \{0,1,2\}, \tag{3.59}$$

and for sufficiently small ε, trajectories of the system (3.51) converge exponentially fast to an $O(\varepsilon^3)$ of the slow manifold defined by $\mathbf{y}_3 = 0$. On this slow manifold, the system behaves approximately according to the reduced order dynamics:

$$\frac{d\tilde{\mathbf{x}}_1}{d\tau} = \sum_{k=1}^{2} \varepsilon^k \tilde{\mathbf{f}}_{1,k}(\tilde{\mathbf{x}}_1,\tilde{\mathbf{x}}_2,0,t,\sigma,\tau) + O(\varepsilon^3), \tag{3.60a}$$

$$\frac{d\tilde{\mathbf{x}}_2}{d\tau} = \sum_{k=1}^{2} \varepsilon^k \tilde{\mathbf{f}}_{2,k}(\tilde{\mathbf{x}}_1, \tilde{\mathbf{x}}_2, 0, t, \sigma, \tau) + O(\varepsilon^3), \tag{3.60b}$$

which is on the averaging canonical form. We may, therefore, perform second order averaging to obtain the system:

$$\frac{d\bar{\tilde{\mathbf{x}}}_1}{d\tau} = \varepsilon^2 \bar{\tilde{\mathbf{f}}}_{1,2}(\bar{\tilde{\mathbf{x}}}_1, \bar{\tilde{\mathbf{x}}}_2, t, \sigma) + O(\varepsilon^3), \tag{3.61a}$$

$$\frac{d\bar{\tilde{\mathbf{x}}}_2}{d\tau} = \sum_{k=1}^{2} \varepsilon^k \bar{\tilde{\mathbf{f}}}_{2,k}(\bar{\tilde{\mathbf{x}}}_1, \bar{\tilde{\mathbf{x}}}_2, t, \sigma) + O(\varepsilon^3), \tag{3.61b}$$

where the exact expressions for the vector fields $\bar{\tilde{\mathbf{f}}}_{j,k}$ can be found in Appendix E. By re-scaling time to $\sigma = \varepsilon(\tau - t_0) + t_0$ we obtain the system:

$$\frac{d\bar{\tilde{\mathbf{x}}}_1}{d\sigma} = \varepsilon\, \bar{\tilde{\mathbf{f}}}_{1,2}(\bar{\tilde{\mathbf{x}}}_1, \bar{\tilde{\mathbf{x}}}_2, t, \sigma), \tag{3.62a}$$

$$\frac{d\bar{\tilde{\mathbf{x}}}_2}{d\sigma} = \bar{\tilde{\mathbf{f}}}_{2,1}(\bar{\tilde{\mathbf{x}}}_1, \bar{\tilde{\mathbf{x}}}_2, t, \sigma) + \varepsilon\, \bar{\tilde{\mathbf{f}}}_{2,2}(\bar{\tilde{\mathbf{x}}}_1, \bar{\tilde{\mathbf{x}}}_2, t, \sigma), \tag{3.62b}$$

We apply another coordinate shift:

$$\bar{\tilde{\mathbf{y}}}_2 = \bar{\tilde{\mathbf{x}}}_2 - \sum_{k=0}^{1} \varepsilon^k \boldsymbol{\phi}_k(\bar{\tilde{\mathbf{x}}}_1, t, \sigma) \tag{3.63}$$

where the map $\boldsymbol{\phi}_1$ is to be defined later. Under this coordinate shift, the system becomes:

$$\frac{d\bar{\tilde{\mathbf{x}}}_1}{d\sigma} = \varepsilon\, \tilde{\bar{\tilde{\mathbf{f}}}}_{1,2}(\bar{\tilde{\mathbf{x}}}_1, \bar{\tilde{\mathbf{y}}}_2, t, \sigma) + O(\varepsilon^2) \tag{3.64}$$

$$\frac{d\bar{\tilde{\mathbf{y}}}_1}{d\sigma} = \tilde{\bar{\tilde{\mathbf{f}}}}_{2,1}(\bar{\tilde{\mathbf{x}}}_1, \bar{\tilde{\mathbf{y}}}_2, t, \sigma) + \varepsilon\, \tilde{\bar{\tilde{\mathbf{f}}}}_{2,2}(\bar{\tilde{\mathbf{x}}}_1, \bar{\tilde{\mathbf{y}}}_2, t, \sigma) + O(\varepsilon^2) \tag{3.65}$$

where the exact expressions for the vector fields $\tilde{\bar{\tilde{\mathbf{f}}}}_{j,k}$ can be found in Appendix E. We observe that:

$$\tilde{\bar{\tilde{\mathbf{f}}}}_{2,1}(\bar{\tilde{\mathbf{x}}}_1, 0, t, \sigma) = 0 \tag{3.66}$$

We proceed to define the map $\boldsymbol{\phi}_1$ by requiring that:

$$\tilde{\bar{\mathbf{f}}}_{2,2}(\bar{\tilde{\mathbf{x}}}_1, 0, t, \sigma) = 0 \tag{3.67}$$

which leads to the equation:

$$\partial_\sigma \boldsymbol{\phi}_1(\cdot, \sigma) = \mathbf{A}_{\boldsymbol{\phi}}(\cdot, \sigma)\boldsymbol{\phi}_1(\cdot, \sigma) + \mathbf{b}_{\boldsymbol{\phi}}(\cdot, \sigma) \tag{3.68}$$

where the vector $\mathbf{b}_{\boldsymbol{\phi}}$ is given by:

$$\mathbf{b}_{\boldsymbol{\phi}}(\bar{\tilde{\mathbf{x}}}_1, t, \sigma) = \tilde{\bar{\mathbf{f}}}_{2,2}(\bar{\tilde{\mathbf{x}}}_1, 0, t, \sigma) - \partial_1 \boldsymbol{\phi}_0(\bar{\tilde{\mathbf{x}}}_1, t, \sigma)\tilde{\bar{\mathbf{f}}}_{1,2}(\bar{\tilde{\mathbf{x}}}_1, \bar{\tilde{\mathbf{y}}}_2, t, \sigma) - \partial_t \boldsymbol{\phi}_0(\bar{\tilde{\mathbf{x}}}_1, t, \sigma) \tag{3.69}$$

We define the map $\boldsymbol{\phi}_1$ by:

$$\boldsymbol{\phi}_1(\cdot, \sigma) = \left(\mathbf{I} - \boldsymbol{\Phi}_{\mathbf{A}_{\boldsymbol{\phi}}}(\sigma + T_2, \sigma)\right)^{-1} \int_\sigma^{\sigma+T_2} \boldsymbol{\Phi}_{\mathbf{A}_{\boldsymbol{\phi}}}(\sigma + T_2, \nu)\mathbf{b}_{\boldsymbol{\phi}}(\cdot, \nu)\, d\nu, \tag{3.70}$$

where $\boldsymbol{\Phi}_{\mathbf{A}_{\boldsymbol{\phi}}}$ is the fundamental matrix. Observe that in this case we have:

$$\tilde{\bar{\mathbf{f}}}_{2,i}(\bar{\tilde{\mathbf{x}}}_1, 0, t, \sigma) = 0, \qquad \forall i \in \{1, 2\} \tag{3.71}$$

which implies that the trajectory converges exponentially fast to an $O(\varepsilon^2)$ neighborhood of the slow manifold $\bar{\tilde{\mathbf{y}}}_2 = 0$. On the slow manifold, the system is governed by the equations:

$$\frac{d\bar{\tilde{\mathbf{x}}}_1}{d\sigma} = \varepsilon\, \tilde{\bar{\mathbf{f}}}_{1,2}(\bar{\tilde{\mathbf{x}}}_1, 0, t, \sigma) + O(\varepsilon^2) \tag{3.72}$$

which is again on the averaging canonical form. We may, therefore, perform first order averaging to obtain the system:

$$\frac{d\bar{\tilde{\mathbf{x}}}_1}{d\sigma} = \varepsilon\, \bar{\tilde{\mathbf{f}}}_{1,2}(\bar{\tilde{\mathbf{x}}}_1, t) + O(\varepsilon^2) \tag{3.73}$$

where the vector field $\bar{\bar{\mathbf{f}}}_{1,2}$ is given by:

$$\bar{\bar{\mathbf{f}}}_{1,2}(\bar{\bar{\mathbf{x}}}_1, t) = \frac{1}{T_2}\int_0^{T_2} \tilde{\bar{\mathbf{f}}}_{1,2}(\bar{\bar{\mathbf{x}}}_1, 0, t, \sigma)\, d\sigma \tag{3.74}$$

By changing back to the slowest time variable $t = \varepsilon(\sigma - t_0) + t_0$, we obtain the fully averaged reduced order model:

$$\dot{\bar{\bar{\mathbf{x}}}}_1 = \bar{\bar{\mathbf{f}}}_{1,2}(\bar{\bar{\mathbf{x}}}_1, t), \qquad \bar{\bar{\mathbf{x}}}_1(t_0) = \mathbf{x}_{1,0} \tag{3.75a}$$

$$\bar{\bar{\mathbf{x}}}_2 = \boldsymbol{\phi}_0(\bar{\bar{\mathbf{x}}}_1, t, \sigma) \tag{3.75b}$$

$$\bar{\bar{\mathbf{x}}}_3 = \boldsymbol{\varphi}_0(\bar{\bar{\mathbf{x}}}_1, \boldsymbol{\phi}_0(\bar{\bar{\mathbf{x}}}_1, t, \sigma), t, \sigma) \tag{3.75c}$$

We give the relation between the trajectories of the system (3.41) and the trajectories of the system (3.75).

Theorem 3.5.1. *Let Assumption* 3.5.1 *be satisfied, and let* $\mathcal{B}_2 \times \mathcal{B}_3 \subset \mathbb{R}^{n_2} \times \mathbb{R}^{n_3}$ *be arbitrary but bounded and* $D \in (0, \infty)$ *be arbitrary. In addition, let a bounded subset* $\mathcal{B}_1 \subset \mathbb{R}^{n_1}$*, a compact subset* $\mathcal{N} \subset \mathbb{R}^{n_1}$*, and a positive constant* $L \in (0, \infty)$ *be such that unique trajectories* $\bar{\bar{\mathbf{x}}}_1(t; t_0, \mathbf{x}_{1,0})$ *for the system (3.75) exist and* $\bar{\bar{\mathbf{x}}}_1(t; t_0, \mathbf{x}_{1,0}) \in \mathcal{N}$*,* $\forall t \in [t_0, t_0 + L]$*,* $\forall t_0 \in \mathbb{R}$*,* $\forall \mathbf{x}_{1,0} \in \mathcal{B}_1$*. Then,* $\exists \varepsilon^* \in (0, \varepsilon_0)$ *and positive constants* $\lambda_\sigma, \gamma_\sigma, \lambda_\tau, \gamma_\tau$ *such that* $\forall t_0 \in \mathbb{R}$*,* $\forall (\mathbf{x}_{1,0}, \mathbf{x}_{2,0} - \boldsymbol{\phi}_0(\mathbf{x}_{1,0}, t_0, t_0), \mathbf{x}_{3,0} - \boldsymbol{\varphi}_0(\mathbf{x}_{1,0}, \boldsymbol{\phi}_0(\mathbf{x}_{1,0}, \mathbf{x}_{2,0}, t_0, t_0, t_0)) \in \mathcal{B}_1 \times \mathcal{B}_2 \times \mathcal{B}_3$*,* $\forall t \in [t_0, t_0 + L]$*,* $\forall \varepsilon \in (0, \varepsilon^*)$*,* $\sigma = \varepsilon^{-1}(t - t_0) + t_0$*, and* $\tau = \varepsilon^{-2}(t - t_0) + t_0$*, unique trajectories* $(\mathbf{x}_1(t; t_0, \mathbf{x}_{1,0}), \mathbf{x}_2(t; t_0, \mathbf{x}_{2,0}), \mathbf{x}_3(t; t_0, \mathbf{x}_{3,0}))$ *for the system (3.41) exist and satisfy the estimates:*

$$\|\mathbf{x}_1(t) - \bar{\bar{\mathbf{x}}}_1(t)\| < D \tag{3.76}$$

$$\|\mathbf{x}_2(t) - \boldsymbol{\phi}_0(\bar{\bar{\mathbf{x}}}(t), t, \sigma)\| < \gamma_\sigma \|\mathbf{x}_{2,0} - \boldsymbol{\phi}_0(\mathbf{x}_{1,0}, t_0, t_0)\|\, \mathrm{e}^{-\lambda_\sigma (\sigma - t_0)} + D \tag{3.77}$$

$$\begin{aligned} &\|\mathbf{x}_3(t) - \boldsymbol{\varphi}_0(\bar{\bar{\mathbf{x}}}_1(t), \boldsymbol{\phi}_0(\bar{\bar{\mathbf{x}}}_1(t), t, \sigma), t, \sigma)\| < \\ &\qquad \gamma_\tau \|\mathbf{x}_{3,0} - \boldsymbol{\varphi}_0(\mathbf{x}_{1,0}, \boldsymbol{\phi}_0(\mathbf{x}_{1,0}, t_0, t_0), t_0, t_0)\|\, \mathrm{e}^{-\lambda_\tau (\tau - t_0)} + D \end{aligned} \tag{3.78}$$

With this trajectory approximation result, we are now able to state the following theorem:

Theorem 3.5.2. *Let Assumption* 3.5.1 *be satisfied and suppose that a compact subset* $\mathcal{S}$ *is GUAS for the system (3.32). Then, the subset* $\mathcal{S}$ *is sSPUAS for the system (3.75).*

Theorem 3.5.1 and Theorem 3.5.2 combine the results from the previous sections into a multiple time-scales setting. The proofs follow essentially the same steps as in the proofs of the previous sections, therefore we omit them. The main application of the results in this section are in the source seeking problem considered in the next chapter.

Chapter 4

Bio-Inspired 3D Source Seeking

Source seeking is the problem of locating a target that emits a scalar measurable signal, typically without any global positioning information. Many control problems and phenomena can be abstracted as a source seeking problem. For example, the navigation of a robot, operating in a GPS-denied environment, and tasked with locating and homing onto the source of a signal is an instance of a source seeking problem. This setting may arise, for example, when a vehicle is operating under water, under ice, or in a cave [31]. The situation also arises whenever position and attitude information are no longer available for measurement as a consequence of the absence of a global reference frame. Remarkably, many organisms are constantly faced with the source seeking problem in their environment. Bacteria need to follow the gradient of chemical concentration to find food. Sperm cells ascend the concentration gradient to find the egg. Nematodes estimate and follow thermal gradients for thermoregulation. As with every other natural phenomenon, there is an incredible diversity of the behavior displayed by the organisms in solving the source seeking problem. Some strategies, such as bacterial chemotaxis, are inherently stochastic. Other strategies, such as that common in organisms with paired receptors, employ a spatial approach to the estimation of the gradient by simultaneously comparing stimuli between paired receptors. More

relevant to us here is the strategy employed by organisms with a single receptor. Such organisms cannot estimate the gradient spatially. Rather, they estimate the gradient in a temporal fashion. When the temporal estimation of the gradient happens through periodic movements of the body, the behavior of the organism is called klinotaxis. It turns out that klinotaxis is essentially an extremum seeking-based solution to the source-seeking problem. We investigate this novel connection in depth in the next chapter. In this chapter, we propose and analyze several source seeking algorithms inspired by this novel connection.

Extensive work has been done on the source seeking problem using extremum seeking control, of which we mention a few. For velocity-actuated point-like kinematics (i.e. single integrator dynamics), the source seeking problem can be easily solved using several non-resonating extremum seeking controllers if we assume full control authority on the velocity in all degrees of freedom. For double integrator dynamics, the problem is more difficult and requires careful considerations [32]. The situation is also difficult for kinematic models of planar rigid bodies under nonholonomic constraints, yet solutions have been proposed [33, 28]. Further difficulties arise when one considers the 2D underactuated dynamics with acceleration, rather than velocity, control [34]. However, most of the work in the literature focuses on the two dimensional case where the rigid body kinematics is described by a unicycle model. The pioneering work on the 3D case by Cochran et al [35] considers the 3D source seeking problem for an under-actuated vehicle with a rigid body kinematic model. However, they employ a parameterization of the rotation group SO(3) through Euler angles. In particular, the control law proposed in [35] assumes direct control authority on the Euler angle rates, which is not convenient for practical implementation; actuating the Euler angle rates requires measurement of the angles themselves. The situation is similar with all subsequent algorithms proposed for the 3D source seeking problem [36, 37, 38, 39, 40, 41, 42]. To elaborate, consider Euler's rigid body equations of motion:

$$\dot{\mathbf{q}} = \mathbf{R}\mathbf{v}, \qquad m\,\dot{\mathbf{v}} + m\,\boldsymbol{\Omega} \times \mathbf{v} = \mathbf{T} \tag{4.1a}$$

$$\dot{\mathbf{R}} = \mathbf{R}\widehat{\mathbf{\Omega}}, \qquad \mathbf{J}\,\dot{\mathbf{\Omega}} + \mathbf{\Omega} \times \mathbf{J}\,\mathbf{\Omega} = \mathbf{M} \tag{4.1b}$$

written in the body frame of reference, where $\mathbf{q}$ is the position of the center of the mass m, $\mathbf{R}$ is the rotation matrix relating the body axes to the axes of an inertial frame of reference, $\mathbf{v}$ and $\mathbf{\Omega}$ are the linear and angular velocities in body coordinates, $\widehat{\mathbf{\Omega}}$ is the skew-symmetric matrix associated with the vector $\mathbf{\Omega}$, $\mathbf{J}$ is the moment of inertia matrix around the center of mass represented in the body frame, and the $\mathbf{T}$ and $\mathbf{M}$ are the body net forces and torques, respectively. The control of free rigid body motion is achieved through the body forces and torques $\mathbf{T}$ and $\mathbf{M}$. All kinematic models are approximations of (4.1) when $\mathbf{T}$ and $\mathbf{M}$ are such that:

$$\mathbf{T} = -\mathbf{D}_1\,(\mathbf{v} - \mathbf{u}), \qquad \mathbf{M} = -\mathbf{D}_2\,(\mathbf{\Omega} - \mathbf{\Lambda}) \tag{4.2}$$

where $\mathbf{\Lambda}$ and $\mathbf{u}$ are free, and the matrices $\mathbf{D}_i$ for $i \in \{1, 2\}$ are positive definite with minimum eigenvalues that are much greater than the mass m and the maximum eigenvalue of the inertia tensor $\mathbf{J}$. Such an assumption is satisfied in the locomotion of microorganisms that swim in a low Reynolds number where viscous forces dominate inertia, or when high-gain velocity feedback is employed to enforce sufficient damping. If such an assumption is satisfied, a singular perturbation argument leads to the quasi-steady approximation:

$$\dot{\mathbf{q}} = \mathbf{R}\mathbf{v}, \qquad \mathbf{v} = \mathbf{u} \tag{4.3a}$$

$$\dot{\mathbf{R}} = \mathbf{R}\widehat{\mathbf{\Omega}}, \qquad \mathbf{\Omega} = \mathbf{\Lambda} \tag{4.3b}$$

Notably, the free parameters (i.e. the control inputs) in the quasi-steady approximation (4.3) are the linear and angular velocities in body coordinates.

If we are to design a source seeking controller for the kinematic model (4.3) that does not employ any global information, we must not use any information on either the position $\mathbf{q}$ or

the orientation $\mathbf{R}$. However, a parameterization of the rotation matrix $\mathbf{R}$ through an Euler angle triplet $\boldsymbol{\theta}$ leads to relations of the form:

$$\dot{\boldsymbol{\theta}} = \boldsymbol{\Phi}(\boldsymbol{\theta})\boldsymbol{\Omega} \tag{4.4}$$

where $\boldsymbol{\Phi}$ involves the jacobian of the parameterization. As such, even if the motion stays within the range of attitudes in which the map $\boldsymbol{\Phi}$ is non-singular, any control authority over the Euler angles rates $\dot{\boldsymbol{\theta}}$ is achieved by inverting the map $\boldsymbol{\Phi}$ since one must only assume control over the angular velocities $\boldsymbol{\Omega}$ in body coordinates when working with kinematic models of free rigid body motion. Hence, assuming direct control authority on the Euler angle rates $\dot{\boldsymbol{\theta}}$ implicitly requires measurement of the angles $\boldsymbol{\theta}$.

4.1 3D Gradient Alignment

Recall that the kinematics of a rigid body in 3D space are given by:

$$\dot{\mathbf{q}} = \mathbf{R}\mathbf{v}, \qquad \dot{\mathbf{R}} = \mathbf{R}\widehat{\boldsymbol{\Omega}} \tag{4.5}$$

First, we consider the problem of orienting a 3D rigid body with a fixed position such that one of the body axes points along the gradient of a signal strength field at the initial fixed position. A solution to this problem is interesting on its own and constitutes the first step towards solving the 3D source seeking problem. To that end, we assume a model of the vehicle such that the origin of the body frame is fixed (i.e. $\mathbf{v} = 0$), and two of the angular velocities in body coordinates are the control inputs:

$$\boldsymbol{\Omega} = \Omega_{\parallel}\mathbf{e}_1 + \Omega_{\perp}\mathbf{e}_3 \tag{4.6}$$

In addition, we assume that a non-collocated sensor is attached at the location $\mathbf{q}_s$ where:

$$\mathbf{q}_s = \mathbf{q} + r\mathbf{R}\mathbf{e}_2 \tag{4.7}$$

We would like to design a control law that aligns the body axis $\mathbf{R}\,\mathbf{e}_1$ with the gradient $\nabla\mathbf{c}(\mathbf{q})$ of a smooth signal strength field $c(\mathbf{q})$ at the fixed position $\mathbf{q}$, assuming that $\nabla\mathbf{c}(\mathbf{q}) \neq 0$. That is, we would like to stabilize the compact subset:

$$\mathcal{S}_{\mathbf{q}}^{+} = \{\mathbf{R} \in \mathrm{SO}(3) : \nabla\mathbf{c}(\mathbf{q})^{\intercal}\mathbf{R}\,\mathbf{e}_1 = \|\nabla\mathbf{c}(\mathbf{q})\|\} \tag{4.8}$$

We propose the linear dynamic feedback law:

$$\dot{\mathbf{y}} = \varepsilon^{-2}\,\mathbf{F}\,\mathbf{y} + \varepsilon^{-2}\,\mathbf{B}\,c(\mathbf{q}_s), \qquad \Omega_{\perp} = \varepsilon^{-1}\,\mathbf{H}\,\mathbf{y}, \qquad \Omega_{\parallel} = \varepsilon^{-2} \tag{4.9}$$

where $\mathbf{y} \in \mathbb{R}^2$, and $\mathbf{F}, \mathbf{B}, \mathbf{H}$ are given by:

$$\mathbf{F} = \begin{bmatrix} -1 & 1 \\ 0 & -1 \end{bmatrix}, \qquad \mathbf{B} = \begin{bmatrix} 0 \\ 1 \end{bmatrix}, \qquad \mathbf{H} = \begin{bmatrix} -4 & 4 \end{bmatrix} \tag{4.10}$$

Observe how the feedback law does not contain any information on the attitude of the vehicle and only employs the measured cost function $c(\mathbf{q}_s)$. In the 'distinguished limit' [43] where the offset r of the sensor from the center of the vehicle is small: $r = O(\varepsilon) = r_0\varepsilon$, as $\varepsilon \to 0$ for some $r_0 > 0$, we have the following proposition:

Proposition 4.1.1. *For a fixed* $\mathbf{q}$ *such that* $\nabla\mathbf{c}(\mathbf{q}) \neq 0$*, the compact subset* $\mathcal{S}_{\mathbf{q}}^{+}$ *is a proper subset of* $SO(3)$ *and is singularly (almost) semi-globally practically uniformly asymptotically stable for the system defined by equations (4.5) and (4.6) under the feedback law (4.9).*

Before we proceed with the proof of this proposition, we remark on the word 'almost' inside the parenthesis in its statement. Topological considerations [44] prohibit asymptotic stabil-

ity via continuous feedback on the group SO(3). As such, it is impossible to conclude global practical stability results, since the reduced order averaged system cannot be globally uniformly asymptotically stable. Instead, we can prove 'almost' semi-global practical stability which is a straightforward extension of Definition 3.3.1.

Proof. Let $\mathbf{R}_0 = \exp\left(\varepsilon^{-2} t\, \widehat{\mathbf{e}}_1\right)$, $\mathbf{P} = \mathbf{R}\mathbf{R}_0^\intercal$, and compute:

$$\dot{\mathbf{P}} = \dot{\mathbf{R}}\mathbf{R}_0^\intercal + \mathbf{R}\dot{\mathbf{R}}_0^\intercal = \Omega_\perp \mathbf{R}\widehat{\mathbf{e}}_3\mathbf{R}_0^\intercal = \Omega_\perp \mathbf{P}\mathbf{R}_0\widehat{\mathbf{e}}_3\mathbf{R}_0^\intercal = \Omega_\perp \mathbf{P}\widehat{\mathbf{R}_0\mathbf{e}_3} \tag{4.11}$$

Let $\mathbf{\Lambda}(\mathbf{y}, \varepsilon^{-2}t) = \mathbf{H}\,\mathbf{y}\,\mathbf{R}_0\mathbf{e}_3$ and observe that:

$$\dot{\mathbf{P}} = \varepsilon^{-1}\,\mathbf{P}\widehat{\mathbf{\Lambda}}(\mathbf{y}, \varepsilon^{-2}t) \tag{4.12}$$

To simplify the presentation, we embed SO(3) into $\mathbb{R}^9$ by partitioning the matrix $\mathbf{P} = [\mathbf{p}_1,\, \mathbf{p}_2,\, \mathbf{p}_3]$, defining the state vector $\mathbf{p} = [\mathbf{p}_1^\intercal,\, \mathbf{p}_2^\intercal,\, \mathbf{p}_3^\intercal]^\intercal$, and restricting the initial conditions for $\mathbf{p}$ to lie on the compact submanifold $\mathcal{M} = \left\{\mathbf{p}_i \in \mathbb{R}^3 :\, \mathbf{p}_i^\intercal\mathbf{p}_j = \delta_{ij},\ \mathbf{p}_i \times \mathbf{p}_j = \epsilon_{ijk}\mathbf{p}_k\right\}$ (which is the image of SO(3) under the embedding), where δ_{ij} is the Kronecker symbol and ϵ_{ijk} is the Levi-Civita symbol. On $\mathcal{M} \times \mathbb{R}^2$, the system is governed by:

$$\dot{\mathbf{p}}_i = \varepsilon^{-1} \sum_{j,k=1}^{3} \Lambda_j(\mathbf{y}, \varepsilon^{-2}t)\epsilon_{ijk}\mathbf{p}_k \tag{4.13a}$$

$$\dot{\mathbf{y}} = \varepsilon^{-2}\left(\mathbf{F}\,\mathbf{y} + \,\mathbf{B}\,c(\mathbf{q}_s)\right) \tag{4.13b}$$

where $\mathbf{q}_s$ is now given by:

$$\mathbf{q}_s = \mathbf{q} + r\left(\cos(\varepsilon^{-2}t)\,\mathbf{p}_2 + \sin(\varepsilon^{-2}t)\,\mathbf{p}_3\right) \tag{4.14}$$

The signal strength field at $\mathbf{q}_s$ can be expanded as a series in $r = r_0\varepsilon$ using Taylor's theorem:

$$c(\mathbf{q}_s) = c(\mathbf{q}) + r_0\varepsilon\,\nabla c(\mathbf{q})^\intercal(\cos(\varepsilon^{-2}t)\mathbf{p}_2 + \sin(\varepsilon^{-2}t)\mathbf{p}_3) + r_0^2\varepsilon^2\boldsymbol{\rho}(\mathbf{q}, \mathbf{q}_s, \varepsilon^{-2}t, \varepsilon) \tag{4.15}$$

where the remainder $\boldsymbol{\rho}$ is differentiable in all of its arguments. Now, observe that the system defined by the equations (4.13) and (4.15) belongs to the class of systems described by (3.24). Hence, we may employ Theorem 3.4.1 and Theorem 3.4.2 in analyzing the stability of the system. In order to proceed, the reduced order averaged system must be computed. First, we observe that $\boldsymbol{\varphi}_0 = \mathbb{1}c(\mathbf{q})$ is the zeroth-order quasi-steady state for the singularly perturbed part of the system. We proceed to compute the first-order periodic correction $\boldsymbol{\varphi}_1$ as given in equations (3.29). The vector $\mathbf{b}_1$ in this case is given by:

$$\mathbf{b}_1 = r_0\mathbf{B}\,\nabla c(\mathbf{q})^\intercal(\cos(\tau)\mathbf{p}_2 + \sin(\tau)\mathbf{p}_3) \tag{4.16}$$

Direct computation using equations (3.29c) and (3.29d) shows that:

$$\boldsymbol{\varphi}_1 = \frac{r_0}{2}\begin{bmatrix} (\sin(\tau)\mathbf{p}_2 - \cos(\tau)\mathbf{p}_3)^\intercal\nabla c(\mathbf{q}) \\ (\cos(\tau)(\mathbf{p}_2 - \mathbf{p}_3) + \sin(\tau)(\mathbf{p}_2 + \mathbf{p}_3))^\intercal\nabla c(\mathbf{q}) \end{bmatrix} \tag{4.17}$$

Therefore, the reduced order averaged system as defined by the formulas given in equations (3.32) is:

$$\begin{bmatrix} \dot{\bar{\mathbf{p}}}_1 \\ \dot{\bar{\mathbf{p}}}_2 \\ \dot{\bar{\mathbf{p}}}_3 \end{bmatrix} = \begin{bmatrix} r_0\left(\bar{\mathbf{p}}_2\bar{\mathbf{p}}_2^\intercal + \bar{\mathbf{p}}_3\bar{\mathbf{p}}_3^\intercal\right)\nabla c(\mathbf{q}) \\ -r_0\bar{\mathbf{p}}_1\bar{\mathbf{p}}_2^\intercal\nabla c(\mathbf{q}) \\ -r_0\bar{\mathbf{p}}_1\bar{\mathbf{p}}_3^\intercal\nabla c(\mathbf{q}) \end{bmatrix} \tag{4.18}$$

We claim that the subset $\mathcal{S}_{\mathbf{q}}^+$ is (almost) globally uniformly asymptotically stable for the

system (4.18). To prove this statement, we define the candidate Lyapunov function:

$$V = \|\nabla c(\mathbf{q})\| - \nabla c(\mathbf{q})^\intercal \bar{\mathbf{p}}_1 \tag{4.19}$$

which is clearly positive definite on $\mathcal{M}\backslash\mathcal{S}_{\mathbf{q}}^+$, and $V = 0$ if and only if $\mathbf{p} \in \mathcal{S}_{\mathbf{q}}^+$. We compute the derivative of V to obtain:

$$\dot{V} = r_0 \nabla c(\mathbf{q})^\intercal \left(\bar{\mathbf{p}}_2 \bar{\mathbf{p}}_2^\intercal + \bar{\mathbf{p}}_3 \bar{\mathbf{p}}_3^\intercal\right) \nabla c(\mathbf{q}) \tag{4.20}$$

However, it is not difficult to see that:

$$\bar{\mathbf{p}}_2 \bar{\mathbf{p}}_2^\intercal + \bar{\mathbf{p}}_3 \bar{\mathbf{p}}_3^\intercal = \mathbf{I} - \bar{\mathbf{p}}_1 \bar{\mathbf{p}}_1^\intercal \tag{4.21}$$

where $\mathbf{I}$ is the identity matrix. Hence, we have that:

$$\dot{V} = r_0 \|\nabla c(\mathbf{q})\|^2 - r_0 \left(\nabla c(\mathbf{q})^\intercal \bar{\mathbf{p}}_1\right)^2 \leq 0 \tag{4.22}$$

Observe that $\dot{V} = 0$ if and only if $\mathbf{p} \in \mathcal{S}_{\mathbf{q}}^+$ or $\mathbf{p} \in \mathcal{S}_{\mathbf{q}}^-$ where:

$$\mathcal{S}_{\mathbf{q}}^- = \{\mathbf{R} \in \mathrm{SO}(3) : \nabla \mathbf{c}(\mathbf{q})^\intercal \mathbf{p}_1 = -\|\nabla \mathbf{c}(\mathbf{q})\|\} \tag{4.23}$$

Thus, if we restrict our attention to the subset $\mathcal{M}\backslash\mathcal{S}_{\mathbf{q}}^-$, we have that $\dot{V} \leq 0$ $\forall \mathbf{p} \in \mathrm{SO}(3)\backslash\mathcal{S}_{\mathbf{q}}^-$ and $\dot{V} = 0$ if and only if $\mathbf{p} \in \mathcal{S}_{\mathbf{q}}^+ \subset \mathrm{SO}(3)\backslash\mathcal{S}_{\mathbf{q}}^-$. We conclude that $\mathcal{S}_{\mathbf{q}}^+$ is almost globally uniformly asymptotically stable for the system (4.18). Hence, a modification of the statement of Theorem 3.4.2 to account for the zero measure unstable invariant set $\mathcal{S}_{\mathbf{q}}^-$ leads us to conclude that the subset $\mathcal{S}_{\mathbf{q}}^+$ is singularly (almost) semi-globally practically uniformly asymptotically stable. □

We illustrate the behavior of this gradient alignment algorithm on a numerical example. The

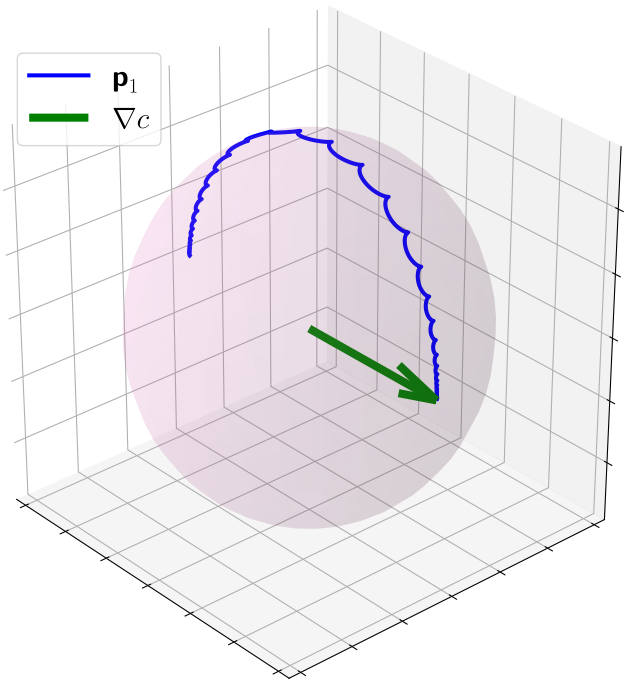

Figure 4.1: Numerical simulation results for the 3D gradient alignment algorithm: the blue curve is the path traced by the tip of the unit vector $\mathbf{p}_1 = \mathbf{R}\,\mathbf{e}_1$, and the green arrow is the direction of the gradient which in this case points along the x-axis.

simulation results are shown in figure 4.1. The signal strength field is taken as the linear field $c(\mathbf{q}) = \mathbf{q}^\intercal \mathbf{e}_1$, the frequency was taken as $\omega = 4\pi$, the parameter $r_0 = 1$, and the initial conditions are taken as $\mathbf{q}(0) = [3,\, -1,\, 3]$, $\mathbf{R}(0) = \exp(-0.99\pi\widehat{\mathbf{e}}_2)$, $\mathbf{z}(0) = [3,\, 3]$.

4.2 Helical 3D Source Seeking with Oscillatory Forward Velocity

Next, we employ the gradient alignment results from the previous section to design a 3D source seeking control law. We assume a vehicle model in which the linear and angular velocity vectors are given in body coordinates by:

$$\mathbf{v} = v\mathbf{e}_1, \qquad \boldsymbol{\Omega} = \Omega_{\|}\mathbf{e}_1 + \Omega_{\perp}\mathbf{e}_3 \tag{4.24}$$

where $\mathbf{e}_i$ for $i \in \{1, 2, 3\}$ are the standard unit vectors. This model is a natural extension of the unicycle model to the 3D setting. It is well known that this system is controllable using first-order Lie brackets [45].

Let $c : \mathbb{R}^3 \to \mathbb{R}$ be the signal strength field emitted by the source, and consider the case of a non-collocated signal strength sensor that is mounted at $\mathbf{q}_s$ as defined in equation (4.7).

Assumption 4.2.1. *Suppose that the signal strength field $c \in \mathcal{C}^3(\mathbb{R}^3; \mathbb{R})$ is radially unbounded, $\exists! \mathbf{q}^* \in \mathbb{R}^3$ such that $\nabla c(\mathbf{q}) = 0 \iff \mathbf{q} = \mathbf{q}^*$, and for some $\kappa > 0$ it satisfies the inequality:*

$$c(\mathbf{q}^*) - c(\mathbf{q}) \leq \kappa \|\nabla c(\mathbf{q})\|^2, \, \forall \mathbf{q} \in \mathbb{R}^n, \tag{4.25}$$

Now, consider the following control law:

$$v = 2\alpha_1 \varepsilon^{-1} \cos(2\varepsilon^{-2} t - c(\mathbf{q}_s)) \tag{4.26a}$$

$$\dot{\mathbf{y}} = \varepsilon^{-2} \mathbf{A}\, \mathbf{y} + \varepsilon^{-2} \mathbf{B}\, c(\mathbf{q}_s) \tag{4.26b}$$

$$\Omega_\perp = 4\alpha_2 \varepsilon^{-1} \mathbf{C}\, \mathbf{y}, \qquad \Omega_\parallel = \varepsilon^{-2} \tag{4.26c}$$

where $\mathbf{y} \in \mathbb{R}^2$, α_1 and α_2 are tuning parameters, and the matrices $\mathbf{A}, \mathbf{B}, \mathbf{C}$ are given by equations (4.10). The static part of this controller, i.e. equation (4.26a) is a 1D extremum seeking control law [28]. Note that other choices of this control law are possible [1]. The dynamic part of this controller, i.e. the equations (4.26b)-(4.26c), is a narrow band-pass filter centered around the frequency ε^{-2}.

In addition, assume that the distance r specifying the offset of the sensor from the center of the frame is such that $r = O(\varepsilon) = r_0 \varepsilon$ for some $r_0 > 0$. This assumption may seem artificial at first glance, though its implication is clear; we require that as the small parameter ε tends to 0, the distance r from the center of the vehicle is small enough so as not to amplify

unwanted nonlinearities in the signal strength field. Alternatively, one may consider this assumption as a "distinguished limit" [43] for the perturbation calculation in the presence of the two parameters ε and r. Under these assumptions, we have the following proposition:

Proposition 4.2.1. *Let Assumption* 4.2.1 *be satisfied, and let* $r = r_0\varepsilon^{-1}$. *Then, the compact subset* $\mathcal{S} = \{\mathbf{q}^*\} \times \mathrm{SO}(3)$ *is sSPUAS for the system defined by equations (4.5), (4.24), (4.7), and (4.26).*

Proof. Let $\mathbf{R}_0 = \exp\left(\varepsilon^{-2} t\, \widehat{\mathbf{e}}_1\right)$, $\mathbf{P} = \mathbf{R}\mathbf{R}_0^\intercal$, and compute:

$$\dot{\mathbf{P}} = \dot{\mathbf{R}}\mathbf{R}_0^\intercal + \mathbf{R}\dot{\mathbf{R}}_0^\intercal = \Omega_\perp \mathbf{R}\widehat{\mathbf{e}}_3\mathbf{R}_0^\intercal = \Omega_\perp \mathbf{P}\mathbf{R}_0\widehat{\mathbf{e}}_3\mathbf{R}_0^\intercal = \Omega_\perp \mathbf{P}\widehat{\mathbf{R}_0\mathbf{e}_3} \tag{4.27}$$

Let $\mathbf{\Lambda}(\mathbf{y}, \varepsilon^{-2}t) = 4\alpha_2 \mathbf{C}\,\mathbf{y}\,\mathbf{R}_0\mathbf{e}_3$ and observe that:

$$\dot{\mathbf{q}} = \mathbf{R}\mathbf{v} = \mathbf{R}\mathbf{R}_0^\intercal\mathbf{R}_0\mathbf{v} = v\,\mathbf{P}\mathbf{R}_0\mathbf{e}_1 = v\,\mathbf{P}\mathbf{e}_1 \tag{4.28}$$

$$\dot{\mathbf{P}} = \sqrt{\omega}\,\mathbf{P}\widehat{\mathbf{\Lambda}}(\mathbf{y}, \varepsilon^{-2}t) \tag{4.29}$$

To simplify the presentation, we embed SO(3) into $\mathbb{R}^9$ by partitioning the matrix $\mathbf{P} = [\mathbf{p}_1, \mathbf{p}_2, \mathbf{p}_3]$, and defining the state vector $\mathbf{p} = [\mathbf{p}_1^\intercal, \mathbf{p}_2^\intercal, \mathbf{p}_3^\intercal]^\intercal$. Restrict the initial conditions for $\mathbf{p}$ to lie on the compact submanifold $\mathcal{M} = \left\{\mathbf{p}_i \in \mathbb{R}^3 : \mathbf{p}_i^\intercal\mathbf{p}_j = \delta_{ij},\ \mathbf{p}_i \times \mathbf{p}_j = \epsilon_{ijk}\mathbf{p}_k\right\}$, where δ_{ij} is the Kronecker symbol and ϵ_{ijk} is the Levi-Civita symbol. On $\mathbb{R}^3 \times \mathcal{M} \times \mathbb{R}^2$, the system is governed by:

$$\dot{\mathbf{q}} = 2\alpha_1\varepsilon^{-1}\cos(2\varepsilon^{-2}t - c(\mathbf{q}_s))\,\mathbf{p}_1 \tag{4.30a}$$

$$\dot{\mathbf{p}}_i = \varepsilon^{-1}\sum_{j,k=1}^{3} \Lambda_j(\mathbf{y}, \varepsilon^{-2}t)\epsilon_{ijk}\mathbf{p}_k \tag{4.30b}$$

$$\dot{\mathbf{y}} = \varepsilon^{-2}\left(\mathbf{A}\,\mathbf{y} + \mathbf{B}\,c(\mathbf{q}_s)\right) \tag{4.30c}$$

The signal strength field can be expanded as a series in the small parameter $r = r_0\varepsilon$ using

Taylor's theorem:

$$c(\mathbf{q}_s) = c(\mathbf{q}) + r_0\varepsilon\,\nabla c(\mathbf{q})^\intercal(\cos(\omega t)\mathbf{p}_2 + \sin(\omega t)\mathbf{p}_3) + \varepsilon^2\boldsymbol{\rho}(\mathbf{q}, \mathbf{q}_s, \omega t, \varepsilon) \tag{4.31}$$

where the remainder $\boldsymbol{\rho}$ is Lipschitz continuous in all of its arguments. Now, observe that the system governed by the equations (4.30a)-(4.30c) belongs to the class of systems described by (3.24). Hence, we may employ Theorem 3.4.1 and Theorem 3.4.2 in analyzing the stability of the system. In order to proceed, the reduced order averaged system needs to be computed. Similar computations to the proof of Proposition 4.1.1 produce the system:

$$\begin{bmatrix} \dot{\bar{\mathbf{q}}} \\ \dot{\bar{\mathbf{p}}}_1 \\ \dot{\bar{\mathbf{p}}}_2 \\ \dot{\bar{\mathbf{p}}}_3 \end{bmatrix} = \begin{bmatrix} \alpha_1\bar{\mathbf{p}}_1\bar{\mathbf{p}}_1^\intercal\nabla c(\bar{\mathbf{q}}) \\ \alpha_2 r_0\left(\bar{\mathbf{p}}_2\bar{\mathbf{p}}_2^\intercal + \bar{\mathbf{p}}_3\bar{\mathbf{p}}_3^\intercal\right)\nabla c(\bar{\mathbf{q}}) \\ -\alpha_2 r_0\bar{\mathbf{p}}_1\bar{\mathbf{p}}_2^\intercal\nabla c(\bar{\mathbf{q}}) \\ -\alpha_2 r_0\bar{\mathbf{p}}_1\bar{\mathbf{p}}_3^\intercal\nabla c(\bar{\mathbf{q}}) \end{bmatrix} \tag{4.32}$$

which can be equivalently written as:

$$\dot{\bar{\mathbf{q}}} = \alpha_1 r_0\bar{\mathbf{P}}\mathbf{e}_1\mathbf{e}_1^\intercal\bar{\mathbf{P}}^\intercal\nabla c(\bar{\mathbf{q}}), \tag{4.33a}$$

$$\dot{\bar{\mathbf{P}}} = \alpha_2 r_0\bar{\mathbf{P}}\widehat{\bar{\boldsymbol{\Lambda}}}(\mathbf{q}, \mathbf{P}) \tag{4.33b}$$

where the average angular velocity vector $\bar{\boldsymbol{\Lambda}}$ is given by:

$$\bar{\boldsymbol{\Lambda}}(\mathbf{q}, \mathbf{P}) = \mathbf{P}^\intercal\nabla c(\mathbf{q}) \times \mathbf{e}_1 \tag{4.34}$$

We claim that the compact subset $\mathcal{S}$ is globally uniformly asymptotically stable for the reduced order averaged system (4.33). To prove this claim, we use the negative of the signal strength field as a Lyapunov function $V_c(\mathbf{q}) = c(\mathbf{q}^*) - c(\mathbf{q})$. Observe that the system (4.33) is autonomous, and so the function V_c is indeed a candidate Lyapunov function for the compact

subset $\mathcal{S}$ due to Assumption 4.2.1 [7]. We proceed to compute the derivative of V_c:

$$\dot{V}_c = -\alpha_1 \nabla c(\bar{\mathbf{q}})^\intercal \bar{\mathbf{P}} \mathbf{e}_1 \mathbf{e}_1^\intercal \bar{\mathbf{P}}^\intercal \nabla c(\bar{\mathbf{q}}) \leq 0 \tag{4.35}$$

Now, consider the subset $\mathcal{N} = \{(\mathbf{q}, \mathbf{P}) \in \mathbb{R}^3 \times \mathrm{SO}(3) : \dot{V}_c = 0\}$, and observe that $\mathcal{S} \subset \mathcal{N}$, and that $\mathcal{S}$ is an invariant subset of the reduced order averaged system (4.33). Suppose that a trajectory $(\bar{\mathbf{q}}(t), \bar{\mathbf{P}}(t))$ of the system (4.33) exists such that $(\bar{\mathbf{q}}(t), \bar{\mathbf{P}}(t)) \in \mathcal{N} \backslash \mathcal{S}$, $\forall t \in I$, where I is the maximal interval of existence and uniqueness of the trajectory. Such a trajectory must satisfy:

$$\nabla c(\bar{\mathbf{q}}(t))^\intercal \bar{\mathbf{P}}(t) \mathbf{e}_1 = 0, \quad \forall t \in I \tag{4.36}$$

The differentiability of the trajectories allows us to compute the derivative of this identity and obtain that:

$$\frac{d}{dt}\big(\nabla c(\bar{\mathbf{q}}(t))^\intercal \bar{\mathbf{P}}(t) \mathbf{e}_1\big) = 0, \quad \forall t \in I \tag{4.37}$$

which simplifies to:

$$\nabla c(\bar{\mathbf{q}}(t))^\intercal \bar{\mathbf{P}}(t) (\bar{\mathbf{\Lambda}}(\bar{\mathbf{q}}(t), \bar{\mathbf{P}}(t)) \times \mathbf{e}_1) = 0 \tag{4.38}$$

Recalling equation (4.34), we see that:

$$\bar{\mathbf{\Lambda}}(\bar{\mathbf{q}}(t), \bar{\mathbf{P}}(t)) \times \mathbf{e}_1 = (\mathrm{Id} - \mathbf{e}_1 \mathbf{e}_1^\intercal) \bar{\mathbf{P}}(t)^\intercal \nabla c(\bar{\mathbf{q}}(t)) = \bar{\mathbf{P}}(t)^\intercal \nabla c(\bar{\mathbf{q}}(t)) \tag{4.39}$$

Hence, the equation (4.38) necessitates that:

$$\|\nabla c(\bar{\mathbf{q}}(t))\|^2 = 0, \quad \forall t \in I \tag{4.40}$$

which is clearly in contradiction with Assumption 4.2.1. Accordingly, it follows from LaSalle's Invariance principle [7, Corollary 4.2 to Theorem 4.4] that the compact subset $\mathcal{S}$ is globally uniformly asymptotically stable for the system (4.33). Hence, we conclude by Theorem 3.4.2 that the subset $\mathcal{S}$ is singularly semi-globally practically uniformly asymptotically stable for the original system defined by (4.5)-(4.10). □

If we attempt to apply the framework of singularly pertubed Lie Bracket Approximation introduced in [4] to the system (4.30a)-(4.30c), then the quasi-steady state of the system will be $\mathbf{y} = [c(\mathbf{q}_s), c(\mathbf{q}_s)]^\intercal$. Hence, according to [4], the reduced order system is:

$$\dot{\mathbf{q}} = \sqrt{4\omega}\cos(2\omega t - c(\mathbf{q}_s))\,\mathbf{p}_1, \qquad \dot{\mathbf{p}}_i = 0 \tag{4.41}$$

which yields the Lie Bracket system:

$$\dot{\bar{\mathbf{q}}} = \bar{\mathbf{P}}\mathbf{e}_1\mathbf{e}_1^\intercal\bar{\mathbf{P}}^\intercal\nabla c(\bar{\mathbf{q}}), \qquad \dot{\bar{\mathbf{P}}} = 0 \tag{4.42}$$

It is clear that the compact subset $\mathcal{S}$ is not asymptotically stable for the Lie Bracket system (4.42), and so the framework in [4] is not suitable for proving the stability of the system (4.30a)-(4.30c).

We now demonstrate the behavior of the proposed algorithm through numerical simulations. In the following example, we have that: $r_0 = 1$, $\alpha_1 = 1$ and $\alpha_2 = 0.5$.

Example 4.2.1. Consider the signal strength field given by

$$c(\mathbf{q}) = \frac{10}{1 + 0.025\mathbf{q}^\intercal\mathbf{q}}, \tag{4.43}$$

which represents a stationary source located at the origin. We take the initial conditions as

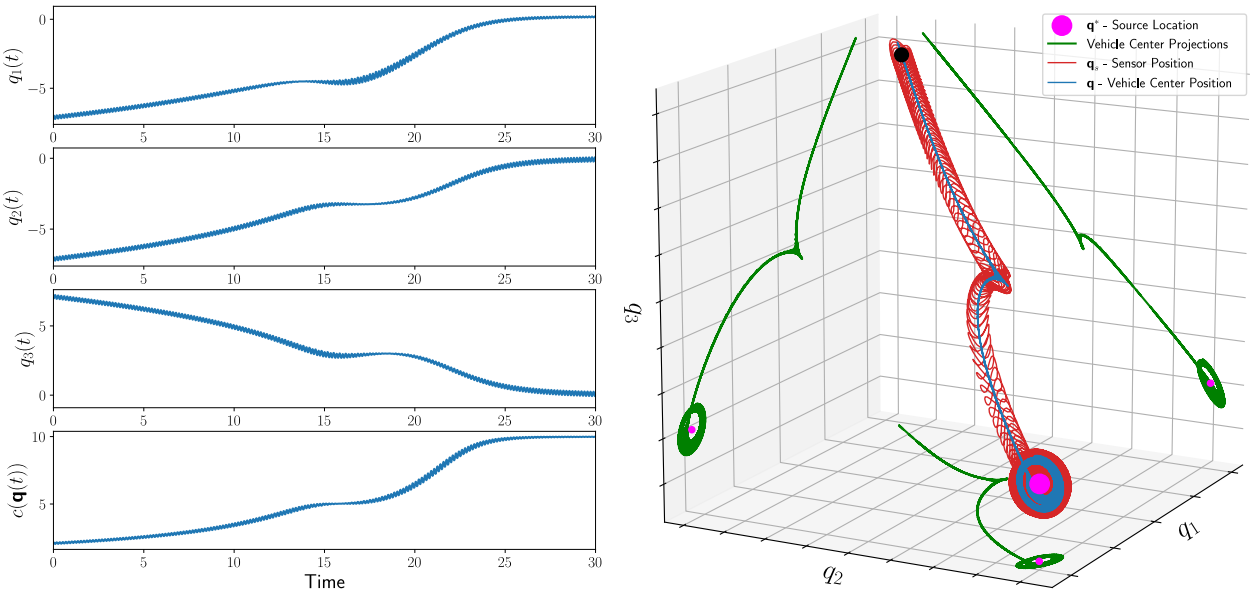

Figure 4.2: Numerical simulation results of the 3D source seeking algorithm for the non-collocated sensor case with oscillatory forward velocity: the history of the signal strength at the vehicle center and the position coordinates (left), and the 3D spatial trajectory with various projections (right)

$\mathbf{q}(0) = [-7, -7, 7]^\intercal$, $\mathbf{R}(0) = [\mathbf{r}_1, \mathbf{r}_2, \mathbf{r}_3]$ where the unit vectors $\mathbf{r}_k$ are given by:

$$\mathbf{r}_1 = -\frac{\nabla c(\mathbf{q}(0))}{\|\nabla c(\mathbf{q}(0))\|}, \qquad \mathbf{r}_2 = \frac{\mathbf{r}_1 \times \mathbf{e}_1}{\|\mathbf{r}_1 \times \mathbf{e}_1\|}, \qquad \mathbf{r}_3 = \mathbf{r}_1 \times \mathbf{r}_2, \tag{4.44}$$

$\mathbf{y}(0) = 0$, and the small parameter as $\varepsilon = 1/\sqrt{6\pi}$. We also take the parameters $\alpha_1 = r_0 = 1$ and $\alpha_2 = 1/2$.

The numerical simulations for the example are shown in figure 4.2. Observe that the behavior near the source is nontrivial, i.e. there is a small non-trivial attractor. However, this complex behavior does not appear in the reduced order averaged system and it can be made arbitrarily small by choosing a sufficiently small ε.

4.3 Helical 3D Source Seeking with Strictly Positive Forward Velocity

In the previous section, the forward velocity of the vehicle was considered as a control input and was employed in the design of the source seeking control law. As a consequence, the velocity was taken as an oscillatory signal, which may be positive or negative. Nevertheless, it may be desirable to maintain a strictly positive forward velocity for the vehicle. In this case, the algorithm of the previous subsection becomes obsolete and a different algorithm is needed. In this section, we tackle such a problem.

Recall that the 3D kinematics of a rigid body are given by:

$$\dot{\mathbf{q}} = \mathbf{R}\mathbf{v}, \qquad \dot{\mathbf{R}} = \mathbf{R}\widehat{\boldsymbol{\Omega}} \tag{4.45}$$

Let us assume a vehicle model in which the velocities in body coordinates are given by equations (4.24), such that the forward velocity $v = \alpha_1 > 0$ is strictly positive and constant, and the angular velocity components $\Omega_{\parallel}$ and $\Omega_{\perp}$ are treated as inputs. Suppose that the assumptions on the sensor location and the signal strength field stated in the previous sections are satisfied and consider the following control law:

$$\dot{z} = \varepsilon^{-1}(c(\mathbf{q}_s) - z) \tag{4.46a}$$

$$\dot{\mathbf{y}} = \varepsilon^{-2}\,\mathbf{A}\,\mathbf{y} + \varepsilon^{-2}\,\mathbf{B}\,c(\mathbf{q}_s) \tag{4.46b}$$

$$\Omega_{\perp} = 4\alpha_2\varepsilon^{-1}\,\mathbf{C}\,\mathbf{y} + 2\alpha_3\varepsilon^{-1}\cos(\varepsilon^{-2}t)\,(c(\mathbf{q}_s) - z), \qquad \Omega_{\parallel} = \varepsilon^{-2} \tag{4.46c}$$

where $z \in \mathbb{R}, \mathbf{y} \in \mathbb{R}^2$, α_i, $i \in \{1, 2, 3\}$ are tuning parameters, and the matrices $\mathbf{A}, \mathbf{B}, \mathbf{C}$ are given by equations (4.10).

Proposition 4.3.1. *In the limit $\varepsilon \to 0$, the trajectory $\boldsymbol{q}$ of the system (4.45) under the*

control law (4.46) converge to the trajectories of the following system:

$$\dot{\bar{\bar{\mathbf{q}}}} = \alpha_1 \bar{\bar{\mathbf{h}}}_1 \tag{4.47a}$$

$$\dot{\bar{\bar{\mathbf{h}}}}_1 = r_0\alpha_2 \left(\mathbf{I} - \bar{\bar{\mathbf{h}}}_1\bar{\bar{\mathbf{h}}}_1^\intercal\right) \nabla c(\bar{\bar{\mathbf{q}}}) + \alpha_1\alpha_3 \bar{\bar{\mathbf{h}}}_2\bar{\bar{\mathbf{h}}}_1^\intercal \nabla c(\bar{\bar{\mathbf{q}}}) \tag{4.47b}$$

$$\dot{\bar{\bar{\mathbf{h}}}}_2 = \alpha_1\alpha_3 \bar{\bar{\mathbf{h}}}_1\bar{\bar{\mathbf{h}}}_2^\intercal \nabla c(\bar{\bar{\mathbf{q}}}) - r_0\alpha_2 \left(\mathbf{I} - \bar{\bar{\mathbf{h}}}_2\bar{\bar{\mathbf{h}}}_2^\intercal\right) \nabla c(\bar{\bar{\mathbf{q}}}) \tag{4.47c}$$

Proof. Let $\mathbf{R}_0 = \exp\left(\varepsilon^{-2} t\, \widehat{\mathbf{e}}_1\right)$, $\mathbf{R}_1 = \exp\left(\alpha_3 z\, \widehat{\mathbf{e}}_3\right)$, $\mathbf{P} = \mathbf{R}\mathbf{R}_0^\intercal\mathbf{R}_1^\intercal$, and compute:

$$\dot{\mathbf{q}} = v\, \mathbf{R}\mathbf{e}_1 = v\, \mathbf{P}\mathbf{R}_1\mathbf{R}_0\mathbf{e}_1 \tag{4.48a}$$

$$\dot{\mathbf{P}} = \dot{\mathbf{R}}\mathbf{R}_0^\intercal\mathbf{R}_1^\intercal + \mathbf{R}\dot{\mathbf{R}}_0^\intercal\mathbf{R}_1^\intercal + \mathbf{R}\mathbf{R}_0^\intercal\dot{\mathbf{R}}_1^\intercal \tag{4.48b}$$

Now, observe that:

$$\dot{\mathbf{R}}\mathbf{R}_0^\intercal\mathbf{R}_1^\intercal = \varepsilon^{-2}\mathbf{P}\mathbf{R}_1\mathbf{R}_0\widehat{\mathbf{e}}_1\mathbf{R}_0^\intercal\mathbf{R}_1^\intercal + \Omega_\perp\mathbf{P}\mathbf{R}_1\mathbf{R}_0\widehat{\mathbf{e}}_3\mathbf{R}_0^\intercal\mathbf{R}_1^\intercal \tag{4.49}$$

$$\mathbf{R}\dot{\mathbf{R}}_0^\intercal\mathbf{R}_1^\intercal = -\varepsilon^{-2}\mathbf{P}\mathbf{R}_1\mathbf{R}_0\widehat{\mathbf{e}}_1\mathbf{R}_0^\intercal\mathbf{R}_1^\intercal \tag{4.50}$$

$$\mathbf{R}\mathbf{R}_0^\intercal\dot{\mathbf{R}}_1^\intercal = -\alpha_3\varepsilon^{-1}(c(\mathbf{q}_s) - z)\mathbf{P}\widehat{\mathbf{e}}_3 \tag{4.51}$$

In addition, direct computation shows that:

$$\begin{aligned}\Omega_\perp\mathbf{R}_1\mathbf{R}_0\mathbf{e}_3 = 4\alpha_2\varepsilon^{-1}\,\mathbf{C}\,\mathbf{y}\Big(&\sin(\varepsilon^{-2}t)(\sin(z)\mathbf{e}_1 - \cos(z)\mathbf{e}_2) + \cos(\varepsilon^{-2}t)\mathbf{e}_3\Big)\\ &+ \varepsilon^{-1}\alpha_3(c(\mathbf{q}_s) - z)\sin(2\varepsilon^{-2}t)(\cos(z)\mathbf{e}_2 - \sin(z)\mathbf{e}_1)\\ &+ \varepsilon^{-1}\alpha_3(c(\mathbf{q}_s) - z)\cos(2\varepsilon^{-2}t)\mathbf{e}_3 + \alpha_3\varepsilon^{-1}(c(\mathbf{q}_s) - z)\mathbf{e}_3\end{aligned} \tag{4.52}$$

Hence, we have that:

$$\dot{\mathbf{q}} = \alpha_1\, \mathbf{P}(\cos(z)\mathbf{e}_1 + \sin(z)\mathbf{e}_2), \tag{4.53a}$$

$$\dot{\mathbf{P}} = \varepsilon^{-1}\mathbf{P}\widehat{\mathbf{\Lambda}}(\mathbf{y}, z, \varepsilon^{-2}t) \tag{4.53b}$$

$$\dot{z} = \varepsilon^{-1}(c(\mathbf{q}_s) - z) \tag{4.53c}$$

$$\dot{\mathbf{y}} = \varepsilon^{-2}\,\mathbf{A}\,\mathbf{y} + \varepsilon^{-2}\,\mathbf{B}\,c(\mathbf{q}_s) \tag{4.53d}$$

where the angular velocity vector $\mathbf{\Lambda}$ is given by:

$$\begin{aligned}\mathbf{\Lambda}(\mathbf{y}, z, \varepsilon^{-2}t) = 4\alpha_2\mathbf{C}\,\mathbf{y}\Big(\,&\sin(\varepsilon^{-2}t)(\sin(z)\mathbf{e}_1 - \cos(z)\mathbf{e}_2) + \cos(\varepsilon^{-2}t)\mathbf{e}_3\Big)\\ &+ \alpha_3(c(\mathbf{q}_s) - z)\Big(\sin(2\varepsilon^{-2}t)(\cos(z)\mathbf{e}_2 - \sin(z)\mathbf{e}_1) + \cos(2\varepsilon^{-2}t)\mathbf{e}_3\Big)\end{aligned} \tag{4.54}$$

and the sensor location $\mathbf{q}_s$ is given by:

$$\mathbf{q}_s = \mathbf{q} + r\,\mathbf{P}\mathbf{R}_1\mathbf{R}_0\mathbf{e}_2 = \mathbf{q} + r\,\mathbf{P}\big(\cos(\varepsilon^{-2}t)(\cos(z)\mathbf{e}_2 - \sin(z)\mathbf{e}_1) + \sin(\varepsilon^{-2}t)\mathbf{e}_3\big) \tag{4.55}$$

Furthermore, we embed SO(3) into $\mathbb{R}^9$ once again by partitioning the matrix $\mathbf{P} = [\mathbf{p}_1,\, \mathbf{p}_2,\, \mathbf{p}_3]$, and defining the state vector $\mathbf{p} = [\mathbf{p}_1^\intercal,\, \mathbf{p}_2^\intercal,\, \mathbf{p}_3^\intercal]^\intercal$. In the new coordinates, the system is governed by:

$$\dot{\mathbf{q}} = \alpha_1\,(\cos(z)\mathbf{p}_1 + \sin(z)\mathbf{p}_2), \tag{4.56a}$$

$$\dot{\mathbf{p}}_i = \varepsilon^{-1}\sum_{j,k=1}^{3}\Lambda_j(\mathbf{y}, z, \varepsilon^{-2}t)\epsilon_{ijk}\mathbf{p}_k \tag{4.56b}$$

$$\dot{z} = \varepsilon^{-1}(c(\mathbf{q}_s) - z) \tag{4.56c}$$

$$\dot{\mathbf{y}} = \varepsilon^{-2}\,(\mathbf{A}\,\mathbf{y} + \,\mathbf{B}\,c(\mathbf{q}_s)) \tag{4.56d}$$

As in the previous section, we may expand $c(\mathbf{q}_s)$ as a Taylor series in the small parameter $r = r_0\varepsilon$ to obtain:

$$c(\mathbf{q}_s) = c(\mathbf{q}) + r_0\varepsilon\,\big(\cos(\varepsilon^{-2}t)(\cos(z)\mathbf{p}_2 - \sin(z)\mathbf{p}_1) + \sin(\varepsilon^{-2}t)\mathbf{p}_3\big)^\intercal\nabla c(\mathbf{q}) + O(\varepsilon^2) \tag{4.57}$$

By substituting for $c(\mathbf{q}_s)$ with its Taylor expansion, we obtain a system that belongs to the class of systems on the form (3.41). Therefore, we may employ Theorem 3.5.1 to approximate

the trajectories of the system. In order to proceed, we need to compute the reduced order recursively averaged system. First, we observe that the quasi-steady states for the singularly perturbed part of the system $z, \mathbf{y}$ are given by $\boldsymbol{\phi}_0(\mathbf{q}, \mathbf{p}) = c(\mathbf{q})$, $\boldsymbol{\varphi}_0(\mathbf{q}, \mathbf{p}, z) = c(\mathbf{q})\mathbb{1}$. Using the formulas provided in Appendix E, we obtain the following reduced order recursively averaged system:

$$\dot{\bar{\bar{\mathbf{q}}}} = \alpha_1 \cos(\alpha_3 c(\bar{\bar{\mathbf{q}}}))\bar{\bar{\mathbf{p}}}_1 + \alpha_1 \sin(\alpha_3 c(\bar{\bar{\mathbf{q}}}))\bar{\bar{\mathbf{p}}}_2 \tag{4.58a}$$

$$\dot{\bar{\bar{\mathbf{p}}}}_1 = r_0\alpha_2 \cos(\alpha_3 c(\bar{\bar{\mathbf{q}}}))\big(\mathbf{I} - \bar{\bar{\mathbf{p}}}_1\bar{\bar{\mathbf{p}}}_1^\intercal\big)\nabla c(\bar{\bar{\mathbf{q}}}) - r_0\alpha_2 \sin(\alpha_3 c(\bar{\bar{\mathbf{q}}}))\bar{\bar{\mathbf{p}}}_2\bar{\bar{\mathbf{p}}}_1^\intercal\nabla c(\bar{\bar{\mathbf{q}}}) \tag{4.58b}$$

$$\dot{\bar{\bar{\mathbf{p}}}}_2 = r_0\alpha_2 \cos(\alpha_3 c(\bar{\bar{\mathbf{q}}}))\bar{\bar{\mathbf{p}}}_1\bar{\bar{\mathbf{p}}}_2^\intercal\nabla c(\bar{\bar{\mathbf{q}}}) - r_0\alpha_2 \sin(\alpha_3 c(\bar{\bar{\mathbf{q}}}))\big(\mathbf{I} - \bar{\bar{\mathbf{p}}}_2\bar{\bar{\mathbf{p}}}_2^\intercal\big)\nabla c(\bar{\bar{\mathbf{q}}}) \tag{4.58c}$$

$$\dot{\bar{\bar{\mathbf{p}}}}_3 = r_0\alpha_2 \sin(\alpha_3 c(\bar{\bar{\mathbf{q}}}))\bar{\bar{\mathbf{p}}}_2\bar{\bar{\mathbf{p}}}_3^\intercal\nabla c(\bar{\bar{\mathbf{q}}}) + r_0\alpha_2 \cos(\alpha_3 c(\bar{\bar{\mathbf{q}}}))\bar{\bar{\mathbf{p}}}_1\bar{\bar{\mathbf{p}}}_3^\intercal\nabla c(\bar{\bar{\mathbf{q}}}) \tag{4.58d}$$

The result of the proposition follows after we perform the following change of coordinates:

$$\bar{\bar{\mathbf{h}}}_1 = \cos(\alpha_3 c(\bar{\bar{\mathbf{q}}}))\bar{\bar{\mathbf{p}}}_1 + \sin(\alpha_3 c(\bar{\bar{\mathbf{q}}}))\bar{\bar{\mathbf{p}}}_2, \tag{4.59a}$$

$$\bar{\bar{\mathbf{h}}}_2 = \sin(\alpha_3 c(\bar{\bar{\mathbf{q}}}))\bar{\bar{\mathbf{p}}}_1 - \cos(\alpha_3 c(\bar{\bar{\mathbf{q}}}))\bar{\bar{\mathbf{p}}}_2 \tag{4.59b}$$

□

The stability of the system given by (4.47) is very intricate; there is a complex attractor near the source whose size does not diminish in the limit $\varepsilon \to 0$. We leave a detailed analysis of this attractor and its stability for future work. Instead, we provide here numerical examples illustrating the behavior of the system.

Example 4.3.1. Consider the signal strength field given by

$$c(\mathbf{q}) = \frac{10}{1 + 0.025\mathbf{q}^\intercal\mathbf{q}}, \tag{4.60}$$

which represents a stationary source located at the origin. We take the initial conditions as

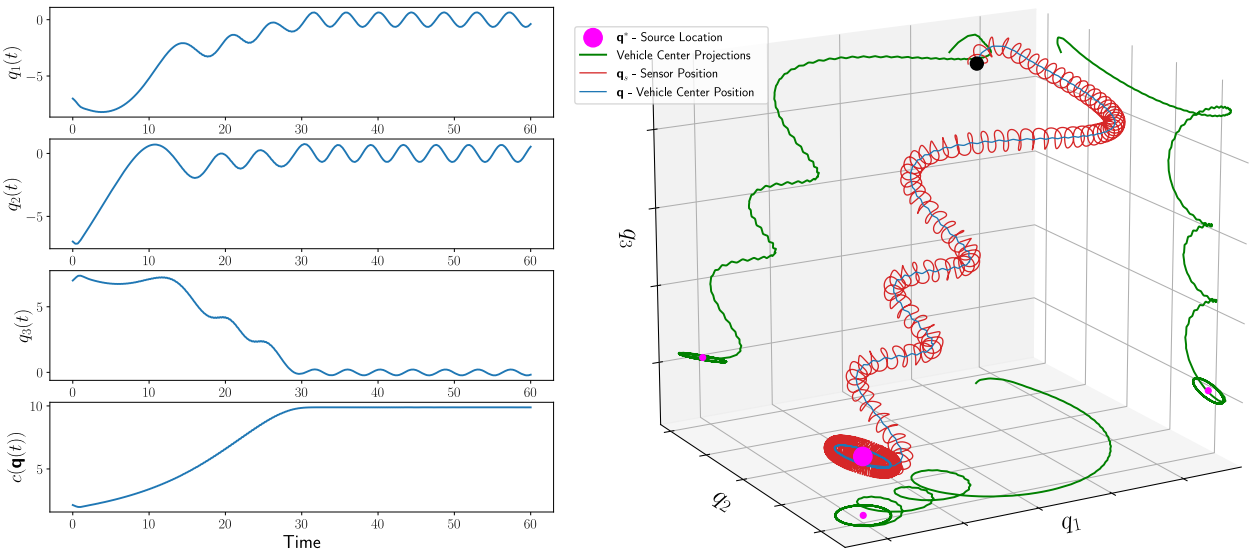

Figure 4.3: Numerical simulation results of the 3D source seeking algorithm for the non-collocated sensor case with strictly positive forward velocity: the history of the signal strength at the vehicle center and the position coordinates (left), and the 3D spatial trajectory with various projections (right)

$\mathbf{q}(0) = [-7, -7, 7]^\intercal$, $\mathbf{R}(0) = [\mathbf{r}_1, \mathbf{r}_2, \mathbf{r}_3]$ where the unit vectors $\mathbf{r}_k$ are given by:

$$\mathbf{r}_1 = -\frac{\nabla c(\mathbf{q}(0))}{\|\nabla c(\mathbf{q}(0))\|}, \qquad \mathbf{r}_2 = \frac{\mathbf{r}_1 \times \mathbf{e}_1}{\|\mathbf{r}_1 \times \mathbf{e}_1\|}, \qquad \mathbf{r}_3 = \mathbf{r}_1 \times \mathbf{r}_2, \tag{4.61}$$

$\mathbf{y}(0) = \mathbb{1}c(\mathbf{q}(0))$, $z(0) = c(\mathbf{q}(0))$, and the small parameter as $\varepsilon = 1/\sqrt{6\pi}$. Moreover, we take the parameters $\alpha_1 = \alpha_2 = \alpha_3 = r_0 = 1$.

The numerical simulations for the example are shown in figure 4.3. The size of the attractor can be made small by tuning the parameters $\alpha_1, \alpha_2, \alpha_3$, which are controller parameters.

4.4 Spherical 3D Source Seeking

In this section, we consider an alternative 3D source seeking algorithm that, unlike the previous algorithms, works for the case of a collocated sensor. The algorithm proposed here is named 'spherical' due to the nature of the trajectory in 3D space as will be clear later in

the numerical examples towards the end of the section.

The 3D kinematics of a rigid body are given by

$$\dot{\mathbf{q}} = \mathbf{R}\mathbf{v}, \qquad \dot{\mathbf{R}} = \mathbf{R}\widehat{\mathbf{\Omega}} \tag{4.62}$$

We consider a vehicle model in which the velocity $\mathbf{v}$ and angular velocity $\mathbf{\Omega}$ are given by:

$$\mathbf{v} = 2\,\varepsilon^{-1}\,\mathbf{e}_1, \qquad \mathbf{\Omega} = \Omega_{\|}\mathbf{e}_1 + \Omega_{\perp}\mathbf{e}_3 \tag{4.63}$$

where $\Omega_{\|}$ and $\Omega_{\perp}$ are the control inputs, which represent roll and yaw of the body frame, respectively, and ω is a positive parameter. This model is a natural extension of the unicycle model to the 3D setting. It is well known that this system is controllable using depth one Lie brackets [45].

Let $c \in C^2(\mathbb{R}^3;\mathbb{R})$ represent the signal strength field and define the control inputs $\Omega_{\|}$ and $\Omega_{\perp}$ by the dynamic time periodic feedback law:

$$\varepsilon^2\,\dot{z} = c(\mathbf{q}) - z \tag{4.64}$$

$$\Omega_{\perp}(c(\mathbf{q}), z) = \varepsilon^{-2} - \dot{z} \tag{4.65}$$

$$\Omega_{\|}(z, \varepsilon^{-2}t) = 2\alpha\varepsilon^{-1}\sin\left(\varepsilon^{-2}t - z\right) \tag{4.66}$$

where $\varepsilon > 0$, and $\alpha > 0$ are constant parameters.

Remark 4.4.1. *When the motion is confined to the plane (i.e. $\alpha = 0$), this control law is the same as the source seeking algorithm for the unicycle model introduced in [28], which also turns out to be the same algorithm employed by sea urchin sperm cells for seeking the egg in 2D [46]. Here we extend the controller to the 3D setting and establish its practical stability. We emphasize that the 2D source seeking algorithm in [28] does not work directly in 3D.*

Assumption 4.4.1. *Suppose that the signal strength field $c \in C^2(\mathbb{R}^3;\mathbb{R})$ is radially unbounded, $\exists! \boldsymbol{q}^* \in \mathbb{R}^3$ such that $\nabla c(\boldsymbol{q}) = 0 \iff \boldsymbol{q} = \boldsymbol{q}^*$, and for some constant $\kappa > 0$, it satisfies the inequality:*

$$c(\boldsymbol{q}^*) - c(\boldsymbol{q}) \leq \kappa \|\nabla c(\boldsymbol{q})\|^2, \, \forall \boldsymbol{q} \in \mathbb{R}^n \tag{4.67}$$

Then, we have the following theorem:

Theorem 4.4.1. *Let Assumption* 4.4.1 *be satisfied. Then, the compact subset $\{\boldsymbol{q}^*\} \times SO(3)$ is singularly semi-globally practically uniformly asymptotically stable for the control system defined by (4.62)-(4.63) under the dynamic feedback law defined by (4.64)-(4.66).*

Proof. Define $\tau = \varepsilon^{-2}t, \; \sigma = \varepsilon^{-1}t$, and the intermediate rotation $\mathbf{P} = \mathbf{R}\mathbf{R}_1^\intercal \mathbf{R}_2^\intercal$, where:

$$\mathbf{R}_1 = \exp\left((\tau - z)\widehat{\mathbf{e}}_3\right), \qquad \dot{\mathbf{R}}_1 = (\varepsilon^{-2} - \dot{z})\mathbf{R}_1\widehat{\mathbf{e}}_3 \tag{4.68a}$$

$$\mathbf{R}_2 = \exp\left(\alpha\,\sigma\,\widehat{\mathbf{e}}_2\right), \qquad \dot{\mathbf{R}}_2 = \varepsilon^{-1}\alpha\,\mathbf{R}_1\widehat{\mathbf{e}}_2 \tag{4.68b}$$

Then, compute:

$$\dot{\mathbf{P}} = \dot{\mathbf{R}}\mathbf{R}_1^\intercal\mathbf{R}_2^\intercal + \mathbf{R}\dot{\mathbf{R}}_1^\intercal\mathbf{R}_2^\intercal + \mathbf{R}\mathbf{R}_1^\intercal\dot{\mathbf{R}}_2^\intercal \tag{4.69}$$

In addition, observe that:

$$\dot{\mathbf{R}}\mathbf{R}_1^\intercal\mathbf{R}_2^\intercal = \mathbf{P}\mathbf{R}_2\mathbf{R}_1\left(\Omega_\parallel\widehat{\mathbf{e}}_1 + \Omega_\perp\widehat{\mathbf{e}}_3\right)\mathbf{R}_1^\intercal\mathbf{R}_2^\intercal \tag{4.70a}$$

$$\mathbf{R}\dot{\mathbf{R}}_1^\intercal\mathbf{R}_2^\intercal = -\mathbf{P}\mathbf{R}_2\mathbf{R}_1\left(\Omega_\perp\widehat{\mathbf{e}}_3\right)\mathbf{R}_1^\intercal\mathbf{R}_2^\intercal \tag{4.70b}$$

$$\mathbf{R}\mathbf{R}_1^\intercal\dot{\mathbf{R}}_2^\intercal = -\varepsilon^{-1}\alpha\,\mathbf{P}\mathbf{R}_2\widehat{\mathbf{e}}_2\mathbf{R}_2^\intercal \tag{4.70c}$$

Direct computation shows that:

$$\Omega_{\|}\mathbf{R}_1\mathbf{e}_1 = \varepsilon^{-1}\alpha\,\mathbf{e}_2 - \varepsilon^{-1}\alpha\,\sin(2(z-\tau))\mathbf{e}_1 - \varepsilon^{-1}\alpha\,\cos(2(z-\tau))\mathbf{e}_2 \tag{4.71}$$

Hence, we have that:

$$\dot{\mathbf{P}} = \varepsilon^{-1}\,\mathbf{P}\widehat{\mathbf{\Lambda}}(z,\sigma,\tau) \tag{4.72}$$

where

$$\mathbf{\Lambda}(z,\sigma,\tau) = -\alpha\,\sin(2(z-\tau))(\cos(\alpha\,\sigma)\mathbf{e}_1 - \sin(\alpha\,\sigma)\mathbf{e}_3) - \alpha\,\cos(2(z-\tau))\mathbf{e}_2 \tag{4.73}$$

Furthermore, the position kinematics evolves according to the equations:

$$\dot{\mathbf{q}} = \varepsilon^{-1}\mathbf{P}\mathbf{f}(z,\sigma,\tau), \qquad\qquad \mathbf{f}(z,\sigma,\tau) = 2\,\mathbf{R}_2\mathbf{R}_1\mathbf{e}_1 \tag{4.74}$$

Consequently, in the new coordinates, the system is governed by:

$$\dot{\mathbf{q}} = \varepsilon^{-1}\sqrt{2}\,\mathbf{P}\mathbf{f}(z,\sigma,\tau), \qquad \dot{\mathbf{P}} = \varepsilon^{-1}\mathbf{P}\widehat{\mathbf{\Lambda}}(z,\sigma,\tau), \qquad \dot{z} = \varepsilon^{-2}\,(c(\mathbf{q}) - z) \tag{4.75a}$$

We embed the manifold SO(3) into $\mathbb{R}^3 \times \mathbb{R}^3 \times \mathbb{R}^3$ by partitioning the matrix $\mathbf{P}$ into column vectors $\mathbf{P} = [\mathbf{p}_1,\, \mathbf{p}_2,\, \mathbf{p}_3]$. Observe that:

$$\dot{\mathbf{P}} = \mathbf{P}\widehat{\mathbf{\Lambda}} = \mathbf{P}\widehat{\mathbf{\Lambda}}\mathbf{P}^{\intercal}\mathbf{P} = \widehat{\mathbf{P}\mathbf{\Lambda}\mathbf{P}} \tag{4.76}$$

and so it is easy to see that the time evolution of the columns of $\mathbf{P}$ is governed by:

$$\frac{d\mathbf{p}_j}{dt} = \varepsilon^{-1}\sum_{i=1}^{3}\Lambda_i(z,\sigma,\tau)\,\mathbf{p}_i \times \mathbf{p}_j, \qquad\qquad j \in \{1,2,3\} \tag{4.77}$$

Next, define the state vector $\mathbf{x} \in \mathbb{R}^{12}$ by $\mathbf{x} = [\mathbf{q}^\intercal,\, \mathbf{p}_1^\intercal,\, \mathbf{p}_2^\intercal,\, \mathbf{p}_3^\intercal]^\intercal$, and the vector field $\mathbf{X}$ which is given in coordinates by:

$$\mathbf{X}(\mathbf{x}, z, \sigma, \tau) = \begin{bmatrix} \sum_{i}^{3} f_i(z, \sigma, \tau)\mathbf{p}_i \\ \sum_{i,k}^{3} \Lambda_i(z, \sigma, \tau)\epsilon_{i1k}\mathbf{p}_k \\ \sum_{i,k}^{3} \Lambda_i(z, \sigma, \tau)\epsilon_{i2k}\mathbf{p}_k \\ \sum_{i,k}^{3} \Lambda_i(z, \sigma, \tau)\epsilon_{i3k}\mathbf{p}_k \end{bmatrix} \tag{4.78}$$

where ϵ_{ijk} is the Levi-Civita symbol. Restrict the initial conditions to lie on the manifold $\mathcal{M} = \{(\mathbf{x}, z) \in \mathbb{R}^{13} \,|\, \mathbf{p}_i^\intercal \mathbf{p}_j = \delta_{ij},\ \mathbf{p}_i \times \mathbf{p}_j = \epsilon_{ijk}\mathbf{p}_k\}$, where δ_{ij} is the Kronecker symbol. With this embedding, the kinematics can be written succinctly as:

$$\dot{\mathbf{x}} = \varepsilon^{-1}\mathbf{X}(\mathbf{x}, z, \sigma, \tau) \tag{4.79}$$

$$\dot{z} = \varepsilon^{-2}(c(\mathbf{q}) - z) \tag{4.80}$$

which is a system that belongs to the class of systems on the form (3.41). Therefore, we may employ the formulas. Hence, we may apply Theorem 3.5.1 and Theorem 3.5.2 to investigate the stability properties of the system. To proceed, we need to compute the reduced order recursively averaged (RORA) system. We observe that the quasi-steady state $\boldsymbol{\varphi}_0 = c(\mathbf{q})$ is a scalar, and therefore the vector-valued map $\mathbf{b}_{\boldsymbol{\varphi},1}$, which appears on the RHS of equation (3.57), is also a scalar and is given by:

$$b_{\boldsymbol{\varphi},1} = -\sum_{k=1}^{3} f_k(c(\mathbf{q}), \sigma, \tau)\mathbf{p}_k^\intercal \nabla c(\mathbf{q}) \tag{4.81}$$

Proceeding to compute the first-order correction term $\boldsymbol{\varphi}_1$ to the quasi-steady state, we obtain:

$$\varphi_1(\mathbf{x}, \sigma, \tau) = -\frac{1}{1 - \mathrm{e}^{-2\pi}} \int_0^{2\pi} \sum_{k=1} \mathrm{e}^{\nu - 2\pi} f_k(c(\mathbf{q}), \sigma, \tau + \nu)\mathbf{p}_k^\intercal \nabla c(\mathbf{q}) \tag{4.82}$$

Substituting into the formulas in Appendix E, and computing the average, we obtain the reduced order recursively averaged system: By changing the coordinates back, we obtain:

$$\dot{\bar{\bar{\mathbf{q}}}} = \bar{\bar{\mathbf{P}}}\mathbf{Q}\bar{\bar{\mathbf{P}}}^{\intercal}\nabla c(\bar{\bar{\mathbf{q}}}), \qquad \dot{\bar{\bar{\mathbf{P}}}} = \mathbf{0}, \qquad \bar{\bar{z}} = c(\bar{\bar{\mathbf{q}}}) \tag{4.83}$$

where the matrix $\mathbf{Q}$ is given by:

$$\mathbf{Q} = \begin{bmatrix} \frac{1}{2} & 0 & 0 \\ 0 & 1 & 0 \\ 0 & 0 & \frac{1}{2} \end{bmatrix} \tag{4.84}$$

The compact subset $\mathcal{S} = \{(\mathbf{q}, \mathbf{P}) : \quad \mathbf{q} = \mathbf{q}^*\}$ is globally uniformly asymptotically stable for the dynamics defined by (4.83). This is easy to see since the matrix $\bar{\bar{\mathbf{P}}}\mathbf{A}\bar{\bar{\mathbf{P}}}^{\intercal}$ is positive definite $\forall \bar{\bar{\mathbf{P}}} \in \mathrm{SO}(3)$, and $\bar{\bar{\mathbf{P}}}$ does not change. Reverting back to $\bar{\bar{\mathbf{R}}}$ from $\bar{\bar{\mathbf{P}}}$ will not affect this stability result. Therefore, we conclude using Theorem 3.5.2 that the compact subset $\mathcal{S}$ is s-SPUAS, which concludes the proof. □

We now provide a numerical example illustrating the behavior of the algorithm proposed in this section.

Example 4.4.1. Consider the signal strength field given by

$$c(\mathbf{q}) = \frac{10}{1 + 0.025\mathbf{q}^{\intercal}\mathbf{q}}, \tag{4.85}$$

which represents a stationary source located at the origin. We take the initial conditions as $\mathbf{q}(0) = [-7, -7, 7]^{\intercal}$, $\mathbf{R}(0) = [\mathbf{r}_1, \mathbf{r}_2, \mathbf{r}_3]$ where the unit vectors $\mathbf{r}_k$ are given by:

$$\mathbf{r}_1 = -\frac{\nabla c(\mathbf{q}(0))}{\|\nabla c(\mathbf{q}(0))\|}, \qquad \mathbf{r}_2 = \frac{\mathbf{r}_1 \times \mathbf{e}_1}{\|\mathbf{r}_1 \times \mathbf{e}_1\|}, \qquad \mathbf{r}_3 = \mathbf{r}_1 \times \mathbf{r}_2, \tag{4.86}$$

$z(0) = c(\mathbf{q}(0))$, and the small parameter as $\varepsilon = 1/\sqrt{6\pi}$. Moreover, we take the parameter

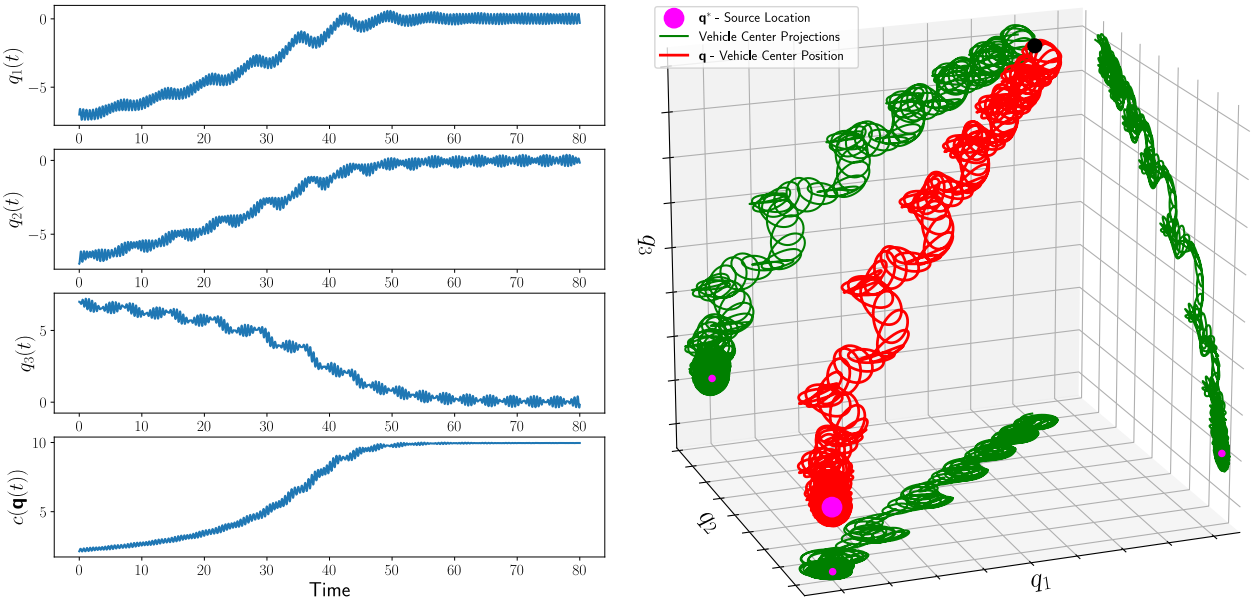

Figure 4.4: Numerical simulation results of the 3D source seeking algorithm for the collocated sensor case with strictly positive forward velocity: the history of the signal strength at the vehicle center and the position coordinates (left), and the 3D spatial trajectory with various projections (right)

$\alpha = 1/4$. The simulation results are shown in figure 4.4. Clearly, the location of the source is asymptotically stable as predicted by our analysis.

Chapter 5

Helical Klinotaxis and Source Seeking

Many organisms are routinely faced with the source seeking problem [31]. A well studied example is that of sperm chemotaxis [47, 48]. To locate an egg in open water, sea urchin sperm evolved to swim up the gradient of the concentration field established by the diffusion of a species-specific chemoattractant, a sperm-activating peptide (SAP), secreted by the eggs [48]. Unlike the inherently stochastic bacterial chemotaxis [49], the navigation strategy of sea urchin sperm can be reasonably described in a deterministic fashion; the cells employ the mean curvature of the flagellum, regulated by intracellular Ca^{2+}, as a steering mechanism to swim in circular paths that drift in the direction of the gradient in 2D, and in helical paths that align with the gradient in 3D [50, 47, 51, 52]. This feedback mechanism is mediated by a complex signaling pathway that regulates the influx and efflux of Ca^{2+} in the cell [53, 54].

In this chapter, we revisit sperm chemotaxis from the perspective of control theory. We frame the search for the egg as a source seeking problem, then we show that the 3D navigation strategy of sea urchin sperm, also known as helical klinotaxis, is in fact a natural implementation of the well-established adaptive control paradigm known as extremum seeking [31, 55, 28].

We illustrate this novel connection by establishing a one-to-one correspondence between the key components of the navigation strategy of sea urchin sperm cells and the hallmark features of an extremum seeking solution to the source seeking problem, which are: i) the injection of periodic perturbation signals to sample the local signal strength, ii) a filter that measures the instantaneous signal strength and extracts the oscillations due to the perturbation signals, iii) the demodulation of the local gradient information from the filter's output, and iv) an integrator that biases the motion in the direction of the gradient [2]. More specifically, we show that the swimming pattern of sea urchin sperm provides the roles of the periodic perturbation, demodulation, and integration components of the standard extremum seeking loop (figure 5.2). As such, the proposed formulation automatically suggests characterizing the chemotactic signaling pathway as an adaptive band pass filter attuned to the frequency of the swimming pattern of the sperm cell. In this manner, the swimming kinematics of sea urchin sperm, together with the signaling pathway, naturally constitute an extremum seeking strategy for chemotaxis.

Based on this formulation, we propose a coarse-grained minimal dynamical description that captures the crucial features of the chemotactic signaling pathway, including the peculiar behavior of sea urchin sperm cells where they seem to switch between two distinct navigation modes: i) the 'on-response' which is a low-gain steering mode when the average velocity vector of the cell is mostly aligned with the gradient, and ii) the 'off-response' which is a high-gain steering mode otherwise [52]. Previous models employed a threshold-based switching logic to account for this behavior [52]. The threshold defining the discontinuous switching boundary was later determined as the solution to an optimal decision problem [56]. Here, we show that the behavior can arise from a continuous dynamical description in a simpler way: it arises as a consequence of the motion pattern and a time-scale separation between the proposed dynamics of the signaling pathway and the average motion. In particular, the proposed model does not exploit any information other than the perceived instantaneous local concentration.

5.1 Modeling the sperm motion

Swimming in a low Reynolds number is dominated by viscous forces, which enables the use of kinematic models as a good approximation to the motion of micro-swimmers, including sperm cells [57]. The kinematics of a rigid body are given by:

$$\dot{\mathbf{x}} = \mathbf{R}\mathbf{v}, \qquad \dot{\mathbf{R}} = \mathbf{R}\widehat{\boldsymbol{\omega}}, \tag{5.1}$$

where the vectors $\mathbf{v}$ and $\boldsymbol{\omega}$ are the linear and angular velocity vectors in the body frame, $\widehat{\boldsymbol{\omega}}$ denotes the skew-symmetric matrix corresponding to the angular velocity vector $\boldsymbol{\omega}$, $\mathbf{x}$ is the instantaneous position of the body with respect to the origin of a fixed frame of reference, and $\mathbf{R}$ is the instantaneous rotation matrix that relates the body frame to the fixed frame. In sea urchin sperm, the mean curvature of the flagellar beating pattern, which is regulated by the chemotactic signaling pathway, controls the angular velocities in the body frame [50, 48]. A common model of the effect of the chemotactic signaling pathway on the swimming kinematics of sea urchin sperm is given by the relations:

$$\mathbf{v} = \begin{bmatrix} v & 0 & 0 \end{bmatrix}^\intercal, \qquad \boldsymbol{\omega} = \begin{bmatrix} \omega_\parallel & 0 & \omega_\perp \end{bmatrix}^\intercal, \tag{5.2}$$

where $v > 0$ is constant, and the angular velocity components $\omega_\parallel$ and $\omega_\perp$ are given by:

$$\omega_\parallel = \omega_{\parallel 0} + \omega_{\parallel 1}\eta, \qquad \omega_\perp = \omega_{\perp 0} + \omega_{\perp 1}\eta, \tag{5.3}$$

with $\omega_{\perp 0}, \omega_{\perp 1}, \omega_{\parallel 0}, \omega_{\parallel 1}$ as constant coefficients, and η is a dynamic feedback term representing the effect of the signaling pathway [58, 47, 52].

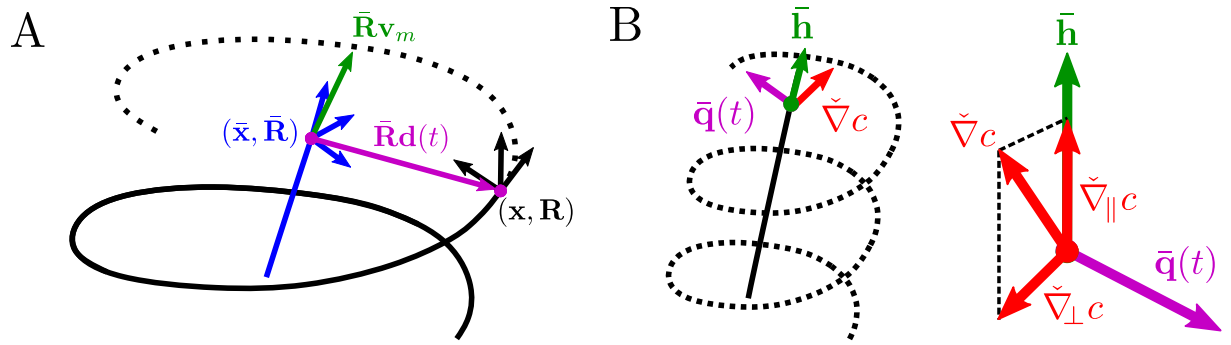

Figure 5.1: The geometry of helical swimming. **A**: the helical nature of the trajectory suggests decomposing the motion $(\mathbf{x}, \mathbf{R})$ into an average part along the helical centerline $(\bar{\mathbf{x}}, \bar{\mathbf{R}})$ and a periodic excursion $\bar{\mathbf{R}}\mathbf{d}(t)$ that is orthogonal to the centerline. **B**: the direction of the gradient $\check{\nabla}c$ can be decomposed into two parts, one along the helical centerline $\bar{\mathbf{h}}$ (denoted as $\check{\nabla}_{\parallel}c$), and another orthogonal to it (denoted as $\check{\nabla}_{\perp}c$) which is contained in the same plane as the direction $\bar{\mathbf{q}}(t)$ of the periodic excursion $\bar{\mathbf{R}}\mathbf{d}(t)$.

5.2 An extremum seeking loop

The constant forward velocity $v > 0$, along with the constant angular velocity components $\omega_{\parallel 0}$ and $\omega_{\perp 0}$, lead to a periodic swimming pattern, a helical trajectory. The sign of $\omega_{\parallel 0}$ and $\omega_{\perp 0}$ determine the handedness of the helical trajectory. For simplicity, we consider the case in which both $\omega_{\parallel 0}$ and $\omega_{\perp 0}$ are positive. The geometry of helical swimming (see figure 5.1A) suggests decomposing the motion into an average part and an oscillatory part. We define the average instantaneous position $\bar{\mathbf{x}}$ and orientation $\bar{\mathbf{R}}$ of the cell as:

$$\mathbf{R}_0(t) = \exp\big(\widehat{\boldsymbol{\omega}}_0 t\big), \quad \bar{\mathbf{R}} = \mathbf{R}\mathbf{R}_0(t)^{\intercal}, \tag{5.4a}$$

$$\bar{\mathbf{x}} = \mathbf{x} - \bar{\mathbf{R}}\mathbf{d}(t), \tag{5.4b}$$

where the vector $\boldsymbol{\omega}_0$ is given by:

$$\boldsymbol{\omega}_0 = \begin{bmatrix} \omega_{\parallel 0} & 0 & \omega_{\perp 0} \end{bmatrix}^{\intercal} \tag{5.5}$$

and the vector $\mathbf{d}(t)$ is the perturbation in the position due to the helical swimming pattern, and is defined by:

$$\mathbf{v}_m = \overline{\mathbf{R}_0(t)}\mathbf{v}, \qquad \mathbf{d}(t) = \int (\mathbf{R}_0(t)\mathbf{v} - \mathbf{v}_m)\, dt. \tag{5.6}$$

In particular, the periodic perturbation vector $\mathbf{d}(t)$ and the average velocity vector $\mathbf{v}_m$ are orthogonal. The evolution of the average motion variables $\bar{\mathbf{x}}$ and $\bar{\mathbf{R}}$ is governed by the following system of differential equations with periodic coefficients:

$$\dot{\bar{\mathbf{x}}} = \bar{\mathbf{R}}\mathbf{v}_\eta(t)\eta + \bar{\mathbf{R}}\mathbf{v}_m, \qquad \mathbf{v}_\eta(t) = \mathbf{d}(t) \times \boldsymbol{\omega}_\eta(t), \tag{5.7a}$$

$$\dot{\bar{\mathbf{R}}} = \bar{\mathbf{R}}\widehat{\boldsymbol{\omega}}_\eta(t)\eta, \qquad \boldsymbol{\omega}_\eta(t) = \mathbf{R}_0(t)\boldsymbol{\omega}_1, \tag{5.7b}$$

where the vector $\boldsymbol{\omega}_1$ is given by:

$$\boldsymbol{\omega}_1 = \begin{bmatrix} \omega_{\parallel 1} & 0 & \omega_{\perp 1} \end{bmatrix}^\intercal. \tag{5.8}$$

Under the assumption that $|\mathbf{d}(t)| \ll 1$, the instantaneous local concentration $c(\mathbf{x})$ can be approximated as a Taylor series in terms of the average motion variables $\bar{\mathbf{x}}$ and $\bar{\mathbf{R}}$ using equation (5.4b):

$$c(\mathbf{x}) \approx c(\bar{\mathbf{x}}) + \nabla c(\bar{\mathbf{x}})^\intercal \bar{\mathbf{R}}\mathbf{d}(t). \tag{5.9}$$

Clearly, the helical swimming pattern modulates the local gradient information on the amplitude of the perturbation $\bar{\mathbf{R}}\mathbf{d}(t)$, similar to the perturbation stage of the ES control loop. The amplitude of the periodic component $\nabla c(\bar{\mathbf{x}})^\intercal \bar{\mathbf{R}}\mathbf{d}(t)$ of the instantaneous local concentration (5.9) is proportional to the component of the local gradient that is orthogonal to the average swimming direction as defined by $\bar{\mathbf{R}}\mathbf{v}_m$.

It is well known that microorganisms that swim in helical trajectories, including sea urchin sperm, can align the axis of their helical trajectory with the gradient by periodically varying the angular velocities of the cell with the same frequency of the helical trajectory [50, 58]. That is, a sperm cell can align its swimming direction with the gradient provided that the signaling pathway is able to extract the periodic component of the instantaneous local concentration, similar to the role of the filter in the ES control loop. This implication about the role of the signaling pathway is one of the main outcomes of the connection between chemotaxis and ES, as proposed in this paper.

Going back to the governing equations of the kinematics (5.7), we see that the feedback signal η multiplies the periodic feedback coefficients $\mathbf{v}_\eta(t)$ and $\boldsymbol{\omega}_\eta(t)$. Consequently, the local gradient information carried on the periodic component in the signal η is 'demodulated' into the non-zero average component of the product signals $\boldsymbol{\omega}_\eta(t)\,\eta$ and $\mathbf{v}_\eta(t)\,\eta$, similar to the demodulation stage of the ES control loop.

Finally, the demodulated local gradient information passes through the kinematics of the motion represented by equations (5.7), which is responsible for biasing the motion in the direction of the gradient. The closed-loop behavior of the nonholonomic integrator defined by the kinematics is investigated in the next section. A block diagram description of the dynamical equations (5.7) representing the navigation strategy of sea urchin sperm is shown in figure 5.2, where the special integration symbol $\int$ denotes the nonholonomic kinematic integrator corresponding to the equations (5.7). The isomorphism between the block diagrams in figure 1.1 and figure 5.2 clearly reveals the connection between sperm chemotaxis and extremum seeking. We remark that the signaling pathway is more complicated than the simple input-output depiction shown in figure 5.2 (see [48] for more details).

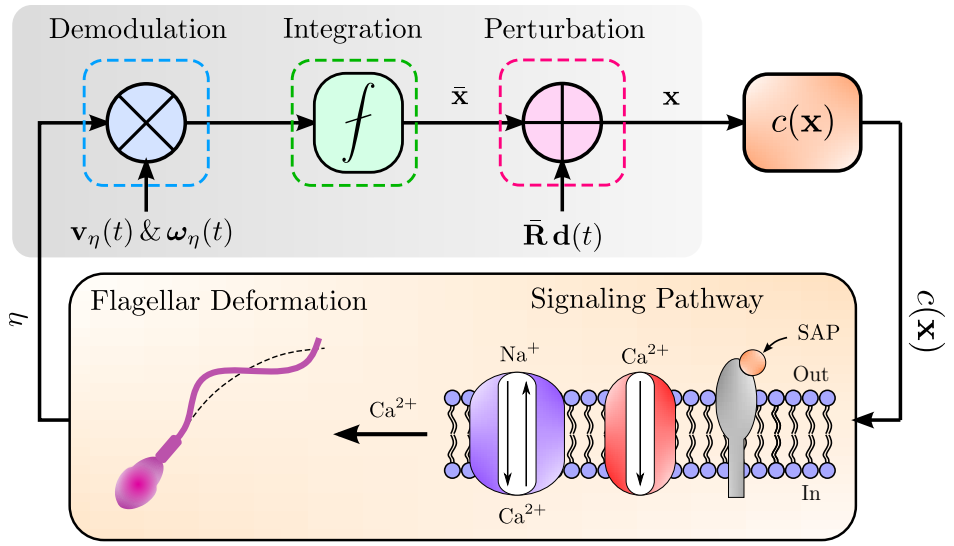

Figure 5.2: A block diagram description of the chemotactic navigation of sperm represented by equations (5.4) and (5.7). The helical swimming pattern injects periodic perturbations into the instantaneous position of the cell which leads to oscillations in the perceived stimulus. The signaling pathway relays the oscillations to the angular velocities through flagellar deformation. Next, the periodic feedback coefficients (i.e. $\mathbf{v}_\eta$ and $\boldsymbol{\omega}_\eta$) of the dynamics of average motion demodulate the gradient information carried by the feedback signal η through signal multiplication. Finally, the kinematic integrator $\int$ biases the motion in the direction of the gradient.

It is note-worthy that the 2D version of the model (5.1)-(5.3) (i.e. when $\omega_{\|} = 0$ and the motion is restricted to a plane) is a well-studied kinematic model in the control community known as the unicycle model. Remarkably, the trajectories generated by an ES-based algorithm for the unicycle model, which was recently proposed in [55, 28] independently from the literature on sperm chemotaxis, are astonishingly similar to the actual trajectories of sea urchin sperm in shallow observation chambers [59].

5.3 Chemotactic Response and Closed Loop Behavior

The evident one-to-one correspondence between the key components of the navigation strategy of sea urchin sperm and ES control immediately clarifies the role of the signaling pathway: it must act as an adaptive band-pass filter attuned to the frequency of the swimming

pattern of the cell. Motivated by this observation, and building upon previous phenomenological models [47, 52], we propose the following coarse-grained dynamical description of the signaling pathway:

$$\sigma\,\dot{\xi} = s(t) - \xi, \tag{5.10a}$$

$$\mu\,\dot{\eta} = \rho\,\dot{\xi} - \eta^3, \tag{5.10b}$$

$$\mu\,\dot{\rho} = \rho - \rho\,\eta^2, \tag{5.10c}$$

where μ and σ are positive constants such that $\sigma < \mu$, and $s(t)$ is the input to the model, which represents the time-varying external stimulus to which the pathway is exposed due to the binding of SAP molecules with the receptors. Without accounting for noise, the stimulus $s(t)$ is customarily approximated by:

$$s(t) \approx \lambda\, c(\mathbf{x}) \tag{5.11}$$

for some positive proportionality constant λ [47, 52]. The proposed model possesses three essential dynamical features: excitation, relaxation, and adaptation. The excitation is modelled by equation (5.10a), which acts as a differentiator that detects changes in the local concentration. The relaxation is modelled by equation (5.10b), which brings the response η back to resting levels when there is no change in the stimulus. Finally, the adaptation is modelled by equation (5.10c), which adjusts the sensitivity of the pathway to the stimulus. A sample trajectory of the equations (5.1)-(5.3) and (5.10) is shown in figure 5.3 along with time-history of the average local concentration $c(\bar{\mathbf{x}})$, the steering response η and the angle ψ between the gradient and the average swimming direction.

We now analyze the closed loop behavior when the dynamics of the pathway is given by the proposed dynamical system (5.10) using analytical calculations based on linear response

theory and averaging, similar to [47, 52]. The details of calculations in this section can be found in the Appendix F. In the parametric regime where $\sigma|\mathbf{v}_m| \ll \mu|\mathbf{v}_m| \ll \sigma|\boldsymbol{\omega}_0| \approx O(1)$, there is a large time-scale separation between the dynamics of average motion (5.7) in the absence of feedback and the dynamics of the pathway (5.10). Consequently, we may approximate the response η due to the time-varying local concentration (5.9) by the quasi-steady response:

$$\eta_{\mathrm{QS}} = \frac{\bar{\mathbf{h}}^{\intercal}\check{\nabla}c + \sqrt{2}\,\beta\,\bar{\mathbf{q}}(t+t_\phi)^{\intercal}\check{\nabla}_{\perp}c}{\sqrt{|\check{\nabla}_{\parallel}c|^2 + \beta^2\,|\check{\nabla}_{\perp}c|^2}}, \tag{5.12}$$

where $\beta = \gamma(\omega)|\mathbf{d}(t)|/(\mu\sqrt{2}|\mathbf{v}_m|)$, $t_\phi = \phi(\omega)/\omega$ with $\gamma(\omega)$ and $\phi(\omega)$ being the gain and phase contributions of the linear part of the system (5.10) at the frequency $\omega = |\boldsymbol{\omega}_0|$, $\check{\nabla}c = \nabla c(\bar{\mathbf{x}})/|\nabla c(\bar{\mathbf{x}})|$ is a unit vector in the direction of the gradient, and we used the following shorthand notations:

$$\bar{\mathbf{h}} = \bar{\mathbf{R}}\mathbf{v}_m/|\mathbf{v}_m|, \qquad \bar{\mathbf{q}}(t) = \bar{\mathbf{R}}\mathbf{d}(t)/|\mathbf{d}(t)|, \tag{5.13}$$

$$\check{\nabla}_{\parallel}c = \bar{\mathbf{h}}\,\bar{\mathbf{h}}^{\intercal}\check{\nabla}c, \qquad \check{\nabla}_{\perp}c = \check{\nabla}c - \check{\nabla}_{\parallel}c, \tag{5.14}$$

to simplify the expression (see figure 5.1B for a geometric illustration of the introduced variables). Notably, the quasi-steady response (5.12) is independent of the ambient concentration $c(\mathbf{x}_0)$ and the stimulus proportionality constant λ, which are irrelevant information from a chemotactic perspective. If we close the loop by replacing η with the quasi-steady approximation η_{QS}, an intricate averaging analysis on the fast time scale $\tau = \omega t$ when $\omega \gg 1$ for the system of equations (5.7a)-(5.7b) coupled with equation (5.12) leads to the following averaged quasi-steady equations:

$$\dot{\bar{\mathbf{x}}}^{\intercal}\bar{\mathbf{h}} = \frac{v\,\omega_{\parallel 0}}{\omega}\left(1 + \frac{\omega_{\perp 0}^2\omega_{\parallel 1}}{\omega^2\omega_{\parallel 0}\alpha}\bar{\mathbf{h}}^{\intercal}\check{\nabla}c\right), \tag{5.15a}$$

$$\dot{\bar{\mathbf{h}}}^{\intercal}\check{\nabla}c = \frac{\gamma(\omega)\,\omega_{\perp 0}^2\omega_{\parallel 1}}{2\mu\omega^2\omega_{\parallel 0}\alpha}\cos(\phi(\omega))|\check{\nabla}_{\perp}c|^2, \tag{5.15b}$$

$$\alpha = \sqrt{|\check{\nabla}_{\parallel} c|^2 + \beta^2 |\check{\nabla}_{\perp} c|^2}. \tag{5.15c}$$

Equation (5.15a) expresses the speed along the average direction of motion $\bar{\mathbf{h}}$, while equation (5.15b) presents the rate of alignment of the average direction of motion $\bar{\mathbf{h}}$ with the gradient.

We now analyze the qualitative dynamic behavior of the quasi-steady averaged equations (5.15) by considering three events and the corresponding response. The first event (the segments highlighted in green in figure 5.3) is when the average swimming direction $\bar{\mathbf{h}}$ is mostly aligned with the gradient (i.e. $\beta|\check{\nabla}_{\perp} c| \ll \bar{\mathbf{h}}^{\intercal} \check{\nabla}_{\parallel} c \approx 1$), in which case the response η_{QS} is approximately given by:

$$\eta_{\mathrm{QS}} \approx 1 + \sqrt{2}\, \beta\, \bar{\mathbf{q}} (t + t_{\phi})^{\intercal} \check{\nabla}_{\perp} c, \tag{5.16}$$

where the second term is small compared to 1 (i.e. the periodic component is attenuated relative to the slope of the ramp component), and the change in the misalignment between the average swimming direction and the gradient is minor. Moreover, the net motion along the average swimming direction $\bar{\mathbf{h}}$ is sped up:

$$\dot{\bar{\mathbf{x}}}^{\intercal} \bar{\mathbf{h}} \approx \frac{v\, \omega_{\parallel 0}}{\omega} \left(1 + \frac{\omega_{\parallel 1} \omega_{\perp 0}^2}{\omega_{\parallel 0} \omega^2} \right), \tag{5.17}$$

The second event (the segments highlighted in purple in figure 5.3) is when the average swimming direction is almost opposite to the gradient (i.e. $\bar{\mathbf{h}}^{\intercal} \check{\nabla}_{\parallel} c \approx -1$), in which case the response is approximately given by:

$$\eta_{\mathrm{QS}} \approx -1 + \sqrt{2}\, \beta\, \bar{\mathbf{q}} (t + t_{\phi})^{\intercal} \check{\nabla}_{\perp} c, \tag{5.18}$$

where once again the periodic term is small. However, the net speed along the average

swimming direction $\bar{\mathbf{h}}$ is reduced:

$$\dot{\mathbf{x}}^{\intercal}\bar{\mathbf{h}} \approx \frac{v\,\omega_{\|0}}{\omega}\left(1 - \frac{\omega_{\|1}\omega_{\perp 0}^2}{\omega_{\|0}\omega^2}\right). \tag{5.19}$$

That is, when the motion is opposite to the gradient, the net motion along the average swimming direction $\bar{\mathbf{h}}$ is slowed down, thereby reducing the helical pitch of the trajectory. This helical pitch reduction can be observed in the purple segment of the trajectory in figure 5.3. Moreover, the average swimming direction defined by $\bar{\mathbf{h}}^{\intercal}\check{\nabla}_{\|}c = -1$ is unstable, so any slight misalignment triggers the transition towards the stable average swimming direction defined by $\bar{\mathbf{h}}^{\intercal}\check{\nabla}_{\|}c \approx 1$.

The third event (the segments highlighted in red in figure 5.3) is when the average swimming direction $\bar{\mathbf{h}}$ is orthogonal to the gradient (i.e. $\bar{\mathbf{h}}^{\intercal}\check{\nabla}_{\|}c \approx 0$ and $|\check{\nabla}_{\perp}c| \approx 1$), in which case the quasi-steady response η_{QS} is dominated by the periodic component in the local concentration:

$$\eta_{\mathrm{QS}} \approx \sqrt{2}\,\bar{\mathbf{q}}(t + t_{\phi})^{\intercal}\check{\nabla}_{\perp}c, \tag{5.20}$$

and the alignment between the average swimming direction and the gradient is increased at a peak rate:

$$\dot{\bar{\mathbf{h}}}^{\intercal}\check{\nabla}c \approx \frac{\omega_{\perp 0}\omega_{\|1}}{\sqrt{2}\,\omega}\cos(\phi(\omega)). \tag{5.21}$$

We remark that near the maximum concentration, the gradient vanishes, and the behavior of the system is dominated by second order effects, due to the Hessian of the concentration field, which are neglected here.

5.4 Discussion

Helical klinotaxis is a ubiquitous mode of taxis in microorganisms. In this study, we used sperm chemotaxis in sea urchins to highlight extremum seeking control as an underlying principle behind helical klinotaxis. This connection sheds light on the role played by the chemotactic signaling pathway and emphasizes the characterization of its dynamics as an adaptive band pass filter. Moreover, we showed that the switching-like behavior of sea urchin sperm can arise from a continuous dynamical description (5.10) without an explicit discontinuous switching logic as in previously proposed models [52, 56]. The key feature of the model (5.10) is that the gain ρ adapts to the filtered stimulus $\dot{\xi}$ rather than the stimulus $s(t)$ directly. As a consequence, the ambient concentration levels do not alter the behavior of the model significantly. The forward velocity v of the cell is treated as a constant in the kinematic model (5.1)-(5.3). Yet, the cell is able to adjust the speed of the net motion along the average swimming direction (i.e. the pitch of the helical trajectory) by dynamically regulating the angular velocity components. Our results suggest that this helical pitch adjustment mechanism is behind the peculiar switching-like behavior. That is, the on-response corresponds to the combined effect of helical pitch increase and the attenuation of the periodic component when the direction of motion is mostly aligned with the gradient. In contrast, the off-response may be explained as the combined effect of helical pitch decrease when the direction of motion is opposite to the gradient followed by amplification of the periodic component when the direction of motion is misaligned with the gradient. The strength of the off-response in our model is determined by the maximum pitch reduction and the peak alignment rate given in equations (5.19) and (5.21), respectively. In particular, the off response is most pronounced when $\omega_{\|1}\omega_{\perp 0}^2 \approx \omega_{\|0}\omega^2$, since that leads to zero helical pitch when the direction of motion is opposite to the gradient. Furthermore, the feedback gain in the peak rate alignment depends on the factor $\cos(\phi(\omega))$, which attains its maximum value when the frequency of the periodic swimming pattern ω is inside the pass-band of

the signaling pathway defined by μ and σ so that the phase lag is minimal. Finally, we remark that the proposed connection between klinotaxis and extremum seeking may guide technological developments in robotic navigation [60, 30]; it may inspire engineers to design source seeking algorithms with minimal sensors, suitable for miniaturized robots.

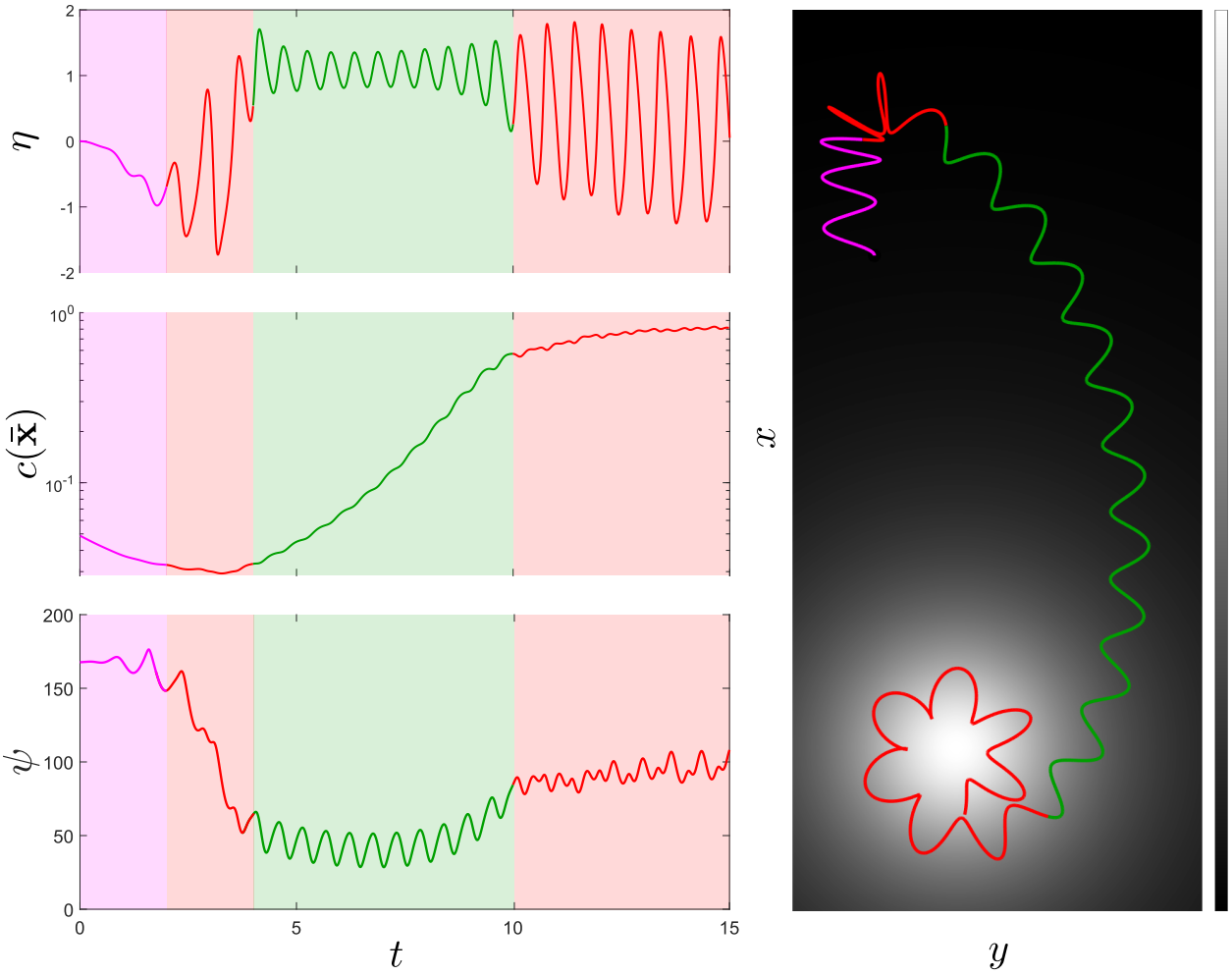

v	$\omega_{\parallel 0}$	$\omega_{\parallel 1}$	$\omega_{\perp 0}$	$\omega_{\perp 1}$	μ	σ	$\eta(t_0)$	$\zeta(t_0)$	$\rho(t_0)$
3.07	3.07	2.30	8.91	1.00	3.07	9.42	0.00	$c(\mathbf{x}_0)$	5.00

Figure 5.3: The three cases of the behavior of the signaling pathway illustrated on a sample trajectory projected on the xy-plane, the response η, the average instantaneous concentration $c(\bar{\mathbf{x}})$, and the angle $\psi = \cos^{-1}(\bar{\mathbf{h}}^{\mathsf{T}}\check{\nabla}c)$ (in degrees) between the gradient and the average direction of motion $\bar{\mathbf{h}}$, in a radial concentration field $c(\mathbf{x}) = 1/(1 + 0.5|\mathbf{x}|^2)$. The initial position is taken as $\mathbf{x}_0 = (6, 1, 0)$, and the initial orientation is $\mathbf{R}(t_0) = \exp(2\pi\hat{\mathbf{e}}_2/5)$, where $\hat{\mathbf{e}}_2 = (0, 1, 0)$. The rest of the initial conditions and parameter values are in the table.

Chapter 6

Averaging for Delay Systems

In this chapter, we investigate the effect of time-delays on the behavior of highly oscillatory systems. The presentation in this chapter is formal as there are no tools for higher-order averaging for time-delay systems. The existing tools in the literature can only tackle first order averaging [61, 62]. Such tools, however, are insufficient to tackle the class of systems we consider here due to the simple fact that the first-order vanishes. Therefore, one must proceed to second-order averaging. It turns out, however, that proceeding to higher-order averages is nontrivial as it requires the computation of the Frechet derivative of an infinite dimensional operator. Nevertheless, by formally following the same methodology of averaging in finite dimensions, one can obtain approximation formulas for systems with constant commensurate time-delays. We compute such formulas in this chapter for the second-order case, leaving the convergence proofs for future work.

6.1 The infinitesmal delay case

Consider a class of delayed systems on the form:

$$\dot{\mathbf{x}} = \sum_{k=1}^{2} \varepsilon^{k-2}\, \mathbf{f}_k(\mathbf{x}, \mathbf{x}_{-1}, \varepsilon^{-2}t) + O(\varepsilon), \qquad \mathbf{x}_{-1}(t) = \mathbf{x}(t - t_d) \tag{6.1}$$

where there is a point time delay of t_d. First, we consider the effect of an infinitesimal time delay on the performance of the trajectories of this system. Specifically, suppose that $t_d = O(\varepsilon^2) = \tau_d \varepsilon^2$. In this case, we can apply the time scaling $\tau = \varepsilon^{-2}t$ to obtain the system:

$$\frac{d\mathbf{x}}{d\tau} = \sum_{k=1} \varepsilon^{k}\, \mathbf{f}_k(\mathbf{x}, \mathbf{x}_{-1}, \tau), \qquad \mathbf{x}_{-1}(\tau) = \mathbf{x}(t - \tau_d) \tag{6.2}$$

This system is on the canonical averaging form. Suppose that the first-order average vanishes:

$$\int_0^T \mathbf{f}_1(\mathbf{x}, \mathbf{x}_{-1}, \tau)\, d\tau = 0 \tag{6.3}$$

Let us attempt to formally apply a near-identity transform defined by:

$$\mathbf{x} = \mathbf{U}(\bar{\mathbf{x}}, \bar{\mathbf{x}}_{-1}, \bar{\mathbf{x}}_{-2}, \tau, \varepsilon) = \bar{\mathbf{x}} + \varepsilon\, \mathbf{u}_1(\bar{\mathbf{x}}, \bar{\mathbf{x}}_{-1}, \tau) + \varepsilon^2 \mathbf{u}_2(\bar{\mathbf{x}}, \bar{\mathbf{x}}_{-1}, \bar{\mathbf{x}}_{-2}, \tau), \tag{6.4}$$

that takes the system (6.2) to a system:

$$\frac{d\bar{\mathbf{x}}}{d\tau} = \varepsilon\, \bar{\mathbf{f}}_1(\bar{\mathbf{x}}, \bar{\mathbf{x}}_{-1}) + \varepsilon^2 \bar{\mathbf{f}}_2(\bar{\mathbf{x}}, \bar{\mathbf{x}}_{-1}, \bar{\mathbf{x}}_{-2}) + \varepsilon^3 \mathbf{h}_3(\bar{\mathbf{x}}, \bar{\mathbf{x}}_{-1}, \bar{\mathbf{x}}_{-2}, \tau, \varepsilon) \tag{6.5}$$

Observe that we included the dependency of the system (6.2) on $\bar{\mathbf{x}}_{-2}$ in anticipation. Under this coordinate transformation, we have that:

$$\begin{aligned}
\frac{d\mathbf{x}}{d\tau} &= \frac{d\bar{\mathbf{x}}}{d\tau} + \varepsilon \left(\partial_\tau \mathbf{u}_1 + \partial_{\bar{\mathbf{x}}} \mathbf{u}_1 \frac{d\bar{\mathbf{x}}}{d\tau} + \partial_{\bar{\mathbf{x}}_{-1}} \mathbf{u}_1 \frac{d\bar{\mathbf{x}}_{-1}}{d\tau} \right) \\
&\quad + \varepsilon^2 \left(\partial_\tau \mathbf{u}_2 + \partial_{\bar{\mathbf{x}}} \mathbf{u}_2 \frac{d\bar{\mathbf{x}}}{d\tau} + \partial_{\bar{\mathbf{x}}_{-1}} \mathbf{u}_2 \frac{d\bar{\mathbf{x}}_{-1}}{d\tau} + \partial_{\bar{\mathbf{x}}_{-2}} \mathbf{u}_2 \frac{d\bar{\mathbf{x}}_{-2}}{d\tau} \right) \\
&= \varepsilon\, \bar{\mathbf{f}}_1(\bar{\mathbf{x}}, \bar{\mathbf{x}}_{-1}) + \varepsilon \partial_\tau \mathbf{u}_1(\bar{\mathbf{x}}, \bar{\mathbf{x}}_{-1}, \tau) + \varepsilon^2 \bar{\mathbf{f}}_2(\bar{\mathbf{x}}, \bar{\mathbf{x}}_{-1}, \bar{\mathbf{x}}_{-2}) + \varepsilon^2 \partial_\tau \mathbf{u}_2(\bar{\mathbf{x}}, \bar{\mathbf{x}}_{-1}, \bar{\mathbf{x}}_{-2}, \tau) \\
&\quad + \varepsilon^2 \partial_{\bar{\mathbf{x}}} \mathbf{u}_1(\bar{\mathbf{x}}, \bar{\mathbf{x}}_{-1}, \tau) \bar{\mathbf{f}}_1(\bar{\mathbf{x}}, \bar{\mathbf{x}}_{-1}) + \varepsilon^2 \partial_{\bar{\mathbf{x}}_{-1}} \mathbf{u}_1(\bar{\mathbf{x}}, \bar{\mathbf{x}}_{-1}, \tau) \mathbf{f}_1(\bar{\mathbf{x}}_{-1}, \bar{\mathbf{x}}_{-2}) + O(\varepsilon^3)
\end{aligned} \tag{6.6}$$

In addition, we have that:

$$\begin{aligned}
\frac{d\mathbf{x}}{d\tau} &= \varepsilon\, \mathbf{f}_1(\mathbf{U}(\bar{\mathbf{x}}, \bar{\mathbf{x}}_{-1}, \bar{\mathbf{x}}_{-2}, \tau, \varepsilon), \mathbf{U}(\bar{\mathbf{x}}_{-1}, \bar{\mathbf{x}}_{-2}, \bar{\mathbf{x}}_{-3}, \tau - \tau_d, \varepsilon), \tau) \\
&\quad + \varepsilon^2 \mathbf{f}_2(\mathbf{U}(\bar{\mathbf{x}}, \bar{\mathbf{x}}_{-1}, \bar{\mathbf{x}}_{-2}, \tau, \varepsilon), \mathbf{U}(\bar{\mathbf{x}}_{-1}, \bar{\mathbf{x}}_{-2}, \bar{\mathbf{x}}_{-3}, \tau - \tau_d, \varepsilon), \tau) \\
&= \varepsilon\, \mathbf{f}_1(\bar{\mathbf{x}}, \bar{\mathbf{x}}_{-1}, \tau) + \varepsilon^2 \partial_{\bar{\mathbf{x}}} \mathbf{f}_1(\bar{\mathbf{x}}, \bar{\mathbf{x}}_{-1}, \tau) \mathbf{u}_1(\bar{\mathbf{x}}, \bar{\mathbf{x}}_{-1}, \tau) \\
&\quad + \varepsilon^2 \partial_{\bar{\mathbf{x}}_{-1}} \mathbf{f}_1(\bar{\mathbf{x}}, \bar{\mathbf{x}}_{-1}, \tau) \mathbf{u}_1(\bar{\mathbf{x}}_{-1}, \bar{\mathbf{x}}_{-2}, \tau - \tau_d) + \varepsilon^2\, \mathbf{f}_2(\bar{\mathbf{x}}, \bar{\mathbf{x}}_{-1}, \tau) + O(\varepsilon^3)
\end{aligned} \tag{6.7}$$

Matching the coefficients of like-power terms in ε, we obtain the homological equations:

$$\partial_\tau \mathbf{u}_1(\bar{\mathbf{x}}, \bar{\mathbf{x}}_{-1}, \tau) = \mathbf{K}_1(\bar{\mathbf{x}}, \bar{\mathbf{x}}_{-1}, \tau) - \bar{\mathbf{f}}_1(\bar{\mathbf{x}}, \bar{\mathbf{x}}_{-1}) \tag{6.8}$$

$$\partial_\tau \mathbf{u}_2(\bar{\mathbf{x}}, \bar{\mathbf{x}}_{-1}, \bar{\mathbf{x}}_{-2}, \tau) = \mathbf{K}_2(\bar{\mathbf{x}}, \bar{\mathbf{x}}_{-1}, \bar{\mathbf{x}}_{-2}, \tau) - \bar{\mathbf{f}}_2(\bar{\mathbf{x}}, \bar{\mathbf{x}}_{-1}, \bar{\mathbf{x}}_{-2}) \tag{6.9}$$

where we have that:

$$\mathbf{K}_1(\bar{\mathbf{x}}, \bar{\mathbf{x}}_{-1}, \tau) = \mathbf{f}_1(\bar{\mathbf{x}}, \bar{\mathbf{x}}_{-1}, \tau) \tag{6.10}$$

$$\mathbf{K}_2(\bar{\mathbf{x}}, \bar{\mathbf{x}}_{-1}, \bar{\mathbf{x}}_{-2}, \tau) = \mathbf{f}_2(\bar{\mathbf{x}}, \bar{\mathbf{x}}_{-1}, \tau) + \partial_{\bar{\mathbf{x}}_{-1}} \mathbf{f}_1(\bar{\mathbf{x}}, \bar{\mathbf{x}}_{-1}, \tau) \mathbf{u}_1(\bar{\mathbf{x}}_{-1}, \bar{\mathbf{x}}_{-2}, \tau - \tau_d) \tag{6.11}$$

$$+ \partial_{\bar{\mathbf{x}}} \mathbf{f}_1(\bar{\mathbf{x}}, \bar{\mathbf{x}}_{-1}, \tau) \mathbf{u}_1(\bar{\mathbf{x}}, \bar{\mathbf{x}}_{-1}, \tau) - \partial_{\bar{\mathbf{x}}} \mathbf{u}_1(\bar{\mathbf{x}}, \bar{\mathbf{x}}_{-1}, \tau) \bar{\mathbf{f}}_1(\bar{\mathbf{x}}, \bar{\mathbf{x}}_{-1}) \tag{6.12}$$

$$- \partial_{\bar{\mathbf{x}}_{-1}} \mathbf{u}_1(\bar{\mathbf{x}}, \bar{\mathbf{x}}_{-1}, \tau) \bar{\mathbf{f}}_1(\bar{\mathbf{x}}_{-1}, \bar{\mathbf{x}}_{-2}) \tag{6.13}$$

Now, we simply let:

$$\bar{\mathbf{f}}_1(\bar{\mathbf{x}}, \bar{\mathbf{x}}_{-1}) = \frac{1}{T}\int_0^T \mathbf{K}_1(\bar{\mathbf{x}}, \bar{\mathbf{x}}_{-1}, \tau)d\tau \tag{6.14}$$

$$\bar{\mathbf{f}}_2(\bar{\mathbf{x}}, \bar{\mathbf{x}}_{-1}, \bar{\mathbf{x}}_{-2}) = \frac{1}{T}\int_0^T \mathbf{K}_2(\bar{\mathbf{x}}, \bar{\mathbf{x}}_{-1}, \bar{\mathbf{x}}_{-2}, \tau)d\tau \tag{6.15}$$

where T is the period of the right hand side of (6.2). The homological equations are then solvable with the solution having zero average. The actual proof can now be constructed by reversing the argument above. We emphasize that the averaged system depends on a twice delayed state. Moreover, the average vector field $\bar{\mathbf{f}}_2$ depends crucially on the delay τ_d. After truncating the terms of order ε^3 and higher in (6.5), we obtain the system:

$$\frac{d\bar{\mathbf{x}}}{d\tau} = \varepsilon\,\bar{\mathbf{f}}_1(\bar{\mathbf{x}}, \bar{\mathbf{x}}_{-1}) + \varepsilon^2\bar{\mathbf{f}}_2(\bar{\mathbf{x}}, \bar{\mathbf{x}}_{-1}, \bar{\mathbf{x}}_{-2}) \tag{6.16}$$

Since the first order terms vanish, we obtain an averaged system on the form:

$$\frac{d\bar{\mathbf{x}}}{d\tau} = \varepsilon^2\bar{\mathbf{f}}(\bar{\mathbf{x}}, \bar{\mathbf{x}}_{-1}, \bar{\mathbf{x}}_{-2}) \tag{6.17}$$

where the vector field $\bar{\mathbf{f}}$ is given by:

$$\begin{aligned}\bar{\mathbf{f}}(\mathbf{x}, \mathbf{x}_{-1}, \mathbf{x}_{-2}) = \frac{1}{T}\int_0^T \Big(&\mathbf{f}_2(\bar{\mathbf{x}}, \bar{\mathbf{x}}_{-1}, \tau) + \partial_{\bar{\mathbf{x}}}\mathbf{f}_1(\bar{\mathbf{x}}, \bar{\mathbf{x}}_{-1}, \tau)\mathbf{u}_1(\bar{\mathbf{x}}, \bar{\mathbf{x}}_{-1}, \tau) \\ &+ \partial_{\bar{\mathbf{x}}_{-1}}\mathbf{f}_1(\bar{\mathbf{x}}, \bar{\mathbf{x}}_{-1}, \tau)\mathbf{u}_1(\bar{\mathbf{x}}_{-1}, \bar{\mathbf{x}}_{-2}, \tau - \tau_d)\Big)\,d\tau\end{aligned} \tag{6.18}$$

By reversing the time scaling $t = \varepsilon^2\tau$, we obtain the delayed averaged system:

$$\dot{\bar{\mathbf{x}}}(t) = \bar{\mathbf{f}}(\bar{\mathbf{x}}(t), \bar{\mathbf{x}}(t - \varepsilon^2\tau_d), \bar{\mathbf{x}}(t - 2\tau_d\varepsilon^2)) \tag{6.19}$$

We observe that the averaged system depends on a twice-delayed state of the system even when the original system does not. Moreover, the averaged system depends, quite surpris-

ingly, on the coefficient τ_d of the time-delay. This seems to be a characteristic of higher order averaging for delayed system. The dependency on τ_d means that highly oscillatory systems are severely vulnerable to time-delays of order $O(\varepsilon^2)$. To illustrate this vulnerability, we now provide a numerical example.

Consider the following two systems:

$$\dot{x}_1 = \varepsilon^{-1}\left(\cos(\varepsilon^{-2}t) - c(x_1)\sin(\varepsilon^{-2}t)\right), \qquad \dot{x}_2 = \varepsilon^{-1}\cos\left(\varepsilon^{-2}t + c(x_1)\right) \tag{6.20}$$

where $c(\cdot)$ is a smooth function. In the limit $\varepsilon \to 0$, both systems behave on average according to the dynamics of the averaged system:

$$\dot{\bar{x}} = -\frac{dc}{dx} \tag{6.21}$$

That is, both systems have identical behavior on average. Now, consider the situation that arises when there is an infinitesmal delay:

$$\dot{x}_1 = \sqrt{2}\,\varepsilon^{-1}\left(\cos(\varepsilon^{-2}t) - c(x_1(t-\tau_d\varepsilon^2))\sin(\varepsilon^{-2}t)\right), \tag{6.22}$$

$$\dot{x}_2 = \sqrt{2}\,\varepsilon^{-1}\cos\left(\varepsilon^{-2}t + c(x_2(t-\tau_d\varepsilon^2))\right) \tag{6.23}$$

By applying the formulas presented in this section, we obtain the averaged systems:

$$\dot{\bar{x}}_1 = -\frac{dc}{dx}(\bar{x}_1(t-\tau_d\varepsilon^2))\left(\cos(\tau_d) + c(\bar{x}_1(t-2\tau_d\varepsilon^2))\sin(\tau_d)\right) \tag{6.24}$$

$$\dot{\bar{x}}_2 = -\frac{dc}{dx}(\bar{x}_2(t-\tau_d\varepsilon^2))\cos\left(\tau_d + c(\bar{x}_2(t-\tau_d\varepsilon^2)) - c(\bar{x}_2(t-2\tau_d\varepsilon^2))\right) \tag{6.25}$$

For sufficiently small ε, the difference between the state and its delay becomes insignificant. In that case, we have that $\bar{x}_i(t-2\tau_d\varepsilon^2) \approx \bar{x}_i(t-\tau_d\varepsilon^2) \approx \bar{x}_i(t)$, which implies that the averaged

systems may be approximated by finite dimensional counterparts:

$$\dot{\bar{x}}_1 = -\cos(\tau_d)\frac{dc}{dx} - \sin(\tau_d)c(\bar{x}_1)\frac{dc}{dx} \tag{6.26}$$

$$\dot{\bar{x}}_2 = -\frac{dc}{dx}\cos(\tau_d) \tag{6.27}$$

Nevertheless, we observe the drastic difference in behavior between the two systems when $\tau_d \neq 0$. For instance, when $\tau_d = \pi/2$, the averaged systems are given by:

$$\dot{\bar{x}}_1 = -c(\bar{x}_1)\frac{dc}{dx}, \qquad \dot{\bar{x}}_2 = 0 \tag{6.28}$$

To demonstrate the drastic difference in the behavior of these systems, let us consider the situation where the function $c(\cdot)$ is given by:

$$c(x) = \frac{1}{2}x^2 \tag{6.29}$$

Therefore, the two systems will be given by:

$$\dot{\bar{x}}_1 = -\frac{1}{2}\bar{x}_1^3, \qquad \dot{\bar{x}}_2 = 0 \tag{6.30}$$

We observe how the origin for the first system is stable, though it is only asymptotically stable compared to exponential stability when $\tau_d = 0$, whereas the second system is only marginally stable.

Even more disturbingly, as soon as τ_d is larger than $\pi/2$, say $\tau_d = 3\pi/4$, one of the systems becomes unstable while the other system bifurcates leading to the creation of two additional exponentially stable equilibria while simultaneously destabilizing the original equilibrium at the origin:

$$\dot{\bar{x}}_1 = \frac{1}{\sqrt{2}}\bar{x}_1\left(1 - \frac{1}{2}\bar{x}_1^2\right), \qquad \dot{\bar{x}}_2 = \frac{1}{\sqrt{2}}\bar{x}_2 \tag{6.31}$$

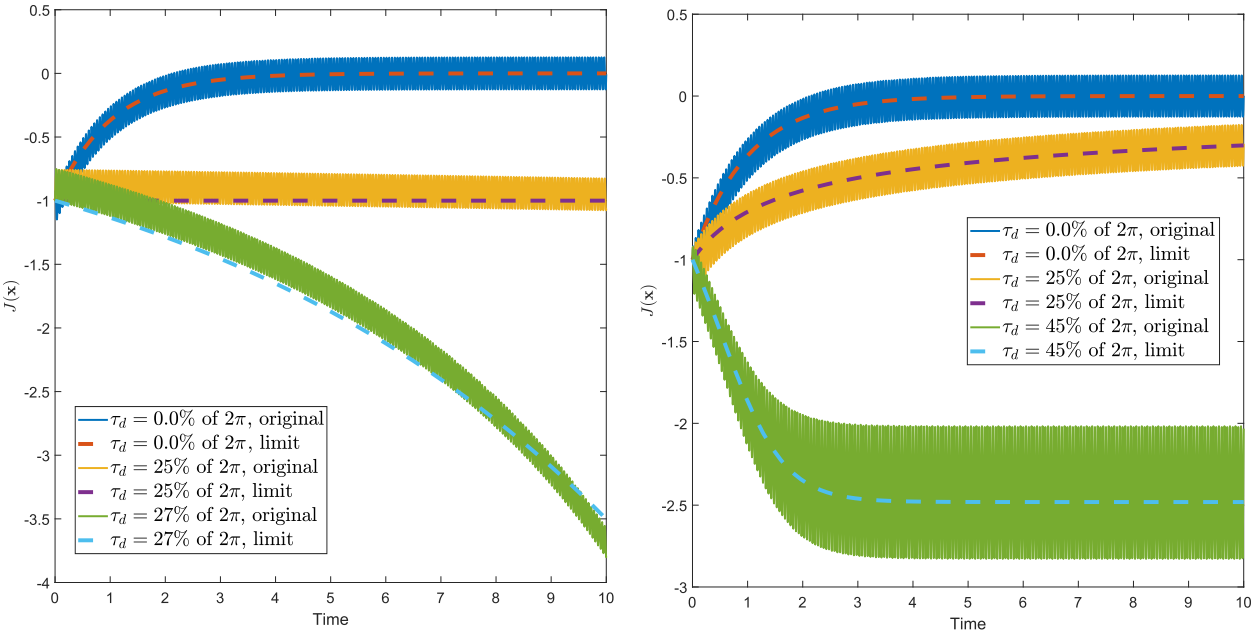

Figure 6.1: Time response of the time-delayed system for various values of τ_d.

We visualise this drastic change in the behavior by providing numerical simulation results for both systems, which are shown in figure 6.1. It is, therefore, clear that highly oscillatory systems are severely vulnerable to infinitesmal delays. One is naturally led to inquire after the reason behind this vulnerability. Intuitively, the reason behind this vulnerability stems from the manner in which higher-order effects manifest in highly oscillatory systems. Second-order effects are aptly named so because they only appear naturally to second-order. In highly oscillatory systems, the vector fields responsible for generating second-order effects are amplified to force their effects to appear as the leading order. As a consequence, minute time-delays in the original time-scale of the dynamics directly affect the phase of the oscillations that interact with one-another and produce the second-order effects. This is understandable since one is attempting to perform first-order actions (i.e. gradient ascent/descent) using zeroth-order information (i.e. function evaluations). In this setting, there is a fundamental trade-off between the speed and domain of attraction and the robustness to infinitesmal time-delays. This has been recognized early on in the literature of open-loop vibrational stabilization [62, 63, 64]. Here, we extend this analysis to the class of highly oscillatory

systems.

It is worth mentioning that this vulnerability does not appear when one allows the dynamics to evolve on their natural time-scale. That is, when second-order effects are not amplified using large gains, the vulnerability to infinitesmal time-delays is no longer present.

6.2 The finite delay case

Now suppose instead that the delay is not infinitesimal. That is, suppose that $t_d = O(1)$. In this case, the time scaling $\tau = \varepsilon^{-2}t$ will lead to a system of the form:

$$\frac{d\bar{\mathbf{x}}}{d\tau} = \varepsilon\, \mathbf{f}_1(\mathbf{x}(\tau), \mathbf{x}(\tau - t_d/\varepsilon^2), \tau) + \varepsilon^2 \mathbf{f}_2(\mathbf{x}(\tau), \mathbf{x}(\tau - t_d/\varepsilon^2), \tau) \tag{6.32}$$

It is clear that the averaging of this system is much more complicated because in the limit as $\varepsilon \to 0$, the delay becomes infinite. Indeed, one cannot perform a time-scale change to put the system on the averaging canonical form. That is, one has to deal with the system in the original time-scale:

$$\dot{\mathbf{x}} = \sum_{k=1}^{2} \varepsilon^{k-2} \mathbf{f}_k(\mathbf{x}, \mathbf{x}_{-1}, \varepsilon^2 t) + O(\varepsilon) \tag{6.33}$$

In order to proceed with the analysis, we shall attempt, at least formally, to use the same near-identity transform:

$$\mathbf{x} = \bar{\mathbf{x}} + \varepsilon\, \mathbf{u}_1(\bar{\mathbf{x}}, \bar{\mathbf{x}}_{-1}\varepsilon^2 t) + \varepsilon^2 \mathbf{u}_2(\bar{\mathbf{x}}, \bar{\mathbf{x}}_{-1}, \bar{\mathbf{x}}_{-2}, \varepsilon^2 t) \tag{6.34}$$

Computing the derivative of both sides with respect to t, we obtain:

$$\begin{aligned}\dot{\mathbf{x}} = \dot{\bar{\mathbf{x}}} + \varepsilon \big(&\varepsilon^{-2}\partial_3 \mathbf{u}_1(\bar{\mathbf{x}}, \bar{\mathbf{x}}_{-1}, \varepsilon^{-2}t) + \partial_1 \mathbf{u}_1(\bar{\mathbf{x}}, \bar{\mathbf{x}}_{-1}, \varepsilon^2 t)\dot{\bar{\mathbf{x}}} + \partial_2 \mathbf{u}_1(\bar{\mathbf{x}}, \bar{\mathbf{x}}_{-1}, \varepsilon^2 t)\dot{\bar{\mathbf{x}}}_{-1}\big) \\ + \varepsilon^2\big(&\varepsilon^{-2}\partial_4 \mathbf{u}_2(\bar{\mathbf{x}}, \bar{\mathbf{x}}_{-1}, \bar{\mathbf{x}}_{-2}, \varepsilon^{-2}t) + \partial_1 \mathbf{u}_2(\bar{\mathbf{x}}, \bar{\mathbf{x}}_{-1}, \bar{\mathbf{x}}_{-2}, \varepsilon^2 t)\dot{\bar{\mathbf{x}}} \\ + &\partial_2 \mathbf{u}_2(\bar{\mathbf{x}}, \bar{\mathbf{x}}_{-1}, \bar{\mathbf{x}}_{-2}, \varepsilon^2 t)\dot{\bar{\mathbf{x}}}_{-1} + \partial_3 \mathbf{u}_2(\bar{\mathbf{x}}, \bar{\mathbf{x}}_{-1}, \bar{\mathbf{x}}_{-2}, \varepsilon^2 t)\dot{\bar{\mathbf{x}}}_{-2}\big)\end{aligned} \tag{6.35}$$

Substituting with the expression for $\mathbf{x}$ and expanding in a Taylor series, we obtain that:

$$\begin{aligned}\dot{\mathbf{x}} = &\varepsilon^{-1}\mathbf{f}_1(\bar{\mathbf{x}}, \bar{\mathbf{x}}_{-1}, \varepsilon^{-2}t) + \partial_1 \mathbf{f}_1(\bar{\mathbf{x}}, \bar{\mathbf{x}}_{-1}, \varepsilon^{-2}t)\mathbf{u}_1(\bar{\mathbf{x}}, \bar{\mathbf{x}}_{-1}, \varepsilon^2 t) \\ &+ \partial_2 \mathbf{f}_1(\bar{\mathbf{x}}, \bar{\mathbf{x}}_{-1}, \varepsilon^{-2}t)\mathbf{u}_1(\bar{\mathbf{x}}_{-1}, \bar{\mathbf{x}}_{-2}, \varepsilon^{-2}(t - t_d)) + O(\varepsilon)\end{aligned} \tag{6.36}$$

Furthermore, we let:

$$\dot{\bar{\mathbf{x}}} = \bar{\mathbf{f}}(\bar{\mathbf{x}}, \bar{\mathbf{x}}_{-1}, \bar{\mathbf{x}}_{-2}, t_d, \varepsilon) \tag{6.37}$$

By matching the coefficient of ε^{-1} we obtain the homological equation:

$$\partial_3 \mathbf{u}_1(\bar{\mathbf{x}}, \bar{\mathbf{x}}_{-1}, \varepsilon^{-2}t) = \mathbf{f}_1(\bar{\mathbf{x}}, \bar{\mathbf{x}}_{-1}, \varepsilon^{-2}t), \tag{6.38}$$

and by matching the coefficient of $O(1)$ we obtain the homological equation:

$$\begin{aligned}\partial_4 \mathbf{u}_2(\bar{\mathbf{x}}, \bar{\mathbf{x}}_{-1}, \bar{\mathbf{x}}_{-2}, \varepsilon^{-2}t) = &\partial_1 \mathbf{f}_1(\bar{\mathbf{x}}, \bar{\mathbf{x}}_{-1}, \varepsilon^{-2}t)\mathbf{u}_1(\bar{\mathbf{x}}, \bar{\mathbf{x}}_{-1}, \varepsilon^{-2}t) \\ &+ \partial_2 \mathbf{f}_1(\bar{\mathbf{x}}, \bar{\mathbf{x}}_{-1}, \varepsilon^{-2}t)\mathbf{u}_1(\bar{\mathbf{x}}_{-1}, \bar{\mathbf{x}}_{-2}, \varepsilon^{-2}t - \varepsilon^{-2}t_d) \\ &- \bar{\mathbf{f}}(\bar{\mathbf{x}}, \bar{\mathbf{x}}_{-1}, \bar{\mathbf{x}}_{-2}, t_d, \varepsilon)\end{aligned} \tag{6.39}$$

If we define:

$$\mathbf{u}_1(\bar{\mathbf{x}}, \bar{\mathbf{x}}_{-1}, \tau) = \int \mathbf{f}_1(\bar{\mathbf{x}}, \bar{\mathbf{x}}_{-1}, \tau)\, d\tau \tag{6.40}$$

where the integral is considered as an anti-derivative, we can define the vector field $\bar{\mathbf{f}}$ by:

$$\begin{aligned}\bar{\mathbf{f}}(\bar{\mathbf{x}}, \bar{\mathbf{x}}_{-1}, \bar{\mathbf{x}}_{-2}, t_d, \varepsilon) = \frac{1}{T}\int_0^T \Big(& \partial_1 \mathbf{f}_1(\bar{\mathbf{x}}, \bar{\mathbf{x}}_{-1}, \tau)\mathbf{u}_1(\bar{\mathbf{x}}, \bar{\mathbf{x}}_{-1}, \tau) \\ & + \partial_2 \mathbf{f}_1(\bar{\mathbf{x}}, \bar{\mathbf{x}}_{-1}, \tau)\mathbf{u}_1(\bar{\mathbf{x}}_{-1}, \bar{\mathbf{x}}_{-2}, \tau - \varepsilon^{-2} t_d) \Big)\, d\tau\end{aligned} \tag{6.41}$$

and the averaged system in this case is given by:

$$\dot{\bar{\mathbf{x}}} = \bar{\mathbf{f}}(\bar{\mathbf{x}}, \bar{\mathbf{x}}_{-1}, \bar{\mathbf{x}}_{-2}, t_d, \varepsilon) \tag{6.42}$$

We observe that the averaged system depends explicitly on t_d and on ε. Notice, however, that the averaged system needs more information than the original system. In particular, the averaged system depends on a twice-delayed state even when the original system depends only on a once-delayed state. This fact translates to an ambiguity regarding the behavior of the averaged system until sufficiently long time has passed. In particular, During the interval $[-t_d, 0)$, the averaged system and the original system have the same initial condition and so they must coincide. However, during the interval $[0, t_d)$, the original system will have started to evolve according to the time-varying first-order dynamics whereas the averaged system is still in the initial condition phase. Therefore, the approximation provided above only works beyond the interval $[-t_d, t_d)$ and we are required to supply the averaged system with the remaining initial condition on the interval $[0, t_d)$. This is done by inverting the near-identity transform:

$$\mathbf{x}(t) = \bar{\mathbf{x}}(t) + \varepsilon\, \mathbf{u}_1(\bar{\mathbf{x}}(t), \mathbf{x}(t - t_d), \varepsilon^{-2} t), \qquad \forall t \in [0, t_d) \tag{6.43}$$

We now illustrate the nature of the approximation using the two systems considered in the previous section.

Consider the two systems:

$$\dot{x}_1 =, \sqrt{2}\,\varepsilon^{-1}\cos\left(\varepsilon^{-2}t + c(x_1(t-t_d))\right) \tag{6.44}$$

$$\dot{x}_2 = \sqrt{2}\,\varepsilon^{-1}\left(\cos(\varepsilon^{-2}t) - c(x_2(t-t_d))\sin(\varepsilon^{-2}t)\right) \tag{6.45}$$

where the function $c(\cdot)$ is a smooth convex function. By applying the formulas presented in this section, we obtain the averaged systems:

$$\dot{\bar{x}}_1 = -\frac{dc}{dx}(\bar{x}_1(t-t_d))\cos\left(t_d\varepsilon^{-2} + c(\bar{x}_1(t-t_d)) - c(\bar{x}_1(t-2t_d))\right) \tag{6.46}$$

$$\dot{\bar{x}}_2 = -\frac{dc}{dx}(\bar{x}_2(t-t_d))\left(\cos(t_d\varepsilon^{-2}) + c(\bar{x}_2(t-2t_d))\sin(t_d\varepsilon^{-2})\right) \tag{6.47}$$

In contrast to the previous section, we can no longer obtain a finite dimensional approximation of these systems due to the fact that the delay is no longer infinitesmal. Yet, the trajectories of the averaged systems faithfully track the trajectories of the original system for sufficiently small ε. We illustrate this fact using numerical simulations. Let us consider the case where the function $c(\cdot)$ is given by:

$$c(x) = \frac{2x^2}{2+x^2} \tag{6.48}$$

Therefore, the averaged systems are given by:

$$\dot{\bar{x}}_1 = -\frac{8\bar{x}_2(t-t_d)}{(2+\bar{x}_1(t-t_d)^2)^2}\cos\left(t_d\varepsilon^{-2} + \frac{2\bar{x}_1(t-t_d)^2}{2+\bar{x}_1(t-t_d)^2} - \frac{2\bar{x}_1(t-2t_d)^2}{2+\bar{x}_1(t-2t_d)^2})\right) \tag{6.49}$$

$$\dot{\bar{x}}_2 = -\frac{8\bar{x}_2(t-t_d)}{(2+\bar{x}_2(t-t_d)^2)^2}\left(\cos(t_d\varepsilon^{-2}) + \frac{2\bar{x}_2(t-2t_d)^2}{2+\bar{x}_2(t-2t_d)^2}\sin(t_d\varepsilon^{-2})\right) \tag{6.50}$$

First, let us consider the situation in which:

$$\cos(t_d\varepsilon^{-2}) = 1, \qquad \sin(t_d\varepsilon^{-2}) = 0, \tag{6.51}$$

which leads to the relation $t_d = 2\pi\ell\varepsilon^2$ between the delay t_d and the small parameter ε where $\ell \in \mathbb{N}$. Consider the sequence:

$$\{\varepsilon_k\}_{k=1}^{\infty}, \qquad \varepsilon_k = \frac{1}{\sqrt{2\pi k}} \tag{6.52}$$

and observe that $\varepsilon_k \to 0$, and that $t_d = 2\pi\ell\varepsilon_k^2 = \ell/k$. Therefore, we make the delay as large as we want for any k by selecting $\ell \in \mathbb{N}$ sufficiently large. In this situation, the averaged systems reduce to:

$$\dot{\bar{x}}_1 = -\frac{8\bar{x}_1(t-\ell/k)}{(2+\bar{x}_1(t-\ell/k)^2)^2}\cos\left(\frac{2\bar{x}_1(t-\ell/k)^2}{2+\bar{x}_1(t-\ell/k)^2} - \frac{2\bar{x}_1(t-2\ell/k)^2}{2+\bar{x}_1(t-2\ell/k)^2})\right) \tag{6.53}$$

$$\dot{\bar{x}}_2 = -\frac{8\bar{x}_2(t-\ell/k)}{(2+\bar{x}_2(t-\ell/k)^2)^2} \tag{6.54}$$

Fix $k = 12$, and let us consider three situations where $\ell \in \{1, 8, 16\}$. Simulation results are shown in figure 6.2. We observe that the gradual increase in the time-delay leads to gradually increasing the instability of the system. Indeed, when the delay becomes sufficiently large, a limit cycle appears in the averaged system. Nevertheless, the averaged systems described by our formulas faithfully track the original system.

We now consider a different situation where:

$$\cos(t_d\varepsilon^{-2}) = 0, \qquad\qquad \sin(t_d\varepsilon^{-2}) = 1, \tag{6.55}$$

which leads to the relation $t_d = (\pi/2 + 2\pi\ell)\varepsilon^2$ between the delay t_d and ε where $\ell \in \mathbb{N}$. Once again, consider the sequence:

$$\{\varepsilon_k\}_{k=1}^{\infty}, \qquad \varepsilon_k = \frac{1}{\sqrt{2\pi k}} \tag{6.56}$$

and observe that $\varepsilon_k \to 0$. In addition, observe that $t_d = (4\ell+1)/(4k)$, and therefore, by selecting ℓ sufficiently large, we can make the delay as large as we want. We observe that in

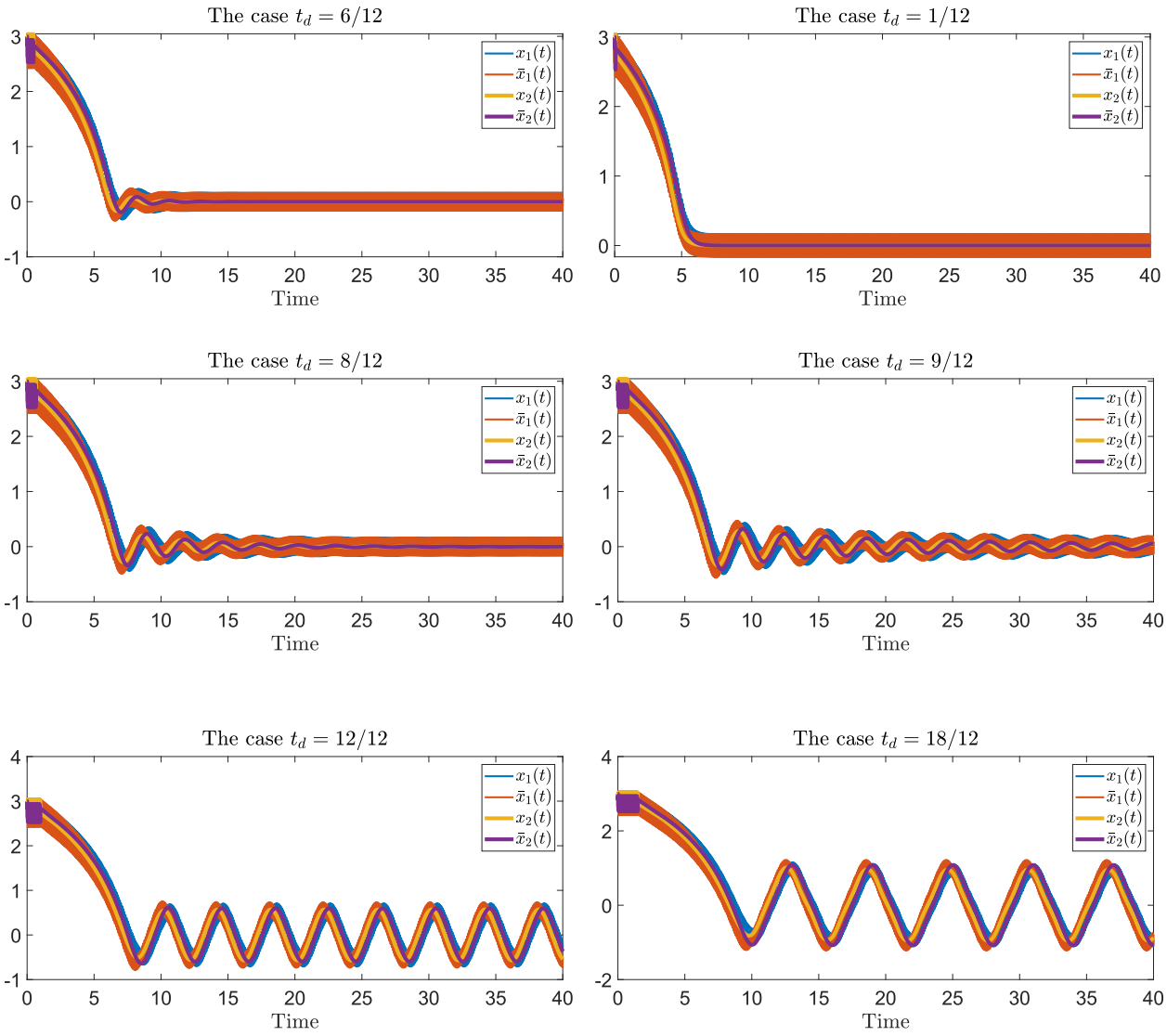

Figure 6.2: Time response of the time-delayed system for various values of t_d.

this situation, the averaged systems simplify to:

$$\dot{\bar{x}}_1 = 0 \tag{6.57}$$

$$\dot{\bar{x}}_2 = -\frac{16\bar{x}_2(t-\ell/k)\bar{x}_2(t-2t_d)^2}{(2+\bar{x}_2(t-\ell/k)^2)^2(2+\bar{x}_2(t-2t_d)^2)} \tag{6.58}$$

Let us fix $k = 12$, and simulate the system for various values of ℓ. The response is shown in figure 6.3. We observe how the first system is marginally stable for all values of the time-delay where as the gradual increase in the delay progressively degrades the stability of the

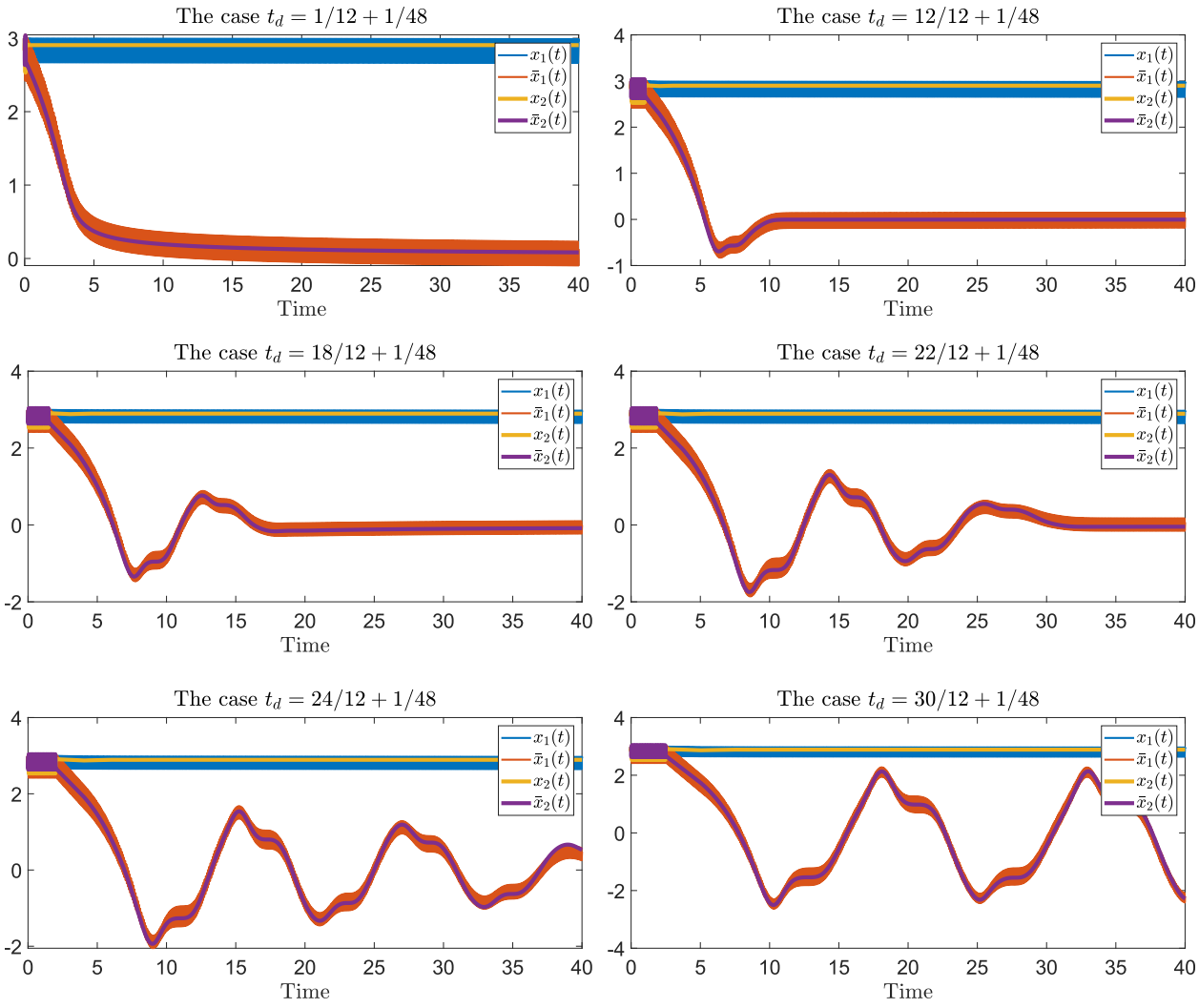

Figure 6.3: The response of the averaged delayed systems for $t_d = (4\ell + 1)/(48)$, $\ell \in \{1, 12, 18, 22, 24, 30\}$.

equilibrium point at the origin until it becomes a limit cycle. In both cases, the averaged systems faithfully track the trajectories of the original systems.

Finally, let us consider the situation in which:

$$\cos(t_d\varepsilon^{-2}) = -\frac{1}{\sqrt{2}}, \qquad \sin(t_d\varepsilon^{-2}) = \frac{1}{\sqrt{2}} \tag{6.59}$$

which leads to the relation $t_d\varepsilon^{-2} = 3\pi/8 + 2\pi\ell$ between the delay t_d and ε where $\ell \in \mathbb{N}$. We

observe that in this situation, the averaged systems simplify to:

$$\dot{\bar{x}}_1 = -\frac{4\sqrt{2}\bar{x}_2(t-t_d)}{(2+\bar{x}_1(t-t_d)^2)^2}\cos\left(\frac{3\pi}{8}+\frac{2\bar{x}_1(t-t_d)^2}{2+\bar{x}_1(t-t_d)^2}-\frac{2\bar{x}_1(t-2t_d)^2}{2+\bar{x}_1(t-2t_d)^2})\right) \tag{6.60}$$

$$\dot{\bar{x}}_2 = -\frac{4\sqrt{2}\bar{x}_2(t-t_d)}{(2+\bar{x}_2(t-t_d)^2)^2}\left(\frac{2\bar{x}_2(t-2t_d)^2}{2+\bar{x}_2(t-2t_d)^2}-1\right) \tag{6.61}$$

Once again, consider the sequence:

$$\{\varepsilon_k\}_{k=1}^{\infty}, \qquad \varepsilon_k = \frac{1}{\sqrt{2\pi k}} \tag{6.62}$$

and observe that $\varepsilon_k \to 0$. In addition, observe that $t_d = (8\ell+3)/(8k)$, and therefore, by selecting ℓ sufficiently large, we can make the delay as large as we want. We fix $k = 12$ and simulate the system for various values of ℓ. The simulation results are shown in figure 6.4. As predicted by our formulas, there are two additional equilibria at $x = \pm\sqrt{2}$ for the second system. Moreover, these equilibria are exponentially stable when the delay is small. Furthermore, as the delay is gradually increased, the stability of the equilibria degrades progressively until, for sufficiently high delay, they turn into limit cycles. Furthermore, the first system is unstable as predicted by our formulas. Finally, we observe that the trajectories of the averaged systems faithfully track their original counterparts.

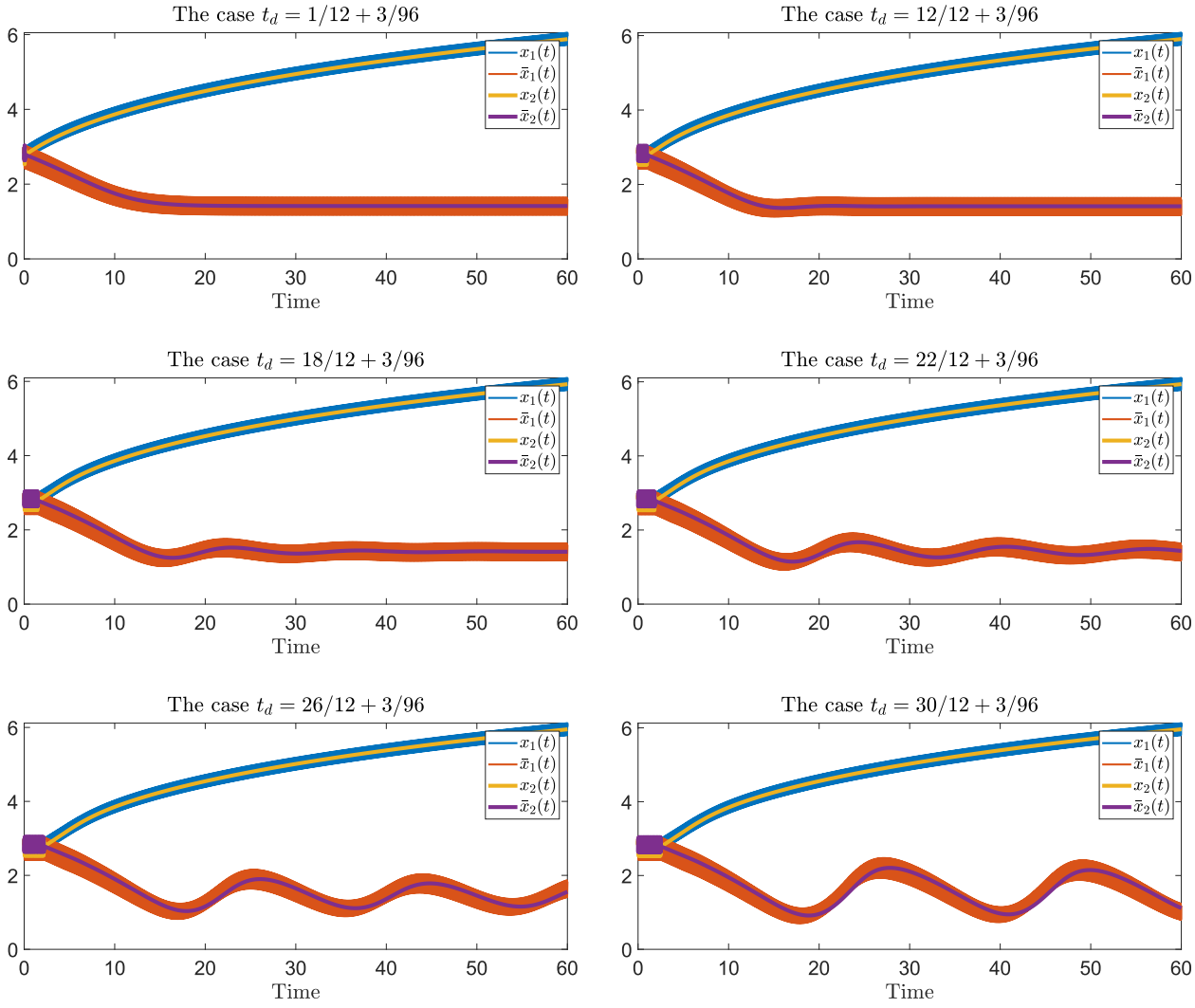

Figure 6.4: The response of the averaged delayed systems for $t_d = (8\ell + 3)/(96)$, $\ell \in \{1, 12, 18, 22, 26, 30\}$.

Chapter 7

Conclusion and Future Work

In this thesis, we revisited the theory of higher-order averaging, particularly second-order averaging, with an emphasis on highly oscillatory systems. We have shown that the averaging theorem is applicable to this class of systems. In addition, we combined singular perturbation and averaging on multiple scales in order to analyze a class of highly oscillatory systems that arises in extremum seeking applications. Finally, we investigated the effect of time-delays, infinitesmal and finite, on the behavior of highly oscillatory systems using the methodology of averaging and numerical simulations.

In addition to the theoretical contributions of the thesis, we considered the application of sperm chemotaxis in biology. We established a novel connection between helical klinotaxis, the navigation strategy of sea urchin sperm cells, and extremum seeking control. Using the tools developed in this thesis, we were able to show that the seemingly discontinuous observed behavior of sperm cells may arise from a continuous dynamical description provided that an appropriate time-scale separation exists between the dynamics of motion and the dynamics of the signaling pathway. Unlike previous models of this phenomenon in the literature, our model is continuous and does not employ any threshold-based switching rules, thereby

making it more natural for a cellular implementation.

Based on the novel connection we established in this thesis, we were able to propose several 3D source seeking algorithms for different kinematic vehicle configurations. Unlike all existing algorithms in the literature, our algorithms do not require any information on the attitude of th seeking agent. We analyze the behavior of the proposed algorithms using the theoretical tools of singularly perturbed averaging on multiple scales that were developed in the thesis.

The work in this thesis can be extended on several fronts. We now discuss such extensions that will be pursued in the future.

7.1 Bio-Inspired 3D Source Seeking

The algorithms proposed for 3D source seeking were inspired by the chemotactic navigation of sperm cells. Since sperm cells swim in the low Reynolds number fluid regime, their motion can be well-approximated with kinematic models. Nevertheless, robots that swim on the macro scale swim in a relatively high Reynolds number fluid regime, and therefore the effects of inertia cannot be neglected. It is, therefore, of practical importance to consider extensions of the methods developed in this thesis to the case where inertial effects are not neglected.

In addition, in the presence of obstacles, it may be of interest to navigate the environment while circumventing the obstacles. Moreover, one may consider the situation in which multiple, rather than a single, vehicles employ 3D source seeking algorithms for cooperative targeting. Each of these extensions will be considered in future work.

7.2 Convergence Proofs for Averaging Time-Delayed Systems

Our analysis of highly oscillatory time-delayed systems in this thesis has been formal. Despite the fact that such an analysis is absent from the literature, it is important to obtain rigorous convergence proofs to relate the trajectories of the averaged and the original systems.

It is worth noting that such an endeavour is not trivial. Already for the first-order averaging case and finite delays, one has to work with ordinary differential equations on infinite dimensional abstract Banach spaces [61].

In addition, it is of interest to attempt to exploit this vulnerability to infinitesmal time-delays in an adversarial setting where an attacker attempts to confuse or destabilize a stable highly oscillatory system.

Finally, knowing this vulnerability, are there any solutions one can implement in order to increase the robustness of the system. That is, with an incomplete information regarding the time-delay, is it possible to estimate and compensate for the presence of the delay in a highly oscillatory system. Such questions may be addressed in future work.

Bibliography

[1] Victoria Grushkovskaya, Alexander Zuyev, and Christian Ebenbauer. On a class of generating vector fields for the extremum seeking problem: Lie bracket approximation and stability properties. *Automatica*, 94:151–160, 2018.

[2] Miroslav Krstic and Hsin-Hsiung Wang. Stability of extremum seeking feedback for general nonlinear dynamic systems. *Automatica-Kidlington*, 36(4):595–602, 2000.

[3] Hans-Bernd Dürr, Miloš S Stanković, Christian Ebenbauer, and Karl Henrik Johansson. Lie bracket approximation of extremum seeking systems. *Automatica*, 49(6):1538–1552, 2013.

[4] Hans-Bernd Dürr, Miroslav Krstić, Alexander Scheinker, and Christian Ebenbauer. Singularly perturbed lie bracket approximation. *IEEE Transactions on Automatic Control*, 60(12):3287–3292, 2015.

[5] Wensheng Liu. An approximation algorithm for nonholonomic systems. *SIAM Journal on Control and Optimization*, 35(4):1328–1365, 1997.

[6] Jan A Sanders, Ferdinand Verhulst, and James Murdock. *Averaging methods in nonlinear dynamical systems*, volume 59. Springer, 2007.

[7] Hassan Khalil. *Nonlinear Systems*. Prentice Hall, 2002.

[8] Nikolaĭ Nikolaevich Bogoliubov and Yurij Alekseevich Mitropolskii. *Asymptotic methods in the theory of non-linear oscillations*, volume 10. CRC Press, 1961.

[9] Andrei Alexandrovich Agrachev and Revaz Valer'yanovich Gamkrelidze. The exponential representation of flows and the chronological calculus. *Matematicheskii Sbornik*, 149(4):467–532, 1978.

[10] Francesco Bullo. Series expansions for the evolution of mechanical control systems. *SIAM Journal on Control and Optimization*, 40(1):166–190, 2001.

[11] Francesco Bullo. Averaging and vibrational control of mechanical systems. *SIAM Journal on Control and Optimization*, 41(2):542–562, 2002.

[12] Andrey V Sarychev. Lie-and chronologico-algebraic tools for studying stability of time-varying systems. *Systems & Control Letters*, 43(1):59–76, 2001.

[13] P.A. Vela and Jared Burdick. A general averaging theory via series expansions. *Proceedings of the 2003 American Control Conference, 2003.*, 2:1530–1535, 2003.

[14] Marco Maggia, Sameh A Eisa, and Haithem E Taha. On higher-order averaging of time-periodic systems: reconciliation of two averaging techniques. *Nonlinear Dynamics*, 99(1):813–836, 2020.

[15] James A Ellison, Albert W Sáenz, and H Scott Dumas. Improved nth order averaging theory for periodic systems. *Journal of differential equations*, 84(2):383–403, 1990.

[16] Maurice Leblanc. Sur l'electrification des chemins de fer au moyen de courants alternatifs de frequence elevee. *Revue générale de l'électricité*, 12(8):275–277, 1922.

[17] Kartik B Ariyur and Miroslav Krstic. *Real-time optimization by extremum-seeking control*. John Wiley & Sons, 2003.

[18] Ying Tan, William H Moase, Chris Manzie, Dragan Nešić, and Iven MY Mareels. Extremum seeking from 1922 to 2010. In *Proceedings of the 29th Chinese control conference*, pages 14–26. IEEE, 2010.

[19] H.J. Sussmann and W. Liu. Limits of highly oscillatory controls and the approximation of general paths by admissible trajectories. In *[1991] Proceedings of the 30th IEEE Conference on Decision and Control*, pages 437–442 vol.1, 1991.

[20] Wensheng Liu. Averaging theorems for highly oscillatory differential equations and iterated lie brackets. *SIAM journal on control and optimization*, 35(6):1989–2020, 1997.

[21] Jaroslav Kurzweil and Jiří Jarník. Limit processes in ordinary differential equations. *Zeitschrift für angewandte Mathematik und Physik ZAMP*, 38(2):241–256, 1987.

[22] Andrew R Teel, Joan Peuteman, and Dirk Aeyels. Semi-global practical asymptotic stability and averaging. *Systems & control letters*, 37(5):329–334, 1999.

[23] Luc Moreau and Dirk Aeyels. Practical stability and stabilization. *IEEE Transactions on Automatic Control*, 45(8):1554–1558, 2000.

[24] Alexander Scheinker and Miroslav Krstić. Non-c2 lie bracket averaging for nonsmooth extremum seekers. *Journal of Dynamic Systems, Measurement, and Control*, 136(1), 2014.

[25] Raik Suttner and Sergey Dashkovskiy. Exponential stability for extremum seeking control systems. *IFAC-PapersOnLine*, 50(1):15464–15470, 2017.

[26] Raik Suttner. Extremum seeking control with an adaptive dither signal. *Automatica*, 101:214–222, 2019.

[27] James A Murdock. Some asymptotic estimates for higher order averaging and a comparison with iterated averaging. *SIAM Journal on Mathematical Analysis*, 14(3):421–424, 1983.

[28] Alexander Scheinker and Miroslav Krstić. Extremum seeking with bounded update rates. *Systems & Control Letters*, 63:25–31, 2014.

[29] Lev Semenovich Pontryagin and LV Rodygin. Periodic solution of a system of ordinary differential equations with a small parameter in the terms containing derivatives. In *Doklady Akademii Nauk*, volume 132, pages 537–540. Russian Academy of Sciences, 1960.

[30] Mahmoud Abdelgalil and Haithem Taha. Recursive averaging with application to bio-inspired 3d source seeking. *arXiv*, 2022.

[31] Miroslav Krstic and Jennie Cochran. Extremum seeking for motion optimization: From bacteria to nonholonomic vehicles. In *2008 Chinese Control and Decision Conference*, pages 18–27. IEEE, 2008.

[32] Chunlei Zhang, Antranik Siranosian, and Miroslav Krstić. Extremum seeking for moderately unstable systems and for autonomous vehicle target tracking without position measurements. *Automatica*, 43(10):1832–1839, 2007.

[33] Jennie Cochran and Miroslav Krstic. Nonholonomic source seeking with tuning of angular velocity. *IEEE Transactions on Automatic Control*, 54(4):717–731, 2009.

[34] Raik Suttner and Miroslav Krstić. Source seeking with a torque-controlled unicycle. *IEEE Control Systems Letters*, 7:79–84, 2022.

[35] Jennie Cochran, Antranik Siranosian, Nima Ghods, and Miroslav Krstic. 3-d source seeking for underactuated vehicles without position measurement. *IEEE Transactions on Robotics*, 25(1):117–129, 2009.

[36] Jinbiao Lin, Shiji Song, Keyou You, and Cheng Wu. 3-d velocity regulation for nonholonomic source seeking without position measurement. *IEEE Transactions on Control Systems Technology*, 24(2):711–718, 2015.

[37] Jinbiao Lin, Shiji Song, Keyou You, and Miroslav Krstic. Overshoot-free nonholonomic source seeking in 3-d. *International Journal of Adaptive Control and Signal Processing*, 31(9):1285–1295, 2017.

[38] Mohammad Ali Ghadiri-Modarres, Mohsen Mojiri, and Hamid RZ Zangeneh. Nonholonomic source localization in 3-d environments without position measurement. *IEEE Transactions on Automatic Control*, 61(11):3563–3567, 2016.

[39] Ruggero Fabbiano, Carlos Canudas De Wit, and Federica Garin. Source localization by gradient estimation based on poisson integral. *Automatica*, 50(6):1715–1724, 2014.

[40] Alexey S Matveev, Michael C Hoy, and Andrey V Savkin. 3d environmental extremum seeking navigation of a nonholonomic mobile robot. *Automatica*, 50(7):1802–1815, 2014.

[41] Alexey S Matveev and Anna A Semakova. Range-only-based three-dimensional circumnavigation of multiple moving targets by a nonholonomic mobile robot. *IEEE Transactions on Automatic Control*, 63(7):2032–2045, 2017.

[42] Trevor T Ashley and Sean B Andersson. Tracking a diffusing three-dimensional source via nonholonomic extremum seeking. *IEEE Transactions on Automatic Control*, 63(9):2855–2866, 2017.

[43] Jirair K Kevorkian and Julian D Cole. *Multiple scale and singular perturbation methods*, volume 114. Springer Science & Business Media, 2012.

[44] Sanjay P Bhat and Dennis S Bernstein. A topological obstruction to continuous global stabilization of rotational motion and the unwinding phenomenon. *Systems & control letters*, 39(1):63–70, 2000.

[45] Naomi E Leonard and PS Krishnaprasad. Averaging for attitude control and motion planning. In *Proceedings of 32nd IEEE Conference on Decision and Control*, pages 3098–3104. IEEE, 1993.

[46] Mahmoud Abdelgalil, Yasser Aboelkassem, and Haithem Taha. Sea urchin sperm exploit extremum seeking control to find the egg. *arXiv preprint arXiv:2108.13634*, 2021.

[47] Benjamin M Friedrich and Frank Jülicher. Chemotaxis of sperm cells. *Proceedings of the National Academy of Sciences*, 104(33):13256–13261, 2007.

[48] Luis Alvarez, Benjamin M Friedrich, Gerhard Gompper, and U Benjamin Kaupp. The computational sperm cell. *Trends in cell biology*, 24(3):198–207, 2014.

[49] Shu-Jun Liu and Miroslav Krstic. Stochastic source seeking for nonholonomic unicycle. *Automatica*, 46(9):1443–1453, 2010.

[50] Hugh C Crenshaw. Orientation by helical motion—iii. microorganisms can orient to stimuli by changing the direction of their rotational velocity. *Bulletin of Mathematical Biology*, 55(1):231–255, 1993.

[51] Benjamin M Friedrich and Frank Jülicher. Steering chiral swimmers along noisy helical paths. *Physical review letters*, 103(6):068102, 2009.

[52] Jan F Jikeli, Luis Alvarez, Benjamin M Friedrich, Laurence G Wilson, René Pascal, Remy Colin, Magdalena Pichlo, Andreas Rennhack, Christoph Brenker, and U Benjamin Kaupp. Sperm navigation along helical paths in 3d chemoattractant landscapes. *Nature communications*, 6(1):1–10, 2015.

[53] U Benjamin Kaupp, Johannes Solzin, Eilo Hildebrand, Joel E Brown, Annika Helbig, Volker Hagen, Michael Beyermann, Francesco Pampaloni, and Ingo Weyand. The signal flow and motor response controling chemotaxis of sea urchin sperm. *Nature cell biology*, 5(2):109–117, 2003.

[54] Daniel A Priego-Espinosa, Alberto Darszon, Adán Guerrero, Ana Laura González-Cota, Takuya Nishigaki, Gustavo Martínez-Mekler, and Jorge Carneiro. Modular analysis of the control of flagellar ca2+-spike trains produced by catsper and cav channels in sea urchin sperm. *PLoS computational biology*, 16(3):e1007605, 2020.

[55] Alexander Scheinker et al. Model independent beam tuning. In *Proceedings of the 2013 International Particle Accelerator Conference, Shanghai, China*, 2013.

[56] Justus A Kromer, Steffen Märcker, Steffen Lange, Christel Baier, and Benjamin M Friedrich. Decision making improves sperm chemotaxis in the presence of noise. *PLoS computational biology*, 14(4):e1006109, 2018.

[57] Benjamin M Friedrich, Ingmar H Riedel-Kruse, Jonathon Howard, and Frank Jülicher. High-precision tracking of sperm swimming fine structure provides strong test of resistive force theory. *Journal of Experimental Biology*, 213(8):1226–1234, 2010.

[58] H. C. Crenshaw. A new look at locomotion in microorganisms: rotating and translating. *American Zoologist*, 36(6):608–618, 1996.

[59] Martin Böhmer, Qui Van, Ingo Weyand, Volker Hagen, Michael Beyermann, Midori Matsumoto, Motonori Hoshi, Eilo Hildebrand, and Ulrich Benjamin Kaupp. Ca2+ spikes in the flagellum control chemotactic behavior of sperm. *The EMBO journal*, 24(15):2741–2752, 2005.

[60] John H Long, Adam C Lammert, Charles A Pell, Mathieu Kemp, James A Strother, Hugh C Crenshaw, and Matthew J McHenry. A navigational primitive: biorobotic implementation of cycloptic helical klinotaxis in planar motion. *IEEE Journal of Oceanic Engineering*, 29(3):795–806, 2004.

[61] JK Hale and SM Verduyn Lunel. Averaging in infinite dimensions. *The Journal of integral equations and applications*, pages 463–494, 1990.

[62] Brad Lehman and Steven P Weibel. Fundamental theorems of averaging for functional differential equations. *Journal of differential equations*, 152(1):160–190, 1999.

[63] Brad Lehman, Joseph Bentsman, Sjoerd Verduyn Lunel, and Erik I Verriest. Vibrational control of nonlinear time lag systems with bounded delay: averaging theory, stabilizability, and transient behavior. *IEEE Transactions on Automatic Control*, 39(5):898–912, 1994.

[64] Khalil Shujaee and Brad Lehman. Vibrational feedback control of time delay systems. *IEEE transactions on automatic control*, 42(11):1529–1545, 1997.

Appendix A

Proofs of Chapter 1

A.1 Proof of Theorem 2.0.1

Proof. Let $J_0 > 0$ be such that the level set

$$\mathcal{L}_{J_0} = \left\{ \mathbf{x} \in \mathbb{R}^n \middle| \tilde{J}(\mathbf{x}) \leq J_0 \right\} \subset D \tag{A.1}$$

Fix an $\epsilon > 0$, and let:

$$y_0 > \frac{1}{2\kappa_1}\left(1 + \sqrt{1 + 8\kappa_1\epsilon}\right), \quad z_0 > J_0 + y_0 \tag{A.2}$$

The functions $F_s(\cdot), s \in \{1, 2\}$ are locally Lipschitz in Δ_ϵ. Hence, absolutely continuous maximal solutions of (2.6) with $\boldsymbol{\theta}(0) \in \Delta_\epsilon$ exist and are unique. We consider a maximal solution $\boldsymbol{\theta} : I \to \Delta_\epsilon$ of (2.6) with $\boldsymbol{\theta}(0) \in \Delta_0$ and apply Lemma 2.0.1 to the functions $g_i,\ i \in \{1, 2, 3\}$ defined by Eq. (2.4). The next step is to establish the bounds on $F^{g_i}, R_1^{g_i}, R_2^{g_i}$

in Lemma 2.0.2 for $g_i(\cdot), i \in \{1,2,3\}$. We compute

$$F^{g_1}(\boldsymbol{\theta}) = -\left\|\nabla J(\mathbf{x})\right\|^2 \tag{A.3a}$$

$$F^{g_2}(\boldsymbol{\theta}) = -z + J(\mathbf{x}) \tag{A.3b}$$

$$F^{g_3}(\boldsymbol{\theta}) = \frac{\eta(\tilde{J}(\mathbf{x})^{2-\frac{1}{m}})}{(z - J(\mathbf{x}))} - \frac{\eta(\tilde{J}(\mathbf{x})^{2-\frac{1}{m}})\left\|\nabla J(\mathbf{x})\right\|^2}{(z - J(\mathbf{x}))^2} \tag{A.3c}$$

$$- \frac{\left(2-\frac{1}{m}\right)\tilde{J}(\mathbf{x})^{1-\frac{1}{m}}\eta'(\tilde{J}(\mathbf{x})^{2-\frac{1}{m}})\left\|\nabla J(\mathbf{x})\right\|^2}{z - J(\mathbf{x})} \tag{A.3d}$$

where $\eta(y) = \tanh(y)$. We note that in case of g_2, the remainder terms $R_1^{g_2}, R_2^{g_2}$ in Lemma 2.0.1 identically vanish, and the only remaining term inside the integral is

$$F^{g_2}(\boldsymbol{\theta}) = -z + J(\mathbf{x}) < 0, \ \forall \boldsymbol{\theta} \in \mathrm{epi}_S(J) \tag{A.4}$$

We conclude, similar to the proof of Lemma 2.0.2, that $g_2(\boldsymbol{\theta}(t)) \leq 0, \ \forall t \in I, \ \forall \omega \in (0,\infty)$. Due to Assumption 2.0.1, we know that $\forall \boldsymbol{\theta} \in \Delta_\epsilon^1$, we have

$$F^{g_1}(\boldsymbol{\theta}) \leq -\kappa_1 J_0^{2-\frac{1}{m}} \tag{A.5}$$

Furthermore, by definition of $g_3(\cdot)$, and thanks to the property that $\tanh(y) \leq y, \ \forall y \geq 0$ and the choice of y_0, we have:

$$F^{g_3}(\boldsymbol{\theta}) \leq y_0 + \epsilon - \kappa_1 y_0^2 < -\epsilon, \quad \forall \boldsymbol{\theta} \in \Delta_\epsilon^3 \tag{A.6}$$

The bounds on the remainders $R_1^{g_2}, R_2^{g_2}$ can be explicitly computed, as outlined in Lemma 2.0.3. We now apply Lemma 2.0.2 with the bounds established above to conclude that $\exists \omega^* \in (0,\infty)$ such that $\forall \omega \in (\omega^*, \infty), \forall \boldsymbol{\theta}(0) \in \Delta_0$ and maximal solution $\boldsymbol{\theta} : \mathrm{I} \to \Delta_\epsilon$, where $0 \in \mathrm{I} =$

(t_e^-, t_e^+), we have :

$$\limsup_{\tau \to t_e^+} g_i(\boldsymbol{\theta}(\tau)) < \epsilon, \ \forall i \in \{1, 2, 3\} \tag{A.7}$$

We note that the only remaining boundary in the definitions of $\Delta_0, \Delta_\epsilon$ is the point $(\mathbf{x}^*, J(\mathbf{x}^*))$. Clearly $\dot{z}(t) < 0$. Moreover, we have that:

$$\dot{z} = -z + J(\mathbf{x}) \geq -z + J(\mathbf{x}^*) \implies \tilde{z}(t) \geq \tilde{z}(0)e^{-t} > 0, \tag{A.8}$$

where $\tilde{z}(t) = z(t) - J(\mathbf{x}^*)$. Thus for any finite $t_e^+ > 0$, we have that

$$\lim_{\tau \to t_e^+} z(\tau) - J(\mathbf{x}_1(\tau)) > 0 \tag{A.9}$$

This implies that $\forall \omega \in (\omega^*, \infty)$, maximal solutions that start inside Δ_0 do not escape Δ_ϵ in any finite time, hence $[0, \infty) \subset I$. Moreover, since z(t) is bounded below and strictly decreasing, we have that

$$\lim_{\tau \to +\infty} z(\tau) - J(\mathbf{x}_1(\tau)) = 0 \tag{A.10}$$

Consequently, we see that due to the definition of $g_3(\cdot)$, it must be true that

$$\lim_{\tau \to +\infty} \eta(\tilde{J}(\mathbf{x}_1(\tau))^{2-\frac{1}{m}}) = 0 \implies \lim \mathbf{x}_1(\tau) = \mathbf{x}^* \tag{A.11}$$

Combining all of the above, we conclude that:

$$\lim_{\tau \to +\infty} \boldsymbol{\theta}(\tau) = (\mathbf{x}^*, J(\mathbf{x}^*)) \tag{A.12}$$

□

A.2 Proof of Lemma 2.0.2

Proof. Fix $\delta \in (0, \epsilon)$. If $g_i(\boldsymbol{\zeta}(t)) < \delta, \forall t \in [0, t_e^+)$, the proof is complete. If not, then, by continuity of $g_i \circ \boldsymbol{\zeta}$ and the Intermediate Value Theorem, $\exists t_1, t_2 \in I,\ t_2 > t_1 \geq 0$, where $g_i(\boldsymbol{\zeta}(t_1)) = 0,\ g_i(\boldsymbol{\zeta}(t_2)) = \delta$, and $\boldsymbol{\zeta}(t) \in \Delta_\epsilon^i,\ \forall t \in [t_1, t_2]$. Using the bounds on $R_1^{g_i}, R_2^{g_i}, F^{g_i}$ and Lemma 2.0.1, we get

$$g_i(\boldsymbol{\zeta}(t_2)) \leq \cancelto{0}{g_i(\boldsymbol{\zeta}(t_1))} + \frac{2c_1^{g_i}}{\sqrt{\omega}} + \int_{t_1}^{t_2} \left(-b^{g_i} + \frac{c_2^{g_i}}{\sqrt{\omega}} \right) dt$$

We define

$$\omega^* = \max_{i \in \{1,2,\ldots,r\}} \left\{ \left(\frac{2c_1^{g_i}}{\delta} \right)^2, \left(\frac{c_2^{g_i}}{b^{g_i}} \right)^2 \right\}$$

and observe that $\forall \omega \in (\omega^*, \infty), \forall i \in \{1, 2, ..., r\}$, we have

$$g_i(\boldsymbol{\zeta}(t_2)) < \delta \implies \limsup_{\tau \to t_e^+} g_i(\boldsymbol{\zeta}(\tau)) < \epsilon \quad \square$$

$\square$

A.3 Proof of Lemma 2.0.3

Proof. Via direct integration, the following bounds can be established

$$|U_{\lambda_1}(t)| \leq \frac{a_1}{\sqrt{\omega}}, \quad |U_{\lambda_1,\lambda_2}(t)| \leq \frac{a_1}{\omega}, \tag{A.13a}$$

$$|U_{\lambda_1,\lambda_2}(t) u_{\lambda_3}(t)| \leq \frac{a_1}{\sqrt{\omega}} \tag{A.13b}$$

$\forall \lambda_1, \lambda_2, \lambda_3 \in \Lambda, \forall t \in \mathbb{R}$, where $a_1 > 0$ depends on the choice of the frequencies ω_j. Due to space constraints, we only show how to establish a bound on one of the highest order terms

in $R_2^{g_3}(\cdot,\cdot)$. The rest of the bounds can be established following the same approach. Let $y = z - J(\mathbf{x})$. We compute

$$L_{\mathbf{f}_{(i,1)}} L_{\mathbf{f}_{(i,1)}} L_{\mathbf{f}_{(i,1)}} g_3(\boldsymbol{\theta}) = \partial_i^3 g_3(\boldsymbol{\theta}) F_1(y)^3 - 2\partial_i^2 g_3(\boldsymbol{\theta}) \tag{A.14a}$$

$$\times F_1'(y) F_1(y)^2 \partial_i J(\mathbf{x}) - \partial_i^2 g_3(\boldsymbol{\theta}) F_1'(y) F_1(y)^2 \partial_i J(\mathbf{x}) \tag{A.14b}$$

$$+\partial_i g_3(\boldsymbol{\theta}) F_1''(y) F_1(y)^2 \partial_i J(\mathbf{x})^2 + \partial_i g_3(\boldsymbol{\theta}) F_1'(y)^2 \tag{A.14c}$$

$$\times F_1(y) \partial_i J(\mathbf{x})^2 - \partial_i g_3(\boldsymbol{\theta}) F_1'(y) F_1(y)^2 \partial_i^2 J(\mathbf{x}) \tag{A.14d}$$

It can be shown by direct computation that, for $y > 0$, we have

$$\begin{aligned}
|F_1(y)| \leq & \sqrt{y},\ |F_1'(y)| \leq \frac{2}{\sqrt{y}},\ |F_2''(y)| \leq \frac{2}{y\sqrt{y}} \\
\partial_i g_3(\boldsymbol{\theta}) = & (2 - \frac{1}{m}) \frac{\tilde{J}(\mathbf{x})^{1-\frac{1}{m}} \partial_i J(\mathbf{x})}{z - J(x)} \operatorname{sech}(\tilde{J}(\mathbf{x})^{2-\frac{1}{m}})^2 \\
& + \frac{\tanh(\tilde{J}(\mathbf{x})^{2-\frac{1}{m}}) \partial_i J(\mathbf{x})}{(z - J(x))^2} \\
|\partial_i g_3(\boldsymbol{\theta})| \leq & \frac{2\tilde{J}(\mathbf{x})^{1-\frac{1}{m}} |\partial_i J(\mathbf{x})|}{|z - J(x)|} + \frac{\tilde{J}(\mathbf{x})^{2-\frac{1}{m}} |\partial_i J(\mathbf{x})|}{(z - J(x))^2}
\end{aligned}$$

Using Assumption 2.0.1, we can see that

$$|\partial_i J(\mathbf{x})| \leq \|\nabla J(\mathbf{x})\| \leq \sqrt{\kappa_2} \tilde{J}(\mathbf{x})^{1-\frac{1}{2m}}$$

Moreover, we know that

$$\frac{\tanh(J(\mathbf{x})^{2-\frac{1}{m}})}{z - J(\mathbf{x})} \leq y_0 + \epsilon, \quad \forall \boldsymbol{\theta} \in \Delta_\epsilon^3$$

Thus, it holds that

$$|\partial_i g_3(\boldsymbol{\theta})| \leq \sqrt{\kappa_2}(y_0 + \epsilon) \frac{\tilde{J}(\mathbf{x})^{2-\frac{3}{2m}}}{\tanh(\tilde{J}(\mathbf{x})^{2-\frac{1}{m}})} (2 + \tilde{J}(x)) \tag{A.15}$$

For $\theta \in \Delta_\epsilon^3$, we have $\tilde{J}(\mathbf{x}) \leq J_0$, and $|F'(y)F(y)| \leq 2$. Thus, we have:

$$|\partial_i g_3(\boldsymbol{\theta})F'(y)F(y)\partial_i J(\mathbf{x})| \leq a_2 \frac{\tilde{J}(\mathbf{x})^{2-\frac{1}{m}}}{\tanh(\tilde{J}(\mathbf{x})^{2-\frac{1}{m}})}$$

where $a_2 = \kappa_2 J_0^{1-\frac{1}{m}}(y_0 + \epsilon)(2 + J_0)$. Finally, it can be shown that

$$\frac{\tilde{J}(\mathbf{x})^{2-\frac{1}{m}}}{\tanh(\tilde{J}(\mathbf{x})^{2-\frac{1}{m}})} \leq \tilde{J}(\mathbf{x})^{2-\frac{1}{m}} + 1$$

This leads to the bound:

$$|\partial_i g_3(\boldsymbol{\theta})F'(y)F(y)\partial_i J(\mathbf{x})| \leq a_3$$

where $a_3 = a_2(1 + J_0^{2-\frac{1}{m}})$. Following a similar approach, it can be shown that all the terms in the Lie derivative are bounded, $|L_{\mathbf{f}_{(i,1)}} L_{\mathbf{f}_{(i,1)}} L_{\mathbf{f}_{(i,1)}} g_3(\boldsymbol{\theta})| \leq a_4$, where $a_4 > 0$ is the sum of all the bounds on the individual terms. Consequently, we have established the bound

$$|L_{\mathbf{f}_{(i,1)}} L_{\mathbf{f}_{(i,1)}} L_{\mathbf{f}_{(i,1)}} g_3(\boldsymbol{\theta}) U_{(i,1),(i,1)}(t) u_{(i,1)}(t)| \leq \frac{a_5}{\sqrt{\omega}}$$

$\forall \boldsymbol{\theta} \in \Delta_\epsilon^3, \forall t \in \mathbb{R}$, where $a_5 = a_1 a_4 > 0$. Following this procedure for each individual term in the remainders will give the explicit bounds on $R_1^{g_i}, R_2^{g_i}, i \in \{1, 2, 3\}$ in terms of the constants $\kappa_1, \kappa_2, \gamma_1, \gamma_2, \epsilon, J_0, y_0, z_0, \omega_j$. □

Appendix B

Proof of Theorem 3.2.1

Proof. The idea of the proof hinges on a two-step procedure in which the first step is second-order averaging of the system (3.8) on the time-scale $\varepsilon^{-2}t$, followed by first-order averaging of the resulting system on the time-scale $\varepsilon^{-1}t$; hence the 'recursive' nature. We begin the proof by applying the time-scaling $\tau = \varepsilon^{-2}(t - t_0) + t_0$ thus yielding the system:

$$\frac{d\mathbf{x}}{d\tau} = \sum_{k=1} \varepsilon^k \, \mathbf{f}_k(\mathbf{x}, \varepsilon^2\tau, \varepsilon\tau, \tau) + O(\varepsilon^3) \tag{B.1}$$

which is on the averaging canonical form. Note that we suppressed the dependency on the initial time t_0 for brevity, but it is implied. By applying the stroboscopic averaging procedure for systems with slow time dependence to second-order in ε [6, Section 3.3], we obtain the system:

$$\frac{d\bar{\mathbf{x}}}{d\tau} = \varepsilon^2 \bar{\mathbf{f}}(\bar{\mathbf{x}}, \varepsilon^2\tau, \varepsilon\tau) \tag{B.2}$$

where the vector field $\bar{\mathbf{f}}$ is given by:

$$\bar{\mathbf{f}}(\bar{\mathbf{x}}, t, \sigma) = \frac{1}{T_2} \int_0^{T_2} \left(\mathbf{f}_2(\bar{\mathbf{x}}, t, \sigma, \tau) + \frac{1}{2} \Big[\int_0^{\tau} \mathbf{f}_1(\bar{\mathbf{x}}, t, \sigma, \nu) d\nu, \mathbf{f}_1(\bar{\mathbf{x}}, t, \sigma, \tau) \Big] \right) d\tau \tag{B.3}$$

A second time-scale change to $\sigma = \varepsilon(\tau - t_0) + t_0$ leads to the system:

$$\frac{d\bar{\mathbf{x}}}{d\sigma} = \varepsilon \, \bar{\mathbf{f}}(\bar{\mathbf{x}}, \varepsilon\sigma, \sigma) \tag{B.4}$$

which is again on the averaging canonical form. By applying the stroboscopic periodic averaging procedure for systems with slow time dependence to first-order in ε [6, Section 3.3], we obtain the system:

$$\frac{d\bar{\bar{\mathbf{x}}}}{d\sigma} = \varepsilon \, \bar{\bar{\mathbf{f}}}(\bar{\bar{\mathbf{x}}}, \varepsilon\sigma) \tag{B.5}$$

A final time-scale change to $t = \varepsilon(\sigma - t_0) + t_0$ brings the system to the fully averaged form:

$$\dot{\bar{\bar{\mathbf{x}}}} = \bar{\bar{\mathbf{f}}}(\bar{\bar{\mathbf{x}}}, t), \qquad \bar{\bar{\mathbf{x}}}(t_0) = \mathbf{x}_0 \tag{B.6}$$

From the assumptions of the theorem, we know that $\forall \mathbf{x}_0 \in \mathcal{K}, \ \forall t_0 \in \mathbb{R}$, a unique trajectory $\bar{\bar{\mathbf{x}}}(t)$ of the system (B.6) exists on the compact time interval $t \in [t_0, t_0 + t_f]$. Moreover. we know that the vector fields $\mathbf{f}_k$ are uniformly bounded in the second argument, which implies that there exists a compact subset $\mathcal{M} \subset \mathbb{R}^{n_1}$ such that $\bar{\bar{\mathbf{x}}}(t) \in \mathcal{M}$, $\forall t \in [t_0, t_0 + t_f]$, $\forall \mathbf{x}_0 \in \mathcal{K}$, $\forall t_0 \in \mathbb{R}$. Hence, the first-order periodic averaging theorem [6] ensures the existence of $\varepsilon_1, C_1 \in (0, \infty)$ such that $\forall \varepsilon \in (0, \varepsilon_1)$, $\forall \mathbf{x}_0 \in \mathcal{K}$, $\forall t_0 \in \mathbb{R}$, a unique trajectory $\bar{\mathbf{x}}(\sigma)$ of the system (B.4) exists on the time interval $\sigma \in [t_0, t_0 + t_f/\varepsilon]$ and satisfies:

$$\|\bar{\bar{\mathbf{x}}}(\varepsilon\sigma) - \bar{\mathbf{x}}(\sigma)\| \leq C_1 \varepsilon, \qquad \forall \sigma \in [t_0, t_0 + t_f/\varepsilon] \tag{B.7}$$

Equivalently, a unique trajectory $\bar{\mathbf{x}}(\varepsilon\tau)$ of the system (B.2) exists on the compact time interval $\tau \in [t_0, t_0 + t_f/\varepsilon^2]$ and $\bar{\mathbf{x}}(\varepsilon\tau) \in \mathcal{M}_{\varepsilon_1}$, where the compact subset $\mathcal{M}_{\varepsilon_1}$ is defined by $\mathcal{M}_{\varepsilon_1} = \{\bar{\mathbf{x}} \in \mathbb{R}^{n_1} \mid \inf_{\mathbf{x}\in\mathcal{K}} \|\mathbf{x} - \bar{\mathbf{x}}\| \leq C_1\varepsilon_1\}$. Hence, the conditions of the second-order periodic averaging theorem with trade-off [6, Section 2.9], [27] are satisfied and we are guaranteed the existence of $\varepsilon_2 \in (0, \infty)$ such that $\forall\varepsilon \in (0, \varepsilon_2)$, $\forall\mathbf{x}_0 \in \mathcal{K}$, $\forall t_0 \in \mathbb{R}$ a unique trajectory $\mathbf{x}_1(\tau)$ of the system (B.1) exists on the compact time interval $\tau \in [t_0, t_0 + t_f/\varepsilon^2]$ and satisfies:

$$\|\bar{\mathbf{x}}(\varepsilon\tau) - \mathbf{x}_1(\tau)\| \leq C_2\varepsilon, \qquad \forall\tau \in \left[0, t_f/\varepsilon^2\right] \tag{B.8}$$

Let $\varepsilon^* = \min\{\varepsilon_1, \varepsilon_2\}$ and observe that it follows from the triangle inequality that $\exists C > 0$ such that $\forall\varepsilon \in (0, \varepsilon^*)$:

$$\|\bar{\bar{\mathbf{x}}}(t) - \mathbf{x}_1(t)\| \leq C\,\varepsilon, \qquad \forall t \in [t_0, t_0 + t_f] \tag{B.9}$$

□

Appendix C

Proof of Theorem 3.3.1

Proof. Define the coordinate shift:

$$\mathbf{y}_2 = \mathbf{x}_2 - \sum_{k=0}^{1} \varepsilon^k \boldsymbol{\phi}_k(\mathbf{x}_1, t, \sigma) \tag{C.1}$$

where the map $\boldsymbol{\phi}_1$ by the formula:

$$\boldsymbol{\phi}_1(\cdot, \sigma) = \big(\mathbf{I} - \boldsymbol{\Phi}_{\mathbf{A}_{\boldsymbol{\phi}}}(\sigma + T_2, \sigma)\big)^{-1} \int_{\sigma}^{\sigma+T_2} \boldsymbol{\Phi}_{\mathbf{A}_{\boldsymbol{\phi}}}(\sigma + T_2, \nu) \mathbf{b}_{\boldsymbol{\phi}}(\cdot, \nu)\, d\nu, \tag{C.2}$$

where the matrix-valued map $\mathbf{A}_{\boldsymbol{\phi}}$ is defined by:

$$\mathbf{A}_{\boldsymbol{\phi}}(\mathbf{x}_1, t, \sigma) = \partial_2 \mathbf{f}_{2,1}(\mathbf{x}_1, \boldsymbol{\phi}_0(\mathbf{x}_1, t, \sigma), t, \sigma), \tag{C.3}$$

the matrix-valued map $\boldsymbol{\Phi}_{\mathbf{A}_{\boldsymbol{\phi}}}$ is the fundamental matrix associated with the linear time-periodic system:

$$\frac{d\mathbf{y}_2}{d\sigma} = \mathbf{A}_{\boldsymbol{\phi}}(\cdot, \sigma)\mathbf{y}_2, \tag{C.4}$$

and the vector-valued map $\mathbf{b}_{\boldsymbol{\phi}}$ is defined by:

$$\begin{aligned}\mathbf{b}_{\boldsymbol{\phi}}(\mathbf{x}_1,t,\sigma) &= \mathbf{f}_{2,2}(\mathbf{x}_1,\boldsymbol{\phi}_0(\mathbf{x}_1,t,\sigma),t,\sigma) - \partial_t\boldsymbol{\phi}_0(\mathbf{x}_1,t,\sigma)\\ &\quad - \partial_1\boldsymbol{\phi}_0(\mathbf{x}_1,t,\sigma)\mathbf{f}_{1,2}(\mathbf{x}_1,\boldsymbol{\phi}_0(\mathbf{x}_1,t,\sigma),t,\sigma)\end{aligned} \tag{C.5}$$

Then, change the timescale to $\sigma = \varepsilon^{-1}(t-t_0)+t_0$ to obtain the system:

$$\frac{d\mathbf{x}_1}{d\sigma} = \varepsilon\,\tilde{\mathbf{f}}_{1,2}(\mathbf{x}_1,\mathbf{y}_2,t,\sigma) + O(\varepsilon^2), \qquad \mathbf{x}_1(t_0) = \mathbf{x}_{1,0} \tag{C.6}$$

$$\frac{d\mathbf{y}_2}{d\sigma} = \sum_{k=1}^{2}\varepsilon^{k-1}\tilde{\mathbf{f}}_{2,k}(\mathbf{x}_1,\mathbf{y}_2,t,\sigma) + O(\varepsilon^2), \qquad \mathbf{y}_2(t_0) = \mathbf{x}_{2,0} - \sum_{k=0}^{1}\varepsilon^k\boldsymbol{\phi}_k(\mathbf{x}_{1,0},t_0,t_0) \tag{C.7}$$

where the vector fields $\tilde{\mathbf{f}}_{j,k}$ are given by:

$$\tilde{\mathbf{f}}_{2,1}(\mathbf{x}_1,\mathbf{y}_2,t,\sigma) = \mathbf{f}_{2,1}(\mathbf{x}_1,\mathbf{y}_2+\boldsymbol{\phi}_0(\mathbf{x}_1,t,\sigma),t,\sigma) - \partial_\sigma\boldsymbol{\phi}_0(\mathbf{x}_1,t,\sigma) \tag{C.8a}$$

$$\tilde{\mathbf{f}}_{1,2}(\mathbf{x}_1,\mathbf{y}_2,t,\sigma) = \mathbf{f}_{1,2}(\mathbf{x}_1,\mathbf{y}_2+\boldsymbol{\phi}_0(\mathbf{x}_1,t,\sigma),t,\sigma) \tag{C.8b}$$

$$\begin{aligned}\tilde{\mathbf{f}}_{2,2}(\mathbf{x}_1,\mathbf{y}_2,t,\sigma) &= \mathbf{f}_{2,2}(\mathbf{x}_1,\mathbf{y}_2+\boldsymbol{\phi}_0(\mathbf{x}_1,t,\sigma),t,\sigma)\\ &\quad + \partial_2\mathbf{f}_{2,1}(\mathbf{x}_1,\mathbf{y}_2+\boldsymbol{\phi}_0(\mathbf{x}_1,t,\sigma),t,\sigma)\boldsymbol{\phi}_1(\mathbf{x}_1,t,\sigma)\\ &\quad - \partial_1\boldsymbol{\phi}_0(\mathbf{x}_1,t,\sigma)\tilde{\mathbf{f}}_{1,2}(\mathbf{x}_1,\mathbf{y}_2,t,\sigma) - \partial_t\boldsymbol{\phi}_0(\mathbf{x}_1,t,\sigma)\\ &\quad - \partial_\sigma\boldsymbol{\phi}_1(\mathbf{x}_1,t,\sigma)\end{aligned} \tag{C.8c}$$

We observe that, due to Assumption 3.3.1 and the definition of the map $\boldsymbol{\phi}_1$, we have that:

$$\tilde{\mathbf{f}}_{2,1}(\mathbf{x}_1,0,t,\sigma) = 0, \qquad \tilde{\mathbf{f}}_{2,2}(\mathbf{x}_1,0,t,\sigma) = 0 \tag{C.9}$$

Let $(\mathbf{x}_1(\sigma;t_0,\mathbf{x}_{1,0}),\mathbf{y}_2(\sigma;t_0,\mathbf{y}_{2,0}))$ denote the unique maximal solution starting at the initial condition $\mathbf{x}_1(t_0)=\mathbf{x}_{1,0}$ and $\mathbf{y}_2(t_0)=\mathbf{y}_{2,0}$. Define the time σ_e by:

$$\begin{aligned}\sigma_e = \inf_T\{T\in(0,\infty) :&\exists!(\mathbf{x}_1(\sigma;t_0,\mathbf{x}_{1,0}),\mathbf{y}_2(\sigma;t_0,\mathbf{y}_{2,0})),\\ &\forall\sigma\in[t_0,t_0+T), t_0\in\mathbb{R}, (\mathbf{x}_{1,0},\mathbf{y}_{2,0})\in\mathcal{B}_1\times\mathcal{B}_2\}\end{aligned} \tag{C.10}$$

Consider the trajectories of the reduced order system given by:

$$\frac{d\tilde{\mathbf{x}}_1}{d\sigma} = \varepsilon\, \tilde{\mathbf{f}}_{1,1}(\tilde{\mathbf{x}}_1, 0, t, \sigma), \qquad \tilde{\mathbf{x}}_1(t_0) = \mathbf{x}_{1,0} \tag{C.11}$$

From the averaging theorem, we know that $\exists \varepsilon_0 \in (0, \infty)$ such that $\forall \mathbf{x}_{1,0} \in \mathcal{B}_1$, $\forall t_0 \in \mathbb{R}$, and $\forall \varepsilon \in (0, \varepsilon_0)$, unique trajectories $\tilde{\mathbf{x}}_1(\sigma; t_0, \mathbf{x}_{1,0})$ of the system (C.11) exist $\forall \sigma \in [t_0, t_0 + t_f/\varepsilon]$ and are contained in a compact subset $\mathcal{N}_1 \subset \mathbb{R}^{n_1}$. Define a tubular neighborhood $\mathcal{O}_1(\sigma)$ around $\tilde{\mathbf{x}}_1(\sigma; t_0, \mathbf{x}_{1,0})$ by:

$$\mathcal{O}_1(\sigma) = \{\mathbf{x}_1 \in \mathbb{R}^{n_1} : \|\mathbf{x}_1 - \tilde{\mathbf{x}}_1(\sigma; t_0, \mathbf{x}_{1,0})\| < D/2\} \tag{C.12}$$

and observe that the component $\mathbf{x}_1(\sigma; t_0, \mathbf{x}_{1,0})$ of the solution $(\mathbf{x}_1(\sigma; t_0, \mathbf{x}_{1,0}), \mathbf{y}_2(\sigma; t_0, \mathbf{y}_{2,0}))$ starts inside $\mathcal{O}_1(\sigma)$. Define the compact subset:

$$\mathcal{M}_1 = \overline{\{\mathbf{x}_1' \in \mathbb{R}^{n_1} : \inf_{\mathbf{x}_1 \in \mathcal{N}_1} \|\mathbf{x}_1 - \mathbf{x}_1'\| < D/2\}} \tag{C.13}$$

From the continuity of solutions we have that one of the following two cases holds: C1) $\exists \sigma_D \in (0, t_0)$ such that $\mathbf{x}_1(\sigma; t_0, \mathbf{x}_{1,0}) \in \mathcal{O}_1(\sigma)$, $\forall \sigma \in [t_0, t_0 + \sigma_D)$ and $\|\tilde{\mathbf{x}}_1(\sigma_D; t_0, \mathbf{x}_{1,0}) - \mathbf{x}_1(\sigma_D; t_0, \mathbf{x}_{1,0})\| = D/2$, or C2) $\mathbf{x}_1(\sigma; t_0, \mathbf{x}_{1,0}) \in \mathcal{O}_1(\sigma)$, $\forall \sigma \in [t_0, t_0 + \sigma_e)$. The proof in case C2) is trivial. Suppose that case C1) holds and observe that $\mathbf{x}_1(\sigma; t_0, \mathbf{x}_{1,0}) \in \mathcal{M}_1, \forall \sigma \in [t_0, t_0 + \sigma_D]$. Let $c \in (0, \infty)$ be such that the compact subset $\mathcal{N}_2 = \{\mathbf{y}_2 \in \mathbb{R}^{n_2} : \|\mathbf{y}_2\| \leq \sqrt{c/\kappa_2}\}$ contains the subset $\mathcal{B}_2$, and define the compact subset $\mathcal{M}_2$ by:

$$\mathcal{M}_2 = \{\mathbf{y}_2 \in \mathbb{R}^{n_2} : \|\mathbf{y}_2\| \leq \sqrt{c/\kappa_1}\} \tag{C.14}$$

In addition, define the compact subset $\mathcal{K} = \mathcal{M}_1 \times \mathcal{M}_2$ and compute the derivative of the Lyapunov function V along the trajectories:

$$\frac{dV}{d\sigma} = \partial_2 V(\mathbf{y}_2, \sigma) + \sum_{k=0}^{1} \varepsilon^k \partial_1 V(\mathbf{y}_2, \sigma) \tilde{\mathbf{f}}_{2,k}(\mathbf{x}_1, \mathbf{y}_2, t, \sigma) + O(\varepsilon^2) \tag{C.15}$$

$$\leq -(\kappa_3 + \varepsilon\, \kappa_4 L_{\mathcal{K},\tilde{\mathbf{f}}_{2,2}}) \|\mathbf{y}_2\|^2 + B_{\mathcal{K},\tilde{\mathbf{f}}_{2,3}} \varepsilon^2 \tag{C.16}$$

where we use the fact that the $O(\varepsilon^2)$-terms are uniformly bounded on the compact subset $\mathcal{K}$, and the vector field $\tilde{\mathbf{f}}_{2,2}$ has an equilibrium point at $\mathbf{y}_2 = 0$ and is Lipschitz continuous. Let $\varepsilon_2 = \min\{\varepsilon_0, \kappa_3/(2\kappa_4 L_{\mathcal{K},\tilde{\mathbf{f}}_{2,2}})\}$, and observe that $\forall \varepsilon \in (0, \varepsilon_2)$, $\forall (\mathbf{x}_1, \mathbf{y}_2) \in \mathcal{K}$, and $\forall \sigma \in \mathbb{R}$, we have that:

$$\frac{dV}{d\sigma} \leq -\frac{\kappa_3}{2} \|\mathbf{y}_2\|^2 + B_{\mathcal{K},\tilde{\mathbf{f}}_{2,3}} \varepsilon^2 \tag{C.17}$$

Next, let $\varepsilon_3 = \min\{\varepsilon_2, \sqrt{(\kappa_3 - \kappa_4\kappa_5)c/(4\kappa_2 B_{\mathcal{K},\tilde{\mathbf{f}}_{2,3}})}\}$, then observe that $\forall \varepsilon \in (0, \varepsilon_3)$, $\forall (\mathbf{x}_1, \mathbf{y}_2) \in \mathcal{M}_1 \times (\mathcal{M}_2 \backslash \mathcal{N}_2)$, and $\forall \sigma \in \mathbb{R}$ we have that $dV/d\sigma \leq 0$, which implies that the solutions $(\mathbf{x}_1(\sigma; t_0, \mathbf{x}_{1,0}), \mathbf{y}_2(\sigma; t_0, \mathbf{y}_{2,0}))$ stay in $\mathcal{K}$, $\forall \sigma \in [t_0, t_0 + \sigma_D]$. Moreover, similar to [7, Theorem 4.18], there exist positive constants $\gamma_\sigma, \lambda_\sigma, \kappa_\sigma$ such that the following estimate holds $\forall \sigma \in [t_0, t_0 + \sigma_D]$:

$$\|\mathbf{y}_2(\sigma)\| < \gamma_\sigma \|\mathbf{y}_{2,0}\| \mathrm{e}^{-\lambda_\sigma(\sigma - t_0)} + \kappa_\sigma\, \varepsilon \tag{C.18}$$

Define the ε-dependent time $\sigma_\varepsilon = \max\{0, \log((\gamma\sqrt{c/\kappa_2})/(\kappa_\sigma \varepsilon))/\lambda\}$, and observe that $\forall \sigma > \sigma_\varepsilon + t_0$ and $\forall \varepsilon \in (0, \varepsilon_3)$ we have that:

$$\gamma_\sigma \|\mathbf{y}_{2,0}\| \, \mathrm{e}^{-\lambda_\sigma(\sigma - t_0)} < \kappa_\sigma\, \varepsilon, \qquad \forall \mathbf{y}_{2,0} \in \mathcal{M}_2 \tag{C.19}$$

We now show that $\exists \varepsilon_4 \in (0, \varepsilon_3)$ such that $\sigma_\varepsilon \leq \sigma_D$, $\forall \varepsilon \in (0, \varepsilon_4)$. To obtain a contradiction, suppose the contrary, and estimate the difference:

$$\|\mathbf{x}_1(\sigma) - \tilde{\mathbf{x}}_1(\sigma)\| \leq \int_{t_0}^{\sigma} B_{\mathcal{K},\tilde{\mathbf{f}}_1} \varepsilon \, d\nu \leq B_{\mathcal{K},\tilde{\mathbf{f}}_1} \varepsilon (\sigma - t_0) \tag{C.20}$$

Therefore, we have that:

$$\|\mathbf{x}_1(t_0 + \sigma_D) - \tilde{\mathbf{x}}_1(t_0 + \sigma_D)\| \leq B_{\mathcal{K},\tilde{\mathbf{f}}_1} \varepsilon \sigma_D \leq B_{\mathcal{K},\tilde{\mathbf{f}}_1} \varepsilon \sigma_\varepsilon \tag{C.21}$$

Observe that $\lim_{\varepsilon \to 0} \varepsilon \sigma_\varepsilon = 0$, and therefore we are guaranteed the existence of $\varepsilon_4 \in (0, \varepsilon_3)$ such that $\forall \varepsilon \in (0, \varepsilon_4)$ we have that $\sigma_\varepsilon \varepsilon < D/(4B_{\mathcal{K},\tilde{\mathbf{f}}_1})$. In other words, we have that $\forall \varepsilon \in (0, \varepsilon_4)$:

$$\|\mathbf{x}_1(\sigma_D) - \tilde{\mathbf{x}}_1(\sigma_D)\| < D/4 \tag{C.22}$$

contradicting the definition of σ_D, which proves the claim. Next, we show the existence of $\varepsilon_5 \in (0, \varepsilon_4)$ such that $\forall \varepsilon \in (0, \varepsilon_5)$ we have that $L/\varepsilon < \sigma_D$. To obtain a contradiction, suppose the contrary and once again estimate the difference $\|\mathbf{x}_1(\sigma) - \tilde{\mathbf{x}}_1(\sigma)\|$ on the interval $\sigma \in [t_0 + \sigma_\varepsilon, t_0 + \sigma_D]$:

$$\|\mathbf{x}_1(\sigma) - \tilde{\mathbf{x}}_1(\sigma)\| \leq \|\mathbf{x}_1(t_0 + \sigma_\varepsilon) - \tilde{\mathbf{x}}_1(t_0 + \sigma_\varepsilon)\| + \varepsilon \left\| \int_{t_0 + \sigma_\varepsilon}^{\sigma} \mathbf{i}(\nu) d\nu \right\| + \int_{t_0 + \sigma_\varepsilon}^{\sigma} B_{\mathcal{K},\tilde{\mathbf{f}}_{1,3}} \varepsilon^2 \, d\nu \tag{C.23}$$

where the integrand $\mathbf{i}$ is given by:

$$\mathbf{i}(\nu) = \tilde{\mathbf{f}}_{1,2}(\mathbf{x}_1(\nu), \mathbf{y}_2(\nu), t(\nu), \nu) - \tilde{\mathbf{f}}_{1,2}(\tilde{\mathbf{x}}_1(\nu), 0, t(\nu), \nu) \tag{C.24}$$

We proceed to estimate:

$$\left\| \int_{t_0+\sigma_\varepsilon}^{\sigma} \mathbf{i}(\nu) d\nu \right\| \leq \int_{t_0+\sigma_\varepsilon}^{\sigma} (\|\mathbf{i}_1(\nu)\| + \|\mathbf{i}_1(\nu)\|) d\nu \tag{C.25}$$

where the integrands $\mathbf{i}_1$ and $\mathbf{i}_2$ are given by:

$$\mathbf{i}_1(\nu) = \tilde{\mathbf{f}}_{1,2}(\mathbf{x}_1(\nu), \mathbf{y}_2(\nu), t(\nu), \nu) - \tilde{\mathbf{f}}_{1,2}(\mathbf{x}_1(\nu), 0, t(\nu), \nu) \tag{C.26}$$

$$\mathbf{i}_2(\nu) = \tilde{\mathbf{f}}_{1,2}(\mathbf{x}_1(\nu), 0, t(\nu), \nu) - \tilde{\mathbf{f}}_{1,2}(\tilde{\mathbf{x}}_1(\nu), 0, t(\nu), \nu) \tag{C.27}$$

Using Lipschitz continuity, we obtain that:

$$\left\| \int_{t_0+\sigma_\varepsilon}^{\sigma} \mathbf{i}(\nu) d\nu \right\| \leq \int_{t_0+\sigma_\varepsilon}^{\sigma} L_{\mathcal{K},\tilde{\mathbf{f}}_{1,2}} (\|\mathbf{y}_2(\nu)\| + \|\mathbf{x}_1(\nu) - \mathbf{x}_2(\nu)\|) d\nu \tag{C.28}$$

Substituting back and simplifying we obtain:

$$\begin{aligned} \|\mathbf{x}_1(\sigma) - \tilde{\mathbf{x}}_1(\sigma)\| \leq \|\mathbf{x}_1(t_0+\sigma_\varepsilon) - \tilde{\mathbf{x}}_1(t_0+\sigma_\varepsilon)\| + \int_{t_0+\sigma_\varepsilon}^{\sigma} L_{\mathcal{K},\tilde{\mathbf{f}}_{1,2}} \varepsilon \, \|\mathbf{y}_2(\nu)\| d\nu \\ + \int_{t_0+\sigma_\varepsilon}^{\sigma} L_{\mathcal{K},\tilde{\mathbf{f}}_{1,2}} \varepsilon \, \|\mathbf{x}_1(\nu) - \mathbf{x}_2(\nu)\| d\nu + B_{\mathcal{K},\tilde{\mathbf{f}}_{1,3}} \sigma_D \varepsilon^2 \end{aligned} \tag{C.29}$$

Recall that:

$$\|\mathbf{x}_1(t_0+\sigma_\varepsilon) - \tilde{\mathbf{x}}_1(t_0+\sigma_\varepsilon)\| \leq B_{\mathcal{K},\tilde{\mathbf{f}}_1} \sigma_\varepsilon \varepsilon \tag{C.30}$$

$$\|\mathbf{y}_2(\sigma)\| \leq 2\kappa\, \varepsilon, \quad \forall \sigma \in [t_0+\sigma_\varepsilon, t_0+\sigma_D] \tag{C.31}$$

and therefore, we have that:

$$\|\mathbf{x}_1(\sigma) - \tilde{\mathbf{x}}_1(\sigma)\| \leq \eta(\varepsilon) + \int_{t_0+\sigma_\varepsilon}^{\sigma} L_{\mathcal{K},\tilde{\mathbf{f}}_{1,2}} \varepsilon \, \|\mathbf{x}_1(\nu) - \mathbf{x}_2(\nu)\| d\nu \tag{C.32}$$

where the function $\eta(\varepsilon)$ is given by:

$$\eta(\varepsilon) = B_{\mathcal{K},\tilde{\mathbf{f}}_1}\sigma_\varepsilon\varepsilon + 2\kappa L_{\mathcal{K},\tilde{\mathbf{f}}_{1,2}}\sigma_D\varepsilon^2 + B_{\mathcal{K},\tilde{\mathbf{f}}_{1,3}}\sigma_D\varepsilon^2 \tag{C.33}$$

From Grönwall's inequality, we obtain that:

$$\|\mathbf{x}_1(\sigma) - \tilde{\mathbf{x}}_1(\sigma)\| \leq \eta(\varepsilon)\exp\left(L_{\mathcal{K},\tilde{\mathbf{f}}_{1,2}}\sigma_D\varepsilon\right) \tag{C.34}$$

By assumption, we have that $\sigma_D < L/\varepsilon$, therefore we have that:

$$\|\mathbf{x}_1(\sigma) - \tilde{\mathbf{x}}_1(\sigma)\| \leq \eta(\varepsilon)\exp\left(L_{\mathcal{K},\tilde{\mathbf{f}}_{1,2}}L\right) \tag{C.35}$$

Observe, however, that $\lim_{\varepsilon\to 0}\eta(\varepsilon) = 0$, and so we are guaranteed the existence of $\varepsilon_5 \in (0, \varepsilon_4)$ such that:

$$\eta(\varepsilon) < D\exp\left(-L_{\mathcal{K},\tilde{\mathbf{f}}_{1,2}}L\right)/4 \tag{C.36}$$

which implies that:

$$\|\mathbf{x}_1(t_0 + \sigma_D) - \tilde{\mathbf{x}}_1(t_0 + \sigma_D)\| < D/4 \tag{C.37}$$

contradicting the definition of σ_D, which proves the claim. The lemma follows by reverting back to the original time-scale $t = \varepsilon(\sigma - t_0) + t_0$ and selecting a sufficiently small $\varepsilon^* \in (0, \varepsilon_5)$ such that $\varepsilon\|\boldsymbol{\phi}_1(\mathbf{x}_1, t, \sigma)\| < D/2$. □

Appendix D

Proof of Theorem 3.4.1

Proof. We remark that parts of the proof are inspired by the proof of Lemma 1 in [4]. However, the major difference and a significant technical difficulty in our case compared to [4] lies in the fact that only a single parameter is used to induce the time-scale separation needed for both singular perturbation and averaging. A reader familiar with the literature of perturbation theory will recognize this as a 'distinguished limit' in which several parameters are assumed to have precise asymptotic orders with respect to a single parameter in the system [43]. Due to the nature of the distinguished limit we choose here, the interaction between the fast periodic time variable and the singularly perturbed part of the system is not negligible and must be explicitly accounted for. In fact, the choice of the distinguished limit we make here is precisely why our results capture the stable behavior of the class of systems to which the motivational example (3.22) belongs, whereas the results in [4] fail to do so. We emphasize that our results are not a special case of the results in [4].

We begin by applying the time scaling $\tau = \varepsilon^{-2}(t - t_0) + t_0$. In contrast to the standard singular perturbation analysis (e.g. [7, Chapter 11], [4, Section I]), we augment the standard

coordinate shift with a *near-identity* part:

$$\mathbf{y}_2 = \mathbf{x}_2 - \boldsymbol{\varphi}_0(\mathbf{x}_1, t) - \varepsilon\, \boldsymbol{\varphi}_1(\mathbf{x}_1, t, \tau) - \varepsilon^2 \boldsymbol{\varphi}_2(\mathbf{x}_1, t, \tau), \tag{D.1}$$

where the maps $\boldsymbol{\varphi}_i(\mathbf{x}, t, \tau)$ for $i \in \{1, 2\}$ are the solutions to the linear non-homogeneous two point boundary value problems:

$$\partial_\tau \boldsymbol{\varphi}_i(\mathbf{x}_1, t, \tau) = \mathbf{A}_{\boldsymbol{\varphi}}(\mathbf{x}_1, t, \tau)\, \boldsymbol{\varphi}_i(\mathbf{x}_1, t, \tau) + \mathbf{b}_i(\mathbf{x}_1, t, \tau) \tag{D.2}$$

$$\boldsymbol{\varphi}_i(\mathbf{x}_1, t, \tau) = \boldsymbol{\varphi}_i(\mathbf{x}_1, t, \tau + T) \tag{D.3}$$

for $i \in \{1, 2\}$, where:

$$\mathbf{b}_{\boldsymbol{\varphi},1}(\mathbf{x}_1, t, \tau) = \mathbf{f}_{2,1}(\mathbf{x}_1, \boldsymbol{\varphi}_0(\mathbf{x}_1, t), t, \tau) - \partial_1 \boldsymbol{\varphi}_0(\mathbf{x}_1, t) \mathbf{f}_{1,1}(\mathbf{x}_1, \boldsymbol{\varphi}_0(\mathbf{x}_1, t), t, \tau) \tag{D.4}$$

$$\begin{aligned} \mathbf{b}_{\boldsymbol{\varphi},2}(\mathbf{x}_1, t, \tau) &= \mathbf{f}_{2,2}(\mathbf{x}_1, \boldsymbol{\varphi}_0(\mathbf{x}_1, t), t, \tau) - \partial_1 \boldsymbol{\varphi}_0(\mathbf{x}_1, t) \mathbf{f}_{1,2}(\mathbf{x}_1, \boldsymbol{\varphi}_0(\mathbf{x}_1, t), t, \tau) \\ &\quad - \partial_1 \boldsymbol{\varphi}_1(\mathbf{x}_1, t, \tau) \mathbf{f}_{1,1}(\mathbf{x}_1, \boldsymbol{\varphi}_0(\mathbf{x}_1, t), t, \tau) - \partial_t \boldsymbol{\varphi}_0(\mathbf{x}_1, t) \\ &\quad + \partial_2^2 \mathbf{f}_{0,2}(\mathbf{x}_1, \boldsymbol{\varphi}_0(\mathbf{x}_1, t), t, \tau)[\boldsymbol{\varphi}_1(\mathbf{x}_1, t, \tau)] \end{aligned} \tag{D.5}$$

The following lemma is a simple consequence of Assumption 3.4.1 and standard linear systems theory:

Lemma D.0.1. *Let Assumption* 3.4.1 *be satisfied. Then, the non-homogeneous BVPs (D.2)-(D.3) have unique periodic solutions $\boldsymbol{\varphi}_i$ defined by:*

$$\boldsymbol{\varphi}_i(\mathbf{x}, t, \tau) = \left(\mathbf{I} - \boldsymbol{\Phi}_{\mathbf{A}_{\boldsymbol{\varphi}}}(\tau + T_\tau, \tau)\right)^{-1} \int_\tau^{\tau + T_\tau} \boldsymbol{\Phi}_{\mathbf{A}_{\boldsymbol{\varphi}}}(\tau + T_\tau, \nu) \mathbf{b}_{\boldsymbol{\varphi},i}(\mathbf{x}_1, t, \nu)\, d\nu \tag{D.6}$$

Proof. The result can be verified by direct substitution. □

We observe that under this coordinate change and time scaling, we have that:

$$\frac{d\mathbf{x}_1}{d\tau} = \sum_{k=1}^{2} \varepsilon^k \tilde{\mathbf{f}}_{1,k}(\mathbf{x}_1, \mathbf{y}_2, t, \tau) + O(\varepsilon^3), \qquad \mathbf{x}_1(t_0) = \mathbf{x}_{1,0} \tag{D.7a}$$

$$\frac{d\mathbf{y}_2}{d\tau} = \sum_{k=0}^{2} \varepsilon^k \tilde{\mathbf{f}}_{2,k}(\mathbf{x}_1, \mathbf{y}_2, t, \tau) + O(\varepsilon^3), \qquad \mathbf{y}_2(t_0) = \mathbf{y}_{2,0} \tag{D.7b}$$

where the vector fields $\tilde{\mathbf{f}}_{j,k}$ given by:

$$\tilde{\mathbf{f}}_{1,1}(\mathbf{x}_1, \mathbf{y}_2, t, \tau) = \mathbf{f}_{1,1}(\mathbf{x}_1, \mathbf{y}_2 + \boldsymbol{\varphi}_0(\mathbf{x}_1, t), t, \tau) \tag{D.8a}$$

$$\tilde{\mathbf{f}}_{2,0}(\mathbf{x}_1, \mathbf{y}_2, t, \tau) = \mathbf{f}_{2,0}(\mathbf{x}_1, \mathbf{y}_2 + \boldsymbol{\varphi}_0(\mathbf{x}_1, t), t, \tau)$$

$$\begin{aligned}\tilde{\mathbf{f}}_{1,2}(\mathbf{x}_1, \mathbf{y}_2, t, \tau) &= \mathbf{f}_{1,2}(\mathbf{x}_1, \mathbf{y}_2 + \boldsymbol{\varphi}_0(\mathbf{x}_1, t), t, \tau) \\ &\quad + \partial_2 \mathbf{f}_{1,1}(\mathbf{x}_1, \mathbf{y}_2 + \boldsymbol{\varphi}_0(\mathbf{x}_1, t), t, \tau)\boldsymbol{\varphi}_1(\mathbf{x}_1, t, \tau)\end{aligned} \tag{D.8b}$$

$$\begin{aligned}\tilde{\mathbf{f}}_{2,1}(\mathbf{x}_1, \mathbf{y}_2, t, \tau) &= \mathbf{f}_{2,1}((\mathbf{x}_1, \mathbf{y}_2 + \boldsymbol{\varphi}_0(\mathbf{x}_1, t), t, \tau) \\ &\quad + \partial_2 \mathbf{f}_{2,0}(\mathbf{x}_1, \mathbf{y}_2 + \boldsymbol{\varphi}_0(\mathbf{x}_1, t), t, \tau)\boldsymbol{\varphi}_1(\mathbf{x}_1, t, \tau) \\ &\quad - \partial_1 \boldsymbol{\varphi}_0(\mathbf{x}_1, t)\mathbf{f}_{1,1}(\mathbf{x}_1, \mathbf{y}_2 + \boldsymbol{\varphi}_0(\mathbf{x}_1, t), t, \tau) - \partial_3 \boldsymbol{\varphi}_1(\mathbf{x}_1, t, \tau)\end{aligned} \tag{D.8c}$$

$$\begin{aligned}\tilde{\mathbf{f}}_{2,2}(\mathbf{x}_1, \mathbf{y}_2, t, \tau) &= \mathbf{f}_{2,2}(\mathbf{x}_1, \mathbf{y}_2 + \boldsymbol{\varphi}_0(\mathbf{x}_1, t), t, \tau) \\ &\quad + \partial_2 \mathbf{f}_{2,0}(\mathbf{x}_1, \mathbf{y}_2 + \boldsymbol{\varphi}_0(\mathbf{x}_1, t), t, \tau)\boldsymbol{\varphi}_2(\mathbf{x}_1, t, \tau) \\ &\quad + \partial_2^2 \mathbf{f}_{3,0}(\mathbf{x}_1, \mathbf{y}_2 + \boldsymbol{\varphi}_0(\mathbf{x}_1, t), t, \tau)[\boldsymbol{\varphi}_1(\mathbf{x}_1, t, \tau)] \\ &\quad - \partial_1 \boldsymbol{\varphi}_0(\mathbf{x}_1, t)\mathbf{f}_{1,2}(\mathbf{x}_1, \mathbf{y}_2 + \boldsymbol{\varphi}_0(\mathbf{x}_1, t), t, \tau) \\ &\quad - \partial_1 \boldsymbol{\varphi}_1(\mathbf{x}_1, t, \tau)\mathbf{f}_{1,1}(\mathbf{x}_1, \mathbf{y}_2 + \boldsymbol{\varphi}_0(\mathbf{x}_1, t), t, \tau) \\ &\quad - \partial_t \boldsymbol{\varphi}_0(\mathbf{x}_1, t) - \partial_3 \boldsymbol{\varphi}_2(\mathbf{x}_1, t, \tau)\end{aligned} \tag{D.8d}$$

and the remainder terms are Lipschitz continuous and bounded on every compact subset $\mathcal{K} \subset \mathbb{R}^{n_1} \times \mathbb{R}^{n_2}$, uniformly in $t_0 \in \mathbb{R}$, τ and $\varepsilon \in [0, \varepsilon_0]$ for some $\varepsilon_0 > 0$, with Lipschitz constants $L_{\mathbf{f}_{1,k},\mathcal{K}}, L_{\mathbf{f}_{2,k},\mathcal{K}} > 0$ and bounds $B_{\mathbf{f}_{1,k},\mathcal{K}}, B_{\mathbf{f}_{2,k},\mathcal{K}} > 0$. By virtue of the way in which the maps $\boldsymbol{\varphi}_i(\mathbf{x}_1, t, \tau)$ for $i \in \{1, 2\}$ are defined, we observe that $\tilde{\mathbf{f}}_{1,1}(\mathbf{x}_1, 0, t, \tau) = \tilde{\mathbf{f}}_1(\mathbf{x}_1, t, \tau)$, $\tilde{\mathbf{f}}_{1,2}(\mathbf{x}_1, 0, t, \tau) = \tilde{\mathbf{f}}_2(\mathbf{x}_1, t, \tau)$, and that $\tilde{\mathbf{f}}_{2,1}(\mathbf{x}_1, 0, t, \tau) = \tilde{\mathbf{f}}_{2,2}(\mathbf{x}_1, 0, t, \tau) = 0$, $\forall \mathbf{x}_1 \in \mathbb{R}^{n_1}$, $\forall \tau \in \mathbb{R}$.

That is, the origin $\mathbf{y}_2 = 0$ is an equilibrium point for the boundary layer model:

$$\frac{d\mathbf{y}_2}{d\tau} = \sum_{k=0}^{2} \varepsilon^k \tilde{\mathbf{f}}_{2,k}(\mathbf{x}_1, \mathbf{y}_2, t, \tau), \qquad \mathbf{y}_2(t_0) = \mathbf{y}_{2,0} \tag{D.9}$$

when $\mathbf{x}_1$ and t are treated as parameters. From second-order averaging [30, 6], we know that $\exists \varepsilon_0 \in (0, \infty)$ such that $\forall \mathbf{x}_{1,0} \in \mathcal{B}_1$, $\forall t_0 \in \mathbb{R}$, $\forall \varepsilon \in (0, \varepsilon_0)$, unique trajectories $\tilde{\mathbf{x}}_1(t; t_0, \mathbf{x}_{1,0})$ of the system (3.28) exist and $\tilde{\mathbf{x}}_1(t; t_0, \mathbf{x}_{1,0}) \in \mathcal{N}_1, \forall t \in [t_0, t_0 + t_f]$ for some compact subset $\mathcal{N}_1$. Equivalently, we know that $\tilde{\mathbf{x}}_1(\tau; t_0, \mathbf{x}_{1,0}) \in \mathcal{N}_1, \forall \tau \in [t_0, t_0 + t_f \varepsilon^{-2}]$. Due to Assumption 3.4.1, we know that $\forall (\mathbf{x}_{1,0}, \mathbf{y}_{2,0}) \in \mathcal{B}_1 \times \mathcal{B}_2$, and $\forall \varepsilon \in (0, \varepsilon_0)$, unique trajectories of the system (D.7) exist. Let $[t_0, t_0 + \tau_e)$ with $\tau_e \in (0, \infty)$ be the maximal interval of existence and uniqueness of a given solution $(\mathbf{x}_1(\tau; t_0, \mathbf{x}_{1,0}), \mathbf{y}_2(\tau; t_0, \mathbf{y}_{2,0}))$. Define an open tubular neighborhood $\mathcal{O}_1(\tau)$ around $\tilde{\mathbf{x}}_1(\tau; t_0, \mathbf{x}_{1,0})$ by:

$$\mathcal{O}_1(\tau) = \{\mathbf{x} \in \mathbb{R}^{n_1} \ : \ \|\mathbf{x} - \tilde{\mathbf{x}}_1(\tau; t_0, \mathbf{x}_{1,0})\| < D\}, \tag{D.10}$$

and observe that the $\mathbf{x}_1$-component of the solution to (D.7) is initially inside $\mathcal{O}_1(0)$. Moreover, define the compact subset

$$\mathcal{M}_1 = \overline{\{\mathbf{x}_1 \in \mathbb{R}^{n_1} : \inf_{\mathbf{x}' \in \mathcal{N}_1} \|\mathbf{x} - \mathbf{x}'\| < D\}} \tag{D.11}$$

From Assumption 3.4.1, we know that there exists a function $V \in \mathcal{C}^1(\mathbb{R}^{n_2} \times \mathbb{R})$, and positive constants κ_i, $i \in \{1, 2, 3, 4\}$ such that:

$$\kappa_1 \|\mathbf{y}_2\|^2 \leq V(\mathbf{y}_2, \tau) \leq \kappa_2 \|\mathbf{y}_2\|^2 \tag{D.12a}$$

$$\partial_2 V(\mathbf{y}_2, \tau) + \partial_1 V(\mathbf{y}_2, \tau) \tilde{\mathbf{f}}_{2,0}(\mathbf{x}_1, \mathbf{y}_2, t, \tau) \leq -\kappa_3 \|\mathbf{y}_2\|^2 \tag{D.12b}$$

$$\|\partial_1 V(\mathbf{y}_2, \tau)\| \leq \kappa_4 \|\mathbf{y}_2\| \tag{D.12c}$$

Let $c \in (0, \infty)$ be such that the compact subset $\mathcal{N}_2 = \{\mathbf{y}_2 \in \mathbb{R}^{n_2} : \|\mathbf{y}_2\| \leq \sqrt{c/\kappa_2}\}$ contains

the bounded set $\mathcal{B}_{\mathbf{y}_2}$, and define the compact subset $\mathcal{M}_2 = \{\mathbf{y}_2 \in \mathbb{R}^{n_2} : \|\mathbf{y}_2\| \leq \sqrt{c/\kappa_1}\}$, and let $\mathcal{K} = \mathcal{M}_1 \times \mathcal{M}_2$. Finally, define the time τ_D as follows: $\mathbf{x}_1(\tau; t_0, \mathbf{x}_{1,0}) \in \mathcal{O}_1(\tau)$, $\forall \tau \in [t_0, t_0 + \tau_D)$, and $\|\mathbf{x}_1(t_0 + \tau_D; t_0, \mathbf{x}_{1,0}) - \tilde{\mathbf{x}}_1(t_0 + \tau_D; t_0, \mathbf{x}_{1,0})\| = D$, or $\tau_D = \tau_e$ if $\mathbf{x}_1(\tau; t_0, \mathbf{x}_{1,0}) \in \mathcal{O}_1(\tau)$, $\forall \tau \in [t_0, t_0 + \tau_e)$. Then, we have the following lemma adapted from a portion of the proof of Lemma 1 in [4]:

Lemma D.0.2. *[4] Let the assumptions of Theorem* 3.4.1 *be satisfied. Then, there exist constants $\lambda_\tau > 0$, $\kappa_\tau > 0$, $\gamma_\tau > 0$, and $\varepsilon_2 \in (0, \varepsilon_0)$ such that $\forall \varepsilon \in (0, \varepsilon_2)$, $\forall (\mathbf{x}_{1,0}, \mathbf{y}_{2,0}) \in \mathcal{B}_1 \times \mathcal{B}_2$, the solution $(\mathbf{x}_1(\tau; t_0, \mathbf{x}_{1,0}), \mathbf{y}_2(\tau; t_0, \mathbf{y}_{2,0}))$ stays inside $\mathcal{K}$, $\forall \tau \in [t_0, t_0 + \tau_D]$, and:*

$$\|\mathbf{y}_2(\tau; t_0, \mathbf{y}_{2,0})\| < \gamma_\tau \|\mathbf{y}_{2,0}\| \mathrm{e}^{-\lambda_\tau(\tau - t_0)} + \kappa_\tau \varepsilon^{\frac{3}{2}} \tag{D.13}$$

where the constants $\lambda_\tau > 0$, $\kappa_\tau > 0$, $\gamma_\tau > 0$ are independent from the choice of ε.

We proceed to define $\varepsilon_3 = \min\{\varepsilon_1, \varepsilon_2\}$, and an ε-dependent time τ_ε by requiring that the following inequality is satisfied:

$$\gamma_\tau \|\mathbf{y}_{2,0}\| \mathrm{e}^{-\lambda_\tau(\tau - t_0)} < \kappa_\tau \varepsilon^{\frac{3}{2}}, \qquad \forall \mathbf{y}_{2,0} \in \mathcal{M}_2,\ \forall \tau > \tau_\varepsilon + t_0 \tag{D.14}$$

We note that this is always possible for $\varepsilon > 0$. In fact, it can be shown that $\tau_\varepsilon = \max\{(3/(2\lambda)) \log((\gamma\sqrt{c/\alpha_2})/(\alpha\,\varepsilon)), 0\}$ satisfies the inequality (D.14). Now, we show that $\exists \varepsilon_4 \in (0, \varepsilon_3)$ such that $\tau_\varepsilon < \tau_D$, $\forall \varepsilon \in (0, \varepsilon_4)$. To obtain a contradiction, suppose that there exists a bounded subset $\mathcal{B}_1 \times \mathcal{B}_2 \subset \mathbb{R}^{n_1} \times \mathbb{R}^{n_2}$, and a $D \in (0, \bar{D})$, such that $\forall \varepsilon_4 \in (0, \varepsilon_3)$, $\exists \varepsilon \in (0, \varepsilon_4)$ such that $\tau_\varepsilon \geq \tau_D$. We estimate the difference:

$$\|\mathbf{x}_1(\tau_D; t_0, \mathbf{x}_{1,0}) - \tilde{\mathbf{x}}_1(\tau_D; t_0, \mathbf{x}_{1,0})\| \leq \int_{t_0}^{t_0 + \tau_D} B_{\mathcal{K}, \mathbf{f}_1} \varepsilon \, d\tau \leq B_{\mathcal{K}, \mathbf{f}_1} \tau_D \varepsilon \leq B_{\mathcal{K}, \mathbf{f}_1} \tau_\varepsilon \, \varepsilon, \tag{D.15}$$

where $B_{\mathcal{K}, \mathbf{f}_1} > 0$ is a uniform upper bound on the norm of the integrand inside the compact subset $\mathcal{K}$ whose existence is guaranteed by Assumption 3.4.1. Now, observe that $\lim_{\varepsilon \to 0} \tau_\varepsilon \, \varepsilon =$

0, and so $\exists \varepsilon_4 \in (0, \varepsilon_3)$ such that $B_{\mathcal{K},\mathbf{f}_1} \tau_\varepsilon \, \varepsilon \leq D/2$, $\forall \varepsilon \in (0, \varepsilon_4)$. Hence, we have that $\forall \varepsilon \in (0, \varepsilon_4)$, $\|\mathbf{x}_1(\tau_D; t_0, \mathbf{x}_{1,0}) - \tilde{\mathbf{x}}_1(\tau_D; t_0, \mathbf{x}_{1,0})\| \leq D/2$ which contradicts the definition of τ_D. Accordingly, we have that $\exists \varepsilon_4 \in (0, \varepsilon_3)$, such that $\forall \varepsilon \in (0, \varepsilon_4)$, $\forall (\mathbf{x}_{1,0}, \mathbf{y}_{2,0}) \in \mathcal{B}_1 \times \mathcal{B}_2$, we have that $\tau_\varepsilon < \tau_D$.

Next, we show that $\exists \varepsilon_5 \in (0, \varepsilon_4)$ such that $t_f/\varepsilon^2 < \tau_D$, $\forall \varepsilon \in (0, \varepsilon_5)$. To obtain a contradiction, suppose that $\forall \varepsilon_5 \in (0, \varepsilon_4)$, $\exists \varepsilon \in (0, \varepsilon_5)$ such that $t_f/\varepsilon^2 \geq \tau_D$. Once again, we estimate the difference $\|\mathbf{x}_1(\tau; t_0, \mathbf{x}_{1,0}) - \tilde{\mathbf{x}}_1(\tau; t_0, \mathbf{x}_{1,0})\|$ on the interval $[t_0, t_0 + \tau_D]$. We have that:

$$\|\mathbf{x}_1(\tau; t_0, \mathbf{x}_{1,0}) - \tilde{\mathbf{x}}_1(\tau; t_0, \mathbf{x}_{1,0})\| = \left\| \sum_{k=1}^{2} \int_{t_0}^{t_0+\tau_\varepsilon} \Delta \tilde{\mathbf{f}}_{1,k}(s) ds + \int_{t_0+\varepsilon}^{t_0+\tau} \Delta \tilde{\mathbf{f}}_{1,k}(s) ds + O(\varepsilon^3) \right\| \tag{D.16}$$

where the integrands $\Delta \tilde{\mathbf{f}}_{1,k}(s)$ are given by:

$$\Delta \tilde{\mathbf{f}}_{1,k}(s) = \tilde{\mathbf{f}}_{1,k}(\mathbf{x}_1(\tau), \mathbf{y}_2(\tau), t(\tau), \tau) - \tilde{\mathbf{f}}_{1,k}(\tilde{\mathbf{x}}_1(\tau), 0, t(\tau), \tau) \tag{D.17}$$

which leads to the estimate:

$$\|\mathbf{x}_1(\tau) - \tilde{\mathbf{x}}_1(\tau)\| \leq B_{\mathcal{K},\mathbf{f}_1}(\tau_\varepsilon + \tau_D \varepsilon^2)\varepsilon + \|\mathbf{i}_1\|, \qquad \mathbf{i}_1 = \int_{\tau_\varepsilon}^{\tau} \sum_{k=1}^{2} \varepsilon^k \Delta \tilde{\mathbf{f}}_{1,k}(s) ds \tag{D.18}$$

on the interval $[0, \tau_D]$. We proceed to estimate $\|\mathbf{i}_1\|$ as follows:

$$\|\mathbf{i}_1\| \leq \varepsilon(\|\mathbf{i}_2\| + \|\mathbf{i}_3\|) + \varepsilon^2(\|\mathbf{i}_4\| + \|\mathbf{i}_5\|) \tag{D.19}$$

where $\mathbf{i}_i$ for $i \in \{2, 3, 4, 5\}$ are given by:

$$\mathbf{i}_2 = \int_{\tau_\varepsilon}^{\tau} (\tilde{\mathbf{f}}_{1,1}(\mathbf{x}_1(s), \mathbf{y}_2(s), t(s), s) - \tilde{\mathbf{f}}_{1,1}(\mathbf{x}_1(s), 0, t(s), s))\, ds \tag{D.20}$$

$$\mathbf{i}_3 = \int_{\tau_\varepsilon}^{\tau} (\tilde{\mathbf{f}}_{1,1}(\mathbf{x}_1(s), 0, t(s), s) - \tilde{\mathbf{f}}_{1,1}(\tilde{\mathbf{x}}_1(s), 0, t(s), s)) ds \tag{D.21}$$

$$\mathbf{i}_4 = \int_{\tau_\varepsilon}^{\tau} (\tilde{\mathbf{f}}_{1,2}(\mathbf{x}_1(s), \mathbf{y}_2(s), t(s), s) - \tilde{\mathbf{f}}_{1,2}(\mathbf{x}_1(s), 0, t(s), s))\, ds \tag{D.22}$$

$$\mathbf{i}_5 = \int_{\tau_\varepsilon}^{\tau} (\tilde{\mathbf{f}}_{1,2}(\mathbf{x}_1(s), 0, t(s), s) - \tilde{\mathbf{f}}_{1,2}(\tilde{\mathbf{x}}_1(s), 0, t(s), s)) ds \tag{D.23}$$

We estimate each of the integrals above, starting by $\mathbf{i}_2$, $\mathbf{i}_4$ and $\mathbf{i}_5$, which can be estimated as:

$$\|\mathbf{i}_2\| \leq \int_{\tau_\varepsilon}^{\tau} L_{\mathbf{f}_1,\mathcal{K}} \|\mathbf{y}_2(s)\| ds \tag{D.24}$$

$$\|\mathbf{i}_4\| \leq \int_{\tau_\varepsilon}^{\tau} L_{\mathbf{f}_2,\mathcal{K}} \|\mathbf{y}_2(s)\| ds \tag{D.25}$$

$$\|\mathbf{i}_5\| \leq \int_{\tau_\varepsilon}^{\tau} L_{\mathbf{f}_2,\mathcal{K}} \|\mathbf{x}_1(s) - \tilde{\mathbf{x}}_1(s)\| ds \tag{D.26}$$

where $L_{\mathbf{f}_1,\mathcal{K}}, L_{\mathbf{f}_2,\mathcal{K}}, L_{\mathbf{f}_2,\mathcal{K}} > 0$ are Lipschitz constants. Next, we estimate $\|\mathbf{i}_3\|$. We proceed by dividing the interval $\mathcal{I} = [\tau_\varepsilon, \tau]$ into sub-intervals of length T and a left over piece:

$$\mathcal{I} = \left(\bigcup_{i=1}^{N(\varepsilon)} [T_{i-1}, T_i] \right) \bigcup [N(\varepsilon)T, \tau],$$

where $T_i = \tau_\varepsilon + i\,T$, and $N(\varepsilon)$ is the unique integer such that $N(\varepsilon)T \leq \tau < N(\varepsilon)T + T$. Then, we split $\mathbf{i}_3$ into a sum of sub-integrals:

$$\mathbf{i}_3 = \sum_{i=1}^{N(\varepsilon)} \mathbf{i}_{3,i} + \int_{N(\varepsilon)T}^{\tau} (\tilde{\mathbf{f}}_{1,1}(\mathbf{x}_1(s), 0, t(s), s) - \tilde{\mathbf{f}}_{1,1}(\tilde{\mathbf{x}}_1(s), 0, t(s), s))\, ds \tag{D.27}$$

$$\mathbf{i}_{3,i} = \int_{T_{i-1}}^{T_i} (\tilde{\mathbf{f}}_{1,1}(\mathbf{x}_1(s), 0, t(s), s) - \tilde{\mathbf{f}}_{1,1}(\tilde{\mathbf{x}}_1(s), 0, t(s), s))\, ds \tag{D.28}$$

The part of the integral on the leftover piece can be bounded independently from ε as follows:

$$\left\| \int_{N(\varepsilon)T}^{\tau} (\tilde{\mathbf{f}}_{1,1}(\mathbf{x}_1(s), 0, t(s), s) - \tilde{\mathbf{f}}_{1,1}(\tilde{\mathbf{x}}_1(s), 0, t(s), s))\, ds \right\| \leq 2B_{\mathbf{f}_1,\mathcal{K}} T \tag{D.29}$$

Next, we employ Hadamard's lemma to obtain:

$$\mathbf{i}_{3,i} = \int_{T_{i-1}}^{T_i} \mathbf{F}_1(\mathbf{x}_1(s), \tilde{\mathbf{x}}_1(s), s)(\mathbf{x}_1(s)_1 - \tilde{\mathbf{x}}_1(s))ds \tag{D.30}$$

where the matrix valued map $\mathbf{F}_1$ is given by:

$$\mathbf{F}_1(\mathbf{x}_1, \tilde{\mathbf{x}}_1, s) = \int_0^1 \partial_1 \tilde{\mathbf{f}}_{1,1}(\tilde{\mathbf{x}}_1 + \lambda(\mathbf{x}_1 - \tilde{\mathbf{x}}_1), t(s), s)d\lambda \tag{D.31}$$

Through adding and subtracting a term, we may write:

$$\mathbf{i}_{3,i} = \int_{T_{i-1}}^{T_i} \mathbf{F}_1(\mathbf{x}_1(T_{i-1}), \tilde{\mathbf{x}}_1(T_{i-1}), s)\,(\mathbf{x}_1(s) - \tilde{\mathbf{x}}_1(s))ds + \int_{T_{i-1}}^{T_i} \Delta_i\big[\mathbf{F}_1\big](s)\,(\mathbf{x}_1(s) - \tilde{\mathbf{x}}_1(s))ds \tag{D.32}$$

where the term $\Delta_i[\mathbf{F}_1]$ is given by:

$$\Delta_i\big[\mathbf{F}_1\big](s) = \mathbf{F}_1(\mathbf{x}_1(s), \tilde{\mathbf{x}}_1(s), s) - \mathbf{F}_1(\mathbf{x}_1(T_{i-1}), \tilde{\mathbf{x}}_1(T_{i-1}), s)$$

Next, since the matrix-valued map $\mathbf{F}_1$ is periodic with zero average over its third argument when the other arguments are fixed, we have that

$$\int_{T_{i-1}}^{T_i} \mathbf{F}_1(\mathbf{x}_1(T_{i-1}), \tilde{\mathbf{x}}_1(T_{i-1}), s)\,\mathbf{w}\,ds = 0 \tag{D.33}$$

for any fixed $\mathbf{w}$. Thus, we may write:

$$\mathbf{i}_{3,i} = \int_{T_{i-1}}^{T_i} \Delta_i\big[\mathbf{F}_1\big]\,(\mathbf{x}_1(s) - \tilde{\mathbf{x}}_1(s)) + \int_{T_{i-1}}^{T_i} \mathbf{F}_1(\mathbf{x}_1(T_{i-1}), \tilde{\mathbf{x}}_1(T_{i-1}), s)\Delta_i[\mathbf{x} - \tilde{\mathbf{x}}]ds \tag{D.34}$$

where $\Delta_i[\mathbf{x}_1 - \tilde{\mathbf{x}}_1] = (\mathbf{x}_1(s) - \mathbf{x}_1(T_{i-1})) - (\tilde{\mathbf{x}}_1(s) - \tilde{\mathbf{x}}_1(T_{i-1}))$. The fundamental theorem of

calculus yields:

$$(\mathbf{x}_1(s) - \mathbf{x}_1(T_{i-1})) - (\tilde{\mathbf{x}}_1(s) - \tilde{\mathbf{x}}_1(T_{i-1})) \tag{D.35}$$

$$= \varepsilon \int_{T_{i-1}}^{s} (\tilde{\mathbf{f}}_{1,1}(\mathbf{x}_1(\nu), \mathbf{y}_2(\nu), \nu) - \tilde{\mathbf{f}}_1(\tilde{\mathbf{x}}_1(\nu), \nu))d\nu + O(\varepsilon^2) \tag{D.36}$$

$$= \varepsilon \int_{T_{i-1}}^{s} (\tilde{\mathbf{f}}_{1,1}(\mathbf{x}_1(\nu), \mathbf{y}_2(\nu), \nu) - \tilde{\mathbf{f}}_{1,1}(\mathbf{x}_1(\nu), 0, \nu))d\nu \tag{D.37}$$

$$+ \varepsilon \int_{T_{i-1}}^{s} (\tilde{\mathbf{f}}_1(\mathbf{x}_1(\nu), \nu) - \tilde{\mathbf{f}}_1(\tilde{\mathbf{x}}_1(\nu), \nu))d\nu + O(\varepsilon^2) \tag{D.38}$$

Through integration by parts, we obtain:

$$\begin{aligned}\int_{T_{i-1}}^{T_i} \mathbf{F}_1(\mathbf{x}_1(T_{i-1}), \tilde{\mathbf{x}}_1(T_{i-1}), s)\Delta_i[\mathbf{x} - \tilde{\mathbf{x}}]ds = \mathbf{i}_{\mathbf{F},i}(s)\, \Delta_i[\mathbf{x} - \tilde{\mathbf{x}}]\Big|_{s=T_{i-1}}^{s=T_i} - \varepsilon \int_{T_{i-1}}^{T_i} \mathbf{i}_{\mathbf{F},i}(s)\, \Delta[\tilde{\mathbf{f}}_1]ds \\ - \varepsilon \int_{T_{i-1}}^{T_i} \mathbf{i}_{\mathbf{F},i}(s)\, \Delta[\tilde{\mathbf{f}}_{1,1}]ds + O(\varepsilon^2)\end{aligned} \tag{D.39}$$

where we have that:

$$\Delta[\tilde{\mathbf{f}}_{1,1}] = \tilde{\mathbf{f}}_{1,1}(\mathbf{x}_1(s), \mathbf{y}_2(s), t(s), s) - \tilde{\mathbf{f}}_{1,1}(\mathbf{x}_1(s), 0, t(s), s) \tag{D.40}$$

$$\Delta[\tilde{\mathbf{f}}_1] = \tilde{\mathbf{f}}_1(\mathbf{x}_1(s), t(s), s) - \tilde{\mathbf{f}}_1(\tilde{\mathbf{x}}_1(s), t(s), s) \tag{D.41}$$

$$\mathbf{i}_{\mathbf{F},i}(s) = \int_{T_{i-1}}^{s} \mathbf{F}_1(\mathbf{x}_1(T_{i-1}), \tilde{\mathbf{x}}_1(T_{i-1}), \nu)d\nu \tag{D.42}$$

The boundary term coming out of the integration by parts vanishes because the right factor vanishes at $s = T_{i-1}$ and the left factor vanishes at $s = T_i$, leaving only the integral terms. Using Lipschitz continuity and boundedness on compact subsets, it is not hard to see that:

$$\left\| \int_{T_{i-1}}^{T_i} \mathbf{i}_{\mathbf{F},i}(s)\, \Delta[\tilde{\mathbf{f}}_{1,1}]ds \right\| \leq \int_{T_{i-1}}^{T_i} M_{\mathbf{i}_{\mathbf{F}}, \tilde{\mathbf{f}}_{1,1}, \mathcal{K}} \|\mathbf{y}_2(s)\| ds \tag{D.43}$$

$$\left\| \int_{T_{i-1}}^{T_i} \mathbf{i}_{\mathbf{F},i}(s)\, \Delta[\tilde{\mathbf{f}}_1]ds \right\| \leq \int_{T_{i-1}}^{T_i} M_{\mathbf{i}_{\mathbf{F}}, \mathbf{f}_1, \mathcal{K}} \|\Delta[\mathbf{x}]\| ds \tag{D.44}$$

$$\left\| \int_{T_{i-1}}^{T_i} \Delta_i\big[\mathbf{F}_1\big]\, \Delta[\mathbf{x}] ds \right\| \leq \varepsilon \int_{T_{i-1}}^{T_i} L_{\mathbf{F}_1,\mathcal{K}}\, \|\Delta[\mathbf{x}]\| ds \tag{D.45}$$

where $\Delta[\mathbf{x}] = \mathbf{x}_1(s) - \tilde{\mathbf{x}}_1(s)$. By utilizing the above estimates, the integral on the sub-intervals can be shown to satisfy the bound:

$$\|\mathbf{i}_{3,i}\| \leq M_{\mathcal{K}}\, \varepsilon \int_{T_{i-1}}^{T_i} (\|\Delta[\mathbf{x}]\| + \|\mathbf{y}_2(s)\|)\, ds \tag{D.46}$$

for some constant $M_{\mathcal{K}}$. As a consequence, the integral term $\mathbf{i}_3$ satisfies the bound:

$$\|\mathbf{i}_3\| \leq M_{\mathcal{K}}\, \varepsilon \int_{\tau_\varepsilon}^{\tau} (\|\Delta[\mathbf{x}]\| + \|\mathbf{y}_2(s)\|)\, ds + 2B_{\mathbf{f}_1,\mathcal{K}} T \tag{D.47}$$

Combining (D.18), (D.19), (D.24), (D.25), (D.26), and (D.47), in addition to the fact that $\tau_\varepsilon < \tau_D$, $\forall \varepsilon \in (0, \varepsilon_4)$, we can show that the following estimate holds:

$$\begin{aligned} \|\mathbf{x}_1(\tau) - \tilde{\mathbf{x}}_1(\tau)\| &\leq (M_{\mathcal{K},1} + M_{\mathcal{K},2}\tau_\varepsilon + M_{\mathcal{K},3}\tau_D\varepsilon^2)\varepsilon \\ &+ M_{\mathcal{K},4}\varepsilon \int_{\tau_\varepsilon}^{\tau} \|\mathbf{y}_2(s)\| ds + M_{\mathcal{K},5}\varepsilon^2 \int_{\tau_\varepsilon}^{\tau} \|\mathbf{x}_1(s) - \tilde{\mathbf{x}}_1(s)\| ds \end{aligned} \tag{D.48}$$

for some positive constants $M_{\mathcal{K},j}$, $j \in \{1, \ldots, 5\}$. Using the fact that $\|\mathbf{y}_2(\tau)\| < 2\alpha\, \varepsilon^{\frac{3}{2}}$, $\forall \tau \in [\tau_\varepsilon, \tau_D]$ by definition, we obtain that:

$$\int_{\tau_\varepsilon}^{\tau} \|\mathbf{y}_2(s)\| ds \leq 2\alpha\, \tau\, \varepsilon^{\frac{3}{2}} \leq 2\alpha\, \tau_D\, \varepsilon^{\frac{3}{2}} \tag{D.49}$$

Now, remember that in order to obtain a contradiction we assumed that $\tau_D \leq t_f/\varepsilon^2$, and so we will have:

$$\|\mathbf{x}(\tau) - \tilde{\mathbf{x}}_1(\tau)\| \leq \delta(\varepsilon) + \int_{\tau_\varepsilon}^{\tau} M_{\mathcal{K},5}\varepsilon^2 \|\mathbf{x}_1(s) - \tilde{\mathbf{x}}_1(s)\| ds \tag{D.50}$$

where the function $\delta(\varepsilon)$ is given by:

$$\delta(\varepsilon) = M_{\mathcal{K},1}\varepsilon + M_{\mathcal{K},2}\tau_\varepsilon\varepsilon + M_{\mathcal{K},3}t_f\varepsilon + 2M_{\mathcal{K},4}t_f\varepsilon^{\frac{1}{2}} \tag{D.51}$$

An application of Grönwall's inequality yields:

$$\|\mathbf{x}_1(\tau) - \tilde{\mathbf{x}}_1(\tau)\| \leq \delta(\varepsilon)\mathrm{e}^{M_{\mathcal{K},5}\varepsilon^2\tau} \leq \delta(\varepsilon)\mathrm{e}^{M_{\mathcal{K},5}\varepsilon^2\tau_D} \tag{D.52}$$

on the interval $\tau \in [\tau_\varepsilon, \tau_D]$. Once again, recall that we assumed that $\tau_D \leq t_f/\varepsilon^2$, and so we have:

$$\|\mathbf{x}_1(\tau) - \tilde{\mathbf{x}}_1(\tau)\| \leq \delta(\varepsilon)\mathrm{e}^{M_{\mathcal{K},5}t_f} \tag{D.53}$$

Now, observe that $\lim_{\varepsilon\to 0}\delta(\varepsilon) = 0$, and so we are guaranteed the existence of an $\varepsilon_5 \in (0, \varepsilon_4)$ such that $\forall\varepsilon \in (0, \varepsilon_5)$ we have that $\|\mathbf{x}_1(\tau_D) - \tilde{\mathbf{x}}_1(\tau_D)\| \leq D/2$, which contradicts the definition of τ_D. Hence, the assumption that $\tau_D \leq t_f/\varepsilon^2$ is wrong, and we have that $\exists\varepsilon_5 \in (0, \varepsilon_4)$, such that $\forall\varepsilon \in (0, \varepsilon_5)$, $\forall(\mathbf{x}_0, \mathbf{y}_{2,0}) \in \mathcal{B}_1 \times \mathcal{B}_2$, we have that $t_f/\varepsilon^2 < \tau_D$. To summarize, we have proven that $\forall\varepsilon \in (0, \varepsilon_5)$, $\forall(\mathbf{x}_0, \mathbf{y}_{2,0}) \in \mathcal{B}_\mathbf{x} \times \mathcal{B}_{\mathbf{y}_2}$, $\forall\tau \in [0, t_f/\varepsilon^2]$ we have that:

$$\|\mathbf{x}_1(\tau) - \tilde{\mathbf{x}}_1(\tau)\| < D \tag{D.54a}$$

$$\|\mathbf{y}_2(\tau)\| < \gamma\,\|\mathbf{y}_{2,0}\|\mathrm{e}^{-\lambda\tau} + \alpha\,\varepsilon^{\frac{3}{2}} \tag{D.54b}$$

Now recall the definition of $\mathbf{y}_2$, which leads to the bound:

$$\|\mathbf{y}(\tau) - \boldsymbol{\varphi}_0(\mathbf{x}_1(\tau))\| < \gamma\|\mathbf{y}_0 - \boldsymbol{\varphi}_0(\mathbf{x}_0)\| + \bar{\delta}(\varepsilon) \tag{D.55a}$$

$$\bar{\delta}(\varepsilon) = M_{\boldsymbol{\varphi},\mathcal{K}}\varepsilon + \alpha\,\varepsilon^{\frac{3}{2}} \tag{D.55b}$$

where we used the fact that the maps $\boldsymbol{\varphi}_i$ for $i \in \{1, 2\}$ are uniformly bounded in time due to continuity and periodicity. Since $\lim_{\varepsilon\to 0}\bar{\delta}(\varepsilon) = 0$, it follows that $\exists\varepsilon_6 \in (0, \varepsilon_5)$ such

that $\bar{\delta}(\varepsilon) < \bar{D}$. Moreover, it follows from the results in [3, 30] that $\exists \varepsilon_7 \in (0, \varepsilon_6)$ such that $\forall \mathbf{x}_0 \in \mathcal{B}_{\mathbf{x}}$, $\forall \tau \in [0, t_f/\varepsilon^2]$ we have:

$$\|\mathbf{x}_1(\tau) - \tilde{\mathbf{x}}_1(\tau)\| < \bar{D} - D \tag{D.56}$$

Hence, the result follows after an application of the triangle inequality and reversing the time scaling $\tau = \varepsilon^{-2}(t - t_0) + t_0$. □

Appendix E

Vector Fields Expressions

$$\tilde{\mathbf{f}}_{1,1}(\mathbf{x}_1, \mathbf{x}_2, \mathbf{y}_3, t, \sigma, \tau) = \mathbf{f}_{1,1}(\mathbf{x}_1, \mathbf{x}_2, \mathbf{y}_3 + \boldsymbol{\varphi}_0(\mathbf{x}_1, \mathbf{x}_2, t, \sigma), t, \sigma, \tau) \tag{E.1}$$

$$\tilde{\mathbf{f}}_{2,1}(\mathbf{x}_1, \mathbf{x}_2, \mathbf{y}_3, t, \sigma, \tau) = \mathbf{f}_{2,1}(\mathbf{x}_1, \mathbf{x}_2, \mathbf{y}_3 + \boldsymbol{\varphi}_0(\mathbf{x}_1, \mathbf{x}_2, t, \sigma), t, \sigma, \tau) \tag{E.2}$$

$$\tilde{\mathbf{f}}_{3,0}(\mathbf{x}_1, \mathbf{x}_2, \mathbf{y}_3, t, \sigma, \tau) = \mathbf{f}_{3,0}(\mathbf{x}_1, \mathbf{x}_2, \mathbf{y}_3 + \boldsymbol{\varphi}_0(\mathbf{x}_1, \mathbf{x}_2, t, \sigma), t, \sigma, \tau) \tag{E.3}$$

$$\tilde{\mathbf{f}}_{1,2}(\mathbf{x}_1, \mathbf{x}_2, \mathbf{y}_3, t, \sigma, \tau) = \mathbf{f}_{1,2}(\mathbf{x}_1, \mathbf{x}_2, \mathbf{y}_3 + \boldsymbol{\varphi}_0(\mathbf{x}_1, \mathbf{x}_2, t, \sigma), t, \sigma, \tau) \tag{E.4}$$

$$+ \partial_3 \mathbf{f}_{1,1}(\mathbf{x}_1, \mathbf{x}_2, \mathbf{y}_3 + \boldsymbol{\varphi}_0(\mathbf{x}_1, \mathbf{x}_2, t, \sigma), t, \sigma, \tau) \boldsymbol{\varphi}_1(\mathbf{x}_1, \mathbf{x}_2, t, \sigma, \tau) \tag{E.5}$$

$$\tilde{\mathbf{f}}_{2,2}(\mathbf{x}_1, \mathbf{x}_2, \mathbf{y}_3, t, \sigma, \tau) = \mathbf{f}_{2,2}(\mathbf{x}_1, \mathbf{x}_2, \mathbf{y}_3 + \boldsymbol{\varphi}_0(\mathbf{x}_1, \mathbf{x}_2, t, \sigma), t, \sigma, \tau) \tag{E.6}$$

$$+ \partial_3 \mathbf{f}_{2,1}(\mathbf{x}_1, \mathbf{x}_2, \mathbf{y}_3 + \boldsymbol{\varphi}_0(\mathbf{x}_1, \mathbf{x}_2, t, \sigma), t, \sigma, \tau) \boldsymbol{\varphi}_1(\mathbf{x}_1, \mathbf{x}_2, t, \sigma, \tau) \tag{E.7}$$

$$\tilde{\mathbf{f}}_{3,1}(\mathbf{x}_1, \mathbf{x}_2, \mathbf{y}_3, t, \sigma, \tau) = \mathbf{f}_{3,1}(\mathbf{x}_1, \mathbf{x}_2, \mathbf{y}_3 + \boldsymbol{\varphi}_0(\mathbf{x}_1, \mathbf{x}_2, t, \sigma), t, \sigma, \tau) \tag{E.8}$$

$$+ \partial_3 \mathbf{f}_{3,0}(\mathbf{x}_1, \mathbf{x}_2, \mathbf{y}_3 + \boldsymbol{\varphi}_0(\mathbf{x}_1, \mathbf{x}_2, t, \sigma), t, \sigma, \tau) \boldsymbol{\varphi}_1(\mathbf{x}_1, \mathbf{x}_2, t, \sigma, \tau) \tag{E.9}$$

$$- \partial_1 \boldsymbol{\varphi}_0(\mathbf{x}_1, \mathbf{x}_2, t, \sigma) \mathbf{f}_{1,1}(\mathbf{x}_1, \mathbf{x}_2, \mathbf{y}_3 + \boldsymbol{\varphi}_0(\mathbf{x}_1, \mathbf{x}_2, t, \sigma), t, \sigma, \tau) \tag{E.10}$$

$$- \partial_2 \boldsymbol{\varphi}_0(\mathbf{x}_1, \mathbf{x}_2, t, \sigma) \mathbf{f}_{2,1}(\mathbf{x}_1, \mathbf{x}_2, \mathbf{y}_3 + \boldsymbol{\varphi}_0(\mathbf{x}_1, \mathbf{x}_2, t, \sigma), t, \sigma, \tau) \tag{E.11}$$

$$- \partial_\sigma \boldsymbol{\varphi}_0(\mathbf{x}_s, \mathbf{x}_m, t, \sigma) - \partial_\tau \boldsymbol{\varphi}_1(\mathbf{x}_s, \mathbf{x}_m, t, \sigma, \tau) \tag{E.12}$$

$$\tilde{\mathbf{f}}_{3,2}(\mathbf{x}_1, \mathbf{x}_2, \mathbf{y}_3, t, \sigma, \tau) = \mathbf{f}_{3,2}(\mathbf{x}_1, \mathbf{x}_2, \mathbf{y}_3 + \boldsymbol{\varphi}_0(\mathbf{x}_1, \mathbf{x}_2, t, \sigma), t, \sigma, \tau) \tag{E.13}$$

$$+ \partial_3 \mathbf{f}_{3,0}(\mathbf{x}_1, \mathbf{x}_2, \mathbf{y}_3 + \boldsymbol{\varphi}_0(\mathbf{x}_1, \mathbf{x}_2, t, \sigma), t, \sigma, \tau)\boldsymbol{\varphi}_2(\mathbf{x}_1, \mathbf{x}_2, t, \sigma, \tau) \tag{E.14}$$

$$+ \partial_3^2 \mathbf{f}_{3,0}(\mathbf{x}_1, \mathbf{x}_2, \mathbf{y}_3 + \boldsymbol{\varphi}_0(\mathbf{x}_1, \mathbf{x}_2, t, \sigma), t, \sigma, \tau)[\boldsymbol{\varphi}_1(\mathbf{x}_1, \mathbf{x}_2, t, \sigma, \tau)] \tag{E.15}$$

$$- \partial_1 \boldsymbol{\varphi}_0(\mathbf{x}_1, \mathbf{x}_2, t, \sigma)\mathbf{f}_{1,2}(\mathbf{x}_1, \mathbf{x}_2, \mathbf{y}_3 + \boldsymbol{\varphi}_0(\mathbf{x}_1, \mathbf{x}_2, t, \sigma), t, \sigma, \tau) \tag{E.16}$$

$$- \partial_2 \boldsymbol{\varphi}_0(\mathbf{x}_1, \mathbf{x}_2, t, \sigma)\mathbf{f}_{2,2}(\mathbf{x}_1, \mathbf{x}_2, \mathbf{y}_3 + \boldsymbol{\varphi}_0(\mathbf{x}_1, \mathbf{x}_2, t, \sigma), t, \sigma, \tau) \tag{E.17}$$

$$- \partial_1 \boldsymbol{\varphi}_1(\mathbf{x}_1, \mathbf{x}_2, t, \sigma)\mathbf{f}_{1,1}(\mathbf{x}_1, \mathbf{x}_2, \mathbf{y}_3 + \boldsymbol{\varphi}_0(\mathbf{x}_1, \mathbf{x}_2, t, \sigma), t, \sigma, \tau) \tag{E.18}$$

$$- \partial_2 \boldsymbol{\varphi}_1(\mathbf{x}_1, \mathbf{x}_2, t, \sigma)\mathbf{f}_{2,1}(\mathbf{x}_1, \mathbf{x}_2, \mathbf{y}_3 + \boldsymbol{\varphi}_0(\mathbf{x}_1, \mathbf{x}_2, t, \sigma), t, \sigma, \tau) \tag{E.19}$$

$$- \partial_\sigma \boldsymbol{\varphi}_1(\mathbf{x}_1, \mathbf{x}_2, t, \sigma, \tau) - \partial_t \boldsymbol{\varphi}_0(\mathbf{x}_1, \mathbf{x}_2, t, \sigma) - \partial_\tau \boldsymbol{\varphi}_2(\mathbf{x}_1, \mathbf{x}_2, t, \sigma, \tau) \tag{E.20}$$

$$\mathbf{b}_{\boldsymbol{\varphi},1}(\mathbf{x}_1, \mathbf{x}_2, t, \sigma, \tau) = \mathbf{f}_{3,1}(\mathbf{x}_1, \mathbf{x}_2, \boldsymbol{\varphi}_0(\mathbf{x}_1, \mathbf{x}_2, t, \sigma), t, \sigma, \tau) - \partial_\sigma \boldsymbol{\varphi}_0(\mathbf{x}_1, \mathbf{x}_2, t, \sigma) \tag{E.21}$$

$$- \partial_1 \boldsymbol{\varphi}_0(\mathbf{x}_1, \mathbf{x}_2, t, \sigma)\mathbf{f}_{1,1}(\mathbf{x}_1, \mathbf{x}_2, \boldsymbol{\varphi}_0(\mathbf{x}_1, \mathbf{x}_2, t, \sigma), t, \sigma, \tau) \tag{E.22}$$

$$- \partial_2 \boldsymbol{\varphi}_0(\mathbf{x}_1, \mathbf{x}_2, t, \sigma)\mathbf{f}_{2,1}(\mathbf{x}_1, \mathbf{x}_2, \boldsymbol{\varphi}_0(\mathbf{x}_1, \mathbf{x}_2, t, \sigma), t, \sigma, \tau), \tag{E.23}$$

$$\mathbf{b}_{\boldsymbol{\varphi},2}(\mathbf{x}_1, \mathbf{x}_2, t, \sigma, \tau) = \mathbf{f}_{3,2}(\mathbf{x}_1, \mathbf{x}_2, \boldsymbol{\varphi}_0(\mathbf{x}_1, \mathbf{x}_2, t, \sigma), t, \sigma, \tau) - \partial_t \boldsymbol{\varphi}_0(\mathbf{x}_1, \mathbf{x}_2, t, \sigma) \tag{E.24}$$

$$- \partial_1 \boldsymbol{\varphi}_0(\mathbf{x}_1, \mathbf{x}_2, t, \sigma)\mathbf{f}_{1,2}(\mathbf{x}_1, \mathbf{x}_2, \boldsymbol{\varphi}_0(\mathbf{x}_1, \mathbf{x}_2, t, \sigma), t, \sigma, \tau) \tag{E.25}$$

$$- \partial_2 \boldsymbol{\varphi}_0(\mathbf{x}_1, \mathbf{x}_2, t, \sigma)\mathbf{f}_{2,2}(\mathbf{x}_1, \mathbf{x}_2, \boldsymbol{\varphi}_0(\mathbf{x}_1, \mathbf{x}_2, t, \sigma), t, \sigma, \tau) \tag{E.26}$$

$$- \partial_1 \boldsymbol{\varphi}_1(\mathbf{x}_1, \mathbf{x}_2, t, \sigma)\mathbf{f}_{1,1}(\mathbf{x}_1, \mathbf{x}_2, \boldsymbol{\varphi}_0(\mathbf{x}_1, \mathbf{x}_2, t, \sigma), t, \sigma, \tau) \tag{E.27}$$

$$- \partial_2 \boldsymbol{\varphi}_1(\mathbf{x}_1, \mathbf{x}_2, t, \sigma)\mathbf{f}_{2,1}(\mathbf{x}_1, \mathbf{x}_2, \boldsymbol{\varphi}_0(\mathbf{x}_1, \mathbf{x}_2, t, \sigma), t, \sigma, \tau) \tag{E.28}$$

$$- \mathbf{Q}(\mathbf{x}_1, \mathbf{x}_2, t, \sigma, \tau)[\boldsymbol{\varphi}_1(\mathbf{x}_1, \mathbf{x}_2, t, \sigma, \tau)] - \partial_\sigma \boldsymbol{\varphi}_1(\mathbf{x}_1, \mathbf{x}_2, t, \sigma, \tau), \tag{E.29}$$

$$\mathbf{Q}(\mathbf{x}_1, \mathbf{x}_2, t, \sigma, \tau) = \partial_3^2 \mathbf{f}_{3,0}(\mathbf{x}_1, \mathbf{x}_2, \boldsymbol{\varphi}_0(\mathbf{x}_1, \mathbf{x}_2, t, \sigma), t, \sigma, \tau) \tag{E.30}$$

$$\bar{\tilde{\mathbf{f}}}_{1,1}(\mathbf{x}_1,\mathbf{x}_2,t,\sigma) = \frac{1}{T_1}\int_0^{T_1} \tilde{\mathbf{f}}_{1,1}(\mathbf{x}_1,\mathbf{x}_2,0,t,\sigma,\tau)\,d\tau \tag{E.31}$$

$$\bar{\tilde{\mathbf{f}}}_{2,1}(\mathbf{x}_1,\mathbf{x}_2,t,\sigma) = \frac{1}{T_1}\int_0^{T_1} \tilde{\mathbf{f}}_{2,1}(\mathbf{x}_1,\mathbf{x}_2,0,t,\sigma,\tau)\,d\tau \tag{E.32}$$

$$\bar{\tilde{\mathbf{f}}}_{1,2}(\mathbf{x}_1,\mathbf{x}_2,t,\sigma) = \frac{1}{T_1}\int_0^{T_1} \tilde{\mathbf{f}}_{1,2}(\mathbf{x}_1,\mathbf{x}_2,0,t,\sigma,\tau)\,d\tau \tag{E.33}$$

$$+ \frac{1}{T_1}\int_0^{T_1} \partial_1\tilde{\mathbf{f}}_{1,1}(\mathbf{x}_1,\mathbf{x}_2,0,t,\sigma,\tau)\int_0^{\tau} \tilde{\mathbf{f}}_{1,1}(\mathbf{x}_1,\mathbf{x}_2,0,t,\sigma,\nu)d\nu\,d\tau \tag{E.34}$$

$$+ \frac{1}{T_1}\int_0^{T_1} \partial_2\tilde{\mathbf{f}}_{1,1}(\mathbf{x}_1,\mathbf{x}_2,0,t,\sigma,\tau)\int_0^{\tau} \tilde{\mathbf{f}}_{2,1}(\mathbf{x}_1,\mathbf{x}_2,0,t,\sigma,\nu)d\nu\,d\tau \tag{E.35}$$

$$- \frac{1}{T_1}\int_0^{T_1}\int_0^{\tau} \partial_1\tilde{\mathbf{f}}_{1,1}(\mathbf{x}_1,\mathbf{x}_2,0,t,\sigma,\nu)\,\bar{\tilde{\mathbf{f}}}_{1,1}(\mathbf{x}_1,\mathbf{x}_2,t,\sigma)d\nu\,d\tau \tag{E.36}$$

$$- \frac{1}{T_1}\int_0^{T_1}\int_0^{\tau} \partial_2\tilde{\mathbf{f}}_{1,1}(\mathbf{x}_1,\mathbf{x}_2,0,t,\sigma,\nu)\,\bar{\tilde{\mathbf{f}}}_{2,1}(\mathbf{x}_1,\mathbf{x}_2,t,\sigma)d\nu\,d\tau \tag{E.37}$$

$$- \frac{1}{T_1}\int_0^{T_1}\int_0^{\tau} \partial_\sigma\tilde{\mathbf{f}}_{1,1}(\mathbf{x}_1,\mathbf{x}_2,0,t,\sigma,\nu)\,d\nu d\tau \tag{E.38}$$

$$\bar{\tilde{\mathbf{f}}}_{2,2}(\mathbf{x}_1,\mathbf{x}_2,t,\sigma) = \frac{1}{T_1}\int_0^{T_1} \tilde{\mathbf{f}}_{2,2}(\mathbf{x}_1,\mathbf{x}_2,0,t,\sigma,\tau)\,d\tau \tag{E.39}$$

$$+ \frac{1}{T_1}\int_0^{T_1} \partial_1\tilde{\mathbf{f}}_{2,1}(\mathbf{x}_1,\mathbf{x}_2,0,t,\sigma,\tau)\int_0^{\tau} \tilde{\mathbf{f}}_{1,1}(\mathbf{x}_1,\mathbf{x}_2,0,t,\sigma,\nu)d\nu\,d\tau \tag{E.40}$$

$$+ \frac{1}{T_1}\int_0^{T_1} \partial_2\tilde{\mathbf{f}}_{2,1}(\mathbf{x}_1,\mathbf{x}_2,0,t,\sigma,\tau)\int_0^{\tau} \tilde{\mathbf{f}}_{2,1}(\mathbf{x}_1,\mathbf{x}_2,0,t,\sigma,\nu)d\nu\,d\tau \tag{E.41}$$

$$- \frac{1}{T_1}\int_0^{T_1}\int_0^{\tau} \partial_1\tilde{\mathbf{f}}_{2,1}(\mathbf{x}_1,\mathbf{x}_2,0,t,\sigma,\nu)\,\bar{\tilde{\mathbf{f}}}_{1,1}(\mathbf{x}_1,\mathbf{x}_2,t,\sigma)d\nu\,d\tau \tag{E.42}$$

$$- \frac{1}{T_1}\int_0^{T_1}\int_0^{\tau} \partial_2\tilde{\mathbf{f}}_{2,1}(\mathbf{x}_1,\mathbf{x}_2,0,t,\sigma,\nu)\,\bar{\tilde{\mathbf{f}}}_{2,1}(\mathbf{x}_1,\mathbf{x}_2,t,\sigma)d\nu\,d\tau \tag{E.43}$$

$$- \frac{1}{T_1}\int_0^{T_1}\int_0^{\tau} \partial_\sigma\tilde{\mathbf{f}}_{2,1}(\mathbf{x}_1,\mathbf{x}_2,0,t,\sigma,\nu)\,d\nu\,d\tau \tag{E.44}$$

$$\bar{\tilde{\mathbf{f}}}_{1,1}(\bar{\tilde{\mathbf{x}}}_1,\bar{\tilde{\mathbf{y}}}_2,t,\sigma) = \bar{\tilde{\mathbf{f}}}_{1,1}(\bar{\tilde{\mathbf{x}}}_1,\bar{\tilde{\mathbf{y}}}_2+\boldsymbol{\phi}_0(\bar{\tilde{\mathbf{x}}}_1,t,\sigma),t,\sigma) \tag{E.45}$$

$$\bar{\tilde{\mathbf{f}}}_{2,1}(\bar{\tilde{\mathbf{x}}}_1,\bar{\tilde{\mathbf{y}}}_2,t,\sigma) = \bar{\tilde{\mathbf{f}}}_{2,1}(\bar{\tilde{\mathbf{x}}}_1,\bar{\tilde{\mathbf{y}}}_2+\boldsymbol{\phi}_0(\bar{\tilde{\mathbf{x}}}_1,t,\sigma),t,\sigma) - \partial_\sigma\boldsymbol{\phi}_0(\bar{\tilde{\mathbf{x}}}_1,t,\sigma) \tag{E.46}$$

$$- \partial_1\boldsymbol{\phi}_0(\bar{\tilde{\mathbf{x}}}_1,t,\sigma)\bar{\tilde{\mathbf{f}}}_{1,1}(\bar{\tilde{\mathbf{x}}}_1,\bar{\tilde{\mathbf{y}}}_2,t,\sigma) \tag{E.47}$$

$$\tilde{\bar{\mathbf{f}}}_{1,2}(\tilde{\bar{\mathbf{x}}}_1, \tilde{\bar{\mathbf{y}}}_2, t, \sigma) = \bar{\tilde{\mathbf{f}}}_{1,2}(\tilde{\bar{\mathbf{x}}}_1, \tilde{\bar{\mathbf{y}}}_2 + \boldsymbol{\phi}_0(\tilde{\bar{\mathbf{x}}}_1, t, \sigma), t, \sigma) \tag{E.48}$$

$$+ \partial_2 \bar{\tilde{\mathbf{f}}}_{1,1}(\tilde{\bar{\mathbf{x}}}_1, \tilde{\bar{\mathbf{y}}}_2 + \boldsymbol{\phi}_0(\tilde{\bar{\mathbf{x}}}_1, t, \sigma), t, \sigma)\boldsymbol{\phi}_1(\tilde{\bar{\mathbf{x}}}_1, t, \sigma) \tag{E.49}$$

$$\tilde{\bar{\mathbf{f}}}_{2,2}(\tilde{\bar{\mathbf{x}}}_1, \tilde{\bar{\mathbf{y}}}_2, t, \sigma) = \bar{\tilde{\mathbf{f}}}_{2,2}(\tilde{\bar{\mathbf{x}}}_1, \tilde{\bar{\mathbf{y}}}_2 + \boldsymbol{\phi}_0(\tilde{\bar{\mathbf{x}}}_1, t, \sigma), t, \sigma) \tag{E.50}$$

$$+ \partial_2 \bar{\tilde{\mathbf{f}}}_{2,1}(\tilde{\bar{\mathbf{x}}}_1, \tilde{\bar{\mathbf{y}}}_2 + \boldsymbol{\phi}_0(\tilde{\bar{\mathbf{x}}}_1, t, \sigma), t, \sigma)\boldsymbol{\phi}_1(\tilde{\bar{\mathbf{x}}}_1, t, \sigma) \tag{E.51}$$

$$- \partial_1 \boldsymbol{\phi}_0(\tilde{\bar{\mathbf{x}}}_1, t, \sigma)\tilde{\bar{\mathbf{f}}}_{1,2}(\tilde{\bar{\mathbf{x}}}_1, \tilde{\bar{\mathbf{y}}}_2, t, \sigma) \tag{E.52}$$

$$- \partial_1 \boldsymbol{\phi}_1(\tilde{\bar{\mathbf{x}}}_1, t, \sigma)\tilde{\bar{\mathbf{f}}}_{1,1}(\tilde{\bar{\mathbf{x}}}_1, \tilde{\bar{\mathbf{y}}}_2, t, \sigma) - \partial_t \boldsymbol{\phi}_0(\tilde{\bar{\mathbf{x}}}_1, t, \sigma) \tag{E.53}$$

$$- \partial_\sigma \boldsymbol{\phi}_1(\tilde{\bar{\mathbf{x}}}_1, t, \sigma) \tag{E.54}$$

Appendix F

Derivation of Sperm Chemotaxis Equations

If the angular velocity components $\omega_\perp$ and $\omega_\parallel$ are given by:

$$\omega_\perp = \omega_{\perp 0} + \omega_{\perp 1}\eta, \tag{F.1}$$

$$\omega_\parallel = \omega_{\parallel 0} + \omega_{\parallel 1}\eta, \tag{F.2}$$

then we may rewrite the rotational kinematics as:

$$\dot{\mathbf{R}} = \mathbf{R}\left(\widehat{\boldsymbol{\omega}}_0 + \widehat{\boldsymbol{\omega}}_1\eta\right) \tag{F.3}$$

where the vectors $\boldsymbol{\omega}_0$ and $\boldsymbol{\omega}_1$ are given by:

$$\boldsymbol{\omega}_0 = \begin{bmatrix} \omega_{\parallel 0} \\ 0 \\ \omega_{\perp 0} \end{bmatrix}, \qquad \boldsymbol{\omega}_1 = \begin{bmatrix} \omega_{\parallel 1} \\ 0 \\ \omega_{\perp 1} \end{bmatrix} \tag{F.4}$$

Let $\mathbf{R}_0(t) = \exp(\widehat{\boldsymbol{\omega}}_0 t)$ and $\bar{\mathbf{R}} = \mathbf{R}\mathbf{R}_0(t)^\intercal$, and compute:

$$\mathbf{R}_0(t) = \begin{bmatrix} \frac{\omega_{\perp 0}^2}{\omega^2}\cos(\omega t) + \frac{\omega_{\parallel 0}^2}{\omega^2} & -\frac{\omega_{\perp 0}}{\omega}\sin(\omega t) & \frac{\omega_{\perp 0}\omega_{\parallel 0}}{\omega^2}(1-\cos(\omega t)) \\ \frac{\omega_{\perp 0}}{\omega}\sin(\omega t) & \cos(\omega t) & -\frac{\omega_{\parallel 0}}{\omega}\sin(\omega t) \\ \frac{\omega_{\perp 0}\omega_{\parallel 0}}{\omega^2}(1-\cos(\omega t)) & \frac{\omega_{\parallel 0}}{\omega}\sin(\omega t) & \frac{\omega_{\parallel 0}^2}{\omega^2}\cos(\omega t) + \frac{\omega_{\perp 0}^2}{\omega^2} \end{bmatrix} \tag{F.5}$$

where $\omega = |\boldsymbol{\omega}_0|$. Then, observe that:

$$\begin{aligned} \dot{\mathbf{x}} &= \mathbf{R}\mathbf{v} = \mathbf{R}\mathbf{R}_0(t)^\intercal \mathbf{R}_0(t)\mathbf{v} = \bar{\mathbf{R}}\mathbf{R}_0(t)\mathbf{v} \\ \dot{\bar{\mathbf{R}}} &= \dot{\mathbf{R}}\mathbf{R}_0(t)^\intercal + \mathbf{R}\dot{\mathbf{R}}_0^\intercal = \mathbf{R}\widehat{\boldsymbol{\omega}}_0\mathbf{R}_0(t)^\intercal + \eta\mathbf{R}\widehat{\boldsymbol{\omega}}_1\mathbf{R}_0(t)^\intercal - \mathbf{R}\widehat{\boldsymbol{\omega}}_0\mathbf{R}_0(t)^\intercal \\ &= \mathbf{R}\mathbf{R}_0(t)^\intercal\mathbf{R}_0(t)\widehat{\boldsymbol{\omega}}_1\mathbf{R}_0(t)^\intercal\eta = \bar{\mathbf{R}}\,\mathbf{R}_0(t)\widehat{\boldsymbol{\omega}}_1\mathbf{R}_0(t)^\intercal\,\eta \end{aligned}$$

Define the average velocity vector $\mathbf{v}_m$ and the vector $\mathbf{d}(t)$ by:

$$\mathbf{v}_m = \overline{\mathbf{R}_0(t)}\mathbf{v} = \frac{\omega}{2\pi}\int_0^{\frac{2\pi}{\omega}} \mathbf{R}_0(t)dt\,\mathbf{v}, \qquad \mathbf{d}(t) = \int (\mathbf{R}_0(t)\mathbf{v} - \mathbf{v}_m)\,dt \tag{F.6}$$

then observe that:

$$\mathbf{R}_0(t)\mathbf{v} = \mathbf{v}_m + \dot{\mathbf{d}}(t) \tag{F.7}$$

If $v > 0, \omega_{\parallel 0} > 0, \omega_{\perp 0} > 0$, direct computation shows that:

$$\mathbf{v}_m = \frac{v\omega_{\parallel 0}}{\omega}\begin{bmatrix} \frac{\omega_{\parallel 0}}{\omega} \\ 0 \\ \frac{\omega_{\perp 0}}{\omega} \end{bmatrix}, \quad \dot{\mathbf{d}}(t) = \frac{v\omega_{\perp 0}}{\omega}\begin{bmatrix} \frac{\omega_{\perp 0}}{\omega}\cos(\omega t) \\ \sin(\omega t) \\ -\frac{\omega_{\parallel 0}}{\omega}\cos(\omega t) \end{bmatrix}, \quad \mathbf{d}(t) = \frac{v\omega_{\perp 0}}{\omega^2}\begin{bmatrix} \frac{\omega_{\perp 0}}{\omega}\sin(\omega t) \\ -\cos(\omega t) \\ -\frac{\omega_{\parallel 0}}{\omega}\sin(\omega t) \end{bmatrix} \tag{F.8}$$

Define the average position $\bar{\mathbf{x}} = \mathbf{x} - \bar{\mathbf{R}}\,\mathbf{d}(t)$, which evolves according to:

$$\dot{\bar{\mathbf{x}}} = \dot{\mathbf{x}} - \dot{\bar{\mathbf{R}}}\,\mathbf{d}(t) - \bar{\mathbf{R}}\,\dot{\mathbf{d}}(t) = -\bar{\mathbf{R}}\,\mathbf{R}_0(t)\widehat{\boldsymbol{\omega}}_1\mathbf{R}_0(t)^\intercal\mathbf{d}(t)\,\eta + \bar{\mathbf{R}}\,\mathbf{v}_m \tag{F.9}$$

If we make the identifications:

$$\widehat{\boldsymbol{\omega}}_\eta(t) = \mathbf{R}_0(t)\widehat{\boldsymbol{\omega}}_1\mathbf{R}_0(t)^\intercal \tag{F.10}$$

$$\mathbf{v}_\eta(t) = -\widehat{\boldsymbol{\omega}}_\eta(t)\mathbf{d}(t) \tag{F.11}$$

then the evolution of the average motion variables $\bar{\mathbf{x}}$ and $\bar{\mathbf{R}}$ is governed by:

$$\dot{\bar{\mathbf{x}}} = \bar{\mathbf{R}}\mathbf{v}_\eta(t)\eta + \bar{\mathbf{R}}\mathbf{v}_m \tag{F.12}$$

$$\dot{\bar{\mathbf{R}}} = \bar{\mathbf{R}}\widehat{\boldsymbol{\omega}}_\eta(t)\eta \tag{F.13}$$

We compute the expressions for $\mathbf{v}_\eta(t), \boldsymbol{\omega}_\eta(t)$ which turn out to be:

$$\boldsymbol{\omega}_\eta(t) = \frac{\omega_{\parallel 1}\omega_{\parallel 0} + \omega_{\perp 1}\omega_{\perp 0}}{\omega}\begin{bmatrix} \frac{\omega_{\parallel 0}}{\omega} \\ 0 \\ \frac{\omega_{\perp 0}}{\omega} \end{bmatrix} + \frac{\omega_{\parallel 1}\omega_{\perp 0} - \omega_{\perp 1}\omega_{\parallel 0}}{\omega}\begin{bmatrix} \frac{\omega_{\perp 0}}{\omega}\cos(\omega t) \\ \sin(\omega t) \\ -\frac{\omega_{\parallel 0}}{\omega}\cos(\omega t) \end{bmatrix} \tag{F.14}$$

$$\mathbf{v}_\eta(t) = \frac{v\omega_{\perp 0}\left(\omega_{\perp 1}\omega_{\parallel 0} - \omega_{\parallel 1}\omega_{\perp 0}\right)}{\omega^3}\begin{bmatrix} \frac{\omega_{\parallel 0}}{\omega} \\ 0 \\ \frac{\omega_{\perp 0}}{\omega} \end{bmatrix} - \frac{v\omega_{\perp 0}\left(\omega_{\parallel 1}\omega_{\parallel 0} + \omega_{\perp 1}\omega_{\perp 0}\right)}{\omega^3}\begin{bmatrix} \frac{\omega_{\perp 0}}{\omega}\cos(\omega t) \\ \sin(\omega t) \\ -\frac{\omega_{\parallel 0}}{\omega}\cos(\omega t) \end{bmatrix} \tag{F.15}$$

Observe that the feedback coefficients $\mathbf{v}_\eta, \boldsymbol{\omega}_\eta$ are periodic with non zero average in general, whereas the periodic perturbation $\mathbf{d}(t)$ always has zero average. In the absence of feedback, the instantaneous local concentration $c(\mathbf{x})$ may be approximated by its Taylor series:

$$c(\mathbf{x}) = c(\bar{\mathbf{x}} + \bar{\mathbf{R}}\mathbf{d}(t)) = c(\bar{\mathbf{x}}) + \nabla c(\bar{\mathbf{x}})^\intercal\bar{\mathbf{R}}\mathbf{d}(t) + O(|\mathbf{d}(\cdot)|^2) \tag{F.16}$$

By employing the fundamental theorem of calculus, the local concentration at the average position $c(\bar{\mathbf{x}})$ can be written as:

$$c(\bar{\mathbf{x}}) = c(\bar{\mathbf{x}}_0) + \int_{t_0}^{t} \nabla c(\bar{\mathbf{x}}(\nu))^\intercal \dot{\bar{\mathbf{x}}}(\nu)\, d\nu = c(\bar{\mathbf{x}}_0) + \int_{t_0}^{t} \nabla c(\bar{\mathbf{x}}(\nu))^\intercal \bar{\mathbf{R}}(\nu)\left(\mathbf{v}_\eta(\nu)\,\eta + \mathbf{v}_m\right)\, d\nu \tag{F.17}$$

where $\bar{\mathbf{x}}_0$ is the initial average position of the cell at the initial time t_0. Hence, in the absence of feedback, the instantaneous local concentration may be approximated by:

$$c(\mathbf{x}) = c(\bar{\mathbf{x}}_0) + \int_{t_0}^{t} \nabla c(\bar{\mathbf{x}}(\nu))^\intercal \bar{\mathbf{R}}(\nu)\mathbf{v}_m\, d\nu + \nabla c(\bar{\mathbf{x}})^\intercal \bar{\mathbf{R}}\,\mathbf{d}(t) + O(|\mathbf{d}(\cdot)|^2) \tag{F.18}$$

The dynamics of the signaling pathway is modelled by:

$$\sigma\,\dot{\xi} = s(t) - \xi, \tag{F.19}$$

$$\mu\,\dot{\eta} = \rho\,\dot{\xi} - \eta^3, \tag{F.20}$$

$$\mu\,\dot{\rho} = \rho - \rho\,\eta^2, \tag{F.21}$$

We employ a coordinate change to study the behavior of the signal pathway. Let $\zeta_2 = \xi$, $\zeta_1 = \xi - \eta/\rho$, which leads to:

$$\mu\,\dot{\zeta}_1 = \zeta_2 - \zeta_1 \tag{F.22}$$

$$\sigma\,\dot{\zeta}_2 = s(t) - \zeta_2 \tag{F.23}$$

$$\mu\,\rho = \rho\,(1 - \rho^2\zeta^2) \tag{F.24}$$

$$\zeta = \zeta_2 - \zeta_1, \quad \eta = \rho\,\zeta \tag{F.25}$$

We take the stimulus to be $s(t) = \lambda c(\mathbf{x})$ for some proportionality constant λ. Under the assumption that $\mu|\mathbf{v}_m| \ll 1$ and $\sigma|\mathbf{v}_m| \ll 1$ in the absence of feedback, there is enough time-scale separation between the dynamics of the average motion variables $\bar{\mathbf{x}}, \bar{\mathbf{R}}$ and the dynamics

of ζ_1 and ζ_2, which allows approximating the signal $\zeta = \zeta_2 - \zeta_1$ by its quasi-steady state in which the average motion variables $\bar{\mathbf{x}}, \bar{\mathbf{R}}$ are treated as constants. In this quasi-steady approximation, the local concentration maybe taken as:

$$c(\mathbf{x}) \approx c(\bar{\mathbf{x}}_0) + \nabla c(\bar{\mathbf{x}})^\intercal \bar{\mathbf{R}} \mathbf{v}_m \Delta t + \nabla c(\bar{\mathbf{x}})^\intercal \bar{\mathbf{R}} \mathbf{d}(t) + O(|\mathbf{d}(\cdot)|^2) \tag{F.26}$$

where $\Delta t = t - t_0$. This form of the local concentration is treated as an input for the dynamics of the signaling pathway. Accordingly, we obtain the quasi-steady output for ζ, denoted as ζ_{QS}, which can be computed from standard linear systems theory:

$$\zeta \approx \zeta_{\mathrm{QS}} = \lambda\, \mu \nabla c(\bar{\mathbf{x}})^\intercal \bar{\mathbf{R}} \mathbf{v}_m + \lambda\, \gamma(\omega)\, \nabla c(\bar{\mathbf{x}})^\intercal \bar{\mathbf{R}}\, \mathbf{d}(t + \phi(\omega)/\omega) \tag{F.27}$$

where $\gamma(\omega)$ and $\phi(\omega)$ are the gain and phase contribution at the frequency ω, and are defined by:

$$\gamma(\omega) = \frac{\omega\,(\mu + \sigma)}{\sqrt{(1 + \mu^2\omega^2)(1 + \sigma^2\omega^2)}}, \tag{F.28}$$

$$\sin(\phi(\omega)) = \frac{1 - \mu\sigma\omega^2}{\sqrt{(1 + \mu^2\omega^2)(1 + \sigma^2\omega^2)}}, \qquad \cos(\phi(\omega)) = \frac{\mu\omega + \sigma\omega}{\sqrt{(1 + \mu^2\omega^2)(1 + \sigma^2\omega^2)}} \tag{F.29}$$

Hence, a quasi steady approximation of the adaptation rule for the signaling pathway becomes:

$$\mu\, \dot{\rho} = \rho\, \left(1 - \rho^2 \zeta_{\mathrm{QS}}^2\right) \tag{F.30}$$

and the motion evolves, in the quasi-steady sense, according to the equations:

$$\dot{\bar{\mathbf{x}}} = \bar{\mathbf{R}}\, \mathbf{v}_\eta(t)\, \rho\, \zeta_{\mathrm{QS}} + \bar{\mathbf{R}}\, \mathbf{v}_m \tag{F.31}$$

$$\dot{\bar{\mathbf{R}}} = \bar{\mathbf{R}}\, \widehat{\boldsymbol{\omega}}_\eta(t)\, \rho\, \zeta_{\mathrm{QS}} \tag{F.32}$$

$$\mu\, \dot{\rho} = \rho\, \left(1 - \rho^2\, \zeta_{\mathrm{QS}}^2\right) \tag{F.33}$$

$$\zeta_{\mathrm{QS}} = \lambda\,\mu\nabla c(\bar{\mathbf{x}})^{\intercal}\bar{\mathbf{R}}\mathbf{v}_m + \lambda\,\gamma(\omega)\,\nabla c(\bar{\mathbf{x}})^{\intercal}\bar{\mathbf{R}}\,\mathbf{d}(t+\phi(\omega)/\omega) \tag{F.34}$$

To proceed with the rest of the analysis, we make several definitions that will simplify the calculations. First, we define the three unit vectors:

$$\mathbf{i}_1(t) = \frac{\mathbf{d}(t)}{|\mathbf{d}(t)|} = \begin{bmatrix} \frac{\omega_{\perp 0}}{\omega}\sin(\omega t) \\ -\cos(\omega t) \\ -\frac{\omega_{\parallel 0}}{\omega}\sin(\omega t) \end{bmatrix}, \qquad \mathbf{i}_2(t) = \frac{1}{\omega}\frac{d\mathbf{i}_1(t)}{dt} = \begin{bmatrix} \frac{\omega_{\perp 0}}{\omega}\cos(\omega t) \\ \sin(\omega t) \\ -\frac{\omega_{\parallel 0}}{\omega}\cos(\omega t) \end{bmatrix}, \tag{F.35}$$

$$\mathbf{i}_3 = \frac{\mathbf{v}_m}{|\mathbf{v}_m|} = \begin{bmatrix} \frac{\omega_{\parallel 0}}{\omega} \\ 0 \\ \frac{\omega_{\perp 0}}{\omega} \end{bmatrix} \tag{F.36}$$

and we observe that:

$$\mathbf{i}_1(t)\times\mathbf{i}_2(t) = \mathbf{i}_3, \qquad \mathbf{i}_2(t)\times\mathbf{i}_3 = \mathbf{i}_1(t), \qquad \mathbf{i}_3\times\mathbf{i}_1(t) = \mathbf{i}_2(t) \tag{F.37}$$

$$\mathbf{i}_1(t)\cdot\mathbf{i}_2(t) = 0, \qquad \mathbf{i}_2(t)\cdot\mathbf{i}_3 = 0, \qquad \mathbf{i}_3\cdot\mathbf{i}_1(t) = 0 \tag{F.38}$$

where $\times$ and $\cdot$ are the cross product and the dot product between 3D vectors, respectively. In other words, the vector triplet $\{\mathbf{i}_1(t),\, \mathbf{i}_2(t),\, \mathbf{i}_3\}$ comprises a right-handed orthogonal rotating coordinate basis for the 3D space. Next, we observe that:

$$\mathbf{d}(t) = \frac{v\,\omega_{\perp 0}}{\omega^2}\,\mathbf{i}_1(t), \qquad \mathbf{v}_m = \frac{v\,\omega_{\parallel 0}}{\omega}\,\mathbf{i}_3 \tag{F.39}$$

and that:

$$\boldsymbol{\omega}_\eta(t) = \frac{\omega_{\parallel 1}\omega_{\perp 0} - \omega_{\perp 1}\omega_{\parallel 0}}{\omega}\mathbf{i}_2(t) + \frac{\omega_{\parallel 1}\omega_{\parallel 0} + \omega_{\perp 1}\omega_{\perp 0}}{\omega}\mathbf{i}_3 \tag{F.40}$$

$$\mathbf{v}_\eta(t) = \frac{v\omega_{\perp 0}}{\omega^2}\left(-\frac{\left(\omega_{\parallel 1}\omega_{\parallel 0} + \omega_{\perp 1}\omega_{\perp 0}\right)}{\omega}\mathbf{i}_2(t) + \frac{\left(\omega_{\perp 1}\omega_{\parallel 0} - \omega_{\parallel 1}\omega_{\perp 0}\right)}{\omega}\mathbf{i}_3\right) \tag{F.41}$$

We apply the time scaling $\tau = \omega t$, which leads to the equations:

$$\frac{d\bar{\mathbf{x}}}{d\tau} = \frac{1}{\omega}\rho\,\zeta_{\mathrm{QS}}\,\bar{\mathbf{R}}\,\mathbf{v}_\eta(\tau) + \frac{1}{\omega}\bar{\mathbf{R}}\,\mathbf{v}_m \tag{F.42}$$

$$\frac{d\bar{\mathbf{R}}}{d\tau} = \frac{1}{\omega}\rho\,\zeta_{\mathrm{QS}}\,\bar{\mathbf{R}}\,\widehat{\boldsymbol{\omega}}_\eta(\tau) \tag{F.43}$$

$$\frac{d\rho}{d\tau} = \frac{1}{\mu\omega}\rho\,\left(1-\rho^2\,\zeta_{\mathrm{QS}}^2\right) \tag{F.44}$$

$$\zeta_{\mathrm{QS}} = \lambda\,\mu\nabla c(\bar{\mathbf{x}})^\intercal\bar{\mathbf{R}}\mathbf{v}_m + \lambda\,\gamma(\omega)\,\nabla c(\bar{\mathbf{x}})^\intercal\bar{\mathbf{R}}\,\mathbf{d}(\tau+\phi(\omega)) \tag{F.45}$$

Up to this point, the analysis is valid irrespective of the asymptotic orders of the terms in the equations as long as the assumptions $\mu|\mathbf{v}_m| \ll 1$, $\sigma|\mathbf{v}_m| \ll 1$ and $|\mathbf{d}(\cdot)| \ll 1$ are valid. Before we proceed to perform an averaging analysis, all the terms in the equations must be assigned a precise asymptotic order, in relation to the frequency ω, that is consistent with the assumptions adopted so far. There are several choices for this asymptotic order assignment, each of them corresponds to a different 'distinguished limit' in which the behavior of the system is qualitatively different. We investigate the particular distinguished limit in which we have:

$$\mu = O(1/\sqrt{\omega}), \qquad \sigma = O(1/\omega), \qquad v = O(\sqrt{\omega}), \qquad \omega_{\perp 0} = O(\omega), \tag{F.46}$$

$$\omega_{\perp 1} = O(1), \qquad \omega_{\parallel 0} = O(\sqrt{\omega}), \qquad \omega_{\parallel 1} = O(\sqrt{\omega}), \tag{F.47}$$

First, we verify that this limit is consistent with the assumptions:

$$\mu|\mathbf{v}_m| = \frac{\mu v\,\omega_{\parallel 0}}{\omega} = O(1/\sqrt{\omega}) \ll 1, \qquad \sigma|\mathbf{v}_m| = \frac{\sigma v\,\omega_{\parallel 0}}{\omega} = O(1/\omega) \ll 1, \tag{F.48}$$

$$|\mathbf{d}(t)| = \frac{v\omega_{\parallel 0}}{\omega^2} = O(1/\sqrt{\omega}) \ll 1 \tag{F.49}$$

which is true in the limit $\omega \to \infty$. We proceed to define the vector $\bar{\mathbf{h}} = \bar{\mathbf{R}}\,\mathbf{i}_3$, which evolves according to the equation:

$$\frac{d\bar{\mathbf{h}}}{d\tau} = \frac{d\bar{\mathbf{R}}}{d\tau}\,\mathbf{i}_3 = \frac{1}{\omega}\rho\,\zeta_{\text{QS}}\,\bar{\mathbf{R}}\,\widehat{\boldsymbol{\omega}}_\eta(\tau)\mathbf{i}_3 = \frac{1}{\omega}\rho\,\zeta_{\text{QS}}\,\bar{\mathbf{R}}\,\widehat{\boldsymbol{\omega}}_\eta(\tau)\mathbf{i}_3 = \frac{1}{\omega}\rho\,\zeta_{\text{QS}}\,\bar{\mathbf{R}}\,\widehat{\boldsymbol{\omega}}_\eta(\tau)\bar{\mathbf{R}}^\intercal\bar{\mathbf{R}}\,\mathbf{i}_3 \quad \text{(F.50)}$$

We compute:

$$\bar{\mathbf{R}}\,\widehat{\boldsymbol{\omega}}_\eta(\tau)\bar{\mathbf{R}}^\intercal = \frac{\omega_{\parallel 1}\omega_{\perp 0} - \omega_{\perp 1}\omega_{\parallel 0}}{\omega}\bar{\mathbf{R}}\,\widehat{\mathbf{i}}_2\bar{\mathbf{R}}^\intercal + \frac{\omega_{\parallel 1}\omega_{\parallel 0} + \omega_{\perp 1}\omega_{\perp 0}}{\omega}\bar{\mathbf{R}}\,\widehat{\mathbf{i}}_3\bar{\mathbf{R}}^\intercal \quad \text{(F.51)}$$

Hence, we have that:

$$\bar{\mathbf{R}}\,\widehat{\boldsymbol{\omega}}_\eta(\tau)\bar{\mathbf{R}}^\intercal\,\bar{\mathbf{R}}\mathbf{i}_3 = \frac{\omega_{\parallel 1}\omega_{\perp 0} - \omega_{\perp 1}\omega_{\parallel 0}}{\omega}\bar{\mathbf{R}}\,\mathbf{i}_1(\tau) \implies \frac{d\bar{\mathbf{h}}}{d\tau} = \frac{\omega_{\parallel 1}\omega_{\perp 0} - \omega_{\perp 1}\omega_{\parallel 0}}{\omega^2}\,\rho\,\zeta_{\text{QS}}\bar{\mathbf{R}}\,\mathbf{i}_1(\tau) \quad \text{(F.52)}$$

Moreover, it easy to verify through direct computation that:

$$\mathbf{d}(\tau + \phi(\omega)) = \frac{v\,\omega_{\perp 0}}{\omega^2}\,\cos(\phi(\omega))\,\mathbf{i}_1(\tau) + \frac{v\,\omega_{\perp 0}}{\omega^2}\,\sin(\phi(\omega))\,\mathbf{i}_2(\tau) \quad \text{(F.53)}$$

which implies that:

$$\zeta_{\text{QS}} = \lambda\left(\frac{\mu v\,\omega_{\parallel 0}}{\omega}\bar{\mathbf{R}}\,\mathbf{i}_3 + \frac{v\,\omega_{\perp 0}\gamma(\omega)}{\omega^2}\,\left(\cos(\phi(\omega))\,\bar{\mathbf{R}}\,\mathbf{i}_1(\tau) + \sin(\phi(\omega))\,\bar{\mathbf{R}}\,\mathbf{i}_2(\tau)\right)\right)^\intercal \nabla c(\bar{\mathbf{x}}) \quad \text{(F.54)}$$

Hence, we have:

$$\frac{d\bar{\mathbf{h}}}{d\tau} = \bar{\mathbf{R}}\,\left(\alpha_1\,\mathbf{i}_1(\tau)\mathbf{i}_3^\intercal + \alpha_2\,\mathbf{i}_1(\tau)\mathbf{i}_1(\tau)^\intercal + \alpha_3\,\mathbf{i}_1(\tau)\mathbf{i}_2(\tau)^\intercal\right)\,\bar{\mathbf{R}}^\intercal\,\rho\,\nabla c(\bar{\mathbf{x}}) + O(\rho/\omega^{3/2}) \quad \text{(F.55)}$$

where the coefficients α_i for $i \in \{1,2,3\}$ are given by:

$$\alpha_1 = \frac{\mu v\, \omega_{\perp 0}\omega_{\|0}\omega_{\|1}}{\omega^3}, \quad \alpha_2 = \frac{v\, \omega_{\perp 0}^2\omega_{\|1}\gamma(\omega)}{\omega^4}\cos(\phi(\omega)), \quad \alpha_3 = \frac{v\, \omega_{\perp 0}^2\omega_{\|1}\gamma(\omega)}{\omega^4}\sin(\phi(\omega)) \tag{F.56}$$

In the distinguished limit defined above, we have that:

$$\alpha_1 = O(1/\omega), \quad \alpha_2 = O(1/\omega), \quad \alpha_3 = O(1/\omega)$$

Next, we compute:

$$\bar{\mathbf{R}}\,\mathbf{v}_m = \frac{v\,\omega_{\|0}}{\omega}\,\bar{\mathbf{R}}\,\mathbf{i}_3, \tag{F.57}$$

$$\bar{\mathbf{R}}\,\mathbf{v}_\eta(\tau) = -\frac{v\omega_{\perp 0}}{\omega^3}\left(\left(\omega_{\|1}\omega_{\|0} + \omega_{\perp 1}\omega_{\perp 0}\right)\bar{\mathbf{R}}\,\mathbf{i}_2(\tau) + \left(\omega_{\perp 1}\omega_{\|0} - \omega_{\|1}\omega_{\perp 0}\right)\bar{\mathbf{R}}\,\mathbf{i}_3\right) \tag{F.58}$$

which implies that:

$$\frac{d\bar{\mathbf{x}}}{d\tau} = \bar{\mathbf{R}}\,\left(\beta_1\mathbf{i}_3\mathbf{i}_3^\intercal + \beta_2\mathbf{i}_3\mathbf{i}_1(\tau)^\intercal + \beta_3\mathbf{i}_3\mathbf{i}_2(\tau)^\intercal\right)\,\bar{\mathbf{R}}^\intercal\,\rho\,\nabla c(\bar{\mathbf{x}}) + \frac{v\,\omega_{\|0}}{\omega^2}\bar{\mathbf{R}}\,\mathbf{i}_3 + O(\rho/\omega^2) \tag{F.59}$$

where the coefficients β_i for $i \in \{1,2,3\}$ are given by:

$$\beta_1 = \frac{\mu v^2\omega_{\perp 0}^2\omega_{\|0}\omega_{\|1}}{\omega^5}, \quad \beta_2 = \frac{v^2\omega_{\perp 0}^3\omega_{\|1}\gamma(\omega)}{\omega^6}\cos(\phi(\omega)), \quad \beta_3 = \frac{v^2\omega_{\perp 0}^3\omega_{\|1}\gamma(\omega)}{\omega^6}\sin(\phi(\omega)) \tag{F.60}$$

In the distinguished limit defined above, we have that:

$$\beta_1 = O(1/\omega^{3/2}), \quad \beta_2 = O(1/\omega^{3/2}), \quad \beta_3 = O(1/\omega^{3/2})$$

In addition, we have that:

$$\mu\omega = O(\sqrt{\omega}), \quad \frac{v\,\omega_{\|0}}{\omega^2} = O(1/\omega), \quad \frac{\mu v\,\omega_{\|0}}{\omega} = O(1/\sqrt{\omega}), \quad \frac{v\,\omega_{\perp 0}\gamma(\omega)}{\omega^2} = O(1/\sqrt{\omega}) \quad \text{(F.61)}$$

Recall that the evolution equation for the adaptive gain ρ is given by:

$$\frac{d\rho}{d\tau} = \frac{1}{\mu\omega}\rho\left(1-\rho^2\,\zeta_{\mathrm{QS}}^2\right) \quad \text{(F.62)}$$

$$\zeta_{\mathrm{QS}} = \left(\frac{\mu v\,\omega_{\|0}}{\omega}\bar{\mathbf{R}}\,\mathbf{i}_3 + \frac{v\,\omega_{\perp 0}\gamma(\omega)}{\omega^2}\left(\cos(\phi(\omega))\,\bar{\mathbf{R}}\,\mathbf{i}_1(\tau) + \sin(\phi(\omega))\,\bar{\mathbf{R}}\,\mathbf{i}_2(\tau)\right)\right)^{\intercal}\nabla c(\bar{\mathbf{x}}) \quad \text{(F.63)}$$

which has equilibrium points: $\{0, \pm 1/|\zeta_{\mathrm{QS}}|\}$. We are only interested in the behavior of ρ around the equilibrium point $\rho = 1/|\zeta_{\mathrm{QS}}|$, since the equilibrium point $\rho = 0$ is unstable and the equilibrium point $\rho = -1/|\zeta_{\mathrm{QS}}|$ does not satisfy the requirement that $\rho > 0$. We note, however, that in the distinguished limit defined above we have that $\zeta_{\mathrm{QS}} = O(1/\sqrt{\omega})$, which implies that near the equilibrium point $\rho = 1/|\zeta_{\mathrm{QS}}|$ we have that $\rho = O(\sqrt{\omega})$. This implies that ρ will change the asymptotic orders of all the terms in which it appears. In other words, we have that:

$$\alpha_1\rho = O(1/\sqrt{\omega}), \quad \alpha_2\rho = O(1/\sqrt{\omega}), \quad \alpha_3\rho = O(1/\sqrt{\omega})$$
$$\beta_1\rho = O(1/\omega), \qquad \beta_2\rho = O(1/\omega), \qquad \beta_3\rho = O(1/\omega)$$

Now that all terms have been assigned a precise asymptotic order in relation to the frequency ω, we may proceed to average out the equations:

$$\frac{d\bar{\mathbf{h}}}{d\tau} = \bar{\mathbf{R}}\left(\alpha_1\,\mathbf{i}_1(\tau)\mathbf{i}_3^{\intercal} + \alpha_2\,\mathbf{i}_1(\tau)\mathbf{i}_1(\tau)^{\intercal} + \alpha_3\,\mathbf{i}_1(\tau)\mathbf{i}_2(\tau)^{\intercal}\right)\bar{\mathbf{R}}^{\intercal}\,\rho\,\nabla c(\bar{\mathbf{x}}) \quad \text{(F.64)}$$

$$\frac{d\bar{\mathbf{x}}}{d\tau} = \bar{\mathbf{R}}\left(\beta_1\mathbf{i}_3\mathbf{i}_3^{\intercal} + \beta_2\mathbf{i}_3\mathbf{i}_1(\tau)^{\intercal} + \beta_3\mathbf{i}_3\mathbf{i}_2(\tau)^{\intercal}\right)\bar{\mathbf{R}}^{\intercal}\,\rho\,\nabla c(\bar{\mathbf{x}}) + \frac{v\,\omega_{\|0}}{\omega^2}\bar{\mathbf{R}}\,\mathbf{i}_3 \quad \text{(F.65)}$$

$$\frac{d\rho}{d\tau} = \frac{1}{\mu\omega}\rho\left(1-\rho^2\,\zeta_{\mathrm{QS}}^2\right) \quad \text{(F.66)}$$

$$\zeta_{\mathrm{QS}} = \lambda \left(\frac{\mu v\, \omega_{\|0}}{\omega} \bar{\mathbf{R}}\, \mathbf{i}_3 + \frac{v\, \omega_{\perp 0} \gamma(\omega)}{\omega^2} \left(\cos(\phi(\omega))\, \bar{\mathbf{R}}\, \mathbf{i}_1(\tau) + \sin(\phi(\omega))\, \bar{\mathbf{R}}\, \mathbf{i}_2(\tau) \right) \right)^{\intercal} \nabla c(\bar{\mathbf{x}}) \tag{F.67}$$

We compute:

$$\zeta_{\mathrm{QS}}^2/\lambda^2 = \frac{\mu^2 v^2\, \omega_{\|0}^2}{\omega^2} \left(\bar{\mathbf{h}}^{\intercal} \nabla c(\bar{\mathbf{x}}) \right)^2 + \frac{v^2\, \omega_{\perp 0}^2 \gamma(\omega)^2}{\omega^4} \cos(\phi(\omega))^2 \left(\nabla c(\bar{\mathbf{x}})^{\intercal} \bar{\mathbf{R}}\, \mathbf{i}_1(\tau) \right)^2 \tag{F.68}$$

$$+ \frac{v^2\, \omega_{\perp 0}^2 \gamma(\omega)^2}{\omega^4} \sin(\phi(\omega))^2 \left(\nabla c(\bar{\mathbf{x}})^{\intercal} \bar{\mathbf{R}}\, \mathbf{i}_2(\tau) \right)^2 \tag{F.69}$$

$$+ \frac{2\mu v^2\, \omega_{\|0} \omega_{\perp 0} \gamma(\omega)}{\omega^3} \left(\bar{\mathbf{h}}^{\intercal} \nabla c(\bar{\mathbf{x}}) \right) \left(\cos(\phi(\omega)) \, \left(\nabla c(\bar{\mathbf{x}})^{\intercal} \bar{\mathbf{R}}\, \mathbf{i}_1(\tau) \right) + \sin(\phi(\omega)) \, \left(\nabla c(\bar{\mathbf{x}})^{\intercal} \bar{\mathbf{R}}\, \mathbf{i}_2(\tau) \right) \right) \tag{F.70}$$

$$+ \frac{2v^2\, \omega_{\perp 0}^2 \gamma(\omega)^2}{\omega^4} \sin(\phi(\omega)) \cos(\phi(\omega)) \left(\nabla c(\bar{\mathbf{x}})^{\intercal} \bar{\mathbf{R}}\, \mathbf{i}_2(\tau) \right) \left(\nabla c(\bar{\mathbf{x}})^{\intercal} \bar{\mathbf{R}}\, \mathbf{i}_1(\tau) \right) \tag{F.71}$$

Finally, we apply second order averaging with respect to the parameter $1/\sqrt{\omega}$ to obtain:

$$\frac{d\bar{\mathbf{h}}}{d\tau} = \bar{\mathbf{R}} \left(\alpha_2\, \overline{\mathbf{i}_1(\tau) \mathbf{i}_1(\tau)^{\intercal}} + \alpha_3\, \overline{\mathbf{i}_1(\tau) \mathbf{i}_2(\tau)^{\intercal}} \right) \bar{\mathbf{R}}^{\intercal}\, \rho\, \nabla c(\bar{\mathbf{x}}) \tag{F.72}$$

$$\frac{d\bar{\mathbf{x}}}{d\tau} = \beta_1 \bar{\mathbf{R}}\, \mathbf{i}_3 \mathbf{i}_3^{\intercal} \bar{\mathbf{R}}^{\intercal}\, \rho\, \nabla c(\bar{\mathbf{x}}) + \frac{v\, \omega_{\|0}}{\omega^2} \bar{\mathbf{R}}\, \mathbf{i}_3 \tag{F.73}$$

$$\frac{d\rho}{d\tau} = \frac{1}{\mu\omega} \rho \left(1 - \rho^2\, \overline{\zeta_{\mathrm{QS}}^2} \right) \tag{F.74}$$

where we neglected all terms of non-leading order in each equation. Direct calculation shows that:

$$\overline{\mathbf{i}_1(\tau) \mathbf{i}_1(\tau)^{\intercal}} = \overline{\mathbf{i}_2(\tau) \mathbf{i}_2(\tau)^{\intercal}} = \frac{1}{2} \left(\mathbf{I} - \mathbf{i}_3 \mathbf{i}_3^{\intercal} \right), \qquad \overline{\mathbf{i}_1(\tau) \mathbf{i}_2(\tau)^{\intercal}} = -\overline{\mathbf{i}_2(\tau) \mathbf{i}_1(\tau)^{\intercal}} = \frac{1}{2} \widehat{\mathbf{i}}_3 \tag{F.75}$$

where $\mathbf{I}$ is the identity matrix of appropriate dimension. Hence, the averaged equations are:

$$\frac{d\bar{\mathbf{h}}}{d\tau} = \frac{1}{2} \bar{\mathbf{R}} \left(\alpha_2\, \left(\mathbf{I} - \mathbf{i}_3 \mathbf{i}_3^{\intercal} \right) + \alpha_3\, \widehat{\mathbf{i}}_3 \right) \bar{\mathbf{R}}^{\intercal}\, \rho\, \nabla c(\bar{\mathbf{x}}) \tag{F.76}$$

$$\frac{d\bar{\mathbf{x}}}{d\tau} = \beta_1 \bar{\mathbf{R}}\, \mathbf{i}_3 \mathbf{i}_3^{\intercal} \bar{\mathbf{R}}^{\intercal}\, \rho\, \nabla c(\bar{\mathbf{x}}) + \frac{v\, \omega_{\|0}}{\omega^2} \bar{\mathbf{R}}\, \mathbf{i}_3 \tag{F.77}$$

$$\frac{d\rho}{d\tau} = \frac{1}{\mu\omega} \rho \left(1 - \rho^2\, \overline{\zeta_{\mathrm{QS}}^2} \right) \tag{F.78}$$

$$\overline{\zeta_{\mathrm{QS}}^2} = \lambda^2 \nabla c(\bar{\mathbf{x}})^\intercal \bar{\mathbf{R}} \left(\frac{\mu^2 v^2 \, \omega_{\|0}^2}{\omega^2} \mathbf{i}_3 \mathbf{i}_3^\intercal + \frac{v^2 \, \omega_{\perp 0}^2 \gamma(\omega)^2}{2\omega^4} \, (\mathbf{I} - \mathbf{i}_3 \mathbf{i}_3^\intercal) \right) \bar{\mathbf{R}}^\intercal \nabla c(\bar{\mathbf{x}}) \tag{F.79}$$

Using the definition $\bar{\mathbf{h}} = \bar{\mathbf{R}} \, \mathbf{i}_3$, and some algebraic manipulations, we obtain that:

$$\frac{d\bar{\mathbf{h}}}{d\tau} = \frac{1}{2} \left(\alpha_2 \left(\mathbf{I} - \bar{\mathbf{h}} \, \bar{\mathbf{h}}^\intercal \right) + \alpha_3 \widehat{\bar{\mathbf{h}}} \right) \rho \, \nabla c(\bar{\mathbf{x}}) \tag{F.80}$$

$$\frac{d\bar{\mathbf{x}}}{d\tau} = \beta_1 \bar{\mathbf{h}} \, \bar{\mathbf{h}}^\intercal \, \rho \, \nabla c(\bar{\mathbf{x}}) + \frac{v \, \omega_{\|0}}{\omega^2} \bar{\mathbf{h}} \tag{F.81}$$

$$\frac{d\rho}{d\tau} = \frac{1}{\mu\omega} \rho \left(1 - \rho^2 \, \overline{\zeta_{\mathrm{QS}}^2} \right) \tag{F.82}$$

$$\overline{\zeta_{\mathrm{QS}}^2} = \lambda^2 \frac{v^2}{\omega^2} \left(\mu^2 \omega_{\|0}^2 (\nabla c(\bar{\mathbf{x}})^\intercal \bar{\mathbf{h}})^2 + \frac{\omega_{\perp 0}^2 \gamma(\omega)^2}{\omega^2} \left(|\nabla c(\bar{\mathbf{x}})|^2 - (\nabla c(\bar{\mathbf{x}})^\intercal \bar{\mathbf{h}})^2 \right) \right) \tag{F.83}$$

We observe that ζ_{QS}^2 is strictly positive as long as $|\nabla c(\bar{\mathbf{x}})|$ is strictly positive which implies that the equilibrium point $\rho = 1/\sqrt{\overline{\zeta_{\mathrm{QS}}^2}}$ is well-defined as long as $|\nabla c(\bar{\mathbf{x}})|$ is strictly positive. In addition, we observe that the leading order behavior in $\bar{\mathbf{x}}$ is $O(1/\omega)$ and in $\bar{\mathbf{h}}$ is $O(1/\sqrt{\omega})$, whereas the leading order behavior in ρ is $O(1)$. By employing a singular perturbation argument that exploits this time scale-separation, we obtain the quasi-steady approximation of the dynamics of $\bar{\mathbf{h}}$ and $\bar{\mathbf{x}}$ as:

$$\frac{d\bar{\mathbf{h}}}{d\tau} = \frac{1}{2} \alpha_2 \rho \, \left(\mathbf{I} - \bar{\mathbf{h}} \, \bar{\mathbf{h}}^\intercal \right) \nabla c(\bar{\mathbf{x}}) + \frac{1}{2} \alpha_3 \rho \, \bar{\mathbf{h}} \times \nabla c(\bar{\mathbf{x}}) + O(1/\omega) \tag{F.84}$$

$$\frac{d\bar{\mathbf{x}}}{d\tau} = \beta_1 \bar{\mathbf{h}} \, \bar{\mathbf{h}}^\intercal \, \rho \, \nabla c(\bar{\mathbf{x}}) + \frac{v \, \omega_{\|0}}{\omega^2} \bar{\mathbf{h}} \tag{F.85}$$

$$\rho = \frac{1}{\sqrt{\overline{\zeta_{\mathrm{QS}}^2}}}, \quad \sqrt{\overline{\zeta_{\mathrm{QS}}^2}} = \lambda \frac{v}{\omega} |\nabla c(\bar{\mathbf{x}})| \sqrt{\mu^2 \omega_{\|0}^2 |\check{\nabla}_\| c|^2 + (\omega_{\perp 0} \gamma(\omega)/\sqrt{2} \, \omega)^2 |\check{\nabla}_\perp c|^2} \tag{F.86}$$

We make some definitions to compactify the equations:

$$\check{\nabla} c = \nabla c(\bar{\mathbf{x}}) / |\nabla c(\bar{\mathbf{x}})|, \quad \check{\nabla}_\| c = \bar{\mathbf{h}} \, \bar{\mathbf{h}}^\intercal \check{\nabla} c, \quad \check{\nabla}_\perp c = \left(\mathbf{I} - \bar{\mathbf{h}} \, \bar{\mathbf{h}}^\intercal \right) \check{\nabla} c, \tag{F.87}$$

which leads to the following equations when projected along the vector $\bar{\mathbf{h}}$ and the normalized gradient $\check{\nabla}c$:

$$\dot{\bar{\mathbf{x}}}^{\intercal}\bar{\mathbf{h}} = \frac{v\,\omega_{\|0}}{\omega}\left(1 + \frac{\mu\omega_{\perp 0}^2\omega_{\|1}}{\chi\,\omega^2}\bar{\mathbf{h}}^{\intercal}\check{\nabla}c\right) \tag{F.88}$$

$$\dot{\bar{\mathbf{h}}}^{\intercal}\check{\nabla}c = \frac{\omega_{\perp 0}^2\omega_{\|1}\gamma(\omega)}{2\chi\,\omega^2}\cos(\phi(\omega))(1 - (\bar{\mathbf{h}}^{\intercal}\check{\nabla}c(\bar{\mathbf{x}}))^2) \tag{F.89}$$

$$\chi = \sqrt{\mu^2\omega_{\|0}^2|\check{\nabla}_{\|}c|^2 + (\omega_{\perp 0}\gamma(\omega)/\sqrt{2}\,\omega)^2|\check{\nabla}_{\perp}c|^2} \tag{F.90}$$

This may be simplified to:

$$\dot{\bar{\mathbf{x}}}^{\intercal}\bar{\mathbf{h}} = \frac{v\,\omega_{\|0}}{\omega}\left(1 + \frac{\omega_{\perp 0}^2\omega_{\|1}}{\alpha\,\omega^2\omega_{\|0}}\bar{\mathbf{h}}^{\intercal}\check{\nabla}_{\|}c\right), \tag{F.91}$$

$$\dot{\bar{\mathbf{h}}}^{\intercal}\check{\nabla}c = \frac{\gamma(\omega)\,\omega_{\perp 0}^2\omega_{\|1}}{2\mu\omega^2\omega_{\|0}\alpha}\cos(\phi(\omega))|\check{\nabla}_{\perp}c|^2, \tag{F.92}$$

$$\alpha = \sqrt{|\check{\nabla}_{\|}c|^2 + \beta^2|\check{\nabla}_{\perp}c|^2}. \tag{F.93}$$

where $\beta = \gamma(\omega)\omega_{\perp 0}/(\sqrt{2}\omega\mu\omega_{\|0})$. In particular, the quasi-steady signaling pathway response η_{QS} is given by:

$$\eta_{\mathrm{QS}} = \frac{\check{\nabla}_{\|}c + \sqrt{2}\beta(\bar{\mathbf{R}}\mathbf{d}(t)/|\mathbf{d}(t)|)^{\intercal}\check{\nabla}_{\perp}c}{\sqrt{|\check{\nabla}_{\|}c|^2 + \beta^2|\check{\nabla}_{\perp}c|^2}} \tag{F.94}$$